The role of Transferrin 2 and Laminin B2 in Drosophila melanogaster intestinal stem cell homeostasis and ageing

ANONA GALBRAITH

Durham University

The role of Transferrin 2 and Laminin B2 in *Drosophila melanogaster* intestinal stem cell homeostasis and ageing

Anona Christine Galbraith

This thesis is submitted in accordance with the requirements
for the degree of Doctor of Philosophy

Department of Biosciences
Durham University
March 2024

Abstract

Ageing is accompanied by many physiological changes. This is particularly evident in the intestine, where changes in gene expression, gut barrier, and microbiome pre-empt disease and eventual mortality. A wide range of research has been carried out into intestinal homeostasis and loss of homeostasis with age, and the model organism *Drosophila melanogaster* provides an excellent method for ageing research.

Intestinal stem cells (ISCs) have proliferative capacity and can replenish cells that are lost in the intestine because of hazards found in the lumen of the gut. Due to an increased turnover rate compared to some other tissues, the replacement of cells must be controlled tightly to prevent insufficient or excessive cell production, both of which can be fatal to the organism. Many different factors and signalling pathways contribute to the regulation of ISC proliferation, but with age, the balance between different components is lost. Therefore, understanding how intestinal homeostasis is maintained in young flies will help elucidate how this can become disrupted with age.

Stem cell division is controlled by the ISC niche, which consists of a tightly regulated microenvironment of proliferation-inducing and -restricting signals deriving from surrounding tissues such as the muscle and from other epithelial cells. More recent research has revealed that intestinal stem cells also play an active part in contributing to their own niche.

This thesis describes the effects of two proteins, Transferrin 2 and Laminin B2, that are expressed by ISCs and the non-proliferative intestinal progenitor cells called enteroblasts. Changing their expression levels in stem and progenitor cells disrupts intestinal homeostasis, but their relationship to ageing remains unclear.

Table of Contents

List of Figures

List of Tables

List of Abbreviations

BM	Basement membrane
BMP	Bone Morphogenic Protein
BPH	Benign prostate hyperplasia
CAF	Carcinoma-associated fibroblast
Dpp	Decapentaplegic
EB	Enteroblast
EC	Enterocyte
ECM	Extracellular matrix
EE	Enteroendocrine cell
EGF	Epithelial growth factor
EGFR	EGF receptor
EMT	Epithelial-to-mesenchymal transition
ER	Endoplasmic reticulum
ERK	Extracellular signal-regulated kinase
Esg	Escargot
FOV	Field of view
FSC	Follicle stem cell
GS	GeneSwitch
Hh	Hedgehog
Hpo	Hippo
IHC	Immunohistochemistry
iPSC	Induced pluripotent stem cell
ISC	Intestinal stem cell
JAK/STAT	Janus kinase signal transducer and activator of transcription
JNK	Jun N-terminal kinase
LAMC1	Laminin γ1
LanA	Laminin A
LanB1	Laminin B1
LanB2	Laminin B2
LanW	Laminin W
MAPK	Mitogen-activated protein kinase-type

MET	Mesenchymal-to-epithelial transition
mMTf	Membrane-bound melanotransferrin
MTf	Melanotransferrin
Npc2a	Niemann-Pick type C-2a
Nrg	Neuroglian
PCa	Prostate cancer
PERK	PKR-like ER kinase
Plod	Procollagen lysyl hydroxylase
Pros	Prospero
Pvf2	PDGF- and VEGF-related factor 2
Pvr	PDGF- and VEGF-receptor related
RNAi	RNA interference
ROS	Reactive oxygen species
SC	Stem cell
scRNA-seq	Single cell RNA sequencing
SJ	Septate junction
sMTf	Soluble Melanotransferrin
SPARC	Secreted Protein Acidic and Rich in Cysteine
Ssk	Snakeskin
TF	Transcription factor
Tsf2	Transferrin 2
UAS	Upstream activating sequence
Upd	Unpaired
UPR	Unfolded protein response
VM	Visceral muscle
Wb	Wing blister
Wg/Wnt	Wingless/Wingless-related integration site
Yki	Yorkie

Declaration

The work described herein was carried out in the Department of Biosciences, Durham University, between October 2019 and March 2024. All the work is my own, except where specifically stated otherwise. No part has previously been submitted for a degree at this or any other university.

Statement of Copyright

Funding

This project was funded by the BBSRC, UKRI.

Acknowlegements

First of all I would like to thank my supervisor David for taking a chance on me as your first PhD student. Thank you for helping me develop my research skills and for guiding me through the last five and a half years. Here we are, one pandemic and a shattered knee later, but we made it to the finish line.

To the other Doupé lab members, both past and present, particularly my fellow PhD students Fanila and Paula, it has been wonderful to work with you all in such a friendly and helpful atmosphere. Thanks also to the other people of lab 20: Rebecca, Vincent, Abbi, Sophie, and James, it has been a pleasure to work in the same lab as you and I have enjoyed the many laughs we have shared. Thank you also to Helen for your invaluable help. And to Emma, for putting up with all of my many questions and for being so kind and supportive.

Thank you to Dr Adriana Buskin, Prof. Rakesh Heer, and Prof. Craig Robson for supervising my work at Newcastle University.

To Giulia, I am so glad we met during that fire safety demonstration in the first week, and even though, despite your best efforts, DIMO was not meant to be, we provided each other with enough biology gossip and knitting chat to make up for it.

To El and Jess, thank you for bringing fun and just the right amount of chaos to my life to keep me on my toes.

To Franek, thank you for being there for me through all the ups and downs, lockdowns and late lab nights. Now it's your turn! I can't wait to see what the future will bring.

And finally to my family, Mama, Dad, and Màiri. I love you all, thank you so much for your support, both physical and emotional. Thanks for reminding me that as long as I know my Kommaregeln, everything will be fine. Màiri, I will miss our trips to Embleton, but I am sure we will find a new tradition!

Chapter 1: Introduction

Once an organism finishes developing and reaches adulthood, it maintains this state for an extended period of time until a steady decline sets in with old age. In order to do so, organs must maintain their shape and structure for continued function and this process is called homeostasis. This is particularly important for epithelial tissues that interact with the outside world, for example intestinal tissues, the skin, and the lungs, as these experience damage from interactions with their surroundings. Stem cells are proliferative cells that can replace cells that are lost due to damage in order to maintain tissues. Balancing the rate of cell loss and replacement is of particular importance and has therefore been studied extensively. As research on humans is often not possible, a range of model systems have been developed including cell culture and the use of model organisms.

1.1 *Drosophila* as a model organism for studying intestinal homeostasis

The fruit fly *Drosophila melanogaster* (hereafter referred to as *Drosophila* for simplicity) was first bred for research by Charles Woodworth at the start of the 20th century and has since become an indispensable model organism. *Drosophila* research has made key contributions to a vast range of scientific fields including the study of heredity, X-ray-induced mutations, developmental genetics, the olfactory system, innate immunity, and circadian rhythms (https://www.nobelprize.org/).

This introduction will initially consider the use of *Drosophila* and the advantages of this model organism, and subsequently give an overview of the intestine, intestinal stem cells and their regulation, and changes that disrupt the intestine with age.

1.1.1 The life cycle of *Drosophila melanogaster*

The *Drosophila* life cycle has four major distinct stages: embryo, larva, pupa, and the adult fly. After mating, adult females lay eggs on a food source and the embryos within develop for approximately one day at 25°C until they turn into larvae. Larvae moult twice, which divides

this part of the cycle into three different stages (instars). About 4-5 days after the eggs are laid, the larvae crawl out of the food and pupate on the side of the containment vials. During this stage their bodies undergo complete metamorphosis and develop many tissues not present at the previous stages. They eclose and turn into adult flies about 10 days after the start of the cycle and can live for 60 - 80 days. At 18°C the developmental cycle takes approximately 3 weeks (**Figure 1**; reviewed by Jennings, 2011).

The *Drosophila* genome consists of four chromosomes, the X, 2nd, 3rd, and 4th chromosome, coding for around 17,700 genes (Kaufman, 2017). Although the size and complexity of *Drosophila* and human body plans vary significantly, there are nonetheless striking similarities on a smaller scale such as organs like the nervous system and the gut, and as many as 60 - 75% of genes altered in human diseases are conserved in *Drosophila* (Fortini et al., 2000; Reiter et al., 2001).

Drosophila provide an easy, cost-efficient alternative to mammalian models because females can lay several hundreds of eggs which provides a high replicate number for experiments, the life cycle is relatively short, they are fed with a cheap cornmeal-based diet, and they do not take up very much space.

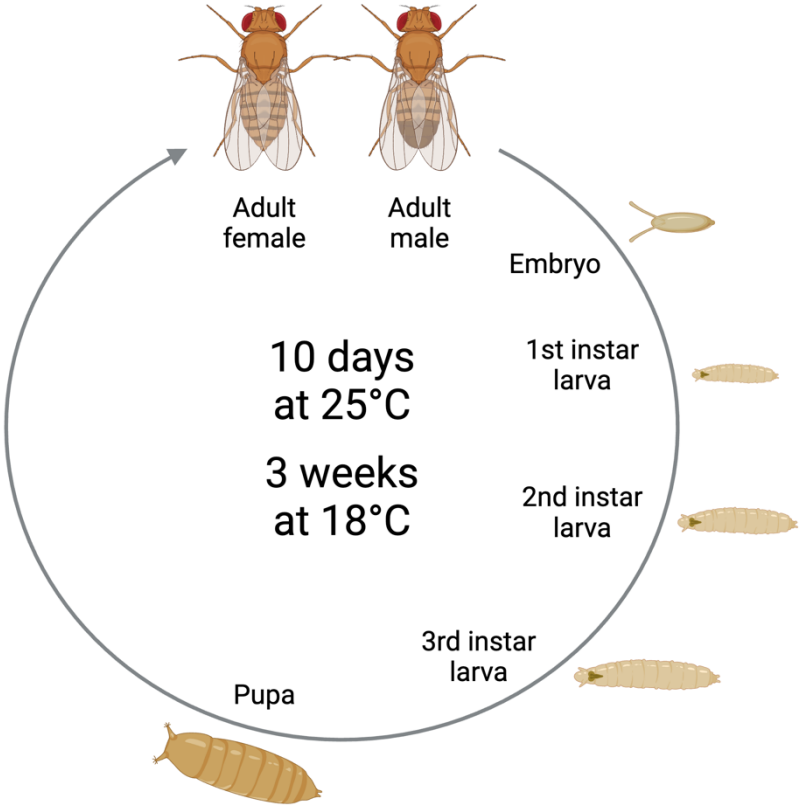

Figure 1: The life cycle of Drosophila melanogaster.

Drosophila flies go through several stages of development. Mated adult female flies lay eggs which hatch into larvae. The larvae go through three stages (instars) and then pupate on the side of the vial. At 25°C the pupae eclose approximately 10 days after the eggs were laid, at 18°C this takes about 3 weeks. This figure was made with Biorender.

1.1.2 Genetic tools

Drosophila melanogaster is a sexually dimorphic species, and as newly eclosed, unmated (virgin) flies can easily be identified, this allows flies with different transgenes to be bred with each other. A vast array of genetic tools has been developed in order to manipulate *Drosophila* gene expression in a temporally and spatially controlled manner. This can be used to label and track proteins or cells, and to increase or decrease the expression of genes of interest. A much smaller number of redundancies between genes simplifies this research. Several different systems can be used for this, including the GAL4/UAS system (Brand & Perrimon, 1993; Fischer et al., 1988), the GeneSwitch system (Osterwalder et al., 2001; Roman et al., 2001) and the AGES system (McClure et al., 2022). The CRISPR/Cas system (Port et al., 2020) can be used for knockout and overexpression among other things, and the Flp-FRT system (Golic & Lindquist, 1989) can be used for lineage tracing of cells.

Both the GAL4/UAS system and the GeneSwitch system have been used extensively in this thesis and are described in more detail below.

1.1.3 The *Drosophila* intestine

The *Drosophila* gut is split into several sections, each with its own distinct gene expression pattern and function. The overall structure can be divided into the foregut, the midgut, and the hindgut (**Figure 2A**). The foregut and hindgut are derived from the developmental ectoderm, while the midgut comes from the endoderm. The foregut is involved in food storage and controls the passage of food into the midgut, which is responsible for digestion and nutrient absorption. The midgut has an anterior part that has a neutral pH, the middle midgut is acidic due to the presence of acid-secreting copper cells, while the posterior midgut has an alkaline pH and is the most similar to the mammalian small intestine. The midgut can be further subdivided into as many as 14 subregions. The hindgut's main function is water reabsorption and waste excretion. Malpighian tubules, which are equated to the mammalian kidney, are connected to the gut at the midgut-hindgut junction (reviewed by Buchon & Osman, 2015).

The posterior midgut consists of four main cell types. Enterocytes (ECs) are polyploid cells that make up the majority of differentiated cells in the gut. They secrete enzymes and absorb nutrients from the lumen, while enteroendocrine cells (EEs), the other group of differentiated cells, are much smaller and are responsible for hormone secretion. Intestinal stem cells (ISCs) are capable of dividing and replenishing lost cells, while enteroblasts (EBs) are non-dividing progenitor cells (Micchelli & Perrimon, 2006; Ohlstein & Spradling, 2006). It was initially thought that EBs differentiate either into EEs or ECs depending on the level of Notch signalling they receive from the ISCs, but more recent studies have shown that there are separate EE progenitor cells that are determined prior to EB formation and EBs differentiate only into ECs (**Figure 2B**; Biteau & Jasper, 2014; Zeng & Hou, 2015).

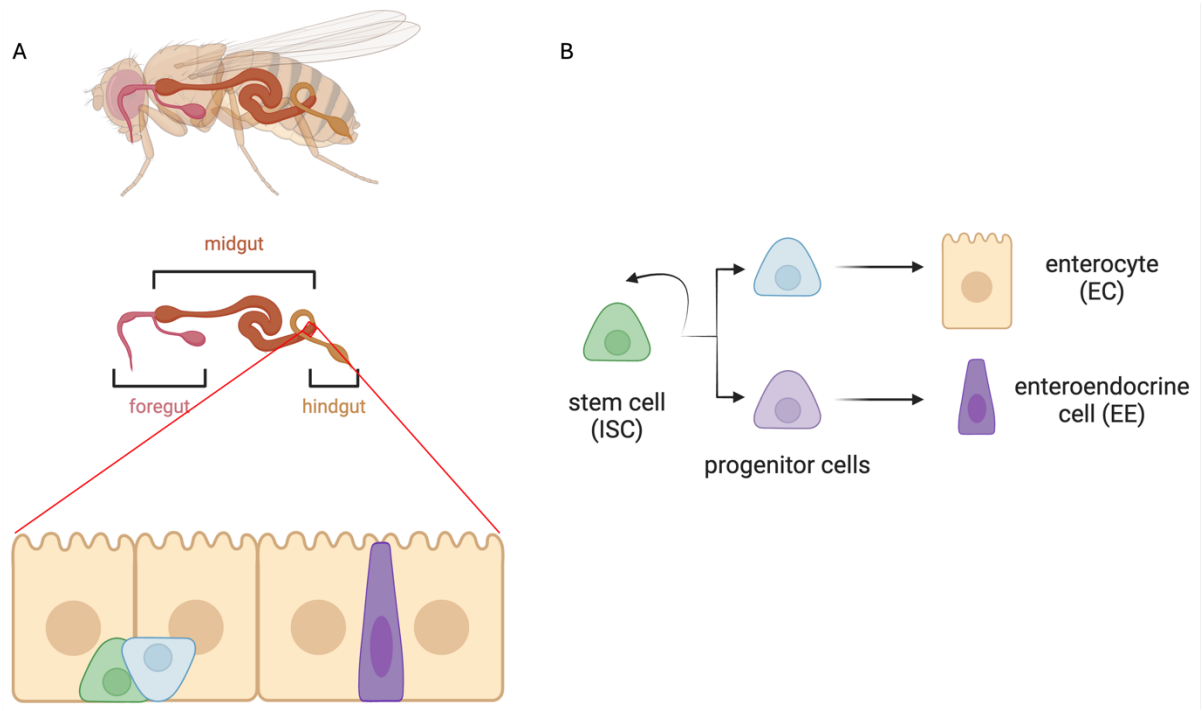

Figure 2: The Drosophila gut.

The structure of the gut consisting of foregut, midgut, and hindgut. The posterior midgut consists of ISCs (green), EBs (blue), EEs (purple), and ECs (beige) (A). ISCs divide, giving rise to more ISCs as well as progenitor cells that differentiate into ECs or EEs (B). This figure was made with Biorender.

The midgut tissue is a pseudostratified epithelium, with ISCs located more basally, close to the basement membrane (BM). The BM is a specialised extracellular matrix (ECM) surrounding the epithelium that contributes to its structure and polarity. It has several core components, including Laminin, Collagen IV, Nidogen, and Perlecan, among others (Töpfer, 2023). Not only does the basal location of ISCs protect them from luminal contents, but it also provides a specialised environment for the ISCs to control their rates of division, with many signals provided from the surrounding cells and tissues including the BM, the visceral muscle (VM), the trachea, and even haemocytes (Ayyaz et al., 2015; Perochon et al., 2021; N. Xu et al., 2011). This environment is called the stem cell niche (Morrison & Spradling, 2008).

As the lumen of the gut, which can be considered as “outside” the body, contains things such as food, bacteria, and digestive enzymes, the intestinal epithelium forms a barrier with junctions between the differentiated cells that prevent the leakage of gut contents into the tissue. Due to digestion, the cells experience mechanical and chemical damage at a higher rate than other tissues, which means the gut also has a higher cell turnover rate. Cell loss is compensated by the production of new cells, and this is tightly regulated. The production of too many cells

can lead to dysplasia and cancer, whereas a depletion of cells will eventually cause loss of tissue integrity, and both outcomes prevent proper gut function and negatively impact the health of the fly (**Figure 3**; Lucchetta & Ohlstein, 2012). ISCs can divide both symmetrically and asymmetrically, depending on cues from their surroundings and on competition between cells (de Navascués et al., 2012).

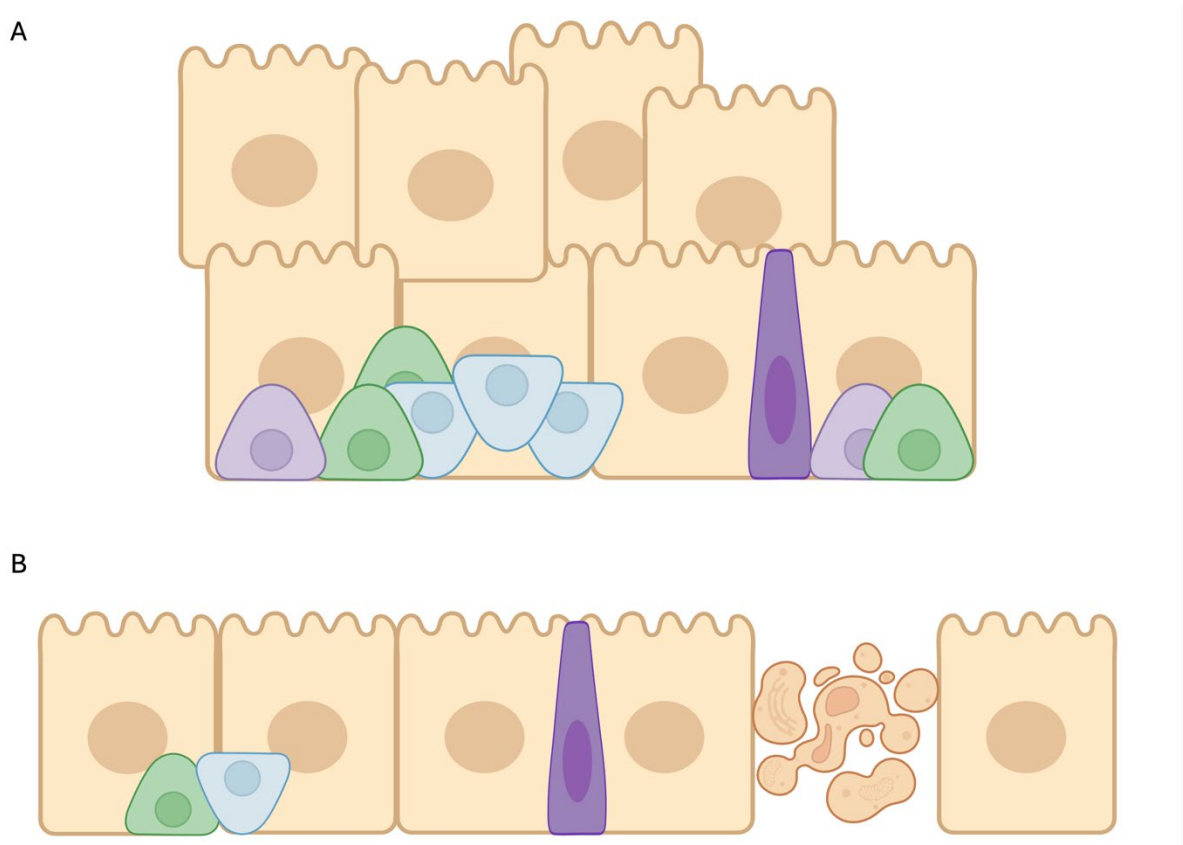

Figure 3: The importance of homeostasis in the Drosophila midgut.

Both overproliferation (A) and underproliferation (B) are detrimental to gut health. This figure was made with Biorender.

The mammalian small intestine consists of similar cell types but has an undulating structure composed of millions of villi that protrude into the lumen, while the ISCs are found at the bottom of the crypts. This architecture results in a clearly defined anatomical niche for mammalian ISCs. As the ISCs divide, the cells move up the crypt and differentiate. The mammalian intestine has progenitor cells called transit-amplifying cells that have a limited proliferative capacity, allowing them to divide a few times before differentiating. This permits the ISCs to remain more quiescent. Due to the similarities between the two systems, the *Drosophila* midgut is a good, simplified model to study the mammalian small intestine (Barker et al., 2007; reviewed by Casali & Batlle, 2009).

1.1.4 ISCs are tightly regulated by their surroundings

Several signalling pathways have been found to regulate proliferation and differentiation in the gut. Most of these are conserved between *Drosophila* and humans, allowing research to be carried out in *Drosophila* that can then be applied in mammalian research. Their methods of action can vary between development, homeostatic regulation, and infection or damage, and they are often misregulated with age which leads to a loss of homeostasis. Below are listed several pathways commonly found activated during loss of homeostasis in *Drosophila* intestines, but this list is non-exhaustive.

1.1.4.1 Notch signalling

When *Drosophila* ISCs divide asymmetrically they do this in such a way that the daughter cell that remains a stem cell stays close to the BM while future EBs segregate upwards and move to fill the free space. The cells that stay ISCs express the Notch ligand Delta, while the cells that become EBs express the receptor Notch (**Figure 4**; Ohlstein & Spradling, 2007). Daughter cell fate is initially stochastic but then reinforced by lateral inhibition (Guisoni et al., 2017), which can be affected by a range of factors, for example space constraints affecting contact areas, the number of other cells in contact, or differentially inherited signalling components (Goulas et al., 2012; Montagne & Gonzalez-Gaitan, 2014). Homeostasis is maintained on a population level, with both symmetric and asymmetric divisions of individual ISCs (de Navascués et al., 2012).

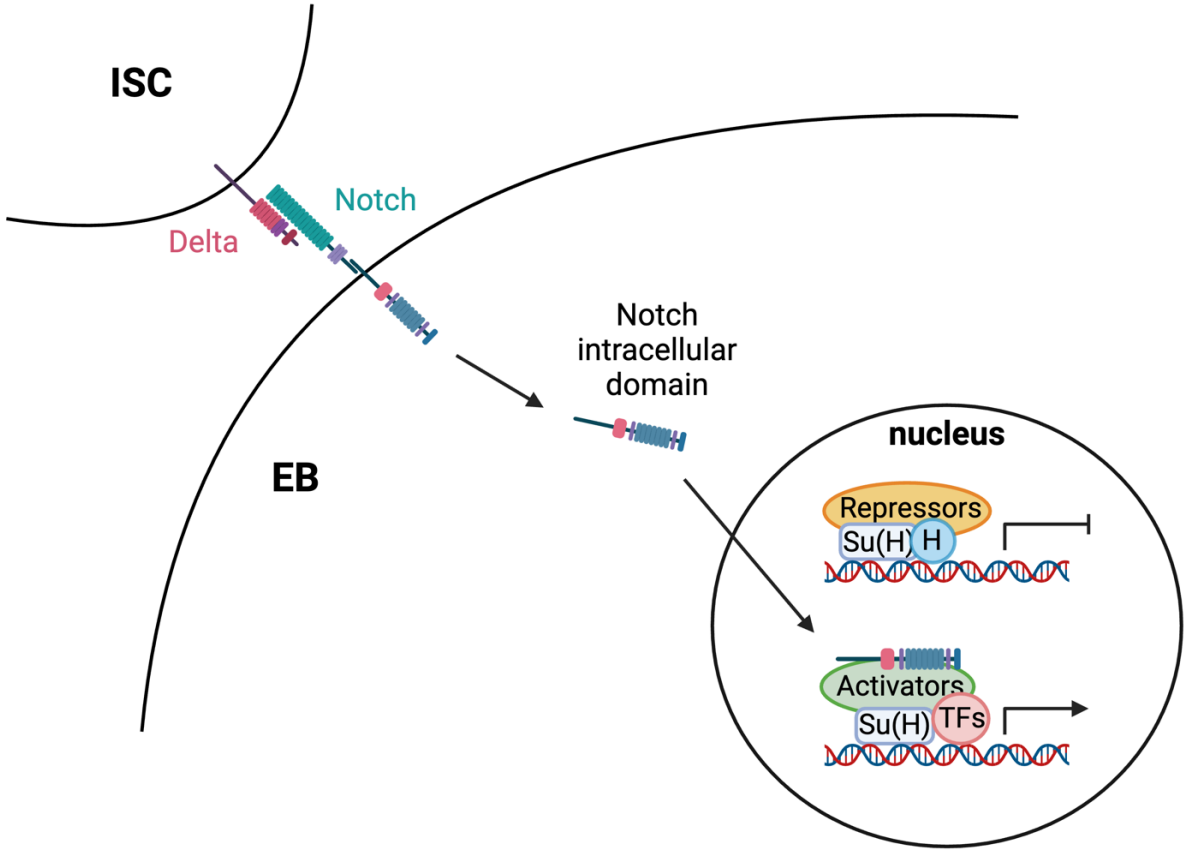

Figure 4: The Notch pathway.

The ligand Delta is expressed by ISCs. It binds its receptor Notch on the neighbouring EB. This induces cleavage and translocation of the intracellular domain to the nucleus, where it binds Su(H) and displaces repressors to activate downstream gene expression. H = Hairless; Su(H) = Suppressor of hairless; TF = transcription factor. This figure was made with Biorender.

1.1.4.2 BMP signalling

Notch signalling between ISCs and EBs is in part controlled by bone morphogenic protein (BMP) ligands Decapentaplegic (Dpp) and Glass bottom boat (Gbb, **Figure 5**), which form a gradient with high basal and low apical levels relative to ISCs. Higher BMP signalling via a Dpp/Gbb heterodimer inhibits Notch signalling, which allows the basal cell during ISC division to express more Delta than Notch and remain an ISC. The BMP ligands are expressed by ECs and trapped at the basal side by collagen in the BM (Tian & Jiang, 2014). Upon injury, BMP ligand production is increased by ECs, promoting symmetric ISC-ISC divisions for faster tissue regeneration, and this is regulated by a negative feedback system to regain homeostatic division levels after regeneration (Tian et al., 2017; J. Zhou et al., 2015). Further studies have found additional sources of BMP ligands, with Dpp expression also seen coming from the trachea (Z. Li et al., 2013) or the VM (Z. Guo et al., 2013; J. Zhou et al., 2015), and potentially conflicting roles in both cell-autonomous or non-autonomous effects on ISC proliferation and EC differentiation, also via the activation of other pathways (Tian & Jiang, 2017).

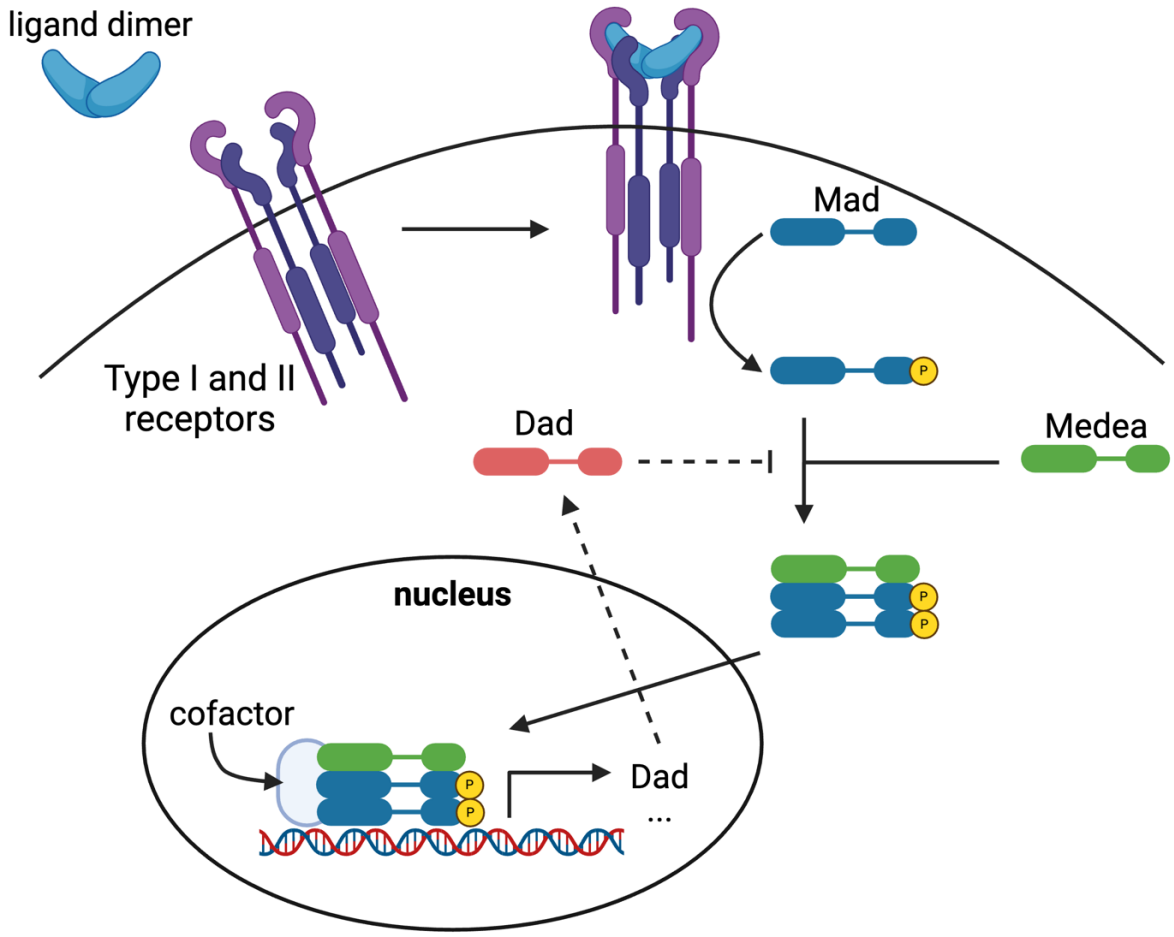

Figure 5: The BMP pathway.

The ligand dimer (consisting of a combination of Dpp, Gbb, and Scw) binds its receptors, which allows the receptors to induce phosphorylation of Mad. A trimer of phosphorylated Mad and Medea forms, which translocates to the nucleus and induces gene expression with a cofactor. Expression of Dad (inhibitory Smad) is induced and forms a negative feedback loop. Dad = Daughters against dpp; Dpp = Decapentaplegic; Gbb = Glass bottom boat; Mad = Mothers against dpp; Scw = Screw. This figure was made with Biorender.

1.1.4.3 JNK signalling

The Jun N-terminal kinase (JNK) pathway consists of a mitogen-activated protein kinase-type (MAPK) cascade (**Figure 6**) which is often triggered in response to stress such as infections or damage. It has both stress-protective and proliferation-inducing functions. With age, chronic JNK signalling causes hyperproliferation and the build-up of misdifferentiated daughter cells (Biteau et al., 2008). Bacterial dysbiosis with age also acts as an inducer of the JNK pathway and contributes to loss of homeostasis (Buchon, Broderick, Chakrabarti, et al., 2009). It can induce proliferation both in ISCs and non-autonomously via ECs by activating other pathways, e.g. by Unpaired (Upd) expression. JNK activation has cell-type specific effects as it can trigger apoptosis in ECs, which in turn stimulates cell turnover (Biteau et al., 2008; H. Jiang et al., 2009; Mundorf et al., 2019).

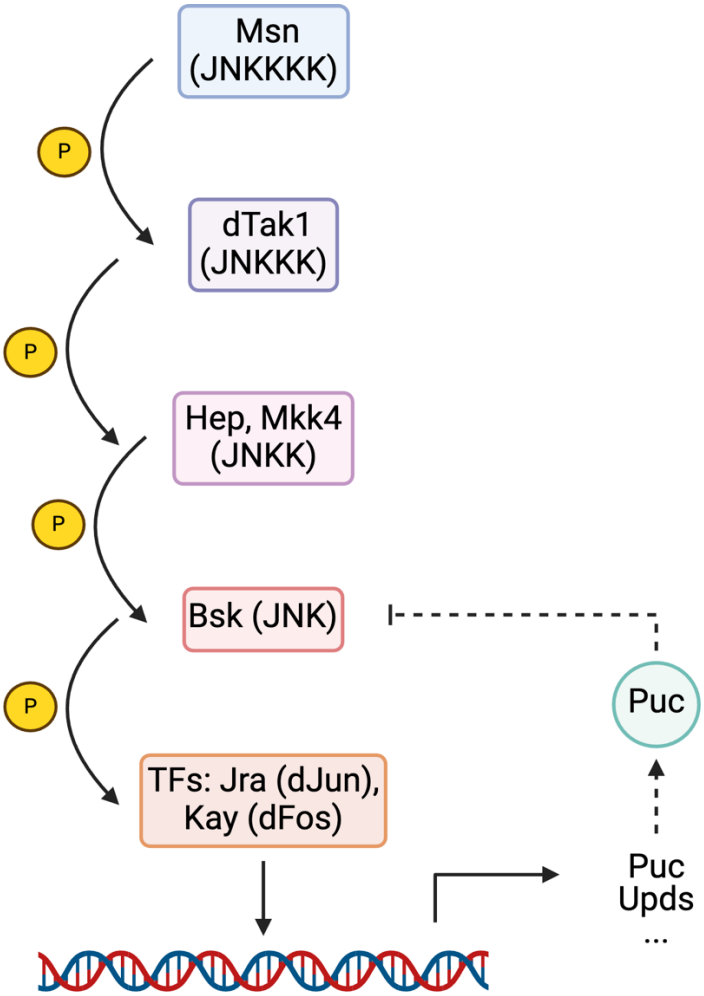

Figure 6: The JNK pathway.

The JNK pathway consists of a series of phosphorylation events carried out by kinases, resulting in the phosphorylation of transcription factors Jra and Kay, which dimerise and induce downstream gene expression. This includes Puc, which forms a negative feedback loop. Bsk = Basket; dTak1 = Drosophila TGF-β activated kinase 1; Hep = Hempiterous; Jra = Jun-related antigen; Kay = Kayak; Mkk4 = MAP kinase kinase 4; Msn = Misshapen; Puc = Puckered. This figure was made with Biorender.

1.1.4.4 Wg signalling

The Wingless (Wg)/Wnt pathway is also key to maintaining ISC fate. An initial study found that Wg secreted by the VM is required and sufficient for ISC proliferation during homeostasis (Lin et al., 2008). A later study found however that during regeneration, Wg from EBs, but not from the VM, is required for ISC proliferation and tissue renewal, while during homeostasis, knockdown of Wg in progenitors or the VM does not affect proliferation (Cordero, Stefanatos, Scopelliti, et al., 2012). The tumour-suppressive Adenomatous Polyposis Coli (APC) functions in ISCs by negatively regulating Wnt signalling in both flies and mammals and is often mutated in cancer (Cordero et al., 2009; Korinek et al., 1997; W.-C. Lee et al., 2009). Additionally, Wg pathway activation in ECs leads to a downregulation of Upd expression by ECs during homeostasis to prevent JAK/STAT-induced ISC overproliferation (Tian et al., 2016).

1.1.4.5 JAK/STAT signalling

The Janus kinase signal transducer and activator of transcription (JAK/STAT) pathway is crucial for controlling gut homeostasis and is often activated downstream of other signalling pathways, as mentioned above. It is mediated by cytokines called Unpaired (Upd) 1, 2, and 3. Apoptotic or damaged ECs secrete Upds (mainly Upd3) to stimulate non-autonomous proliferation of ISCs as well as inducing EB differentiation (H. Jiang et al., 2009; Lin et al., 2010). Infection induces a spike in JAK/STAT signalling, while commensal bacteria maintain a low level of pathway activation which contributes to normal gut renewal (Broderick et al., 2014; Buchon, Broderick, Chakrabarti, et al., 2009; Buchon, Broderick, Poidevin, et al., 2009). JAK/STAT pathway activation in response to infection also induces the expression of EGFR ligands Vein and Spitz from the VM and EBs, respectively, which in turn induces ISC proliferation (H. Jiang et al., 2011; F. Zhou et al., 2013). While some groups have found that JAK/STAT activation is not required for homeostatic proliferation or ISC maintenance in the midgut (Beebe et al., 2010; H. Jiang et al., 2009), others have found that loss of Upds causes a loss of proliferation and/or ISCs (Lin et al., 2010; W. Liu et al., 2010; N. Xu et al., 2011). When looking at the different Upd cytokines, Osman et al showed that while Upd2 and 3 have a larger role in old flies, Upd1 is required for homeostatic ISC proliferation and this occurs in an autocrine manner, as ISCs and EBs express Upd1 (Osman et al., 2012).

1.1.4.6 EGFR signalling

As mentioned above, the epidermal growth factor receptor (EGFR) pathway is another key signalling pathway in the *Drosophila* midgut, both for homeostatic turnover and during regeneration (**Figure 7**). Ligands, which can act in a redundant manner, include Vein, secreted from the VM, and Spitz and Keren secreted by EBs and ECs (Biteau & Jasper, 2011; Buchon et al., 2010; H. Jiang et al., 2011; N. Xu et al., 2011). EGF ligand secretion is controlled further by the protease Rhomboid, which cleaves EGF precursors to allow their secretion. Before cleavage they are bound to the cell membrane in a precursor form that is released to surrounding cells upon apoptosis, linking cell death to the production of new cells (Liang et al., 2017).

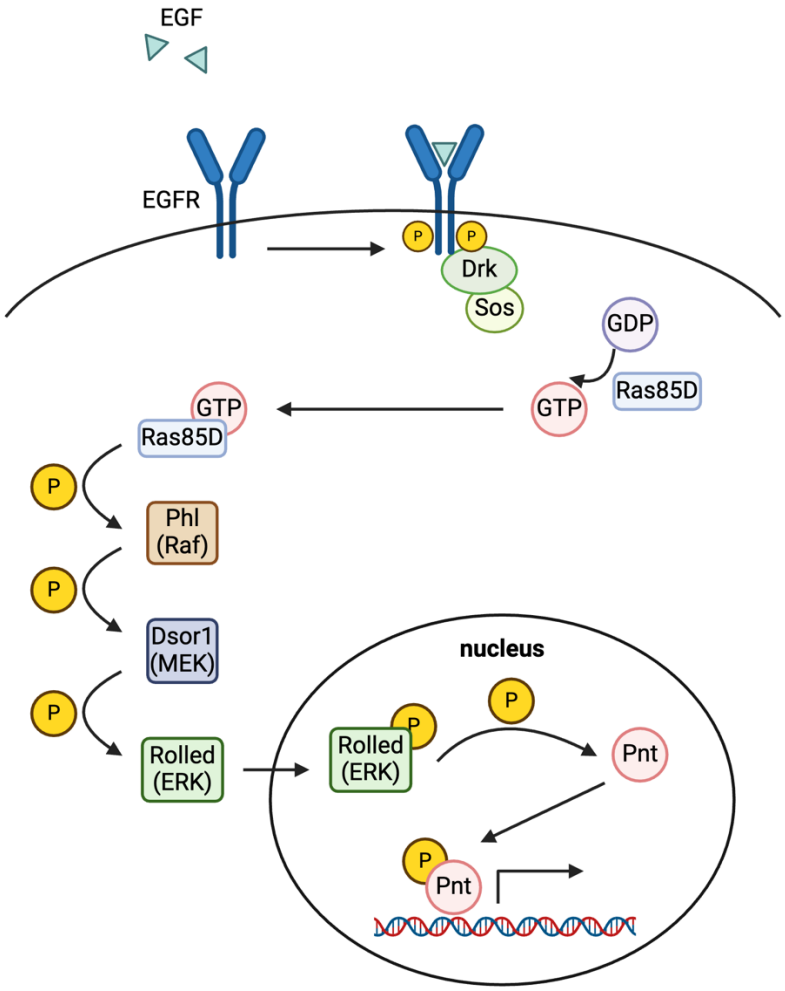

Figure 7: The EGFR and Ras/MAPK pathway.

The EGF ligands (including Keren, Spitz, and Vein) bind their tyrosine kinase receptor EGFR, which induces receptor dimerization and trans-phosphorylation. This recruits Drk and Sos, which converts Ras85D-bound GDP to GTP. Ras85D-GTP induces a phosphorylation cascade, leading to the final MAPK/ERK Rolled translocating to the nucleus, where it phosphorylates the transcription factor Pnt, which in turn induces downstream gene expression. Drk = Downstream of receptor kinase; Dsor1 = Downstream of raf1; EGF = Epidermal growth factor; GDP/GTP = Guanosine di-/triphosphate; Phl = Pole hole; Pnt = Pointed; Ras85D = Ras oncogene at 85D; Sos = Sons of sevenless. This figure was made with Biorender.

1.1.4.7 Hedgehog signalling

When uninduced, the Hedgehog (Hh) pathway is repressed by the promotion of phosphorylation and cleavage of the transcription factor Ci. Upon Hh binding to its receptor Patched, this activates a signalling cascade leading to translocation of Ci to the nucleus to activate Hh target gene transcription including proliferative genes. Hh signalling is not required for homeostatic renewal, but it is necessary for regeneration after damage (Tian et al., 2015). The Hh ligand is expressed by EBs following JNK pathway activation. Hh acts in EBs by inducing Upd2 production which induces ISC proliferation non-cell-autonomously (Tian et al., 2015). Hh expression has also been found to stem from the VM, and Hh was found to be increased in older and in stressed flies (Z. Li et al., 2014).

1.1.4.8 Hippo signalling

The Hippo (Hpo) pathway negatively controls the transcriptional coactivator Yorkie (Yki). During homeostatic turnover, the pathway is active and therefore Yki is inactive; constitutively active Yki expression however is able to induce proliferation. During regeneration, Yki is de-repressed, which allows it to induce the transcription of proliferation-inducing genes, and this is required for regeneration. Yki signalling can induce proliferation both non-autonomously by ECs as well as in an autocrine manner when it is activated in ISCs/EBs. The Hpo pathway ligand Dachsous is expressed by ECs and it activates the Hippo pathway in a juxtacrine manner. When the gut is damaged, juxtacrine signalling may decrease, allowing Yki derepression. Yki activity is induced by the JNK pathway and itself induces Upds and EGFR ligand expression (Karpowicz et al., 2010; Ren et al., 2010; Shaw et al., 2010; Staley & Irvine, 2010).

The signalling pathways mentioned above are often interdependent and induce each other in a cell type-specific and context-dependent manner and can sometimes partially compensate for one another. These relationships can vary between developmental, adult homeostatic, and regenerative conditions (Cordero, Stefanatos, Myant, et al., 2012; H. Jiang et al., 2011; N. Xu et al., 2011).

1.1.5 ISCs contribute to their own niche

Historically it has been thought that stem cells are controlled only by receiving signals originating from surrounding cells and their niche, whereas in recent years the focus has shifted in both *Drosophila* and in mammalian systems to include the study of how stem cells themselves contribute to their niche (Ferraces-Riegas et al., 2022).

1.1.5.1 Feedback from stem cell-derived progeny

While some SCs are surrounded by cells whose function is specifically to act as a niche cell, the progeny of SCs also feed back to regulate proliferation and differentiation, both in a mechanical and a chemical manner. Several pathways involved in feedback from progeny to *Drosophila* ISCs, including from the progenitor EBs, have been listed above. To add to this list, EEs have also been shown to feed back to ISCs. They secrete the ligand Slit which binds to the receptor Robo2 on ISCs to prevent further EE differentiation (Biteau & Jasper, 2014). EEs also secrete Tachykinin in a food-dependent manner to the VM, which in turn signals to

ISCs to induce proliferation (Amcheslavsky et al., 2014). Additionally, EEs secrete the hormone Bursicon to the VM to inhibit EGF ligand Vein secretion and this limits ISC proliferation. This regulation can be disrupted and lead to increased proliferation, for example during old age (Scopelliti et al., 2014).

It has also been shown that the number of cells packed into the epithelium affects cell extrusion and division. This is mediated by the Ca^{2+} ion channel Piezo1 in mammals (Gudipaty et al., 2017) and Piezo in *Drosophila*. Here, Piezo is expressed in EE precursors and when the stretch-sensitive Piezo is activated (e.g., due to a decrease in cell density) or overexpressed, this induces ISC division and EE production by an increase in cytosolic Ca^{2+} which increases extracellular signal-regulated kinase (ERK) signalling and inhibits Notch signalling (He et al., 2018). This allows the gut to respond immediately to changes that could affect the barrier function, for example if a reduction in cell number could affect tissue integrity. Additionally, while insulin signalling plays a major role in young midgut proliferation after feeding (O'Brien et al., 2011), stretching due to food intake may also play a part in this.

Another way a quick response can be achieved is by the formation of progenitor EBs that stay in a paused, undifferentiated state. ISCs and EBs express *escargot* (*esg*), which encodes a transcription factor that maintains stemness by repressing differentiation genes, such as the EC marker *pdm1* (Korzelius et al., 2014; Loza-Coll et al., 2014). *Esg* expression allows EBs to enter a semi-mesenchymal state until local cues signal that they are required, after which *esg* is downregulated and they undergo mesenchymal-to-epithelial transition (MET) and differentiate (Antonello et al., 2015).

1.1.5.2 Stem cells can signal to other cell types and contribute to the microenvironment

Progenitor cells and SCs can themselves also directly signal and thereby actively contribute to the niche and their surroundings. In the murine lung epithelium, basal stem/progenitor cells actively and continuously signal to their progeny, the secretory cells, in order to maintain their state and prevent them from differentiating into ciliated cells (Pardo-Saganta et al., 2015).

Stem cells have also been shown to express ECM components, such as Collagen or Laminin, and ECM regulators, for example in the hair follicle in mice (Morris et al., 2004; Watt & Fujiwara, 2011) and in the *Drosophila* midgut (Hung et al., 2020; Lin et al., 2013). SCs also

express integrins, which mediate cell-ECM interactions, both in mammals (Jones et al., 1995; Jones & Watt, 1993) and in *Drosophila* (Lin et al., 2013; O'Reilly et al., 2008; Rincón-Ortega et al., 2023).

1.1.5.3 Stem cells can signal in an autocrine manner

Mesenchymal cells in the mammalian airway limit proliferation by expressing BMP ligands that signal to the basal stem cells to keep proliferation at a low rate. When the trachea is damaged, this induces a temporary spike of BMP pathway antagonist expression by both the mesenchyme and the stem cells themselves, allowing them to increase proliferation, partly in an autocrine manner, to regenerate the damaged tissue (Tadokoro et al., 2016).

In the murine interfollicular epidermis, SCs control their own fate by expressing Wnt which signals in an autocrine fashion to maintain stemness and induce proliferation, while also expressing longer-range paracrine Wnt inhibitory signals to restrict the pro-proliferative signal (Lim et al., 2013).

Drosophila ISCs express both the ligand Pvf2 and the receptor Pvr of the PDGF- and VEGF-receptor related (Pvr) pathway. This allows them to signal in an autocrine manner during homeostasis to promote proliferation. The pathway is required and sufficient for proliferation and is also responsible for correct differentiation, but lack of Pvr signalling can be overridden during stress situations such as an infection (Bond & Foley, 2012). In mammals, haematopoietic stem cells and blood cancer cells also promote cell proliferation via autocrine VEGF signalling (Gerber & Ferrara, 2003).

The contribution of SC-derived signals to the niche is particularly important in cancer, as cancer stem cells or tumour-initiating cells must colonise a new niche after metastasis. Understanding how they contribute to their niches to make them hospitable for cancer cells while excluding healthy stem cells is therefore important in order to learn how to combat this disease (López de Andrés et al., 2020).

1.2 Ageing

All animals undergo changes as they grow older. Although organisms try to maintain their health and function, this is eventually lost with age and their health decreases until death. While

improvements through scientific discoveries and investment in things such as healthcare and sanitation have increased the average human lifespan, which is defined as the number of years a human will live, the healthspan, which is defined as the number of years that the human will live a healthy life, has not been able to keep up. This has led to an increasing proportion of the population that requires medical care (reviewed by Garmany et al., 2021).

Although this is true for the general population, there is a lot of variability within populations that cannot solely be attributed to differences in diet or exercise. Studying ageing in a model organism such as *Drosophila* can be used to understand these differences and discover treatments to improve or maintain health in old age. Many aspects of *Drosophila* physiology can be manipulated, and they can be bred in large numbers at a time, which enables researchers to carry out lifespan assays to investigate the contribution of different changes that occur throughout life.

Several changes occur with age that have been linked to ill health. These include mental decline, frailty, and loss of bodily functions, as well as chronic diseases such as infections, cancer, or diabetes. Changes to the intestine are well documented, both in humans and in *Drosophila*.

1.2.1 Intestinal changes with age

Because the interplay between the different signalling pathways highlighted previously is very dynamic and requires a fine balance, it comes as no surprise that with age, these pathways can become misregulated, leading to a loss of homeostasis and to disease.

Below is a list of several of the phenotypes and pathways involved in ageing, although there are many more that are not listed here. The phenotypes include dysbiosis, which leads to chronic inflammation and immune pathway activation, loss of proteostasis, chronic JNK pathway activation leading to ISC overproliferation and misdifferentiation of daughter cells, and loss of barrier function. They are all interconnected, which makes dissecting the influence of individual components difficult.

The GI tract is not only the source of nutrient uptake, it also forms a barrier to protect the organism from its contents, and the function of this barrier decreases with age across many species, such as *Drosophila* spp., *C. elegans*, zebrafish, rats, and primates (Dambroise et al.,

2016; Hollander & Tarnawski, 1985; Salazar et al., 2018, 2023; Tran & Greenwood-Van Meerveld, 2013). This is coupled with changes in the gut microbiome, called dysbiosis, with both an overall increase in bacterial load as well as a shift in the proportion of different bacterial species (Buchon, Broderick, Chakrabarti, et al., 2009; Claesson et al., 2012). Dysbiosis is harmful to flies and occurs shortly before barrier dysfunction, and preventing this can extend lifespan (Clark et al., 2015). In *Drosophila*, gut barrier dysfunction can be tested non-invasively by the addition of non-absorbable blue dye to fly food. When the barrier is leaky, the dye permeates throughout the fly and turns it blue, leading to the name "Smurf" fly. It is a precursor to death and therefore a good predictor for a fly's biological age (Rera et al., 2011). Indeed, increasing gut barrier function by overexpressing junction components can extend lifespan and delay dysbiosis significantly (Salazar et al., 2018).

Activation of the immune system is crucial for organismal survival to fight off infections in many species, for example *Drosophila*, humans, and other mammals to name but a few, but it can take a toll on the body and this is especially evident with age, when chronic activation can occur (Chung et al., 2009; Rera et al., 2012; Zerofsky et al., 2005). Immune responses prolong the fly's life by destroying harmful bacteria, but they can also damage the intestine. One of the immune pathways in *Drosophila* is the dual oxidase pathway, which consists of the production of reactive oxygen species (ROS). While these are harmful to bacteria, they can also damage the epithelium and cause EC death (S.-H. Kim & Lee, 2014), which in turn induces ISC proliferation to replace the lost cells. Extended immune activation will eventually lead to ISC overproliferation coupled with misdifferentiation of progeny, which in turn gives rise to dysplasia or cancer (Ullman et al., 2009).

Another factor that contributes to changes with age in the gut is loss of protein homeostasis (proteostasis) in intestinal cells, which is characterised by a build-up of mis- or unfolded proteins in the endoplasmic reticulum that activates the unfolded protein response. In *Drosophila* this is mediated by CncC, the master negative regulator of oxidative stress response (L. Wang et al., 2014). During homeostasis, CncC initiates a checkpoint to stop ISC proliferation when proteostasis is lost, but this capacity is lost with age (Rodriguez-Fernandez et al., 2019). *CncC* is repressed upon ROS challenge specifically in ISCs but not in other cell types to allow ISC proliferation as a response to intestinal damage. With age, overall CncC expression levels decrease, causing an increase in proliferation that can be rescued with CncC overexpression (Hochmuth et al., 2011). PKR-like ER kinase (PERK) is another factor that is

activated by ER stress. It is required for ISC proliferation during regeneration, but chronic activation in old flies leads to ISC overproliferation and eventual death, which can be prevented by knocking down PERK (L. Wang et al., 2015).

As has been mentioned previously, many different signalling pathways contribute to maintaining homeostasis in the stem cell niche of young, healthy fly guts and they become misregulated with age. JNK is one such example. This is a major contributor to loss of homeostasis in old flies and has been researched extensively in this context. Biteau et al found that ISC proliferation and progeny misdifferentiation were increased in old flies, leading to a lack of cell integration into the epithelium. This is caused by excessive JNK and Notch pathway activation (Biteau et al., 2008). JNK signalling in ECs induces JAK/STAT signalling to promote proliferation (H. Jiang et al., 2009). Increased intestinal JAK/STAT signalling occurs with age and reduces lifespan both in flies and in mammals (H. Li et al., 2016; Moskalev et al., 2019; M. Xu et al., 2016). It has also been shown that chronic JNK signalling in old flies causes changes to spindle orientation during cell division, promoting symmetric ISC division to create more ISCs (D. J.-K. Hu & Jasper, 2019). Reducing JNK signalling in old flies is able to prevent dysplasia and extend lifespan (Biteau et al., 2010).

JNK signalling also induces Wg signalling in old flies, which further adds to the overproliferation phenotype and can be ameliorated with Wg knockdown (J. B. Cordero, Stefanatos, Scopelliti, et al., 2012). A similar Wnt-dependent stem cell hyperproliferation has been seen in murine hair follicles (Castilho et al., 2009).

The autocrine Pvr pathway, which is required for homeostatic ISC proliferation in flies (Bond & Foley, 2012) has been shown to become increasingly activated with age due to higher Pvf2 expression, leading to ISC overproliferation. This can also be induced by oxidative stress, and reduction of pathway activation in old flies is able to prevent ageing phenotypes, whereas prolonged activation has the opposite effect (Choi et al., 2008).

The barrier function of the gut has been shown to be particularly important, as leakage of luminal contents through the epithelium can cause damage and inflammation. Overproliferation and improper differentiation prevents the formation of the barrier, as the differentiated cells do not organize into a monolayered epithelium. As septate junctions, which make up this barrier in *Drosophila*, are formed while the progenitor cells are differentiating,

loss of this process prevents barrier formation (Resnik-Docampo et al., 2017; Salazar et al., 2018).

With age, *Drosophila* also experience genetic changes. ISCs accumulate DNA damage and mutations, which has been shown to lead to dysplasia and cancer (Siudeja et al., 2015). They also experience changes in chromatin accessibility, leading to a different gene transcription profile in old versus young flies (Tauc et al., 2021).

These are just some of the examples of how homeostatic signalling is lost with age. Discovering novel homeostatic regulators may therefore provide candidates that can contribute to loss of homeostasis with age, which then can lead to age-related decline in intestinal function.

1.3 Secreted factors are expressed by ISCs/EBs in *Drosophila* and contribute to midgut homeostasis

A recent study looked at gene expression in ISCs and EBs in the adult *Drosophila* midgut using targeted DamID. This couples RNA polymerase II with a DNA adenine methyltransferase (Dam) to give a readout of which genes are transcribed in ISCs and EBs by expressing it under the ISC/EB-specific *esg* promoter (Doupé et al., 2018; Southall et al., 2013). Given the importance of the local microenvironment for stem cell regulation, this approach has the advantage of not requiring cell isolation or tissue breakdown. This was compared to the expression profile of ECs to exclude genes in common as these would most likely be housekeeping genes. The study found the expression of components of several major signalling pathways in intestinal stem and progenitor cells, including Insulin-like peptide Ilp6 and the JNK pathway ligand Eiger, and that manipulating their expression affected proliferation and/or differentiation in the midgut (Doupé et al., 2018). The role of stem/progenitor-derived Eiger in proliferation has been confirmed by subsequent studies (Tamamouna et al., 2020). This is further evidence that *Drosophila* ISCs and EBs play a big part in creating their own niche.

A list of 49 ISC/EB-specific, secreted proteins was curated by intersecting the data from this study with an annotated list of *Drosophila* secreted proteins (Doupé et al., 2018; Y. Hu et al., 2015). The proteins that have high confidence mammalian orthologs, determined using the *Drosophila* RNAi Screening Center Ortholog Prediction Tool (DIOPT) (Y. Hu et al., 2011), were selected and Galbraith et al knocked down 24 of these individually in adult ISCs/EBs for 7 days using the ISC/EB-specific driver *esg^{ts}GFP* (see 2.2.1) to test for effects on midgut homeostasis. This uncovered several hits that showed changes in the proportion of stem and progenitor cells in the posterior midgut (**Figure 8A**), which can be classified as a loss of homeostasis. This was often accompanied by a change in the total cell number per field of view (**Figure 8B**), although this is a less rigorous criterion as gut width and therefore cell density were not taken into account (Galbraith and Doupé, unpublished).

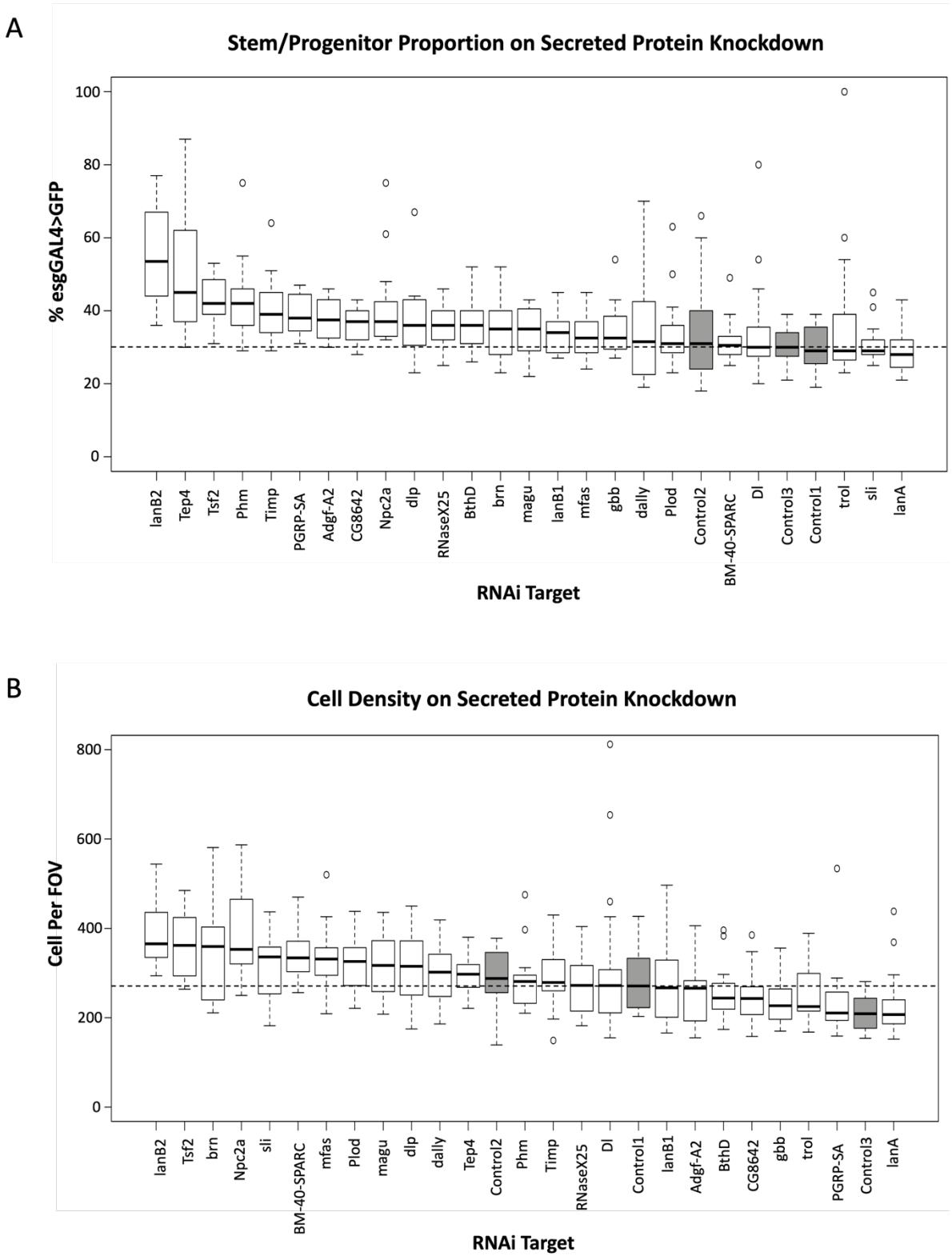

Figure 8: Changes in Drosophila midgut homeostasis upon knockdown of secreted proteins in stem and progenitor cells.

Secreted proteins were knocked down individually in adult ISCs/EBs using esg^{ts}GFP for 7 days. The proportion of stem/progenitor cells in the posterior midgut (A) and the total number of cells per field of view (B) were counted and compared to control knockdown of luciferase RNAi (grey). The boxplots show the median and interquartile ranges, with the whiskers indicating minimum and maximum data points; outliers are also shown. The dotted line represents an average of the medians of all three controls (grey). n≥15 guts combined from three separate replicates/condition.

1.4 Thesis aims

This thesis aims to explore further the roles of stem cell-secreted proteins in the *Drosophila* midgut. It will focus on two key hits from the knockdown screen mentioned above for further analysis.

Laminin B2 (LanB2) had both the highest proportion of stem and progenitor cells and the highest number of cells per field of view upon knockdown and was therefore selected as a target.

Transferrin 2 (Tsf2) has not been well-characterised in *Drosophila*, with only one paper published that focused on this protein. As it also showed a large increase in both criteria in the knockdown screen, this was picked as the second target. This thesis aims to characterise both LanB2 and Tsf2 and their roles specifically in the adult *Drosophila* posterior midgut in relation to homeostasis in young flies and to intestinal ageing.

For each gene the thesis aims to:

- Characterise the expression pattern in the posterior midgut
- Determine the function in normal midgut homeostasis
- Characterise any changes in expression with age, both at a transcriptional and at the protein level
- Assess the effect of changing expression levels on lifespan and healthspan
- Determine potential mechanisms of action
- Assess conservation of expression in mammalian systems

Chapter 2: Materials and Methods

2.1 Fly husbandry

2.1.1 Food preparation

2.1.1.1 Cornmeal food

To prepare fly food, the dry ingredients and water were mixed and microwaved at short intervals until fully dissolved and boiling. This was then placed in the fume hood and allowed to cool for a short while, after which the Nipagin and acid mix were added and mixed in thoroughly. If required, further reagents were added at this stage, e.g., RU486 or blue dye. The food was then dispensed into vials containing either 4 mL (for short term use, e.g., in regularly flipped lifespans) or 8 mL of food (for stock vials and crosses), or into bottles of 75 ml food. The food was left at room temperature overnight to cool and to allow condensation to disperse. It was then stored at 4°C for up to one week. The day before flipping flies into the vials/bottles they were put back at room temperature to allow the food to warm up. Vials, bottles, and stoppers were sourced from Genesee Scientific via SLS.

Table 1: Recipe for 1000 mL of cornmeal food

Reagent	Amount	Source
Agar	10g	SLS FLY1020
Yeast	30g	Genesee Scientific 62-106
Sucrose	19g	Duchefa Biochemie S0809
Dextrose	38g	Melford G32040
Cornmeal	91g	SLS FLY1110
Water (dH_20)	900 mL	n/a
10% Nipagin	15 mL	SLS FLY1136
Acid Mix (4.15% phosphoric acid + 41.8% propionic acid)	11 mL	 VWR 20624.262 Sigma P5561

2.1.1.2 Mifepristone food for GeneSwitch experiments

Mifepristone (Cayman Chemical, 10006317; Merck, M8046), also known as RU486, was added to cornmeal food after Nipagin and acid mix addition. A stock solution of 20 mg/mL was added at a ratio of 250 µL/100 mL food. This dilution is referred to as RU50 as it has a final concentration of 50 µg/mL. As RU486 is dissolved in ethanol, control vials were made with the addition of 250 µL ethanol/100 mL food and this is referred to as RU0.

2.1.1.3 Blue food for Smurf assays

2.5% FD&C blue food dye #1 (Fast Colours, 08BLU00201) was added to the food after Nipagin and acid mix addition and mixed in thoroughly.

2.1.2 Stock and cross maintenance

Fly stocks in active use were kept at room temperature (approximately 23°C) and were flipped every 2 - 3 weeks. Other stocks were kept at 18°C and flipped once a month. Experimental flies were maintained in incubators at 25°C and 60% humidity with a 12-hour light/dark cycle and flipped 3 times per week into 4 mL food vials unless stated otherwise. Temperature shift experiments were set up and maintained in incubators at 18°C, upon induction they were moved to 29°C. They were kept in 8 mL vials and flipped twice per week. Crosses were set up in 8 mL vials, and bottles of stocks, where applicable, contained 75 mL food.

Crosses were set up with virgins that were up to 7 days old and kept at 18°C prior to mating to slow down ageing. After crossing them with males at a ratio of between 5♀:1♂ and 2♀:1♂ and allowing them to mate for 3 days, the parents were cleared and vials kept hydrated. For progeny collections, female progeny were mated and age-matched to within 72 hours. The day of collection was counted as day 1. The vial density across different conditions was kept consistent within each experiment. For experiments requiring changes in gene expression, the females were aged for 7 days (± 1 day) after collection before being treated for 7 days. Stoppers were changed once a week to prevent bacterial overgrowth.

2.2 Induction systems

A vast array of genetic tools exists to change gene expression in *Drosophila*. Two of the induction systems have been used for this thesis and are described below.

2.2.1 GAL4/UAS system

The GAL4/UAS system consists of a yeast transcriptional activator (GAL4) which can bind to an upstream activating sequence (UAS) that contains GAL4 binding sites. This system can be used to induce specific genes in a tissue or cell type of choice by changing the promoter that drives GAL4 expression. The line *esgGAL4* was frequently used in this thesis. It has GAL4 expression under the intestinal stem and progenitor cell-specific *esg* promoter. The sequence downstream of UAS determines what gene is expressed.

Each parent fly has either the GAL4 or the UAS component. Upon mating, their progeny will have both components and the target gene can be induced (Brand & Perrimon, 1993; Fischer et al., 1988). This system can be controlled further by the addition of GAL80, which inhibits GAL4 by binding to it and preventing it binding to the UAS. GAL80 can also be expressed in a subset of cells to restrict target gene expression (T. Lee & Luo, 1999). A temperature-sensitive variant of GAL80, called $GAL80^{ts}$, can be used for temporal regulation of target gene expression. It functions normally at the lower temperature of 18°C to prevent target gene expression, but changes conformation once the flies are moved to 29°C and no longer inhibits GAL4, which allows GAL4 to bind to the UAS and induce the change in gene expression (McGuire et al., 2003). This can be used to study the effects of genes in specific situations, for example by allowing normal expression during development and then knocking down or overexpressing a gene during adult homeostasis. In this thesis *esgGAL4* combined with *tubGAL80^{ts}* used. *TubGAL80^{ts}* suppresses GAL4 ubiquitously at 18°C as tubulin is expressed in all cells. The line is referred to as *esg^{ts}GFP* as it also contains *UAS-GFP* to label all *esg*$^+$ cells.

Knockdown of a target gene can be induced by RNA interference (RNAi), which occurs when the target gene induced by GAL4 is a double-stranded RNA specific for the gene of interest. This targets the mRNA of the gene of interest for degradation. In this thesis, *UAS-RNAi* lines and overexpression lines were used to explore the functions of genes of interest; a list of the lines used can be found in **Table 2** below.

2.2.2 GeneSwitch system

The GeneSwitch system is a drug-inducible version of GAL4/UAS. This has a GAL4 variant that is fused to a progesterone receptor. This GAL4 activates target gene transcription upon addition of RU486, also known as mifepristone (Osterwalder et al., 2001; Roman et al., 2001). RU486 is given to the flies by mixing it into their food. GeneSwitch is used as a method to control for differences in genetic background, as the progeny of one cross can be split into two genetically identical groups, one of which is fed RU486 while the other is not.

The GeneSwitch system was initially characterised for use during development, but more recent studies that included analysis of the effects in adult flies have found some problems with the system. Because it relies on consistent feeding levels and on endogenous enhancers for gene expression and these may change with age, this can affect the level of transgene expression. Furthermore, the system has been shown to be leaky, with aberrant transgene expression without RU486 induction. This is especially prevalent when looking at RNAi expression, more so than for protein coding transgenes (Poirier et al., 2008; Scialo et al., 2016). The drug RU486 also has effects on lifespan, which are described in more detail below in (**2.4 Lifespans**).

In order to look for potential effects induced by RU486 on cell number/proliferation and cell fate during differentiation, the number of cells per field of view and the proportion of EE cells were analysed upon expression of the control RNAi line BL31603 driven by the ISC/EB-specific driver line *5961*^{GS}. While there was no statistically significant difference in the number of cells per field of view between RU0 and RU50 guts, RU50 did induce a significant increase in the proportion of EE cells, from 4.8% ± 0.4 (mean ± SEM to 1dp) to 7.2% ± 0.4 (**Figure 9**). This must be taken into consideration when analysing data using this driver line.

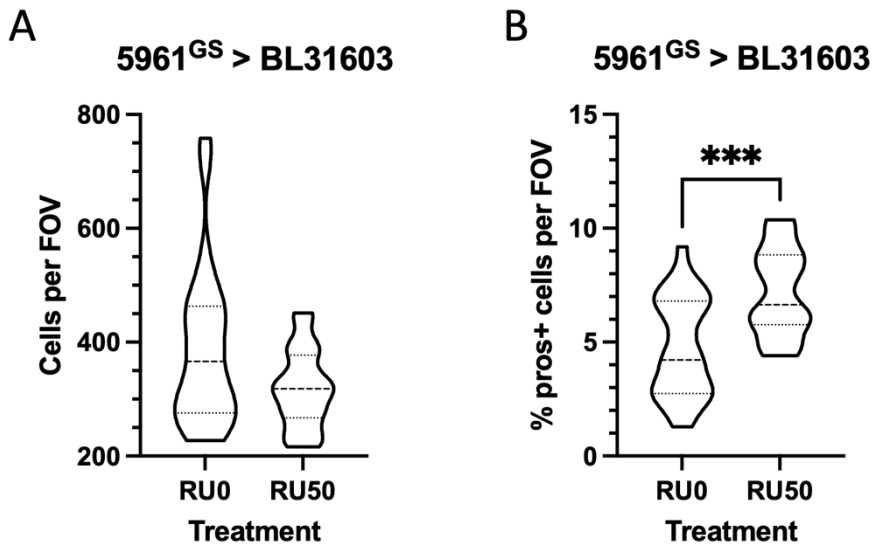

Figure 9: Quantification of the effect of 7 days of RU50 treatment on the 5961^{GS} line.

*Changes in cell number per field of view (A) and the proportion of EE cells (B) after 7 days of RU50 treatment on 5961^{GS} crossed to the control RNAi line BL31603 (luc-RNAi). The plotted lines represent the median and quartiles. The unpaired t test was used for normally distributed data, the Mann-Whitney test was used for non-normally distributed data. n≥21 guts over 3 replicates. No * = ns, ***p<0.001.*

2.3 Fly stocks

Many stocks were sourced from Bloomington Drosophila Stock Center (BDSC) or the Vienna Drosophila Research Center (VDRC).

Table 2: Fly stocks used in this thesis

Designation	Source/ Reference	Source identifier	Function	Genotype
esg^{ts}GFP	Perrimon lab		temperature-inducible ISC/EB-specific driver with ISCs/EBs labelled by GFP	esgGAL4,UAS-GFP,tubGAL80^{ts}
tubG4^{ts}	Perrimon lab		temperature-inducible ubiquitous driver	tubGAL80^{ts}; tubGAL4/TM6B
5961^{GS},UAS-GFP	Walker lab		ISC/EB-specific GS driver with ISCs/EBs labelled by GFP upon induction	
5961^{GS}	O'Brien lab		ISC/EB-specific GS driver	
esg-lacZ	Perrimon lab		ISC/EB reporter	y[1] w[67c23]; P{w[+mC]=lacW}esg[k00606]/CyO
Su(H)GBE-lacZ	(Furriols & Bray, 2001)		Notch signalling reporter	
UAS-EGFP	BDSC	RRID:BDSC_6874	inducible EGFP	w[*]; P{w[+mC]=UAS-2xEGFP}AH2

UAS-GFPnls	BDSC	RRID:BDSC_4775	inducible nuclear GFP	w[1118]; P{w[+mC]=UAS-GFP.nls}14
UAS-mCherrynls	BDSC	RRID:BDSC_38425	inducible nuclear mCherry	w[*]; P{w[+mC]=UAS-mCherry.NLS}2; MKRS/Tm6B, Tb[1]
esgsfGFP	David Doupé, Perrimon lab		CRISPR sfGFP enhancer trap in esg locus	esgsfGFP/CyO
CantonS	Clark lab		wild-type stock	
w^{1118}	Clark lab		white mutant control stock	
BL31603	BDSC	RRID:BDSC_31603	Luciferase RNAi	y[1] v[1]; P{y[+t7.7] v[+t1.8]=TriP.JF01355}attP2
Tsf2_RNAi_1	BDSC	RRID:BDSC_65903	Tsf2 RNAi	y[1] sc[*] v[1] sev[21]; P{TriP.HMC06165}attP40
Tsf2_RNAi_2	VDRC	v330006	Tsf2 shRNAi	P{VSH330006}attP40
Tsf2_RNAi_3	VDRC	v5236	Tsf2 RNAi	w[1118]; P{GD2442}v5236
UAS-Tsf2-GFP	(Tiklová et al., 2010)		inducible GFP-tagged Tsf2 overexpression	w:UAS-GFP-MTf/CyOftzlacZ
LanB2_RNAi_1	BDSC	RRID:BDSC_55388	LanB2 RNAi	y[1] sc[*] v[1] sev[21]; P{TriP.HMC04076}attP40
LanB2_RNAi_2	BDSC	RRID:BDSC_62002	LanB2 RNAi	y[1] v[1]; P{TriP.HMJ23628}attP40
LanB2_RNAi_3	VDRC	v42559	LanB2 RNAi	w[1118]; P{GD2394}v42559
LanAGFP	VDRC	v318155	LanAGFP FlyFos	Pbac{fTRG00574.sfGFP-TVPTBF}VK00033
LanB1GFP	VDRC	v318180	LanB1GFP FlyFos	Pbac{fTRG00681.sfGFP-TVPTBF}VK00033
LanB2 CRIMIC GAL4	BDSC	RRID:BDSC_91283	LanB2 CRIMIC GAL4	y[1] w[*]; TI{CRIMIC.TG4.0}LanB2[CR01721-TG4.0]
UAS-mCas9	VDRC	v340002	inducible mCas9	P{ry[+t7.2]=hsFLP}12, y[1] w[*]; P{y[+t7.7] w[+mC]=UAS-uMCas9}attP40
w^{1118};If/SM6a; TM2/TM6c,Sb’	Clark lab		Double balancer (II and III)	w^{1118};If/SM6a; TM2/TM6c,Sb’
If/SM6a; TIGS	Clark lab		TIGS GS driver line on the third chromosome with balancers	If/SM6a; TIGS/TM2
Su(H)GBE-GFPnls (II)	de Navascués lab/O’Brien lab		nuclear Notch reporter on the second chromosome	Su(H)GBE-GFPnls/CyO; MKRS/TM6B
Su(H)GBE-GFPnls (III)	de Navascués lab/O’Brien lab		nuclear Notch reporter on the third chromosome	If/Cyo; Su(H)GBE-GFPnls/TM6B
UAS-EGFP; LanB2-GAL4	This study (see notes below)		LanB2 CRIMIC GAL4 with inducible EGFP	UAS-EGFP/SM6a; LanB2-GAL4/TM6c,Sb’

5961^{GS},UAS-GFP, Su(H)GBE-lacZ	This study (see notes below)		ISC/EB-specific GS driver with labelled EBs and inducible GFP expression in ISCs/EBs	
5961^{GS},UAS-GFP, UAS-mCas9	This study (see notes below)		ISC/EB-specific driver with GFP and Cas9 expression upon induction	
5961^{GS}; Su(H)GBE-GFPnls	This study (see notes below)		ISC/EB-specific driver with Notch reporter GFPnls	5961^{GS}; Su(H)GBE-GFPnls/TM6c,Sb'
Su(H)GBE-GFPnls;TIGS	This study (see notes below) (David Doupé)		ISC/EB/EC-specific driver with Notch reporter GFPnls	Su(H)GBE-GFPnls/ CyO;TIGS/TM2

UAS-EGFP;LanB2-GAL4 was made by balancing LanB2 CRIMIC GAL4 and *UAS-EGFP* and crossing the balanced stocks to each other.

5961^{GS},UAS-GFP,Su(H)GBE-lacZ was generated by recombination of *5961^{GS},UAS-GFP* and *Su(H)GBE-lacZ*.

5961^{GS},UAS-GFP,UAS-mCas9 was generated by recombination of *5961^{GS},UAS-GFP* and *UAS-mCas9*.

5961^{GS};Su(H)GBE-GFPnls was made by balancing *5961^{GS}* and crossing the balanced stock to *Su(H)GBE-GFPnls* (II).

Su(H)GBE-GFPnls;TIGS was made by crossing Su(H)GBE-GFPnls (III) and If/SM6a; TIGS/TM2.

2.4 Lifespans

2.4.1 Lifespan set-up

Crosses were set up with 15 *5961^{GS}* virgins and 3 - 5 males. They were allowed to lay for 3 days, after which the vials were cleared and kept hydrated. Once the first vial started eclosing, all progeny were collected after approximately 72 hours to make sure the flies were age-matched. They were then allowed to mate for 2 days, after which they were randomly sorted into vials of 30 females each. They were flipped onto fresh food every 2 - 3 days and deaths were counted. Overexpression or knockdown of target genes was induced on day 7 (± 1 day). Flies were counted as censored if they escaped, were squashed by the vial stopper, or if they were stuck to the food but still alive, preventing them from being transferred to the new vial. 10 vials of 30 females each were used per condition.

2.4.2 Potential effects of RU486 on lifespan

Mating induces an increase ISC proliferation and midgut size to support the nutrient demands of egg production (Reiff et al., 2015; Tower et al., 2017). One study showed that RU486 does not affect the lifespan of males or virgin females, but can cause a dose-dependent, significant increase for mated females of some genotypes. It does this by counteracting the negative effect on lifespan that mating and egg production has, as RU486 reduces progeny number and midgut size of mated females. Another study by the same lab also found a lifespan increase in virgin females upon feeding RU486 (Landis et al., 2015, 2021). This was not tested specifically with *5961^{GS}*, the ISC/EB-specific driver used in this thesis. The concentration used in the studies mentioned above was 160 - 200 µg/mL, compared to 50 µg/mL used in this thesis.

To test for effects on lifespan that were not caused by changing the expression levels of genes of interest, several different controls were set up. *5961^{GS}* was crossed to BL6874 (*UAS-EGFP*). Two independent lifespans were set up as described above, although the virgin females used to set up the crosses were collected from the same set of bottles. Both showed a significant reduction in lifespan in response to RU treatment. The first replicate had a median survival of 70 days for the control and 68 days for the treated cohort (**Figure 10A**). The second replicate had a median survival of 68 and 63 days, respectively (**Figure 10B**).

The control *luciferase-RNAi* BL31603, which was used in several experiments in this thesis as a control for RNAi experiments using the temperature-inducible GAL4/UAS system, was also crossed to *5961^{GS}*. The crosses for the first two replicates were set up at the same time with separate virgin females collected from the same bottles, while the third replicate was set up at a different time with virgins collected from a different set of bottles. The first replicate had a significant reduction in lifespan, with median survival at 73 days for the control and 62 days for the treated flies (**Figure 10E**). The second replicate also had a significant reduction, with median survival at 73 and 69 days, respectively (**Figure 10F**). The third replicate had a non-significant reduction in lifespan, with median survival at 65 and 61 days, respectively (**Figure 10G**).

The fly line with a mutation causing white eyes, called *w^{1118}*, is often used as a control fly line. It has been shown recently however that *white* mutant flies have an increased lifespan as the loss of White in ISC prevents age-induced ISC overproliferation by affecting folate metabolism. The study found that feeding RU486 to *5961^{GS}* flies with wild-type White expression reduced lifespan at a non-significant level, whereas driving *white-RNAi* with *5961^{GS}*

showed a significant increase in lifespan (Sasaki et al., 2021). When *5961*^{GS} was crossed to the *white* mutant w^{1118} line as part of this thesis, both replicates showed a non-significant increase in lifespan with RU486, with median survivals of 54 and 56 days for the control and treated cohorts respectively (**Figure 10C,D**).

A final control was carried out using just CantonS flies without crossing them to *5961*^{GS}. The survival curves for control and treated flies matched each other very closely, with the same median survival of 56 days (**Figure 10H**).

Overall this suggests that at the concentration used in this thesis, RU486 does not seem to affect lifespan by itself. However, when it is used to induce changes in gene expression via the GeneSwitch system, this may have a negative impact. This should be taken into account when interpreting lifespan data, as it could suggest that any significant increases in lifespan in treated samples may be even more robust than the analysis suggests, while results showing no changes or significant decreases in lifespan as a result of transgene induction by the GeneSwitch system may have been impacted as well.

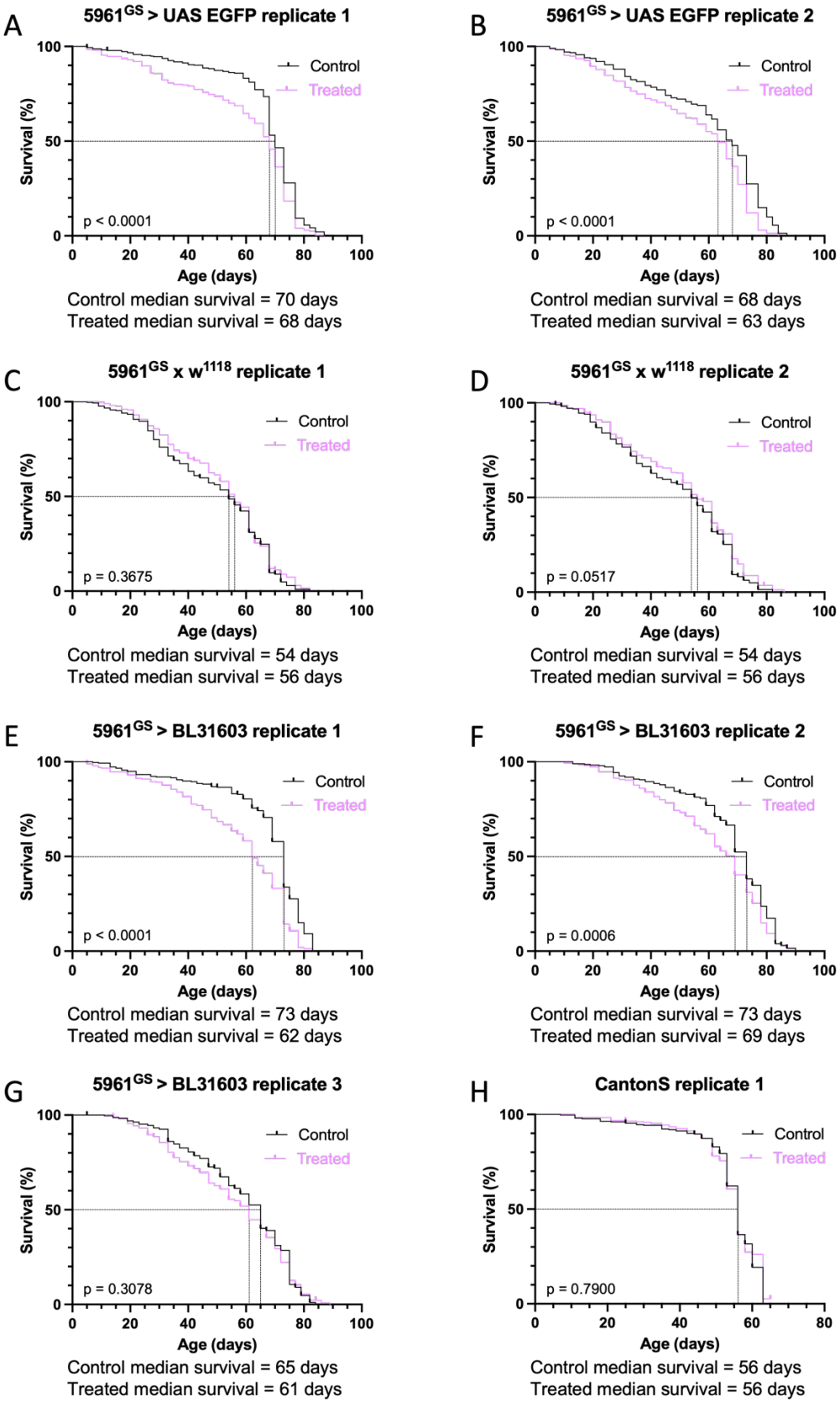

Figure 10: Control lifespans to test the effect of RU486.

Lifespan graphs of 5961^{GS} crossed to BL6874 (UAS-EGFP) (A,B), crossed to w^{1118} (C,D), crossed to BL31603 luc-RNAi (E-G), and CantonS (H). Lifespans were tested with log-rank (Mantel-Cox) test, p values are indicated on each plot. n = 300 mated females/condition.

2.5 Smurf assays

In order to test the barrier integrity of the gut, flies were flipped onto food containing 2.5% FD&C blue food dye #1. The flies were put onto blue food for 24 hours, after which the number of Smurf flies were counted and the flies were flipped back onto non-blue food. When the barrier function of the flies is intact, the blue dye is contained the intestinal tract, whereas if the barrier is leaky, the dye permeates into the haemolymph and surrounding tissue and the fly turns blue (**Figure 11**; Rera et al., 2011). The Smurf assay was carried out every 10 days until less than half the flies were alive.

There may be a batch-dependent, toxic effect of the food dye on fly health. Some lifespans had noticeable drops in survival a few days after each Smurf assay (data not shown). To prevent this from interfering with lifespan analysis, separate lifespans were set up to test Smurf proportions.

Figure 11: Smurf phenotype.

Photograph of two females displaying the barrier dysfunction Smurf phenotype (bottom) and two non-Smurf females with intact gut barriers (top).

2.6 Immunofluorescence

2.6.1 Staining protocol

A protocol previously used by this lab was followed (Doupé et al., 2018).

Dissection

Dissections were done between 10am and 2pm. Keeping a consistent time limits the impact of circadian rhythm on proliferation rates and other signalling pathways (Karpowicz et al., 2013). They were carried out in increments of up to 90 minutes and guts were kept on ice until fixed to prevent degradation of the tissue.

Before beginning the dissection, phosphate-buffered saline (PBS) and two dissection plates were cooled on ice. After drying the plates, one was left on ice and the wells were each filled with 150 µL ice-cold PBS. Each gut was placed into this plate directly after dissecting. The second plate was used to carry out the dissections, also in ice-cold PBS.

Fixation

After dissecting, 50 µL of freshly thawed 16% paraformaldehyde (PFA) was added to each well in the fume hood to make up a final concentration of 4% PFA. The plate was covered with parafilm and foil to prevent evaporation and light exposure and was placed on a rocker for 30 minutes. After removing the PFA in the fume hood, the guts were washed 3 times with PBS. If further dissections needed to be carried out, the dissection plate was covered in parafilm and foil and kept in the fridge.

Blocking

Blocking buffer (PBS + 0.5% Triton X-100 + 0.5% BSA) was made and stored in the fridge for up to 2 weeks. Once the PFA was removed, an aliquot of blocking buffer with 5% normal goat serum (NGS) was made fresh before use. After removing PBS from the wells, 150 µL of the aliquot was added to each well, the plate was covered in parafilm and foil and placed back onto the rocker for 30 minutes.

Primary antibody

During this incubation, the primary antibody mix was prepared in PBS + 0.5% Triton X-100 (PBT) (see **Table 3** for dilutions). After removal of the blocking buffer mix, 150 µL of the antibody mix was added. The plate was then covered in parafilm and foil, labelled, and placed on a rocker at 4°C overnight.

Secondary antibody and DAPI

The following morning, the primary antibody mixture was removed and three 10-minute PBS washes were performed on a rocker. During the third wash, the secondary antibody mixture was prepared in PBT. The antibodies and concentrations used are shown in **Table 3** below. The secondary antibodies are light sensitive and must therefore be covered in foil. After the third PBS wash, the PBS was removed and 150 µL of the secondary antibody mixture was added to each well. The plate was covered in parafilm and foil and incubated on a rocker at room temperature for 2 hours.

Towards the end of the incubation, DAPI was defrosted and an aliquot of 1:2000 was prepared in PBT. After the 2-hour incubation, the secondary antibody mixture was removed and 150 µL of the diluted DAPI was added to each well. The plate was covered in foil and incubated on the rocker for 10 minutes. Finally, the guts were washed three times for 10 minutes each in PBS. Once finished, the plate was either covered in parafilm and foil and left in the fridge to be mounted later in the day, or the samples were mounted directly.

Mounting

Microscope slides were labelled with the dissection date, genotype, replicate/sample number, primary antibodies and concentrations used, fly age, treatment, etc. To mount, a drop of VectaShield was placed in the middle of the slide and spread out to the dimensions of a coverslip using forceps. The guts were placed individually in the mounting medium and spread out carefully with as little handling as possible to prevent damage. They were covered carefully with a coverslip and sealed using nail polish. Once the nail polish was dry, the slides were placed in a slide box and stored in the fridge.

Dissecting for endogenous GFP

When guts were dissected for looking at endogenous GFP levels, they were kept in the dark at all times during the protocol from the moment of dissection.

Staining for phosphorylated signalling pathway components

In order to prevent dephosphorylation, guts were kept in phosphatase inhibitor (PhosSTOP, Roche) until removal of the primary antibody. Tablets were dissolved at a 10X concentration and appropriate amounts were diluted for each staining step. This was done according to the recommended protocol on the antibody suppliers' websites.

Table 3: Immunofluorescence staining reagents

Reagent	Dilution	Company and Cat number	Storage
Primary antibodies			
Rabbit anti-pH3	1/1000	Merck 06-570	Fridge
Chicken anti-GFP	1/2000	Abcam AB13970	Fridge
Rabbit anti-β-galactosidase	1/500	Invitrogen A11132	Fridge
Guinea Pig anti-MTf	1/500	(Tiklová et al., 2010)	Fridge
Mouse anti-prospero	1/100	DSHB MR1A	Fridge
Mouse anti-Coracle	1/250	DSHB C566.9	Fridge
Mouse anti-Delta	1/10 – 1/50	DSHB C594.9B	Fridge
Mouse anti-NICD	1/100	DSHB C17.9C6	Fridge
Mouse anti-NECD	Dilution series	DSHB C458.2H	Fridge
Rabbit anti-collagen IV	1/500	Abcam AB6586	Fridge
Rabbit anti-phospho-p44/42 MAPK	1/100	Cell Signal 4370S	-20°C
Rabbit anti-phospho-SAPK/JNK	1/100	Cell Signal 4668S	-20°C
Rabbit anti-phospho-Smad3	1/250	Abcam AB52903	Fridge
Secondary antibodies			
Goat anti-chicken Alexa488	1/500	Invitrogen A-11039	Fridge
Goat anti-mouse Alexa488	1/500	Invitrogen A1101	Fridge
Goat anti-guinea pig Alexa555	1/500	Invitrogen A21435	Fridge
Goat anti-mouse Alexa546	1/500	Invitrogen A11030	Fridge
Goat anti-rabbit Alexa555	1/500	Invitrogen A21428	Fridge
Goat anti-mouse CF568	1/500	Biotium 20100	-20°C
Other			
PhosSTOP phosphatase inhibitor	1X	Merck Roche 4906845001	Fridge
DAPI	1/2000	Fisher D1306	-20°C
PBS	n/a	Fisher BP2944	Bench top

16% PFA aliquots	n/a	Fisher 11490570	-20°C
BSA	n/a	Fisher BP1600	Fridge
NGS	n/a	Fisher 31872	-20°C
Triton X-100	n/a	Fisher 10102913	Bench top
VectaShield antifade mounting medium	n/a	Vectorlabs H-1000-10	Fridge

2.6.2 Microscopy and image analysis

Images of the posterior midgut were taken right next to the midgut-hindgut junction (**Figure 12**) using a Leica LSM SP5 confocal microscope. The imaged area was kept consistent due to differences in tissue structure, stem cell number, and gene expression found along the gut (Marianes & Spradling, 2013). Bidirectional z stacks of the epithelial layer of the gut were taken (0.88 µm apart) at 200 Hz, 1024x1024 pixels and with a line average of 3, using the 63x objective with a Zoom of 1.2x. The image files were stored as .tif files. Laser settings, gain, and offset were kept the same within each experiment.

Images used for cell counting were converted into composite maximum intensity z projections and then quantified using Fiji ImageJ (Schindelin et al., 2012). The cell numbers were counted using unedited images (with original fluorescence intensity). After analysis, example images with the most representative cell numbers were chosen as representative images and, where necessary, the brightness and contrast were enhanced using the Auto function in Fiji ImageJ to make staining easier to view.

Mean fluorescence intensity was calculated as an initial analysis by drawing as large a rectangle as possible within each gut and using the Fiji measure function for mean grey value. This does not however take into account the cell density or fluorescence intensity per cell.

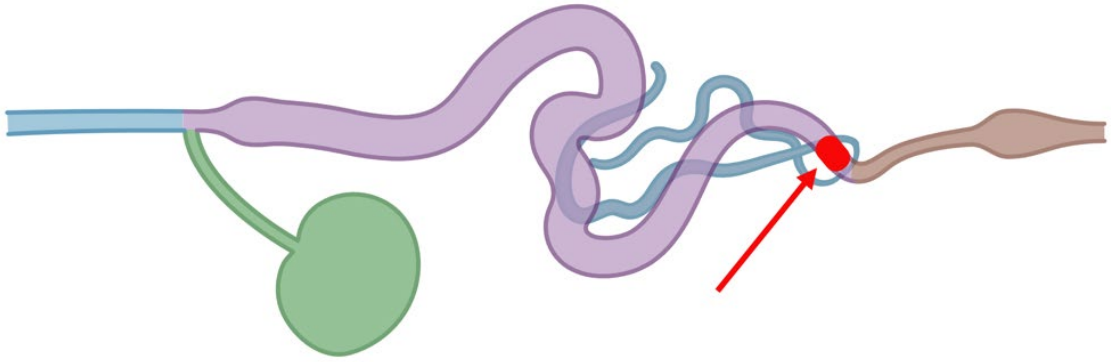

Figure 12: Schematic of the Drosophila gut to show the region that was analysed.

Unless stated otherwise, all images were taken of the posterior midgut epithelium, directly next to the midgut-hindgut junction (imaged area shown in red). This figure was made with Biorender.

2.7 Gene expression analysis

2.7.1 Sample collection and preparation

RNA extraction

Samples for RNA extraction were dissected within the same time window as those for staining. 10 guts were dissected per sample. Experiments for knockdown validation (driven by ubiquitous *tubGAL4^{ts}*) contained whole guts (crop, cardia, whole gut excluding ampula, Malpighian tubules), while all other samples contained only the midgut (excluding crop, cardia, tubules, and hindgut). Samples were either processed immediately or stored at -80°C.

A kit was used to extract the RNA (NEB Monarch Total RNA Miniprep Kit, T2010S). Guts were dissected and homogenised in 300 µL 1X DNA/RNA protection reagent in low retention microcentrifuge tubes. All kit instructions were followed, including any optional steps. Samples were eluted in 50 µL nuclease-free H_2O. They were measured using a Nanodrop (Fisher, ND1000) to detect the concentration of RNA contained in each sample.

cDNA synthesis

The Ultrascript 2.0 cDNA synthesis kit (PCR Biosystems, PB30.31-10 and PB30.32-10) was used for cDNA synthesis. The maximum RNA volume possible was used for the sample with the lowest concentration of RNA, while the other samples within the same experiment (i.e., any samples that would be compared to each other) were added at a ratio of RNA and nuclease-free H_2O in order to give the same concentration of RNA. The samples were incubated at 55°C for 30 minutes and then at 95°C for 10 minutes. An aliquot of 1/5 diluted cDNA was made and all cDNA samples were stored at -20°C.

2.7.2 RT-qPCR

RT-qPCRs were performed using Power SYBR^{TM} Green PCR Master Mix (Fisher, 10658255) on a CFX Connect Real Time System (Bio-Rad, CFX Connect) and a CFX Duet Real Time PCR System (Bio-Rad, CFX96) machine. Each well contained 10 µL made up of 1 µL 1/5 cDNA sample and 9 µL master mix (5 µL SYBR Green, 0.5 µL L + R primer mix, and 3.5 µL nuclease-free H_2O). Plates were pipetted on ice, pipette-mixed, and centrifuged in a plate spinner.

The PCR machine was set as follows: 95°C for 10 minutes, followed by 40 cycles of [95°C for 15 seconds and 60°C for 60 seconds]. This was followed by melt curve calculation to test for correct primer function.

All samples were compared to a housekeeping gene (GAPDH, Actin5C, or rp49) and a standard curve of sequential 1/5 dilutions starting with undiluted samples was used to check primer function. CantonS flies of mixed ages were used for the wild-type expression analysis standards, while guts from the driver lines were prepared for each type of knockdown/overexpression experiment. All samples fell within the standard curve, and housekeeping gene expression levels were compared between control and treated samples to detect large fluctuations.

All primers were ordered from Integrated DNA Technologies. Primer sequences were selected from the FlyPrimerBank (Y. Hu et al., 2013). Whenever possible, exon-spanning primers were used. All primer sequences are listed in **Table 5**.

Table 4: RT-qPCR reagents

Reagent	Company and Cat number	Storage
Ethanol, molecular grade	Fisher BP2818-500	Cabinet
Nuclease-free water	Fisher 10336503	Bench top
Monarch total RNA miniprep kit	NEB T2010S	Bench top
Ultrascript 2.0 cDNA synthesis kit separate oligos	PCR Biosystems PB30.32-10	-20°C
Ultrascript 2.0 cDNA synthesis kit	PCR Biosystems PB30.31-10	-20°C
Power SYBR™ Green PCR Master Mix	Fisher 10658255	-20°C

Table 5: Primers sequences used in this thesis

Gene name	Forward primer	Reverse primer
Actin5C	5' – TTG TCT GGG CAA GAG GAT CAG – 3'	5' – ACC ACT CGC ACT TGC ACT TTC – 3'
Adgf-A2	5' – AGC CGT CAT GCT TTG TGT AAT – 3'	5' – CCT CGG ACG TAA GAT TGG ACA – 3'
Dad	5' – GAG TGT GCA AAG TGA TGC – 3'	5' – CTC ATG CTC AGA AGT TCA GCC CTA – 3'
E(spl)mβ-HLH	5' – AGC ATC GCT GAG AGT TTC CG – 3'	5' – CCG AGA TCC ACA CTC ACT CC – 3'
E(spl)m3-HLH	5' – GTT GAC CGT GGA TCA CAT GAG – 3'	5' – CGG TAC TGG TTG AGG TGG G – 3'
E(spl)m5-HLH	5' – TGG TTT CTT CGA CTG GCT TG – 3'	5' – CCA GAC TTC TGT TAC AAC CTC CA – 3'
E(spl)m8-HLH	5' – GCT GTG AGA TCC GGA GGA G – 3'	5' – AAT TCC ACG AAG CAC AGT CC – 3'
GAPDH	5' – CCA ATG TCT CCG TTG TGG A – 3'	5' – TCG GTG TAG CCC AGG ATT – 3'
LanA	5' – GGG CTC TGC TAG TAA TCC TGG – 3'	5' – CAC ACG TAG CTG TGG CAT AAA T – 3'
LanB1	5' – CTC GCC GGA GAG ATT CTG C – 3'	5' – TTG TAC GGA TCA TGC TTG GTC – 3'

LanB2	5’ – GGC CAC AGA AAT GTC TGC CA – 3’	5’ – CTG CTC ACC ACA GGT ATT AGT TG – 3’
Mesh	5’ – AGC CCG ATC AAT ACT CAG GA – 3’	5’ – CCA TAT ACC AGG CCA GAG GA – 3’
Miple1	5’ – ATC CGT GGA CTG AGT GTG ACA – 3’	5’ – TTC TGA ATG GTT CGC GTT TGG – 3’
Miple2	5’ – ATA CTG GCT TTA ACC ACG GCT – 3’	5’ – ACG TAT GCC ATC AGA AAG GCT – 3’
Npc2a	5’ – GGC GGA GTG CAT CCT CAA G – 3’	5’ – CGT GGA CGA CTG TCT TCA CC – 3’
Plod	5’ – AAA ATC AAA GTG TTC ACT GTG GC – 3’	5’ – AGG GTG GTT ACC TCA ATA TCG T – 3’
Pnt	5’ – CTA CGA GAA GCT GAG TCG CG – 3’	5’ – TAT CGT TTG CCT GCC GTC TT – 3’
Puc	5’ – GCC ACA TCA GAA CAT CAA GC – 3’	5’ – CCG TTT TCC GTG CAT CTT – 3’
rp49	5’ – ATC GGT TAC GGA TCG AAC AA – 3’	5’ – GAC AAT CTC CTT GCG CTT CT – 3’
Socs36E	5’ – ATG GGT CAT CAC CTT AGC AAG T – 3’	5’ – TCC AGG CTG ATC GTC TCT ACT – 3’
SPARC	5’ – CCA GGC CTC TAG GGA GTT TT – 3’	5’ – CAT CGA TGT CGG ACA GGT CG – 3’
Ssk	5’ – CAC TGG ATG CCA CAC CAT T – 3’	5’ – TGG TGT CGC ACA GCT CTC – 3’
Timp	5’ – GAG TCC TTC GCA AAT CGG ATA C – 3’	5’ – GCT TCG GAT GTA GCC TTG TAG G – 3’
Tsf2	5’ – AGC CTC GTT TTT GTG GCT CTA – 3’	5’ – TGT GCT CAT CGT AGT GAT GTT G – 3’

2.8 Human tissue culture

This work was done in collaboration with the laboratories of Professor Rakesh Heer (Newcastle University, Imperial College London) and Professor Craig Robson (Newcastle University).

2.8.1 Patient material

All surgical specimens were collected according to local ethical and regulatory guidelines and included written, informed patient consent (Newcastle REC 2003/11 and Human Tissue Authority License 12 534, Freeman Hospital, Newcastle upon Tyne, United Kingdom).

2.8.2 Spheroid formation

Induced human pluripotent stem cells (iPSCs), derived from the prostates of patients with benign prostatic hyperplasia (Hepburn et al., 2020), were washed with PBS, then incubated in 1 mL of dissociation reagent (Accutase Reagent) for 5 minutes at 37°C. The cells were then detached and suspended by addition of 1 mL of stem cell medium (mTeSR medium) and gentle pipetting, after which they were transferred into a 15 mL conical tube and centrifuged for 5 minutes at 300g. The supernatant was removed and the cells were resuspended in 1 mL of mTeSR medium. An apoptosis inhibitor (ROCK inhibitor Y-27632) was added at 30 µg/mL. A cell count was performed in a haemocytometer using Trypan Blue. The concentration was adjusted to a density of 1000 cells/well in 100 µL of mTeSR1 medium with ROCK inhibitor.

The cells were plated on a round bottom, ultra-low attachment plate and the outer wells were excluded to avoid any edge-effect. The plate was then centrifuged at 300g at 20°C for 10 minutes, after which it was incubated at 37°C with 5% CO_2 and 95% humidity.

The medium was changed every day. The day after the plate was set up was counted as day 0 as this is when the treatment started. Half of the wells were kept on the same mTeSR medium as a control, while the other half were treated with 100 ng/mL Activin A and 1X B27 in RPMI 1640 medium (with 1% Penicillin-Streptomycin and 1% GlutaMAX supplement) to induce endoderm differentiation.

The same three spheroids per condition were imaged on day 0, 1, 3 and 5 using a VisiCam microscope camera.

2.8.3 Spheroid RT-qPCR sample collection

Ten spheroids per sample were combined. The GenElute Mammalian Total RNA Miniprep Kit (Merck, RTN350-1KT) was used for RNA extraction and all optional steps were followed. The samples were eluted in 20 µL. cDNA synthesis was carried out separately by a technician.

2.8.4 Immunohistochemistry

Day 1

Formalin-fixed, paraffin-embedded slides with endodermal spheroids and with human prostate tissue were prepared by a technician.

The slides were de-paraffinated by being placed in xylene for 5 minutes, followed by 15 dips in a second pot of xylene. Then the slides were hydrated by 15 dips each in 100% ethanol, 100% ethanol, 100% ethanol, 95% ethanol, 70% ethanol and 50% ethanol, after which they were placed in running tap water. Antigen retrieval was carried out in a decloaking chamber at 121°C, after which the slides were once again placed in running tap water. They were then placed in a 3% H_2O_2 solution for 10 minutes to remove endogenous peroxidase activity, after which the slides were placed in running tap water for 5 minutes and then in Tris-Buffered Saline (TBS) while the next step was prepared.

The tissue on the slides was outlined with a hydrophobic marker to contain the reagents on the slides, after which the outlined area was covered with horse serum for blocking for 20 minutes and the slides were placed on a tray containing dampened tissues to prevent them from drying out. After blocking, the slides were washed with running tap water for 5 minutes and then placed in TBS while the primary antibody mix was prepared. The antibody dilutions (**Table 6**) were made up in TBS and pipetted onto the slides. The slides were placed on the slide tray with the dampened tissues at 4°C overnight. No-primary-control slides had blocking serum pipetted onto them instead of antibody mix.

Day 2

The slides were washed with TBS for two sets of 5 minutes on a shaker. The anti-rabbit detection kit was applied and the slides were left on the slide tray for 30 minutes, after which they were rinsed with running tap water for 10 minutes and then places in TBS.

The tissue was then stained with 3,3'-Diaminobenzidine (DAB, 1 drop of chromogen in 1 mL diluent) in the fume hood for 5 minutes, after which the excess was poured into sodium hypochlorite solution and the slides were placed in running tap water for 5 minutes.

The slides were then counterstained. They were placed in Gills II Haematoxylin for 15 seconds and then rinsed in tap water until the water ran clear. They were then placed in Scott's tap water for 30 seconds and then back into running tap water.

The slides were then dehydrated with 15 dips each in 50% ethanol, 70% ethanol, 95% ethanol, 100% ethanol, 100% ethanol, 100% ethanol, xylene, xylene, xylene, and then left in xylene until mounted in DPX.

The slides were then imaged by a technician, and images were captured using the Aperio Imagescope software Version 12.4.6.

Table 6: Mammalian experiments reagents

Reagent	Dilution	Company and Cat number	Storage
Spheroid work			
Accutase Reagent		gibco A1110501	-20°C
mTeSR medium		STEMCELL Technologies 85857	Fridge
ROCK inhibitor Y-27632		STEMCELL Technologies 72304	-20°C

Activin A		STEMCELL Technologies 78132.1	-20°C
B27		gibco 17504044	-20°C
RPMI 1640 medium		gibco 61870036	Fridge
GenElute Mammalian Total RNA Miniprep Kit		Merck RTN350-1KT	Bench top
Immunohistochemistry work			
Rabbit anti-MFi2/MTf	1/50	Abcam AB303514	-20°C
Rabbit anti-Laminin γ1	1/200	Abcam AB233389	-20°C
ImmPRESS HRP horse anti-rabbit IgG polymer detection kit, peroxidase	n/a	VectorLabs MP-7401-50ML	Fridge
DAB substrate kit	n/a	Abcam AB64238	Fridge

2.9 Statistical analysis

All statistical analysis was done using Graphpad Prism Version 9 and 10. P values of less than 0.05 were considered as significant, while values slightly above 0.05 were highlighted as non-significant trends where appropriate.

2.9.1 Cell counts

The distribution of the three different replicates, with each replicate containing at least 5 guts, was looked at to ensure that inter-replicate variation did not affect the significance. All replicates were grouped together for statistical analysis.

Outliers were identified using the ROUT method (robust regression and outlier removal) with Q=1% which can identify multiple outliers at once (to prevent masking). If a data point was identified as an outlier, the other values from that gut were also excluded (i.e., cell counts per FOV, %GFP^+ cells, and %$pros^+$ cells). Once outliers were removed, cell counts were tested for Gaussian distribution using the D'Agostino & Pearson test.

When comparing two groups, the unpaired t test was used for normally distributed data and the Mann Whitney test was used for non-normally distributed data. For three or more data sets, the ordinary one-way ANOVA (with Holm-Šídák's multiple comparisons test) and the Kruskal-Wallis test (with Dunn's multiple comparisons test) were used as parametric and nonparametric tests, respectively.

The results were graphed as violin plots that show the range from the minimum to maximum points, with the median and quartiles marked by lines. Cell count results in-text were given as the mean ± standard error of the mean (SEM).

2.9.2 Lifespans and Smurf assays

Lifespans were set up with a minimum of 300 flies per condition. The flies were marked as censored if they escaped or died due to reasons unrelated to the treatment, e.g. being trapped between the stopper and vial, or getting stuck to the food while still alive.

The survival curves were compared using the log-rank (Mantel-Cox) test as this treats deaths at each timepoint as equally important, unlike the Gehan-Breslow-Wilcoxon test, which gives more weight to deaths that occur earlier in the lifespan. As it is not known if the genes act differently throughout the flies' lifespan, using the Gehan-Breslow-Wilcoxon test would place more importance on early effects and might mask effects later in life. The graphs show the % survival, with censored data indicated on the graphs.

The proportions of Smurf flies were compared between control and treated flies for each timepoint using the chi-square test. The graphs display the proportion of Smurf flies out of the total population alive at the time.

2.9.3 RT-qPCRs

All RT-qPCRs were run with 5 or 6 separate biological replicates. Each sample was run multiple times as a technical duplicate or triplicate on the same plate. Technical replicates of the same sample were compared to identify intra-sample outliers if the spread within a sample was too wide. Outliers across replicates were identified using the ROUT method. If any samples were outliers, their corresponding control/treated samples from the same replicate were also excluded. Housekeeping gene expression between the control and treated samples were compared to ascertain that they were less than one cycle in difference. The results were also tested for Gaussian distribution using the D'Agostino & Pearson test ($n \geq 5$) or the Shapiro-Wilk test ($n < 5$).

For each replicate and condition/timepoint, the average gene of interest (GOI) SQ value was divided by the average housekeeping gene (HKG) SQ to give a GOI/HKG value for each

replicate. SQ values were calculated by comparison and normalisation to the standard curve. Statistical significance was calculated by comparing GOI/HKG values for each timepoint/condition, using the unpaired t test or the ordinary one-way ANOVA (with Holm-Šídák's multiple comparisons test) as parametric tests, and the Mann Whitney test or the Kruskal-Wallis test (with Dunn's multiple comparisons test) as the nonparametric equivalent.

SQ value analysis was plotted for samples comparing young and old expression. When comparing knockdown or overexpression experiments, the ΔΔCt method was used to calculate the relative fold change in expression and this value was used for graphs and in-text descriptions, while SQ analysis was used to calculate the statistical significance of the result.

Chapter 3: Changes in expression of intestinal stem cell-secreted protein-encoding genes with age

3.1 Introduction

Intestinal ageing is accompanied by an extensive set of changes, both on the cellular and the tissue level, as well as in the microbiota. As has been described above in Chapter 1, both in mammalian and in *Drosophila* intestinal epithelia there are changes in gene expression, dysregulation of protein synthesis and DNA damage repair, dysbiosis, and stem cell hyperproliferation (López-Otín et al., 2013). *Drosophila* ISCs also become misregulated with age (reviewed by Jasper, 2020; Rodriguez-Fernandez et al., 2020), but the role of ISC-derived signals has not been fully explored. Genes that might be involved in ISC misregulation with age and in midgut homeostasis are of particular interest. The results described below were an initial experiment to characterise which genes change with age by looking at midgut gene expression. The targets that were chosen are part of a list of genes expressed by stem and progenitor cells (Doupé et al., 2018) and were also looked at in the preliminary RNAi screen, some of which showed significant changes in midgut homeostasis upon knockdown (**Figure 8**).

3.1.1 Chapter aim

The aim of this chapter is to identify which of the stem/progenitor-secreted factors change expression with age in order to prioritise candidate regulators that may impact both normal homeostasis and ageing.

3.2 Results

Six different replicates of CantonS flies were set up from separate bottles. The midguts of age-matched, mated CantonS females without gut barrier dysfunction (tested using the Smurf assay for 24h before dissection) were collected for RNA extraction and cDNA synthesis. Each sample contained 10 midguts. Flies were dissected on day 10, day 30 (± 1 day), and day 51 (± 1 day). **Table 7** and **Figure 13** show the results of SQ analysis comparing each timepoint.

Several genes showed a significant change in expression between the three timepoints:

Laminin A (*lanA*) showed a significant increase in mRNA expression levels at day 51, with a 70.0% increase in expression between day 10 and day 51, and a 54.8% increase from day 30 to 51 (**Figure 13B**). Similarly, LanB1 increased by 46.9% from day 10 to day 51, and by 56.1% from day 30 to day 51 (**Figure 13C**).

Niemann-Pick type C-2a (*npc2a*) showed a significant increase of 52.4% between day 10 and day 51, with smaller, non-significant increases from one timepoint to the following (**Figure 13G**).

Procollagen lysyl hydroxylase (*plod*) (**Figure 13H**) showed a significant decrease from day 10 to day 30 (-24.8%), followed by a significant increase from day 30 to day 51 by 56.1%.

Transferrin 2 (*tsf2*) showed significantly increased expression at day 51, with a 61.3% increase from day 10 and a 70.0% increase from day 30 (**Figure 13K**).

An additional set of genes showed trends in gene expression change that were not significant:

Adenosine deaminase-related growth factor A2 (*adgf-A2*) showed an increase of over 40% increase from day 10 to both of the following two timepoints (**Figure 13A**).

Midkine and pleiotrophin 1 (*miple1*) showed a non-significant increase of 34.3% between day 10 and day 51 (**Figure 13E**).

Miple2 had lower expression at day 30 than at day 10 or day 51, but the changes were not significant (**Figure 13F**).

The rest of the genes tested showed no clear trend or significant difference between the timepoints.

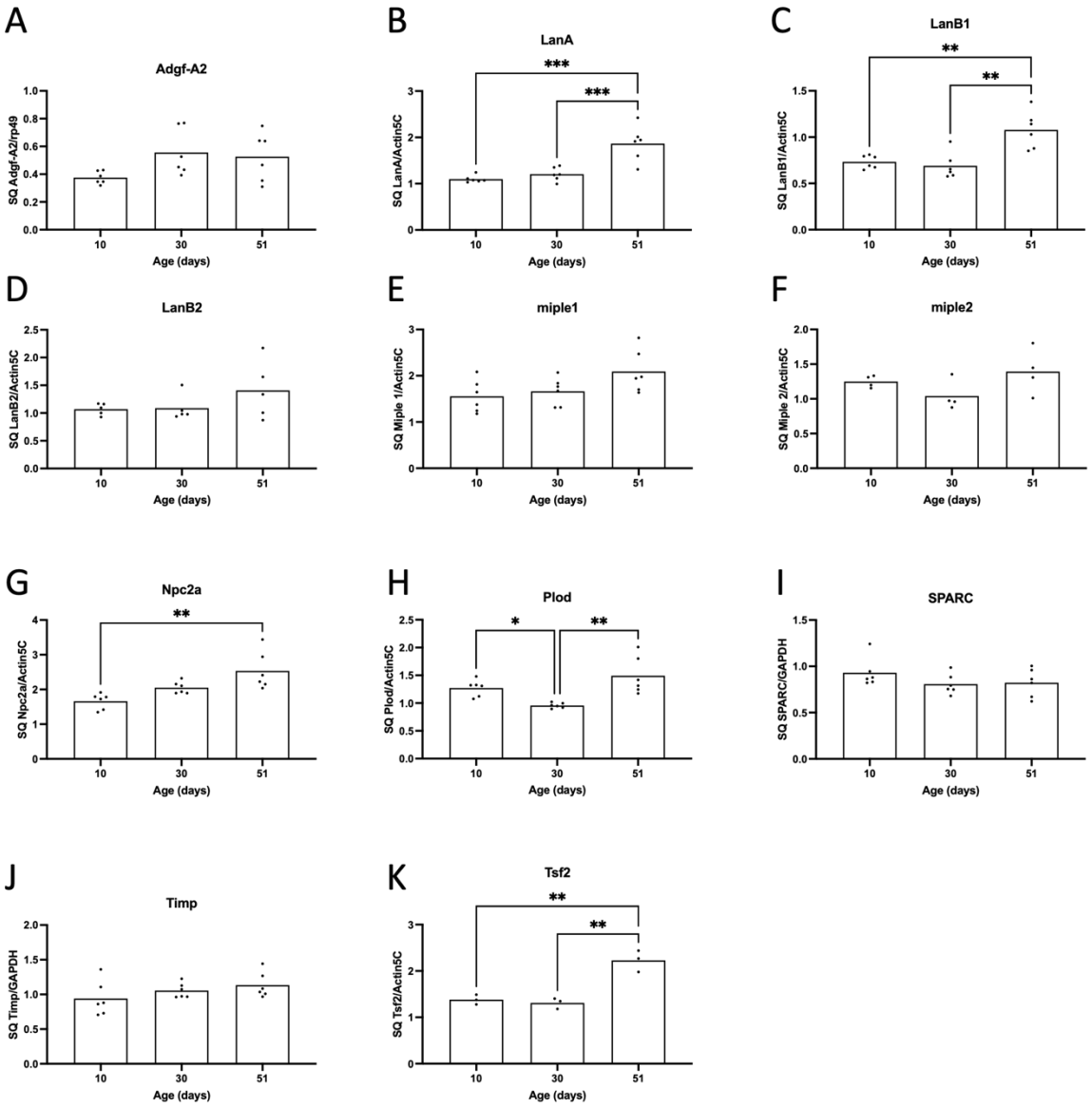

Figure 13: Changes in mRNA expression levels in the Drosophila midgut with age.

Normalised expression levels of Adgf-A2, LanA, LanB1, LanB2, miple1, miple2, Npc2a, Plod, SPARC, Timp and Tsf2 in CantonS midguts on day 10, day 30 (±1) and day 51 (±1) compared to housekeeping gene expression, Actin5C (B-H,K), GAPDH (I,J), and rp49 (A). The bars show mean SQ values of gene of interest/housekeeping gene. Statistical analysis was carried out using the ordinary one-way ANOVA test with Holm-Šídák's multiple comparisons for normally distributed data (Adgf-A2, LanA, LanB1, Miple1, Miple2, Npc2a, Plod, Timp, Tsf2), while the Kruskal-Wallis test with Dunn's multiple comparisons was used for non-normally distributed data (LanB2, SPARC). n=10 midguts/sample, 3-6 replicates. No = ns, *p<0.05, **p<0.01, ***p<0.001.*

Table 7: Changes in mRNA levels in the Drosophila midgut with age.

Normalised expression levels of the genes listed above, comparing day 10, day 30 (±1), and day 51 (±1) mRNA levels. The p-values are listed, all significant changes are in bold. The ordinary one-way ANOVA test with Holm-Šídák's multiple comparisons was used for normally distributed data (Adgf-A2, LanA, LanB1, Miple1, Miple2, Npc2a, Plod, Timp, Tsf2), while the Kruskal-Wallis test with Dunn's multiple comparisons was used for non-normally distributed data (LanB2, SPARC). n≥3.

Gene	Day 10 to 30	Day 10 to 51	Day 30 to 51
Adgf-A2	+48.1% p=0.1305	+40.2% p=0.1690	-5.3% p=0.7251
LanA	+9.8% p=0.4430	**+70.0%** **p=0.0002**	**+54.8%** **p=0.0005**
LanB1	-5.9% p=0.6198	**+46.9%** **p=0.0021**	**+56.1%** **p=0.0012**
LanB2	+1.7% p>0.9999	+31.4% p>0.9999	+29.2% p=0.7737
Miple1	+6.8% p=0.6337	+34.3% p=0.0792	+25.7% p=0.1325
Miple2	-16.7% p=0.4122	+11.4% 0.4122	+33.8% p=0.1693
Npc2a	+23.3% p=0.0781	**+52.4%** **p=0.0021**	+23.5% p=0.0645
Plod	**-24.8%** **p=0.0436**	+17.5% p=0.0936	**+56.1%** **p=0.0017**
SPARC	-13.2% p=0.5293	-11.6% p=0.8385	+1.9% p>0.9999
Timp	+12.2% p=0.5240	+20.6% p=0.2621	+7.5% p=0.5240
Tsf2	-5.1% p=0.6117	**+61.3%** **p=0.0014**	**+70.0%** **p=0.0013**

3.3 Discussion

The results show that there are changes in expression with age of some of the genes tested above. As several genes showed increased expression, while *plod* decreased in expression at day 30, these results do not seem to be generic changes, as they were not seen with all genes. This suggests there are real changes happening at the transcriptional level of the midgut that are worth studying further.

The genes were part of a set identified by targeted DamID as expressed in ISCs/EBs but not in ECs (Doupé et al., 2018), however the RT-qPCR results described above are not cell type-specific. As the samples consisted of dissected midguts, this may include VM or trachea

wrapped around the gut which cannot be fully removed during dissection. This could result in a dilution of any stem/progenitor-specific changes if the genes are expressed in other cell types, for example a significant downregulation of a gene in stem cells could be masked by high levels of expression in the VM. The results therefore need to be followed up with more in-depth study, including at single cell resolution, as has also been done by (Tauc et al., 2021) and others. Immunofluorescence staining pattern changes with age can also show protein localisation to specific cell types, as can be seen with Tsf2 in **Figure 15**. This would be especially interesting as the results above are looking at changes at the mRNA level, which might not correlate to the same changes at the protein level (Becker et al., 2018).

It would also be interesting to have a geriatric data set (e.g., day 70) to see if there are further changes. Not only would this allow comparison with data sets of other expression analysis papers to show reproducibility, but it may also give a more consistent result for old age, as the data for day 51 is more variable than at day 10 and day 30, which may reflect differences in biological age (health) rather than chronological age (age in days).

Another caveat that must be taken into account when interpreting these data is that the flies were placed on food containing blue dye for 24 hours before dissection. This was required to exclude any flies displaying the Smurf phenotype, because they are known to have altered gene expression compared to age-matched, non-Smurf flies (Rera et al., 2012). As mentioned previously, there may be an effect on lifespan when feeding flies blue food dye, so this must be taken into account.

Several genes had significant changes in expression with age and their functions and potential relationship with ageing are described below.

Npc2a is one of a family of eight NPC2-like proteins in the *Drosophila* genome. It has the highest similarity to the single human NPC2 protein (X. Huang et al., 2007), mutations of which cause the Niemann-Pick type C2 disease which presents as an inability to secrete cholesterol from lysosomes (Naureckiene et al., 2000). Npc2a has a partially redundant role with Npc2b in controlling intracellular sterol distribution in *Drosophila* (X. Huang et al., 2007). Npc2a has also been shown to bind microbial components such as lipopolysaccharide, peptidoglycan and lipoteichoic acid *in vitro*, which has also been seen in vertebrates, and has been implicated in activating the immune deficiency pathway (Shi et al., 2012). *Drosophila*

Npc2c is important for ISC maintenance and division in the adult intestine, as well as for regeneration after *Pseudomonas aeruginosa* (*P.a.*) infection (Neophytou et al., 2023). The study also found that Npc2a knockdown in ISCs and EBs decreases *P.a.* infection-induced mitosis, as well as finding decreased *Npc2a* expression with Npc2c knockdown (Neophytou et al., 2023). Both Npc2b and Npc2c knockdown show a decrease in EE cell number. This was described to be due to lower cholesterol availability causing increased Notch signalling, leading to a shift towards EC differentiation (Obniski et al., 2018). Niemann-Pick type C2 patients suffer from premature death due to increasingly severe neurological symptoms (Naureckiene et al., 2000). Similarly, while *npc2a* mutant flies are viable and fertile, they have a reduced lifespan (X. Huang et al., 2007).

Plod is the ortholog of human Lysyl hydroxase 3, mutations of which cause a connective tissue disorder. Plod is expressed in cells that secrete Collagen type IV in *Drosophila* embryos and larvae, such as haemocytes and the fat body, and is required for Collagen secretion (Bunt et al., 2011; H. Ke et al., 2018). As some tissues show increased Collagen expression with age (Blice-Baum et al., 2019), an increase in Plod expression may be required to facilitate this.

Tsf2 and laminins also showed significant increases in midgut expression between the timepoints. Additionally, their knockdowns resulted in significant changes to midgut homeostasis in the RNAi screen (**Figure 8**), suggesting that they may play important functions in contributing to midgut homeostasis and loss of homeostasis with age. They were therefore selected for further study and are the focus of the following three chapters of this thesis.

Chapter 4: The role of Transferrin 2 in midgut homeostasis and ageing

4.1 Introduction

One of the genes found to be expressed in *Drosophila* stem and progenitor cells with targeted DamID profiling was *Transferrin 2* (Doupé et al., 2018) and it was one of the most significant hits of the ISC/EB-specific RNAi screen carried out previously in adult midguts (**Figure 8**). In addition, RT-qPCR data from the previous chapter suggests that its expression in the gut may change with age (**Figure 13**). While its mammalian ortholog Melanotransferrin has been studied extensively in relation to cancer prognosis, only one study has focused on Transferrin 2 in *Drosophila* and its requirement in development. Its mechanisms of action, both in mammals and in the adult fly, have not yet been clearly defined.

4.1.1 Melanotransferrin in mammalian systems

4.1.1.1 Discovery and structure

Human Melanotransferrin (also known as MTf, MELTF, p97, gp95, MFI2, and CD228) was first discovered as a cell-surface antigen on SK-Mel-28 melanoma cells (Brown et al., 1980; Dippold et al., 1980; Woodbury et al., 1980). It is a monomeric iron-binding glycoprotein (Brown, Nishiyama, et al., 1981) with a similar structure to Transferrin and Lactoferrin (Brown et al., 1982; Rose et al., 1986). It has also been suggested that the structure of MTf may allow it to bind Zinc (Garratt & Jhoti, 1992), although this has not been shown experimentally (Richardson, 2000).

Initially thought to have a transmembrane domain, it was shown that MTf is instead anchored to the cell surface by a glycosyl phosphatidylinositol (GPI) anchor which can be cleaved to release it (Alemany et al., 1993; Food et al., 1994).

A second, shorter transcript of *MTf* with only 6 of the total 16 exons has also been found. This does not contain the GPI anchor sequence and is secreted. It is referred to as soluble MTf (sMTf) to distinguish it from membrane-bound MTf (mMTf or just MTf) (Food et al., 1994).

4.1.1.2 Expression pattern

At first MTf was thought only to be expressed by melanoma cells, but later studies with more sensitive assays were able to detect its expression both by other cancers, e.g., breast (Woodbury et al., 1980), kidney (Brown, Woodbury, et al., 1981; Puzanov, 2022), colon (Duś-Szachniewicz et al., 2015), gastric (Sawaki et al., 2019), pancreatic (Real et al., 1988), and lung cancer (Lei et al., 2020), as well as in foetal tissue, such as colon, lung and umbilical cord (Woodbury et al., 1981) and the small intestine (Alemany et al., 1993; Natali et al., 1987). Some healthy adult tissue expression has been found, e.g., in the liver (Richardson & Morgan, 2004; Sciot et al., 1989; Yamada et al., 1999), in sweat glands in the skin (Natali et al., 1987), in the brain (Rothenberger et al., 1996), in the endometrium (Mao et al., 2023) and chondrocytes and cartilage (Kawamoto et al., 1998), but this is usually at very low levels and heterogeneous (Brown, Woodbury, et al., 1981), with different labs disagreeing about expression in the same tissues.

MTf orthologs have also been detected in a wide range of other animals, such as chimpanzees, rhesus monkeys, dogs, rabbits, mice, chicken, and zebrafish (Suryo Rahmanto et al., 2007b).

The similar structure to Transferrin and iron-binding capability of MTf led to the suggestion that it may have a role in iron homeostasis. While MTf can bind iron and donate it to cells (Kennard et al., 1995), it is not required for iron homeostasis, as changing iron levels does not affect MTf levels, and vice versa (Food et al., 2002; Rahmanto & Richardson, 2009; Richardson, 2000; Sekyere et al., 2006). Several studies have shown that MTf is able to transport iron across the blood-brain barrier *in vitro* and in mice (Food et al., 1994; Jefferies et al., 1996; Karkan et al., 2008; Moroo et al., 2003; Rolland et al., 2009; Rothenberger et al., 1996; Singh et al., 2021), possibly via the low-density lipoprotein receptor-related protein which also transports Lactoferrin (Demeule et al., 2002, 2003), although others have disputed the relevance of this due to low uptake in the brain relative to other tissues (Karkan et al., 2008; Richardson & Morgan, 2004).

4.1.1.3 Disputed role in Alzheimer's disease

The research into the relationship between MTf and the brain showed a potential diagnostic role for MTf in Alzheimer's disease (AD) patients. It was found that sMTf levels were elevated in the serum and cerebrospinal fluid of AD patients (Kennard et al., 1996; D. K. Kim et al., 2001), as were post-mortem MTf antibody staining levels of AD patients compared to normal post-mortem tissue, with expression also localised to the β-amyloid plaques found in AD in the

brain (Jefferies et al., 1996; Yamada et al., 1999). In direct contrast, another lab found that sMTf was not upregulated in the serum of AD patients and disagreed with previous data analysis methods (Desrosiers et al., 2003).

4.1.1.4 Disease treatments

Using a vaccine or antibody treatment against human MTf was successfully able to induce an immune response against MTf in mice and monkeys and was able to reduce tumour growth of syngeneic melanoma cell transplants and their lung and brain metastases in mice (Estin et al., 1988, 1989; S. L. Hu et al., 1988; Rolland et al., 2009). MTf has also been found to stimulate an immune response in cells taken from melanoma patients (Röhn et al., 2005). This suggests that a treatment or detection method based on MTf may be able to be developed for melanomas. Creating an MTf-drug conjugate was shown to increase drug delivery to the brain tenfold to treat glioma growth in the mouse brain (Karkan et al., 2008), while another conjugate showed a 10-15-fold increase in drug delivery and a 68% reduction in breast cancer metastases and reduced tumour growth (Gabathuler et al., 2013; Nounou et al., 2016), but this has so far not been tested on melanomas.

Thom et al determined a peptide chain (called MTfp), taken from the full-length MTf, that is easier to conjugate to other proteins and was still able to traverse the murine blood brain barrier. The MTfp-drug conjugate was shown to induce pain relief in a mouse model of neuropathic pain (Singh et al., 2021; Thom et al., 2018). In addition to making drug conjugates, MTfp has been used to transport siRNA to mouse brains to relieve the symptoms of ischemic strokes (Eyford et al., 2021). An antibody against MTf has also been used for trafficking drugs to MTf-expressing murine tumours (Mazahreh et al., 2023).

4.1.1.5 The effect of mMTf vs sMTf on tumorigenesis

MTf was initially discovered as a melanoma marker, with high expression predicting a poor outcome for patients of multiple cancer types, such as clear cell renal carcinoma and oral squamous cell carcinoma (Puzanov, 2022; Yen et al., 2023). Once studies looked at the difference between mMTf and sMTf it was discovered that they likely have opposing effects on tumour growth. Increasing mMTf expression promotes melanoma and endothelial cell migration and invasion and was found to cause an increase in plasmin production, which plays a key role in cell migration and tumour metastasis; treating these cells with antibodies or RNAi against MTf reduces their migratory capacity as well as plasmin production both *in vitro* and *in vivo* when injected into mice (Bertrand et al., 2007; Demeule et al., 2003). Increased sMTf

has the opposite effect, reducing cell migration and plasminogen activation (Demeule et al., 2003; Michaud-Levesque et al., 2005). mMTf and sMTf also affect the production of new blood vessels by endothelial cells (angiogenesis), which is important for tumour growth of melanoma and other cancers. mMTf promotes angiogenesis, while most studies have found that sMTf reduces it (Michaud-Levesque et al., 2006; Rolland et al., 2007, 2009), although some studies contradict this (Lei et al., 2020; Sala et al., 2002).

While almost all studies found that increased MTf expression by mammalian tumours caused a worse outcome, one study showed the opposite, with higher MTf expression resulting in failed tumour growth when melanomas were injected intravenously into mice (Estin et al., 1989). This implies that the effect of differing MTf expression levels on proliferation can be context-dependent. However, as it is not always defined which version of MTf is being described, or sometimes recombinant truncated proteins of an intermediate size are used, this can possibly result in contradictory outcomes.

4.1.1.6 Potential mechanisms of action

Both *MTf* knockout and overexpression mice have been generated. No phenotypic changes were observed in relation to size, behaviour, reproduction, or iron homeostasis, except for a small decrease in red blood cell number in the overexpression mouse (Dunn et al., 2006; Rahmanto & Richardson, 2009; Sekyere et al., 2006). Changes in gene expression from the knockout mouse and from cell line models with altered *MTf* expression were compared. In the mouse, *MTf* knockout resulted in a down- and upregulation of several genes including *transcription factor 4* (*Tcf4*) (Dunn et al., 2006), and *MTf* knockdown and overexpression in melanoma cells showed similar results (Dunn et al., 2006; Suryo Rahmanto et al., 2007a).

Tcf4 mediates Wnt signalling, and another study using SK-Mel-28 melanoma cells found a link between MTf and N-myc downstream regulated gene 1 (NDRG1), which acts as an epithelial-to-mesenchymal transition (EMT) and metastasis repressor and is also involved in Wnt signalling. High MTf expression downregulates NDRG1 expression, which leads to increased nuclear β-catenin localization and Wnt pathway activation, and vice versa (Paluncic et al., 2023).

Increased mMTf has also been shown to upregulate the EMT marker N-cadherin in lung cancer cells. It does this by reducing Krüppel-like factor 4 (Klf4) expression (Lei et al., 2020) as the transcription factor Klf4 inhibits N-cadherin expression and other prometastatic genes (Tiwari

et al., 2013). The same MTf study found meanwhile that sMTf also increases several EMT-related genes in lung cancer cells, e.g., Twist, Snail, N-cadherin, and Vimentin, which are involved in TGF-β, Wnt, and Notch signalling, and promoted lung cancer cell migration. It did however have an inhibitory effect on migration and angiogenesis of endothelial cells by reducing Matrix Metalloproteinase 9 expression, which in turn resulted in decreased Multimerin-2 (MMRN2) degradation (Lei et al., 2020). The ECM-protein MMRN2 has known angiogenesis-inhibitory functions (Lorenzon et al., 2012). This shows that the ratio of mMTf to sMTf is important and they can have opposing, context-dependent functions.

MTf may have different mechanisms of action in different tissues, as it has also been shown to affect EGFR signalling. In oral squamous cell carcinoma, MTf and EGF expression have a positive correlation and MTf is thought to act via the focal adhesion pathway, as *in vitro* MTf knockdown reduces focal adhesion kinase (FAK) phosphorylation, while MTf-induced proliferation is inhibited by pFAK inhibitor (Yen et al., 2023). FAK is involved in cell migration and invasion and in cancer metastasis (Mitra et al., 2005).

MTf has been implicated in taking part in differentiation in some tissues (McNagny et al., 1996; Suardita et al., 2002). A role in the immune system has even been suggested for MTf in the sea cucumber, where it was found to be induced upon challenge by lipopolysaccharide (Ramírez-Gómez et al., 2008).

4.1.2 Tsf2 in *Drosophila melanogaster*

Mammalian MTf has been associated with a range of cancers, and initial studies looking at potential mechanisms of action have been published, but its role in homeostasis has not been defined. *In vivo* models are required to dissect further how MTf functions and in what way changes in expression could lead to the development of cancer.

4.1.2.1 Tsf2 expression

In *Drosophila*, Transferrin 2 (Tsf2) is the closest ortholog to mammalian MTf. Its role during development was investigated in the hindgut and the trachea. It was shown that Tsf2 is required for development, as loss of function mutants are lethal due to elongated, leaky airways. This can be rescued in 60% of mutant flies by mouse *MTf* cDNA expression, which shows conservation of structure and function between *Drosophila* Tsf2 and mammalian mMTf (Tiklová et al., 2010). No soluble form of Tsf2 has been described so far. The phenotypes of

changes in expression of MTf in mammals compared to changing Tsf2 in *Drosophila* are quite different, however.

During early development (embryonic stage 13) Tsf2 is found at the basolateral sides of ectodermal epithelia, such as the hindgut and the trachea, where it binds iron. This leads to endocytosis and transportation to the apicolateral membrane. It interacts with other septate junction components prior to endocytosis, and together they form septate junctions between cells, with Tsf2 bound to the cell membrane by a GPI anchor. The junctions have fully formed by stage 16 in embryos. This does not occur if the iron-binding domains are removed or if the GPI-anchor is replaced by a transmembrane domain, but an iron-binding, soluble, non-GPI-anchored form is sufficient and can be taken up by cells that do not normally express Tsf2. Other septate junction components require Tsf2 expression for correct localisation, and vice versa (Tiklová et al., 2010).

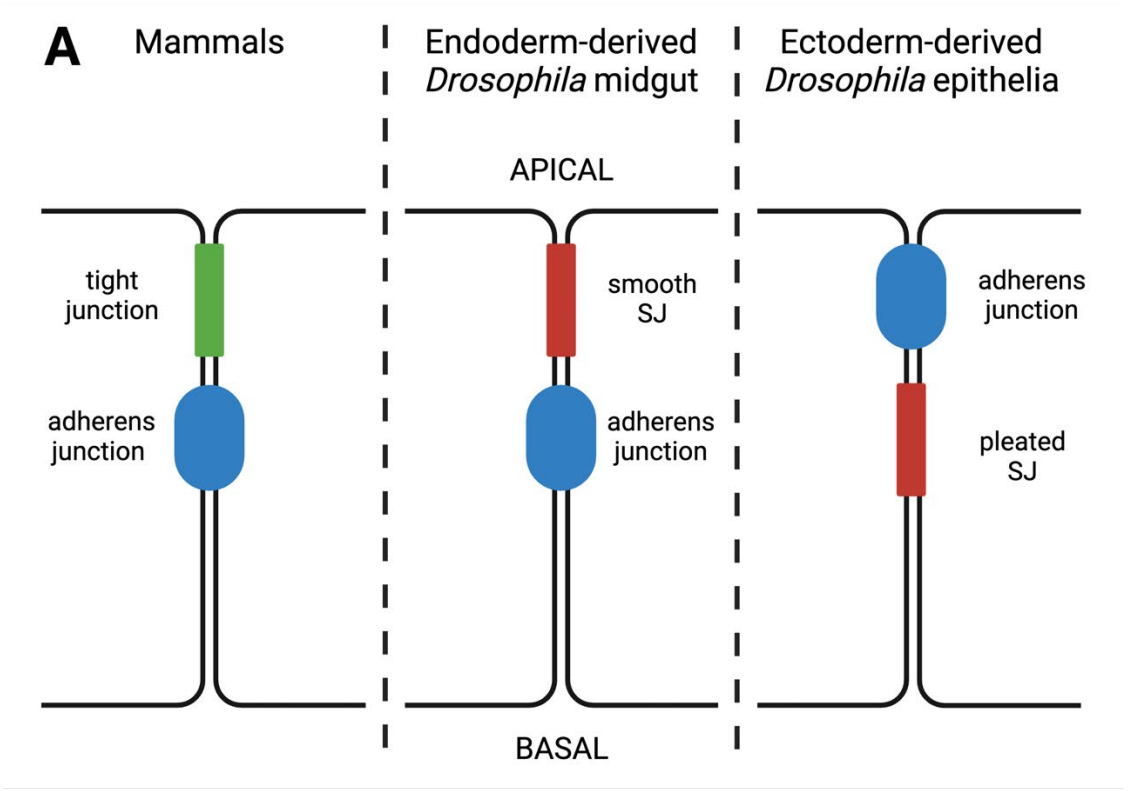

Figure 14: Occluding junction structure.

(A) A basic schematic comparing the location of occluding junctions in mammals (green, tight junctions, left), to apical endoderm-derived smooth septate junctions (SJ) in the Drosophila midgut (red, middle) and more basal pleated septate junctions in other Drosophila epithelia (right). This figure was made with Biorender. (B) Coracle staining (red) is shown surrounding differentiated cells in the Drosophila midgut, while ISCs/EBs are labelled in green. Nuclei are labelled with DAPI in blue. The brightness and contrast have been enhanced for clarity. Scale bar = 30 μm.

4.1.2.2 The function of septate junctions in the intestine

Septate junctions (SJs) act as occluding junctions in *Drosophila* and are the equivalent of mammalian tight junctions. They form a barrier between the lumen and the tissue to prevent luminal contents including the microbiome from moving in an unregulated manner into the epithelium. SJs exist either as pleated SJs (pSJs) in ectoderm-derived epithelia (e.g., foregut, hindgut, trachea), or as smooth SJs (sSJs) in the endoderm-derived midgut as well as in Malpighian tubules. They differ in their shape (wavy versus straight rows, as implied by their names) and in their location on the cell membrane. sSJs, like vertebrate tight junctions, are found apicolaterally close to the apical membrane, whereas pSJs are found more basally in relation to adherens junctions (**Figure 14A**; reviewed by Izumi & Furuse, 2014). SJs can exist either between two adjacent cells as bicellular junctions, or at the meeting point between three cells as tricellular junctions (Noirot-Timothée & Noirot, 1980).

Multiple SJ components have been identified, including but not limited to those listed in **Table 8**. There is some overlap in which components are found in pSJs or in sSJs, while some components are found exclusively in one type of SJ. Furthermore, some SJ members are required specifically in tricellular junctions. Tricellular junctions contribute to stabilizing bicellular junctions during development (Esmangart de Bournonville & Le Borgne, 2020), and loss of the tricellular junction-specific Gli is sufficient to induce barrier dysfunction in the adult intestine of young flies (Resnik-Docampo et al., 2017).

SJs form in adult midguts as the enteroblast progenitor cells are actively differentiating and integrating into the epithelium (J. Chen et al., 2018; J. Chen & St Johnston, 2022; C. Xu et al., 2019). With age, the expression levels of SJ components reduce, leading to a loss of barrier function which precedes death (Clark et al., 2015; Rera et al., 2012). Manipulating different SJ protein levels to simulate ageing causes a range of phenotypes including barrier dysfunction, dysbiosis, shortened lifespan, failed EC differentiation and integration, hyperproliferation, and hypertrophy via both cell-autonomous and non-cell-autonomous effects. Proliferation and signalling are seen before loss of barrier function occurs in SJ knockdowns, as is seen in old age. In reverse, overexpressing SJ components can extend lifespan (Izumi et al., 2019; Resnik-Docampo et al., 2017; Salazar et al., 2018).

In conclusion, a fully functioning gut barrier is integral to maintaining homeostatic proliferation and differentiation rates. If changing Tsf2 expression levels is affecting SJ

assembly in the midgut, this could therefore indirectly affect ISCs/EBs by inducing signalling pathways and could explain the phenotypes seen in the initial RNAi screen (**Figure 8**).

Table 8: Non-exhaustive list of septate junction components

Name	Gene	Reference
Anakonda/Bark beetle	*Aka/Bark*	(Byri et al., 2015; Hildebrandt et al., 2015)
Ankyrin	*Ank*	(Baumann, 2001)
Big Bang	*Bbg*	(Bonnay et al., 2013)
Boudin	*Bou*	(Hijazi et al., 2009)
Coiled	*Cold*	(Nilton et al., 2010)
Contactin	*Cont*	(Faivre-Sarrailh et al., 2004)
Coracle	*Cora*	(Fehon et al., 1994)
Crimpled	*Crim*	(Nilton et al., 2010)
Crooked	*Crok*	(Nilton et al., 2010)
Discs large	*Dlg*	(Woods & Bryant, 1991)
Fasciclin III	*FasIII*	(Snow et al., 1989)
Gliotactin	*Gli*	(Auld et al., 1995; Genova & Fehon, 2003; Schulte et al., 2003)
Hoka	*Hoka*	(Izumi et al., 2020)
Kune-kune	*Kune*	(Nelson et al., 2010)
Lachesin	*Lac*	(Llimargas et al., 2004)
Lethal giant larvae	*Lgl*	(Strand et al., 1994)
M6	*M6*	(Zappia et al., 2011)
Macroglobulin complement-related	*Mcr*	(Bätz et al., 2014)
Megatrachea/Pickel	*Mega/Pck*	(Behr et al., 2003)
Mesh	*Mesh*	(Izumi et al., 2012)
Na+/K+-ATPase α	*ATPα*	(Genova & Fehon, 2003; Paul et al., 2003)
Nervana 2	*Nrv2*	(Genova & Fehon, 2003; Paul et al., 2003)
Neurexin IV	*NrxIV*	(Baumgartner et al., 1996)
Neuroglian	*Nrg*	(Genova & Fehon, 2003)
Pasiflora 1	*Pasi1*	(Deligiannaki et al., 2015)
Pasiflora 2	*Pasi2*	(Deligiannaki et al., 2015)
Sinuous	*Sinu*	(Wu et al., 2004)
Snakeskin	*Ssk*	(Yanagihashi et al., 2012)
Scribble	*Scrib*	(Bilder et al., 2000)
α-spectrin	*α-spec*	(Baumann, 2001)
β-spectrin	*β-spec*	(Baumann, 2001)
Tetraspanin 2A	*Tsp2A*	(Izumi et al., 2016)
Transferrin 2/ Melanotransferrin	*Tsf2/MTf*	(Tiklová et al., 2010)
Undicht	*Udt*	(Petri et al., 2019)
Varicose	*Vari*	(Wu et al., 2007)
Wunen	*Wun*	(Ile et al., 2012)
Würmchen 1	*Wrm1*	(Königsmann et al., 2020)
Yurt	*Yrt*	(Laprise et al., 2006)

4.1.2.3 Signalling pathways and non-occluding functions affected by SJ components

Along with their function of maintaining the gut barrier, several SJ proteins have been implicated in affecting specific signalling pathways involved in stem cell regulation in a variety of ways. As SJs exist between differentiated cells, component expression is very low in EBs,

increasing as they go through the process of differentiation. RNAi against SJ components Tsp2A, Mesh, Ssk, or Cora driven by the ISC/EB-specific driver *esg^{ts}GFP* however results in an increase in proliferation as well as accumulation of pre-ECs that cannot fully differentiate (C. Xu et al., 2019). Furthermore, it was shown that as well as contributing to SJs, Tsp2A is actively endocytosed and in the process interacts with either aPKC or its cofactor Rack1, which are involved in the Hippo pathway, and then the complex is degraded. Upon *tsp2A-RNAi* expression in either EBs or ECs, this leads to build-up of aPKC in the cells, allowing it to inhibit Hippo signalling. This causes build-up of Yki, which in turn induces the proliferative JAK/STAT pathway in ISCs/EBs. This phenotype is enhanced during regeneration. Tsp2A overexpression however slightly reduces damage-induced proliferation (C. Xu et al., 2019).

Similarly, knockdown of Hoka in adult midgut ECs increases aPKC expression, which leads to increased Ras/MAPK and JAK/STAT signalling and overproliferation. As Hoka, Tsp2A, Mesh, and Ssk form a complex and require each other's correct expression for proper SJ formation, knockdown of one of the components affects the localization of other (Izumi et al., 2021). Indeed, knockdown of Tsp2A, Ssk, or Mesh in EBs or ECs has also been shown to increase overproliferation of the midgut via the Hippo, Ras/MAPK, and JAK/STAT pathways (H.-J. Chen et al., 2020; Izumi et al., 2019; Salazar et al., 2018).

Knockdown of Gli induces many ISC proliferation-regulating pathways, such as JNK, EGFR, Hippo, JAK/STAT, and Wg signalling, as well as causing misdifferentiation (Resnik-Docampo et al., 2017). *Ssk-* or *mesh-RNAi* for up to three days does not seem to induce JNK signalling (H.-J. Chen et al., 2020). This may either be due to different roles for different SJ components, or because Gli knockdown was over a longer period (9 days).

Several SJ proteins have also been implicated in maintaining apical-basal cell polarity in epithelia. In ectoderm-derived tissues, where pSJs lie below AJs, lateral localization of Scrib, Dlg, and Lgl are required for cell polarity, as well as the apical Crumbs, Stardust, and the PAR complex including aPKC (Assémat et al., 2008). Loss of Scrib, Dlg, or Lgl allows the spread of apical markers into the basolateral region, causing a loss of polarity (Bilder et al., 2003).

The role of these polarity factors has been disputed in the endoderm-derived midgut epithelium. While one study found that the PAR proteins are required in ISCs for asymmetric cell division (Goulas et al., 2012), others have instead suggested that they are dispensable, with polarity relying on integrin adhesion and tricellular junctions (J. Chen et al., 2018; Izumi et al., 2019;

Yanagihashi et al., 2012), although another study seems to dispute this (Izumi et al., 2016). Due to loss of tissue integrity as cells cannot form the barrier without SJs, it is difficult to pick apart effects on polarity compared to loss of homeostasis and pseudo-stratification with overproliferation.

The response to SJ knockdown is context-dependent and varies in different types of cells. Cora and Neurexin IV are required in blood progenitor cells to induce Hippo signalling, as they are thought to help recruit Merlin, a component of the Hippo pathway, to the cell membrane in the larval lymph gland. Loss of Cora causes Yki-activated expression of Serrate, a ligand for the Notch receptor, and this induces increased differentiation of the blood progenitor cells rather than increasing proliferation as was seen upon loss of SJ components in other cells (Khadilkar & Tanentzapf, 2019).

Neuroglian (Nrg) acts as a SJ protein in pSJs in the adult hindgut, but shows a different expression pattern in the midgut, where it is localized around *esg*$^{+}$ ISCs/EBs but not around ECs (Baumann, 2001; Resnik-Docampo et al., 2021). This has also been confirmed by single cell RNA sequencing (scRNA-seq) of midgut cell types (Hung et al., 2020). Analysis of homeostasis and age-related increases in proliferation show that although Nrg is not required for ISC maintenance, its expression in EBs is required and sufficient to induce non-cell-autonomous ISC proliferation via the EGFR pathway, either directly or indirectly, and reducing expression in older flies reduces overproliferation (Resnik-Docampo et al., 2021).

4.1.3 Chapter aims

This chapter aims to characterise the expression pattern of Tsf2 and establish whether it has the same function in the adult midgut as has been observed in the developing hindgut. This includes looking at the expression of other SJ components in response to changes in Tsf2 expression, as well as determining whether Tsf2 expression changes affect lifespan and gut barrier function. Further, the role of several signalling pathways in Tsf2-dependent loss of homeostasis will be investigated.

4.2 Results

4.2.1 Tsf2 expression in the midgut

An antibody raised against *Drosophila* Tsf2 (Tiklová et al., 2010) was used to identify its localisation in the posterior midgut. CantonS flies were crossed to *esgsfGFP*, and half of the progeny were dissected on day 7 to act as young homeostatic samples. The midguts were stained for GFP and Tsf2 and z stack images were taken of the posterior midgut. The rest of the progeny were aged at 25°C and dissected at 28 days old, representing an ageing population.

The day 7 samples showed Tsf2 localising around the stem and progenitor cells, as well as around a few other small cells which may be EE cells (**Figure 15**). This distinct localisation of Tsf2 is lost in the older samples, with only background levels visible, comparable to areas of the young midgut that didn't contain ISCs/EBs (**Figure 15**). Three independent replicates were set up and all showed the same results.

The Abcam antibody for human MTf (ab303514) was also tested on *Drosophila* midguts but no staining was visible (data not shown).

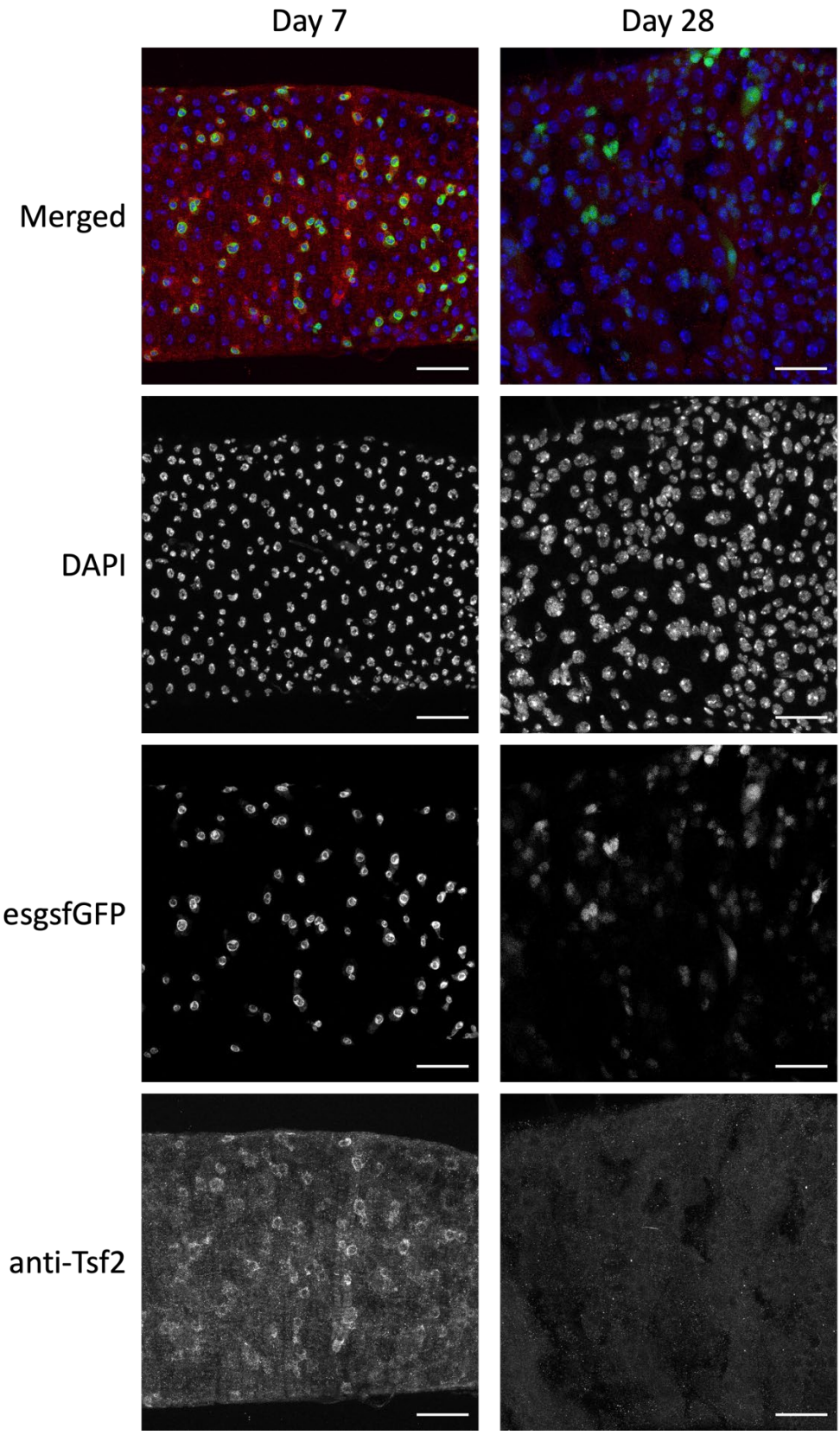

Figure 15: Expression of Tsf2 in young and old posterior midguts.

Representative maximum intensity-projected confocal z stack images with brightness and contrast enhanced for clarity. The images show the posterior midgut of 7-day old and 28-day old CantonS x esgsfGFP flies. Grey-scale images show nuclei (DAPI), ISCs/EBs (esgsfGFP), and Tsf2. Merged images show nuclei (blue), ISCs/EBs (green), and Tsf2 (red). Representative of n=19 across 3 replicates (young), n=12 across 2 replicates (old). Scale bars = 30 μm.

4.2.2 Tsf2 knockdown and overexpression in stem and progenitor cells show opposing effects on midgut homeostasis

The initial RNAi screen only used one RNAi line against Tsf2 (**Figure 8**), leaving open the possibility of off-target effects. In order to rule this out, ISC/EB-specific *esg^{ts}GFP* crosses were set up with three different *tsf2-RNAi* lines to confirm the phenotype: BL65903 (named *Tsf2_RNAi_1*), v330006 (*Tsf2_RNAi_2*) and v5236 (*Tsf2_RNAi_3*). These were compared to the control *luciferase-RNAi* BL31603 (**Figure 16**). *Tsf2_RNAi_1* was set up in a separate set of crosses from *Tsf2_RNAi_2* and *Tsf2_RNAi*_3, indicated by the line separating the knockdown lines in the figures below. Tsf2 knockdown was induced for 7 days at 29°C after ageing the progeny for a week at 18°C. The cell number per field of view (FOV) (**Figure 17A**), the proportion of stem/progenitor cells in the same FOV (**Figure 17B**), as well as the proportion of EE cells (**Figure 17C**) were counted.

Tsf2_RNAi_1 showed a non-statistically significant change in the number of cells per FOV from 343 ± 13 cells (mean ± SEM) to 367 ± 14, whereas *Tsf2_RNAi_2* had a significant increase from 306 ± 14 cells to 375 ± 17 cells, and *Tsf2_RNAi_3* had a significant decrease to 213 ± 11 (**Figure 17A**). The proportion of ISCs/EBs significantly increased for *Tsf2_RNAi_1* from 34.5% ± 1.4 to 39.3% ± 1.3. *Tsf2_RNAi_2* showed no significant difference in % ISCs/EBs with a change from 30.6% ± 0.9 to 32.4% ± 1.2, while *Tsf2_RNAi_3* showed a significant decrease to 23.4% ± 1.9 (**Figure 17B**). The proportion of EE cells increased significantly with *Tsf2_RNAi_1* from 9.5% ± 0.5 to 12.6% ± 0.5, whereas the other two lines showed no significant difference, with *Tsf2_RNAi_2* having 7.5% ± 0.5 and *Tsf2_RNAi_3* having 6.1% ± 0.5 compared to a control of 5.9% ± 0.4 (**Figure 17C**).

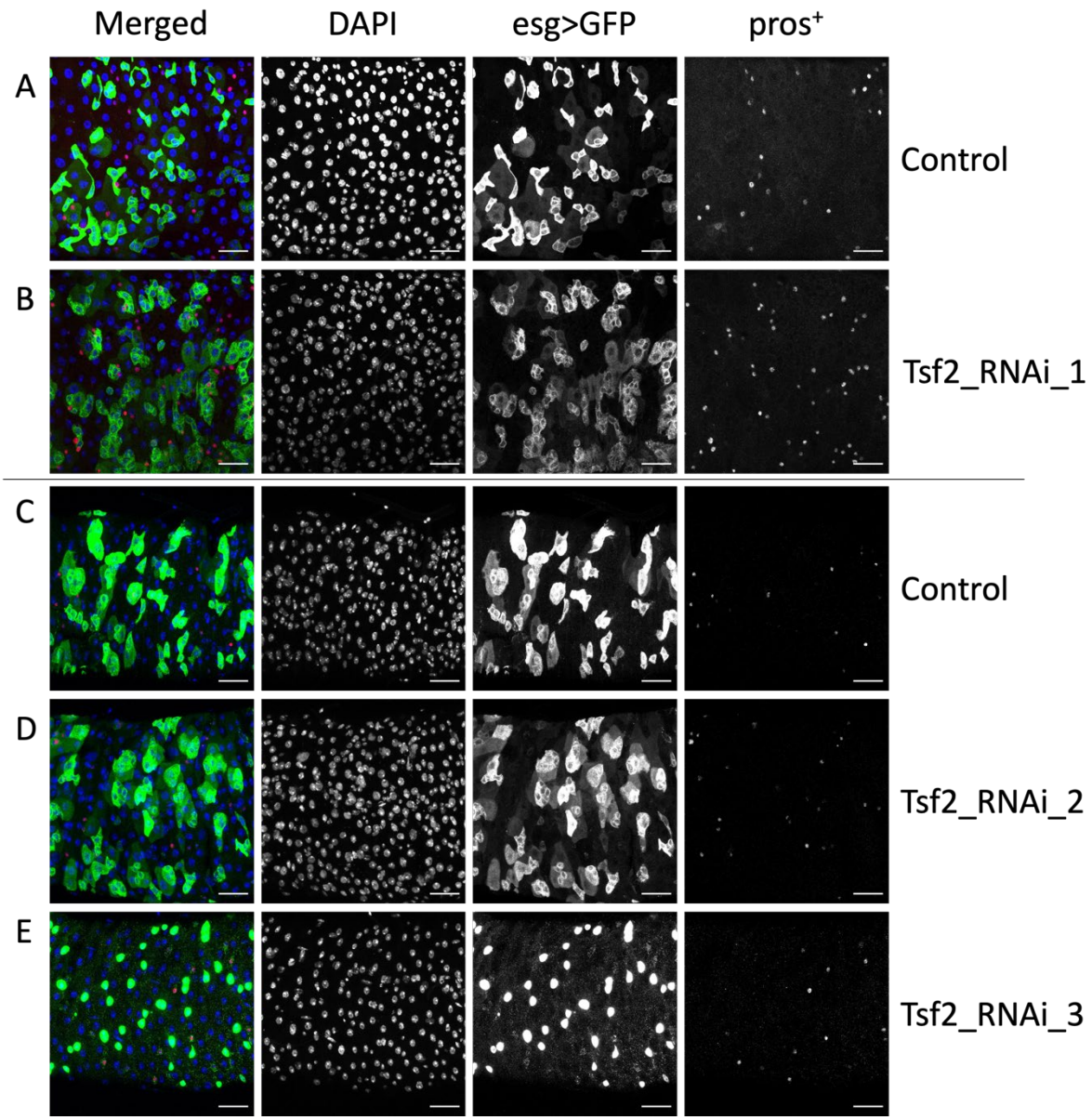

Figure 16: The effect of 7 days of Tsf2 knockdown on cell number and the proportion of stem/progenitor cells and EE cells.

Representative maximum intensity-projected confocal z stack images with brightness and contrast enhanced for clarity of control BL31603 (A,C) and Tsf2 knockdown (B,D,E) lines. C-E were run in a separate set of experiments from A and B. Grey-scale images show cells per field of view (DAPI), ISCs/EBs (esg>GFP), and EE cells (pros^{+}). Merged images show nuclei (blue), ISCs/EBs (green), and EE cells (red). Quantified in the figure below, representative of n≥17. Scale bars = 30 μm.

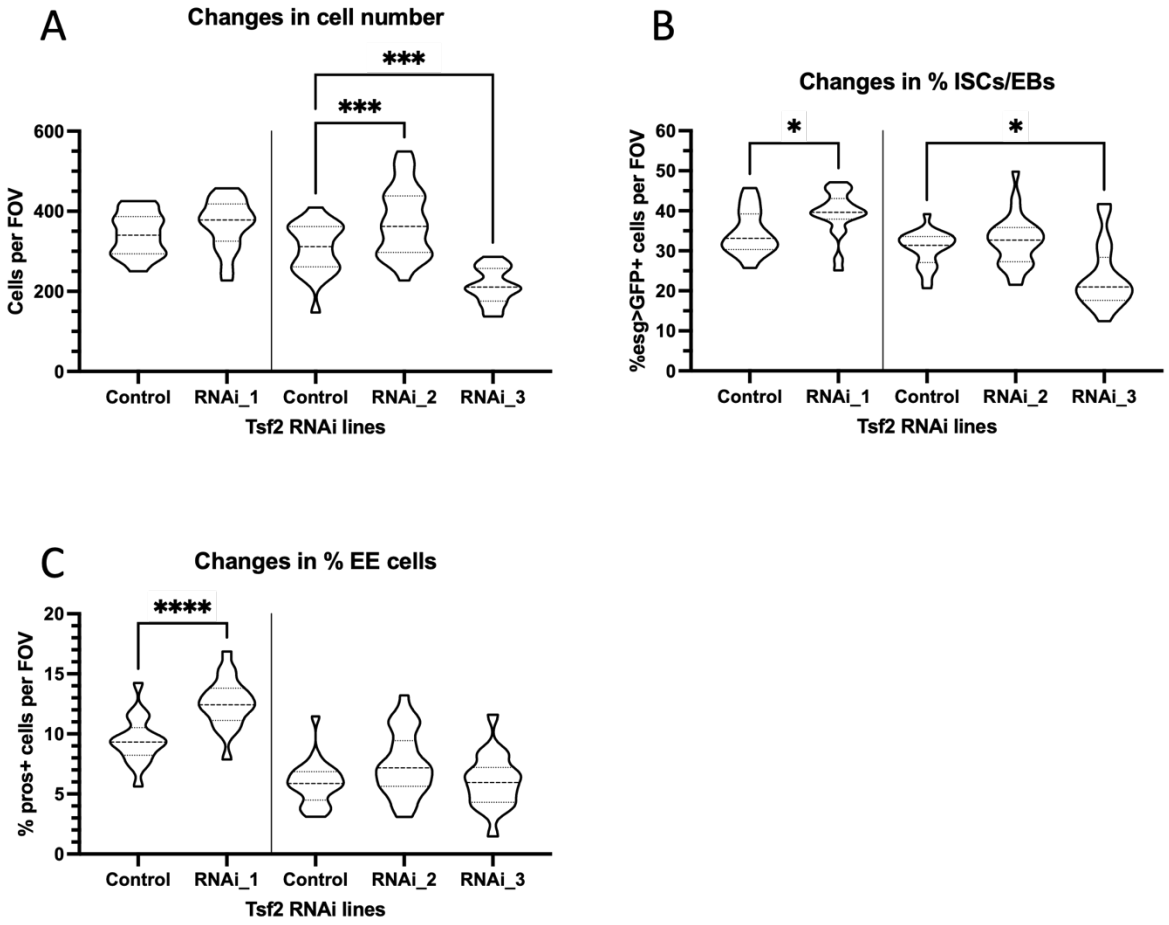

Figure 17: Quantification of the effect of 7 days of Tsf2 knockdown on cell number and the proportion of stem/progenitor cells and EE cells.

Tsf2 was knocked down for 7 days in adult ISCs/EBs using esg^{ts}GFP. Changes in cell number per field of view (A), the proportion of stem/progenitor cells (B), and the proportion of EE cells (C) have been quantified. Tsf2_RNAi_2 and 3 were run separately with their own control, denoted by the vertical line separating them. The plotted lines represent the median and quartiles. Panel A was calculated using an unpaired t test (Tsf2_RNAi_1) and an ordinary one-way ANOVA with Holm-Šídák's multiple comparisons (Tsf2_RNAi_2 and 3). Panel B was calculated using a Mann-Whitney test and a Kruskal-Wallis test with Dunn's multiple comparisons test. Panel C was calculated using an unpaired t test and a Kruskal-Wallis test with Dunn's multiple comparisons test. n≥17 guts from 3 separate replicates. No = ns, *p<0.05, **p,0.01, ****p<0.0001.*

To complement the knockdown approach, Tsf2-GFP (Tiklová et al., 2010) was also overexpressed and compared to a control of *UAS-lacZ* expression (**Figure 18**). The number of cells per FOV did not change significantly (296.6 cells ± 24.7 to 293.1 ± 23.6) (**Figure 19A**), whereas the %ISCs/EBs significantly decreased from 39.3% ± 1.8 to 31.7% ± 0.9 (**Figure 19B**). The control %EE was 8.3% ± 1.0 which changed non-significantly to 7.3% ± 0.6 (**Figure 19C**).

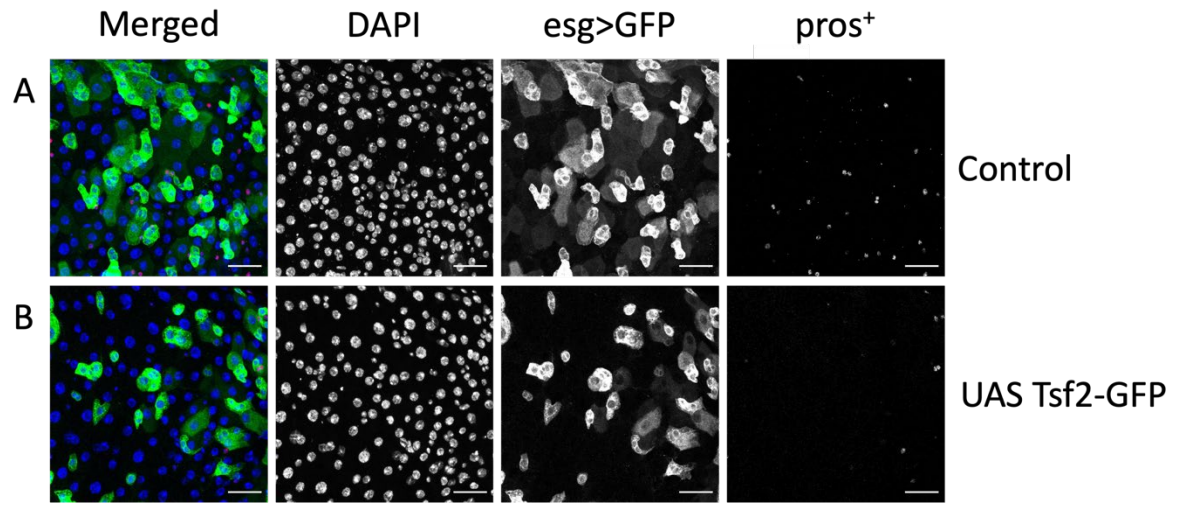

Figure 18: The effect of 7 days of Tsf2 overexpression on cell number and the proportion of stem/progenitor cells and EE cells.

Representative maximum intensity-projected confocal z stack images with brightness and contrast enhanced for clarity of control UAS-lacZ (A) and Tsf2-GFP overexpression (B) lines. Grey-scale images show cells per field of view (DAPI), ISCs/EBs (esg>GFP), and EE cells (pros^{+}). Merged images show nuclei (blue), ISCs/EBs (green), and EE cells (red). Quantified in the figure below, representative of n≥16. Scale bars = 30 μm.

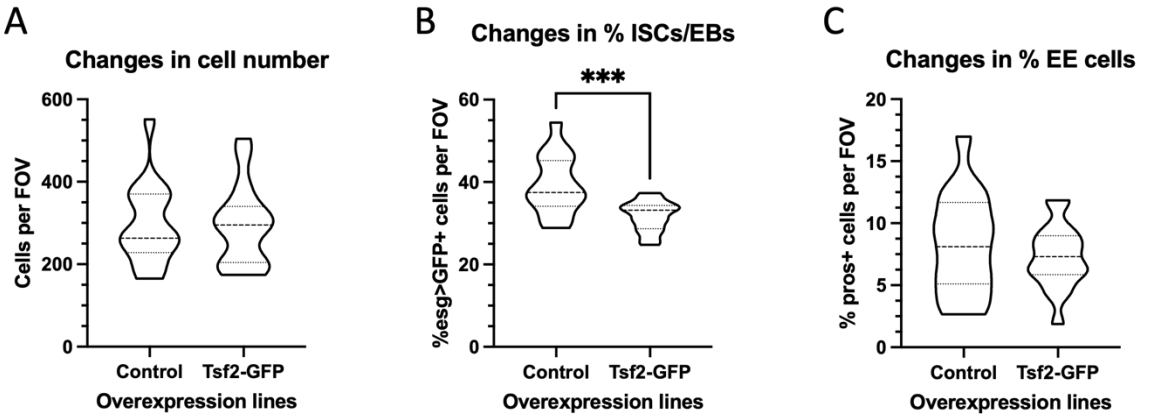

Figure 19: Quantification of the effect of 7 days of Tsf2 overexpression on cell number and the proportion of stem/progenitor cells and EE cells.

UAS-Tsf2-GFP was overexpressed for 7 days in adult ISCs/EBs using esg^{ts}GFP. Changes in cell number per field of view (A), the proportion of stem/progenitor cells (B), and the proportion of EE cells (C) have been quantified. The plotted lines represent the median and quartiles. An unpaired t test was used for all statistical analysis. n≥16 guts from 3 separate replicates. No = ns, * ***p<0.001.*

Using the temperature-inducible GAL4/UAS system requires the use of a control that may be genetically dissimilar to the knockdown or overexpression line. To overcome this problem, knockdown and overexpression experiments were also carried out using *Tsf2_RNAi_1* and *UAS-Tsf2-GFP* driven by the stem/progenitor-specific GeneSwitch driver *5961^{GS}*. As described previously, the GeneSwitch system allows the use of genetically matched flies for control and

treated samples to overcome the problem of different genetic backgrounds. The progeny were aged for 7 days at 25°C and then treated with RU0 or RU50 for 7 days. Changes in cell number per FOV showed the same trends as with *esg^{ts}GFP*: The knockdown control had 388 ± 30 cells (mean ± SEM) and the treated knockdown had 393 ± 23 cells. The overexpression had 311 ± 16 cells while its control had 356 ± 21 cells. The %EE cells in the knockdown flies increased significantly from 3.5% ± 0.5 to 9.2% ± 0.8, while the overexpression decreased significantly from 4.8% ± 0.6 to 2.8% ± 0.4 (**Figure 20**).

Due to the lack of a functioning Tsf2 primer or a sufficient amount of Tsf2 antibody to test knockdown efficiencies of the three RNAi lines, *Tsf2_RNAi_1* was used for subsequent experiments as it showed results that went in the opposite direction to the overexpression line.

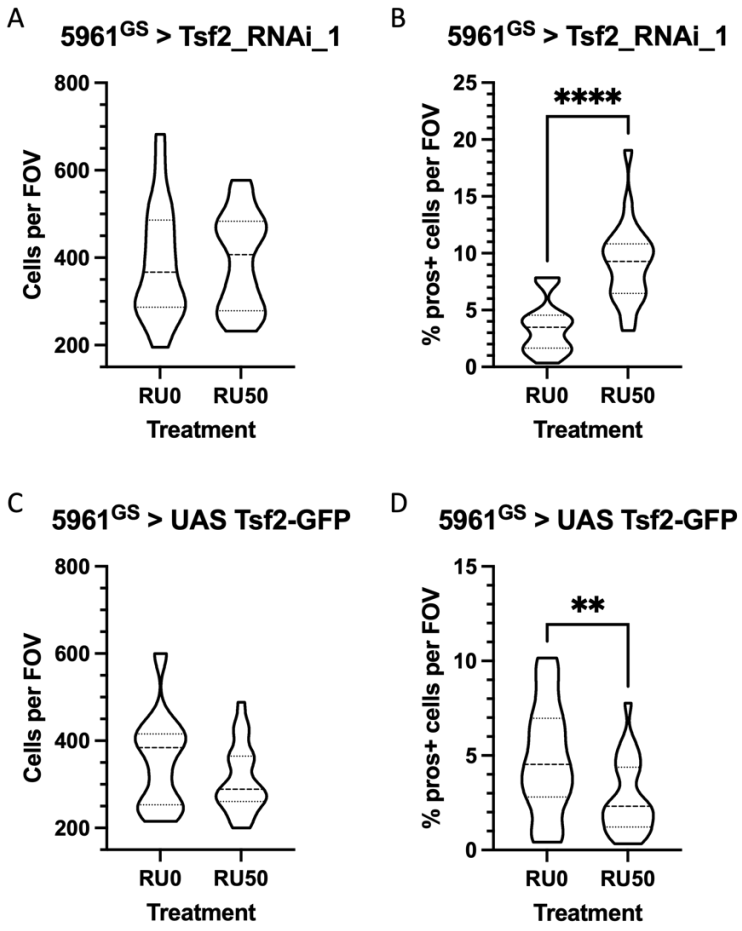

Figure 20: Quantification of the effect of 7 days of Tsf2 knockdown and overexpression using the GeneSwitch system on cell number and the proportion of EE cells.

Tsf2 was knocked down or overexpressed using the 5961^{GS} driver. Changes in cell number per field of view (A,C) and the proportion of EE cells (B,D) after Tsf2 knockdown (A,B) and overexpression (C,D) have been quantified. Tsf2_RNAi_1 was used as the knockdown line. The plotted lines represent the median and quartiles. The unpaired t test was used as all data were normally distributed. n≥19 guts from 3 replicates. No = ns, **p<0.01, ****p<0.0001.*

4.2.3 The effect of changing Tsf2 expression on other septate junction proteins

In order to assess potential effects of changes in Tsf2 expression by stem/progenitor cells, the *5961^{GS}* driver was used to knock down and overexpress Tsf2. After ageing the progeny for 7 days and then treating them with RU0 vs RU50 for a further 7 days, midguts were dissected for RNA extraction and cDNA synthesis. The expression levels of other septate junction proteins were tested using RT-qPCR, however no statistically significant difference was seen in Snakeskin or Mesh expression, neither with Tsf2 knockdown (**Figure 21A**) nor with overexpression (**Figure 21B**). ΔΔCt analysis was used to show fold change in expression relative to the housekeeping gene GAPDH, with 1.0 showing no change.

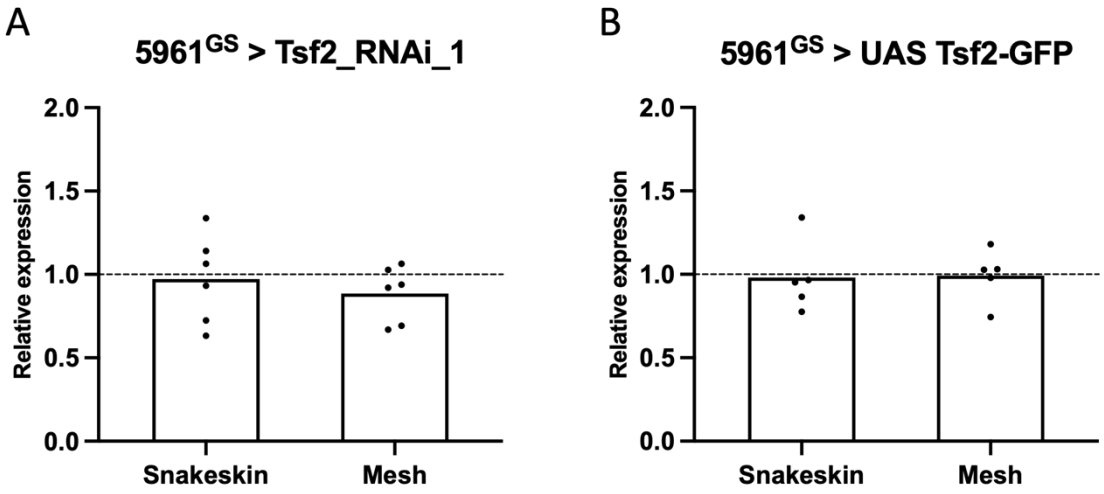

Figure 21: Changing Tsf2 expression does not affect other septate junction components.

Tsf2 knockdown (A) or overexpression (B) in stem/progenitor cells using 5961^{GS} for 7 days does not affect the expression levels of other essential SJ components Snakeskin and Mesh in the midgut. Tsf2_RNAi_1 was used for knockdown. The bars show mean ΔΔCt values relative to GAPDH, the dotted lines represent 1 (no change in expression). Differences in SQ values were tested using the unpaired t test and the Mann-Whitney test. n=10 midguts/sample, 6 (A) and 5 (B) replicates. N = ns.*

Antibody staining was used to see if there was any difference in the localisation of the SJ component Coracle when Tsf2 expression levels were changed. The staining was not consistent enough throughout the images for statistical analysis, even when using varying Triton X-100 concentrations and incubation times of staining protocols. Examples of the range of staining are given below (**Figure 22**). While no quantitative analysis was carried out, there was no obvious difference seen in the images. An example of consistent Cora staining (with colour contrast and brightness enhanced for clarity) is shown in **Figure 14B**.

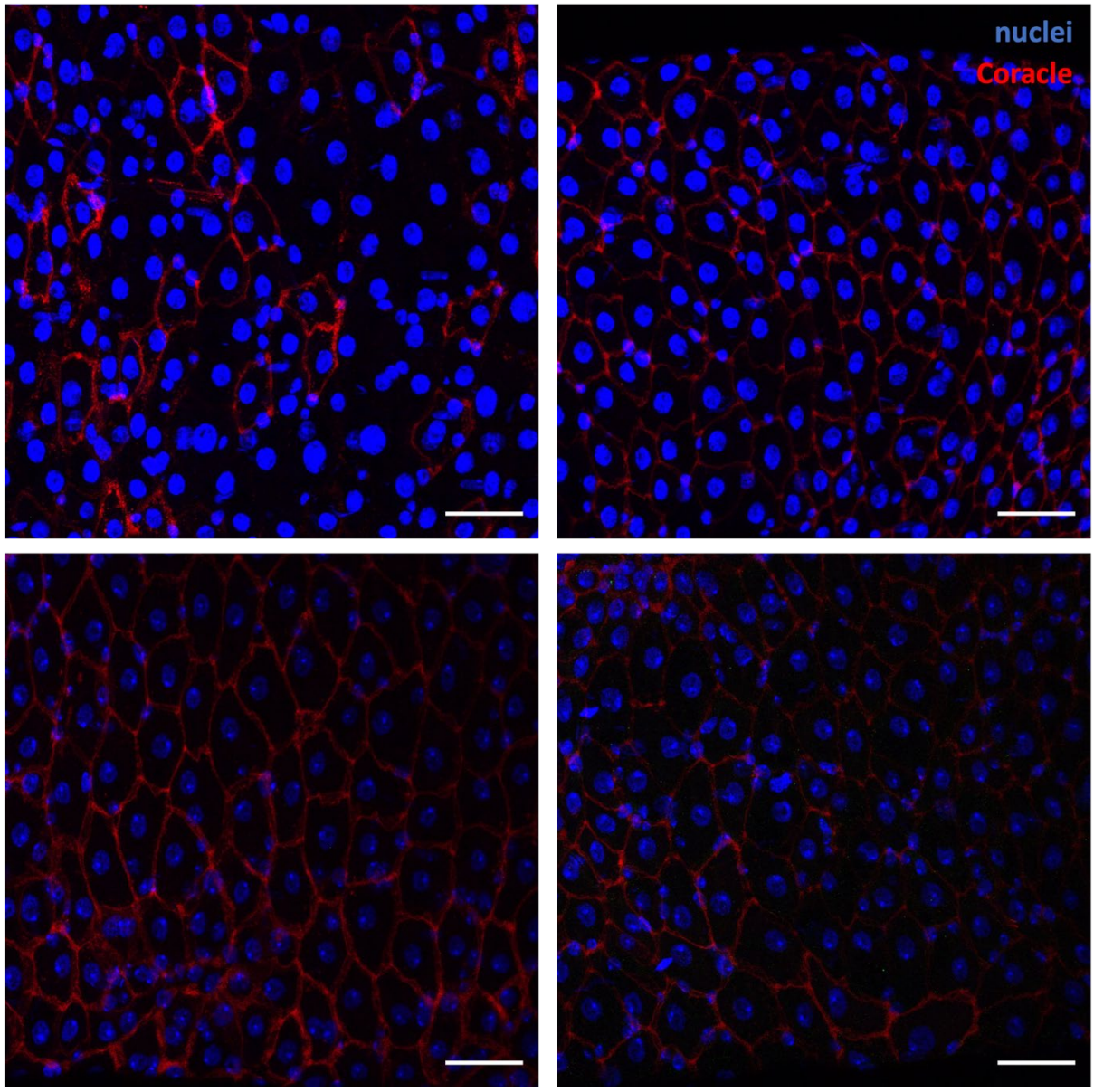

Figure 22: Variable Coracle staining upon Tsf2 overexpression.

A figure to show that Coracle staining is very variable between different images and within the same gut, making quantification difficult. The brightness and contrast have not been altered in these images.

4.2.4 Tsf2 expression change does not affect lifespan or gut barrier function

Knocking down SJ components such as Mesh or Ssk in the midgut causes a strong decrease in lifespan due to a loss of barrier function (Izumi et al., 2019). As Tsf2 expression changes with age (**Figure 13**, **Figure 15**), lifespan and barrier function experiments were therefore carried out with Tsf2. Age-matched, mated *5961^{GS}>Tsf2_RNAi_1* or *UAS-Tsf2-GFP* females were raised on normal cornmeal food for a week and were randomly split into vials of 30 flies each, with 10 vials per condition. From day 7 (± 1 day) onwards, the flies were switched to treated

food (RU0 vs RU50). The deaths in each vial were recorded with every flip onto fresh food (2 - 3 days).

Four replicates of Tsf2 knockdown were carried out, set up independently at different times from different bottles. The log-rank (Mantel-Cox) test was used to analyse differences in survival. The first lifespan showed a significant increase with Tsf2 knockdown, with median survival days of 67 for the control and 71 for the knockdown (**Figure 23A**). However, three subsequent replicates showed no significant difference (**Figure 23B-D**).

Despite the lack of impact on Coracle, Ssk, and Mesh expression upon Tsf2 knockdown in adult midguts described in this thesis, a strong dependency on Tsf2 is known to exist for junction formation in development (Tiklová et al., 2010). The effect of Tsf2 on barrier function was therefore assessed throughout adult life. Two separate lifespans were set up to test the barrier function of the gut with the Smurf assay. The flies were fed blue food once every 10 days for 24 hours. There was no significant difference in the proportion of Smurf flies at any time point for either replicate (n=300/condition/replicate, chi-square test). The Smurf lifespan set up concurrently with lifespan replicate 3 is shown as an example below (**Figure 23G**).

Two replicates of overexpression lifespans were set up in the same way. The first replicate had median survivals of 62 days (control) and 65 days (overexpression), with no difference in lifespan (**Figure 23E**), while the second lifespan was also non-significant with median survival of 69 days for both conditions (**Figure 23F**). Separate lifespans for Smurf assays were also set up with both lifespans, showing no significant differences apart from a decrease in the proportion of Smurf flies in the RU50 cohort on day 20 of replicate 2, with 3.15% in the treated cohort vs 7.97% in the controls (chi-square test). Replicate 1 is shown as an example (**Figure 23H**).

Along with the lifespans and Smurf lifespans, separate sample vials were collected from the same knockdown crosses to look for changes in the number of proliferating cells with age. Flies were dissected and stained for phospho-histone H3 (pH3), and the total number of mitotic cells was counted along the gut at day 10, day 39, and day 64. While the flies showed the expected hyperproliferation that has been described in old flies upon loss of homeostasis (**Figure 24C**; Choi et al., 2008), no difference was seen between the control and the knockdown flies at matching timepoints (**Figure 24D**).

A 7-day Tsf2 knockdown after ageing mated females for 7 days was also carried out using *Tsf2_RNAi_2* and *Tsf2_RNAi_3* in order to look at proliferation rates. While *Tsf2_RNAi_3* showed no significant change (**Figure 24B**), *Tsf2_RNAi_2* showed a small but statistically significant increase in pH3 number in the gut (**Figure 24A**).

Overall, there were no reproducible changes in lifespan, gut barrier dysfunction, or cell proliferation when Tsf2 expression is either increased or decreased.

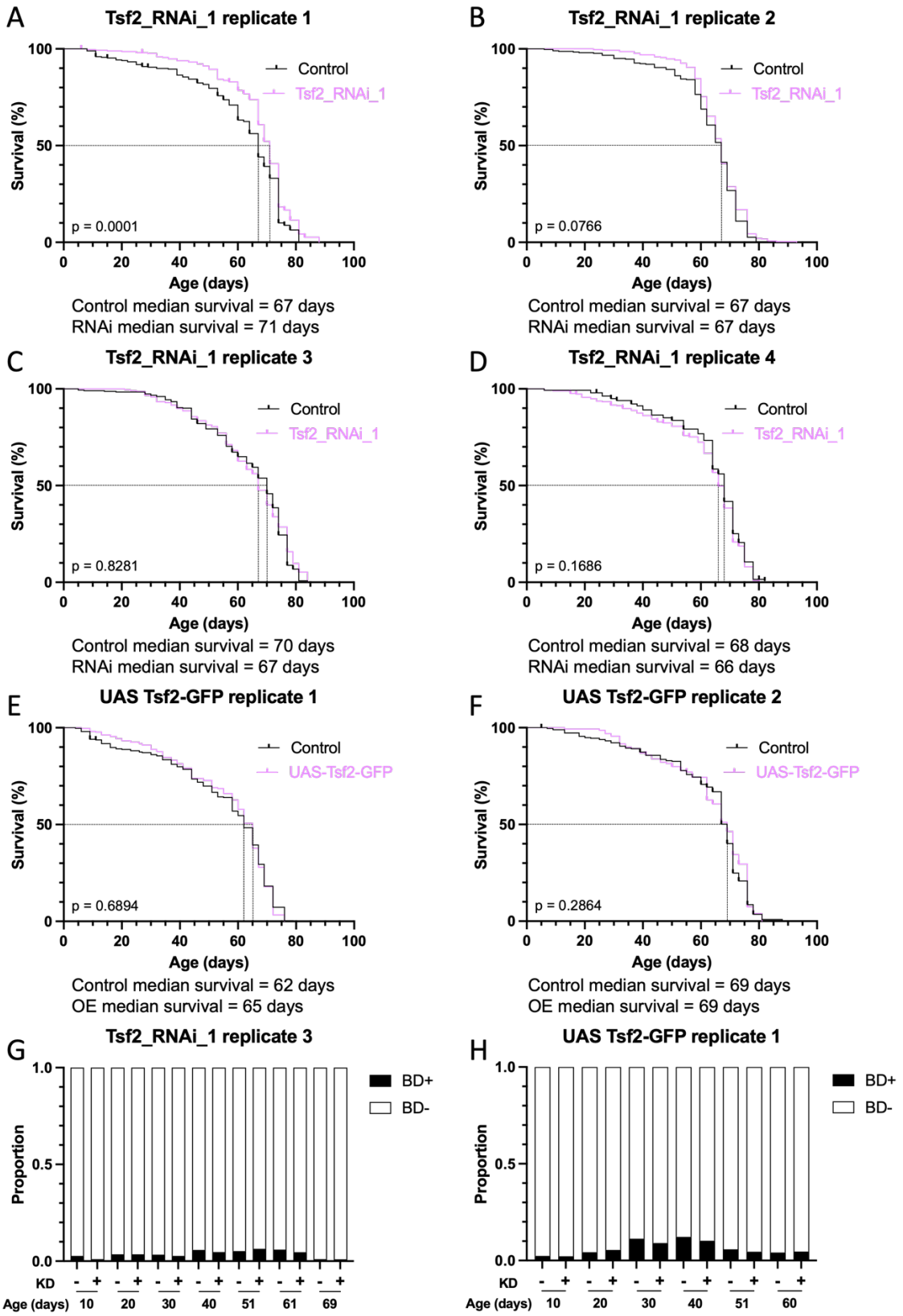

Figure 23: The effect of Tsf2 knockdown and overexpression on lifespan and gut barrier function.

Lifespan graphs of Tsf2 knockdown with Tsf2_RNAi_1 (A-D) and overexpression (E,F) using the driver 5961^{GS}. Smurf proportions of a representative Tsf2_RNAi_1 lifespan (G) and overexpression lifespan (H) taken at 10-day intervals, comparing control (KD-) and knockdown (KD+) flies. BD denotes barrier dysfunction. All Smurf proportions were not significant (chi-square test). Lifespans were tested with log-rank (Mantel-Cox) test, p values are indicated on each plot. n=300 flies/condition.

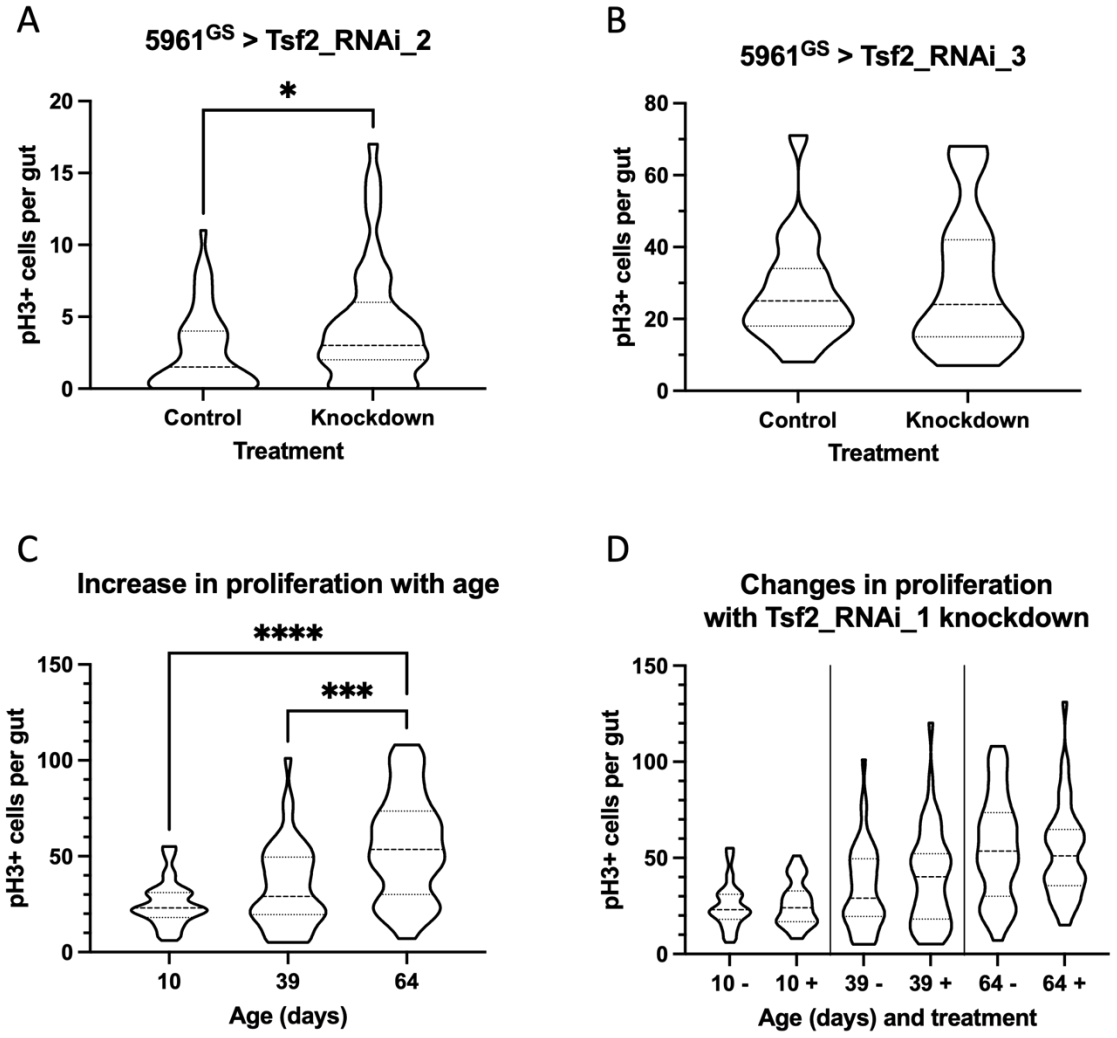

Figure 24: The effect of Tsf2 knockdown on mitosis in the midgut.

The effect of Tsf2_RNAi_2 (A) and Tsf2_RNAi_3 (B) on midgut mitotic cell numbers after 7 days of knockdown. (C) Mitotic cell numbers increase with age in control flies. (D) Tsf2 knockdown throughout adult lifespan does not affect mitosis. Panels A and B were calculated with a Mann-Whitney test, panels C and D were calculated with a Kruskal-Wallis test with Dunn's multiple comparisons. n≥52 from 3 replicates (A), n≥19 from 2 replicates (B), n≥42 from 3 replicates (C), n≥38 from 3 replicates (D). No = ns, *p<0.05, ***p<0.001, ****p<0.0001.*

4.2.5 The effect of changing Tsf2 expression on signalling pathways

In order to understand how the changes in Tsf2 expression described above affect gut homeostasis, some of the main signalling pathways that are involved in proliferation and differentiation were looked at in the context of Tsf2 knockdown and overexpression to look for downstream activation.

4.2.5.1 Notch pathway

The above results show that upon Tsf2 knockdown with *Tsf2_RNAi_1*, there is an increase in the proportion of ISCs/EBs (**Figure 17B**) and an increase in %EE cells (**Figure 17C**, **Figure**

20B), while Tsf2 overexpression results in a decrease in ISCs/EBs (**Figure 19B**) and a decrease in EEs (**Figure 20D**). Tsf2 expression changes in *Drosophila* mimic the *Drosophila notch* phenotype: Notch knockdown results in an increase in progenitor cells and EE cell fate specification, whereas overexpression results in precocious EC differentiation and loss of proliferation (Micchelli & Perrimon, 2006; Ohlstein & Spradling, 2006). Furthermore, as with Tsf2/MTf, the *notch* phenotype is inverse in the mammalian intestine: mammalian ISCs require Notch expression to maintain their stemness and to proliferate (Sancho et al., 2015), while MTf is a potential oncogene in mammals (Brown et al., 1980; Dippold et al., 1980; Woodbury et al., 1980).

Using antibodies against the Notch intracellular domain (NICD), the extracellular domain (NECD), and the ligand Delta in *5961^{GS}>Tsf2_RNAi_1* or *UAS-Tsf2-GFP* midguts was not successful (data not shown).

The Notch reporter *Su(H)GBE-GFPnls* was combined with two different GeneSwitch drivers (*5961^{GS}* and *TIGS*) to allow manipulation of Tsf2 with a Notch signalling readout. The progeny were aged for 7 days, then split in half and treated with RU0 or RU50 for 7 days. During dissection and staining the guts were kept in the dark in order to protect the endogenous GFP levels, with no antibody staining used. The guts were not imageable due to excessive damage across all three replicates set up with each fly line (data not shown). This was possibly due to external factors, such as bacterial contamination in the experimental vials affecting gut homeostasis in a manner unrelated to Tsf2 expression changes. A repeat of the experiments was not possible in the time frame.

A further new transgenic fly line was made by recombining *5961^{GS},UAS-GFP* with *Su(H)GBE-lacZ*. The guts were stained for β-galactosidase. Quantification of these images was not included due to time constraints not allowing a proper analysis and further examination of what any changes in lacZ levels may imply. Images showing the wide range of staining observed for *Su(H)GBE-lacZ* in *5961^{GS}>UAS-Tsf2-GFP* samples are below (**Figure 25**).

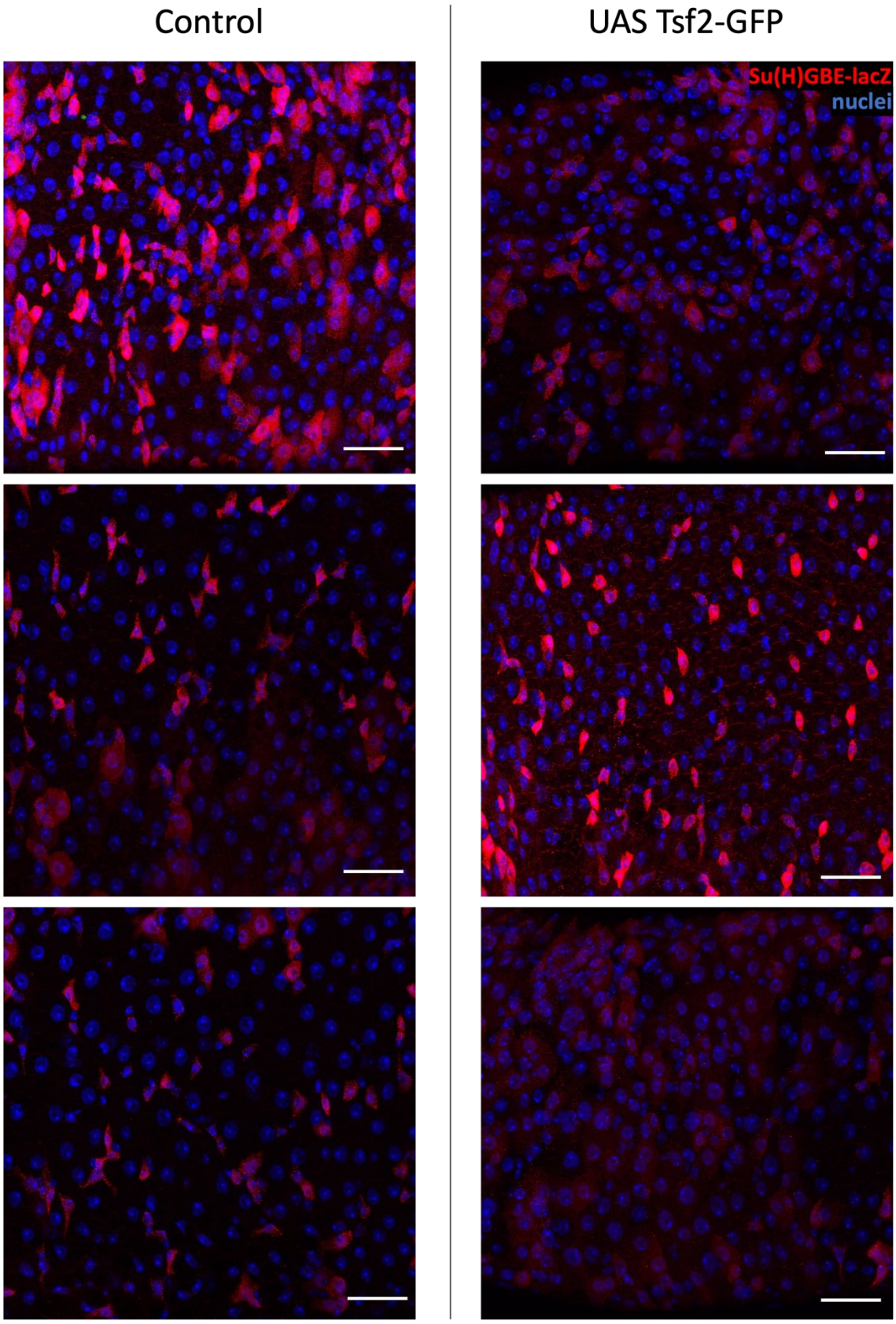

Figure 25: The effect of Tsf2 overexpression on Notch signalling.

The effect of Tsf2 overexpression in stem/progenitor cells using 5961^{GS} for 7 days on Su(H)GBE-lacZ expression in the posterior midgut. Only nuclei (DAPI, blue) and Su(H)GBE-lacZ (red) are shown. The example images are representative of a range of expression observed. N≥39 from 3 replicates. Scale bars = 30 µm.

RT-qPCR was used to look at the expression of several *Enhancer of split* (*E(spl)*) genes, which are directly downstream of Notch signalling (reviewed by Delidakis et al., 2014). Changes in *E(spl)* gene expression may indicate that Notch signalling could be affected by Tsf2. When Tsf2 was overexpressed, there was no significant change in *E(spl)mβ-HLH* or *E(spl)m3-HLH* (**Figure 26B**). Tsf2 knockdown showed no effect on *E(spl)mβ-HLH* expression but a small, significant decrease in *E(spl)m3-HLH* expression by 11.5% (**Figure 26A**). Two further *E(spl)* gene primers *(E(spl)m5-HLH* and *E(spl)m8-HLH)* were tested, but they had to be excluded due to primer dimer formation (data not shown).

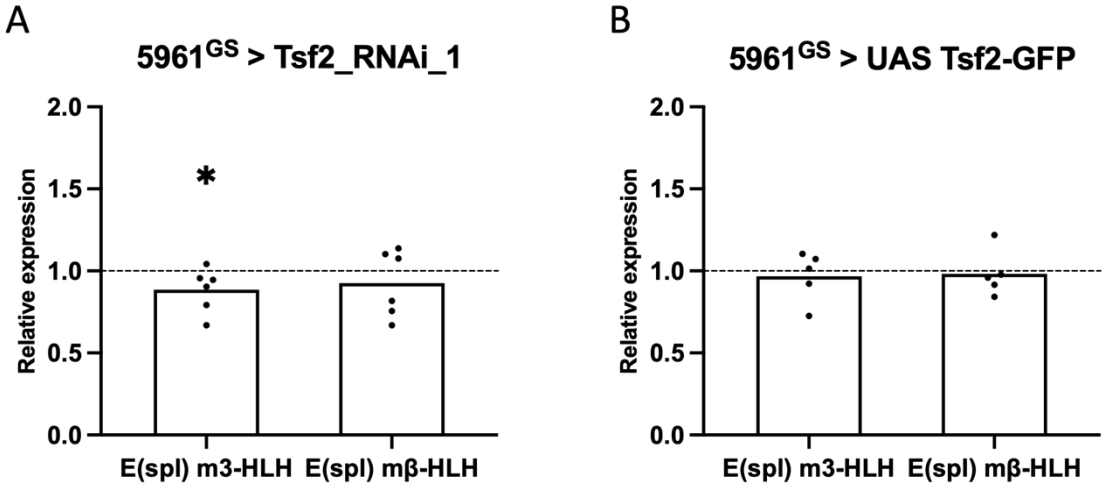

Figure 26: The effect of Tsf2 knockdown and overexpression on Notch signalling targets.

The effect of Tsf2 knockdown (A) and overexpression (B) in stem/progenitor cells using 5961^{GS} for 7 days on E(spl)m3-HLH and E(spl)mβ-HLH in the midgut. Tsf2_RNAi_1 was used for knockdown. The bars show mean ΔΔCt values relative to Actin5C or GAPDH, the dotted lines represent 1 (no change in expression). Differences in SQ values were tested using the unpaired t test and the Mann-Whitney test. n=10 midguts/sample, 6 (A) and 5 (B) replicates. No = ns, *p<0.05.*

4.2.5.2 Other signalling pathways

In order to broaden the assessment of possible downstream effects of Tsf2 on stem/progenitor signalling, other signalling pathway components were also looked at. *5961^{GS}>Tsf2_RNAi_1* knockdown guts were dissected and IF was used to stain for antibodies against phospho-Smad3 (pSmad3) and diphospho-ERK (dpERK). *5961^{GS}>UAS-Tsf2-GFP* overexpression guts were stained for dpERK and phospho-JNK (pJNK). Smad3 is the mammalian ortholog of *Drosophila* Mothers against Dpp (Mad), which is involved in the BMP pathway (**Figure 5**). The antibody detects Smads as well as Mad (H. Li et al., 2013). dpERK is a kinase in the Ras/MAPK pathway (**Figure 7**; Y. Guo et al., 2020). JNK is a kinase in the stress-activated JNK pathway (**Figure 6**; Biteau et al., 2011).

As these pathway components are activated by phosphorylation, the guts were kept in 1X PhosSTOP phosphatase inhibitor after being dissected and throughout the staining process up until the removal of the overnight primary antibody, as phosphorylation and dephosphorylation can occur within a very short time span. This was done according to the recommended protocol on the antibody suppliers' websites.

The staining in these images was inconclusive as only a small number of guts of one replicate for each antibody was imaged, so no concrete conclusions can be drawn from these results. dpERK staining in Tsf2 overexpression guts did not show any stain at all, this may be due to failed staining (data not shown). pSmad3 and dpERK staining on *Tsf2_RNAi_1* guts showed no significant differences between control and knockdown samples (**Figure 27A,B**), while Tsf2 overexpression showed a small, significant decrease in JNK phosphorylation of 32% (**Figure 27C**).

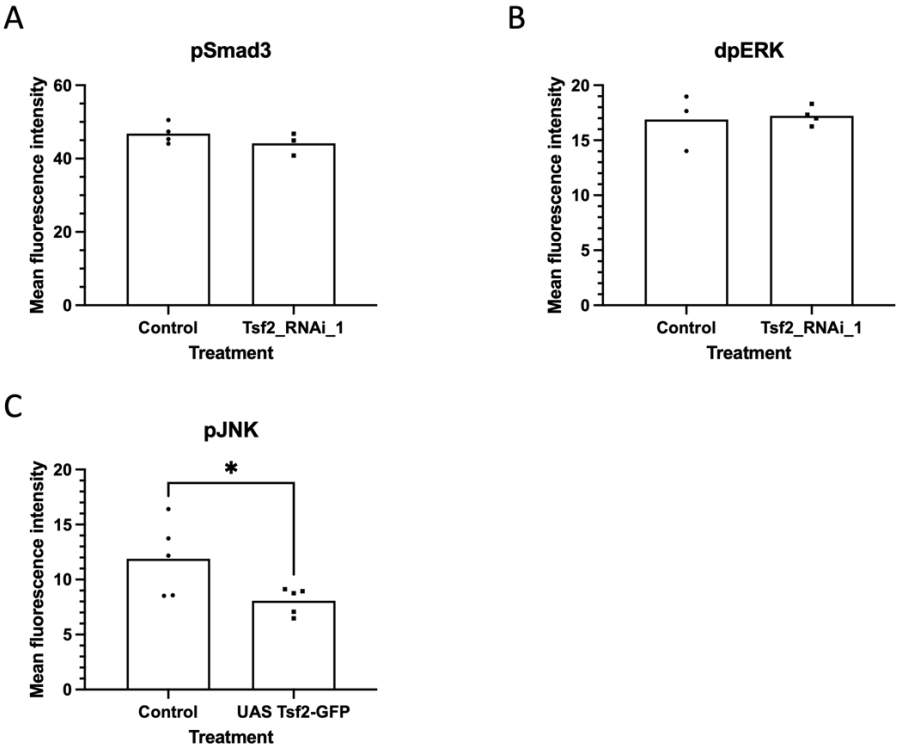

Figure 27: The effect of Tsf2 knockdown and overexpression on signalling pathways.

The effect of Tsf2_RNAi_1 knockdown (A,B) and overexpression (C) in stem/progenitor cells using 5961^{GS} for 7 days on signalling pathway components in the midgut. Mean fluorescence intensity analysis was calculated with the unpaired t test, n≥3 from 1 replicate. No = ns, *p<0.05.*

RT-qPCR analysis was used to look at expression changes of signalling pathway components. Socs36E is a negative regulator of the JAK/STAT pathway in *Drosophila* (Stec et al., 2013). Puckered (Puc) is a negative feedback regulator of the JNK pathway (**Figure 6**; Martin-Blanco

et al., 1998). Daughters against Dpp (Dad) is an inhibitory member of the BMP pathway that creates a negative feedback loop (**Figure 5**; Inoue et al., 1998). Pointed (Pnt) is a transcriptional activator downstream of the Ras/MAPK pathway (**Figure 7**; Klämbt, 1993). No significant changes were seen upon Tsf2 overexpression for either *dad* or *pnt* (**Figure 28B**). Tsf2 knockdown showed no significant effect on *socs36E*. It showed a slight statistically significant decrease of 13% in *puc* expression, but it is not clear if this is also biologically significant (**Figure 28A**).

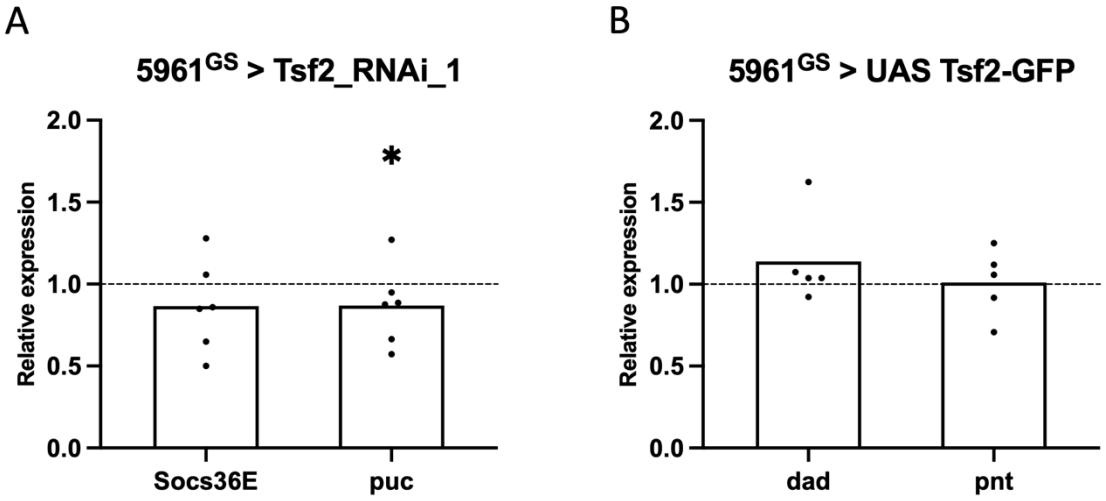

Figure 28: The effect of Tsf2 knockdown and overexpression on signalling pathway component expression.

The effect of Tsf2 knockdown (A) and overexpression (B) in stem/progenitor cells using 5961^{GS} for 7 days on signalling pathway components in the midgut, relative to rp49 (A) and GAPDH (B). Tsf2_RNAi_1 was used for knockdown. The bars show mean ΔΔCt values, the dotted lines represent 1 (no change in expression). Differences in SQ values were tested using the unpaired t test and the Mann-Whitney test. n=10 midguts/sample, 6 (A) and 5 (B) replicates. No = ns, *p<0.05.*

4.3 Discussion

This chapter has investigated the expression pattern of Tsf2 in the *Drosophila* midgut and what effect knocking down or overexpressing Tsf2 has on homeostasis. It was found that knockdown and overexpression have opposing, significant effects on the proportion of stem and progenitor cells in the posterior midgut, but there was no reproducible effect on lifespan or gut barrier function. This suggests that, unlike in the hindgut, Tsf2 does not act as an essential septate junction protein in the midgut. The signalling pathways involved in inducing loss of homeostasis upon manipulating Tsf2 expression levels have not yet been identified.

4.3.1 Tsf2 expression and localisation throughout lifespan in the midgut

Septate junctions are formed as *Drosophila* intestinal progenitor cells are differentiating into ECs and EEs, they connect differentiated cells to one another to form the paracellular gut barrier. This has been shown when looking at other SJ components, which are found at the junctions between differentiated cells (**Figure 14**; J. Chen & St Johnston, 2022). While Tsf2 acts as a SJ protein in pSJs (Tiklová et al., 2010), it has not been found in sSJs so far and indeed is not localised in the same honeycomb pattern surrounding ECs and EE cells (**Figure 15**). It is found instead surrounding the stem and progenitor cells, which is consistent with the original targeted DamID data that led to this study (Doupé et al., 2018) and RNA-seq data showing *tsf2* expression in ISCs (Tauc et al., 2021). This suggests it may have a function in the midgut that is unrelated to SJs. In a similar manner, Nrg is also part of pSJs but is found surrounding ISCs/EBs in the midgut, where it carries out non-occluding functions (Resnik-Docampo et al., 2021).

Tsf2 knockdown or overexpression also did not affect the expression levels of *ssk* or *mesh* (**Figure 21**). While this has not been looked at when changing the expression of other sSJ components, one might hypothesise that it could potentially affect them as a feedback mechanism by inducing a compensatory increase in expression. This can also be seen in old flies, where mRNA levels increase with age, possibly to compensate for reduced protein levels (Resnik-Docampo et al., 2017).

In middle-aged flies (day 28), there is a loss of the ISC/EB-specific Tsf2 protein localisation seen in young flies (**Figure 15**). When looking at *tsf2* mRNA expression in midguts however, there is no change at day 30 compared to day 10, while an increase of over 60% was seen at day 51 compared to the previous timepoints (**Figure 13**). A paper looking at tricellular junction components found that even though mRNA expression of several SJ members is increased in 45-day old vs 5-day old flies, their protein levels decrease with age (Resnik-Docampo et al., 2017), which shows that mRNA levels do not always correlate with protein levels. As stated in Chapter 3, because ISCs and EBs make up such a small number of cells found in the midgut samples used for mRNA expression analysis, it only provides a very crude first look at expression changes and ISC/EB-specific changes may be masked.

Due to having only a very small amount of antibody, it was not possible to carry out further IF experiments. As the antibody against mammalian MTf does not recognise *Drosophila* Tsf2, the production of more Tsf2 antibody would facilitate further analysis of Tsf2 function. It could be used to validate Tsf2 knockdown and overexpression, as well as look for changes in localisation or expression levels when potential upstream mechanisms that determine Tsf2 expression are modified. Creating a reporter, such as an enhancer or protein trap, could be used as an alternative or in addition to antibody usage to look at the sources or localisation of Tsf2. This could be done for example using the CRISPaint approach (Bosch et al., 2020).

4.3.2 Tsf2 knockdown and overexpression phenotypes

Three different knockdown lines were used to look at changes in the posterior midgut. They showed quite different phenotypes, including one increasing the proportion of ISCs/EBs while the other decreased it (**Figure 17**). It is worth noting that while *Tsf2_RNAi_1* and the control *luciferase-RNAi* line BL31603 came from the same stock centre (BDSC), *Tsf2_RNAi_2* and *Tsf2_RNAi_3* were acquired from VRDC, which may lead to variations in genetic background that could affect homeostatic cell proportions. The possibility of potential off-target effects cannot be excluded, which may also contribute to different phenotypes.

Making a driver line containing *5961^{GS}* with *esgsfGFP* could be used to overcome genetic differences potentially affecting the proportions of cell types when looking at phenotypes of knockdown or overexpression experiments, as the control flies in GeneSwitch experiments are taken from the same cross rather than crossing the driver line to a separate control RNAi/overexpression line.

Knockout rather than knockdown experiments are more robust and can have stronger phenotypes if the knockdown is not particularly strong. A recombinant line was created (*5961^{GS},UAS-GFP,UAS-mCas9*) to test this, but due to a lack of time the line was not fully validated or used for experiments.

The use of mosaic analysis with a repressible cell marker (MARCM) clones would also allow quantification of cell fate changes in *tsf2* mutants (T. Lee & Luo, 2001). However, soluble MTf (lacking the GPI anchor) can be taken up by neighbouring cells that do not normally express MTf in mammals. As *Drosophila* Tsf2 is tethered to the cell membrane by a GPI-anchor, this means there is a possibility that the GPI-anchor could be cleaved and Tsf2 could be secreted

and act non-cell-autonomously, as has been seen with pSJ proteins Boudin and Undicht. These are both GPI-anchored pSJ proteins that are secreted and can rescue SJ formation non-cell-autonomously as they can be endocytosed by nearby cells lacking their expression, for example when using MARCM clones (Petri et al., 2019; Tempesta et al., 2017). Creating MARCM clones lacking Tsf2 within a tissue with normal expression may reveal similar non-autonomous functions that can rescue homeostasis via secretion of Tsf2 into regions that are mutant, which would complicate the interpretation of this data.

Tsf2 overexpression resulted in a decrease in the proportion of ISCs/EBs using the *esg^{ts}GFP* driver, and a decrease in the proportion of EE cells which was significant when using the *5961^{GS}* driver but not significant with *esg^{ts}GFP*.

Due to a lack of a functional Tsf2 primer at the start of the project, the efficacy of knockdown by the three different RNAi lines was not tested. This is a big caveat that must be taken into consideration when interpreting the results. Future work should include Tsf2 knockdown with all three RNAi lines and with the overexpression line, driven by the ubiquitous *tubGAL4^{ts}* driver, to validate changes in expression levels. It was not possible to do this due to limited time available after acquiring a functioning Tsf2 primer.

Despite this, *Tsf2_RNAi_1* was chosen for follow-up experiments as it showed the opposite phenotype to the overexpression line, which has previously been used (Tiklová et al., 2010). These opposing results suggest that *Tsf2_RNAi_1* is indeed knocking down Tsf2 to a sufficient level to show its phenotype.

4.3.3 The effect of changing Tsf2 expression on ageing

In stark contrast to knocking down or overexpressing other SJ components (Salazar et al., 2018), no reproducible effects on lifespan were observed when doing so with Tsf2 in ISCs/EBs, further suggesting that it is not involved in SJs in the midgut (**Figure 23A-F**). It did not affect the barrier function of the gut when tested with the Smurf assay. This is another strong phenotype with loss of SJ components, but not when Tsf2 expression is changed in ISCs/EBs (**Figure 23G,H**). Furthermore, there were no differences in mitosis between the control and treated flies at day 10, day 39 or day 64 with *Tsf2_RNAi_1* (**Figure 24D**) or after 7 days of knockdown with *Tsf2_RNAi_3* (**Figure 24B**). Although *Tsf2_RNAi_2* did show a significant

increase, this may not be biologically significant as the number of mitotic cells increased from an average of 2.6 mitotic cells per gut to 4.4 (**Figure 24A**).

As there was a significant effect on posterior midgut homeostasis but no effect on lifespan, Tsf2 expression changes may have a short-term effect that can be compensated for. Tsf2 protein expression appears to be lost with age (**Figure 15**), so inducing expression specifically in old ISCs/EBs may show an ageing phenotype. Additionally, changing Tsf2 expression under different conditions, for example when the gut is damaged or challenged by bacterial infection, as well as looking for changes in Tsf2 expression levels in wild-type flies under stressed conditions, might give more insight into further phenotypes or a possible function that Tfs2 could be having in the midgut.

Studies have shown that the GeneSwitch system can become leaky with age and in particular for RNAi expression (Poirier et al., 2008; Scialo et al., 2016), which could have an impact on any effects seen with Tsf2 expression changes in older flies, for example in lifespan experiments. This could be overcome by using the auxin-inducible gene expression system (AGES), which has not shown aberrant induction in older flies (McClure et al., 2022). It could be particularly relevant due to the changes in *tsf2* mRNA expression and protein levels that have been seen in middle-aged and old flies. Further, it could also be used to see if induction of Tsf2 knockdown or overexpression at a later stage might affect midgut homeostasis. Lifespans using 5961^{GS} crossed to control knockdown/overexpression lines (BL31603 or *UAS-GFP*, respectively), as well as crossed to w^{1118}, and a CantonS x CantonS lifespan were carried out. They show that using the induction system may have an effect on lifespan by itself, without taking into account what gene expression changes are being induced.

4.3.4 Tsf2 involvement in signalling pathways in the midgut

Because Tsf2 expression changes mirrored Notch expression changes in the *Drosophila* midgut regarding effects on ISC/EB numbers and EE differentiation (Micchelli & Perrimon, 2006; Ohlstein & Spradling, 2006), and both have the opposite phenotype in the mammalian intestine (Brown et al., 1980; Dippold et al., 1980; Sancho et al., 2015; Woodbury et al., 1980), involvement of the Notch pathway was investigated. SJ component Mesh has been shown to increase cell-cell adhesion *in vitro* (Izumi et al., 2012). If Tsf2 affects cell-cell adhesion it could

potentially allow for an increase in Delta-Notch binding (Guisoni et al., 2017), or direct interaction with the Notch receptor on the cell surface.

The guts from both *5961^{GS};Su(H)GBE-GFPnls* and *Su(H)GBE-GFPnls;TIGS* progeny were not imageable. This does not seem to be due to excessive damage caused by a Tsf2 phenotype, but rather due to a problem with the fly lines. Other experiments set up at around the same time with the individual component lines used to make the new transgenic lines showed similar problems (data not shown). This may be due to other factors such as vial bacterial contamination or something else. Due to lack of time, these experiments could not be set up again.

Analysis of the Notch reporter *Su(H)GBE-lacZ* does not come without its challenges. While it can be used to quantify the proportion of EBs in a sample, as this is a binary result (positive or negative for expression of lacZ), quantifying the levels of Notch signalling activity in a tissue is more nuanced. When proliferation and/or differentiation are affected, for example by changing Tsf2 expression, their effects on Notch reporter expression needs to be factored in as both proliferation and differentiation rates affect Notch signalling and are affected by it themselves. As there was no immediately obvious difference in lacZ staining when using the *5961^{GS},UAS-GFP,Su(H)GBE-lacZ* reporter line to knock down or overexpress Tsf2, this made analysis of the data difficult. Furthermore, using antibody staining for β-galactosidase may not give representative endogenous expression levels due to the nature of signal amplification with the use of primary and secondary antibodies. The use of endogenous GFP expression with the GFPnls reporters mentioned previously may be better for such quantification. This would also allow live imaging to capture more subtle effects on Notch activation and differentiation (J. L. Martin et al., 2018).

The *E(spl)* complex of genes are direct downstream expression targets of the Notch pathway (Bailey & Posakony, 1995). Changing Notch signalling affects *E(spl)* gene expression levels (Bardin et al., 2010), but only *E(spl)m3-HLH* showed a small change in expression upon Tsf2 knockdown with *Tsf2_RNAi_1*, with knockdown samples having an 11.5% decrease in *E(spl)m3-HLH* expression compared to control samples, while Tsf2 overexpression showed no significant change (**Figure 26**). It is therefore difficult to determine if this change in *E(spl)m3-HLH* is biologically relevant.

These results seem to suggest that Tsf2 does not function by affecting the Notch pathway, but further work is required for conclusive proof.

Additional pathway components were tested with IF staining and RT-qPCR. pSmad3, dpERK, and pJNK staining on knockdown and overexpression guts only gave preliminary results as there was not enough time to image more than one replicate. Staining levels varied a lot within each condition, and the method used for measuring changes in staining levels is a crude way to measure changes in phosphorylation as it does not take into account how many cells are in the area measured or how widely they are spaced apart. While pSmad3 and dpERK did not show any significant changes in staining between control and Tsf2 knockdown samples, Tsf2 overexpression did show a small, statistically significant decrease in JNK phosphorylation. Repeats of these dissections and possibly testing out alterations to the staining protocol could give clearer results. Primers for *socs36E*, *puc*, *dad*, and *pnt* were tested with 7-day Tsf2 knockdown and overexpression samples. While the decrease in *puc* expression was statistically significant, further experiments would need to be carried out to see if the change is biologically relevant. It is worth noting that both significant results were changes involved in JNK signalling, so this may be involved in mediating the phenotypes (changes in the proportion of ISC/EBs and of EE cells) seen upon changes in Tsf2 expression. Future experiments could include staining for a Puc reporter, e.g., *puc-lacZ*, with Tsf2 knockdown or overexpression.

4.3.5 Comparing Tsf2 in *Drosophila* with MTf in mammals

Tiklová et al noted the difference in phenotypes between changing mammalian MTf and *Drosophila* Tsf2 and suggested that this may be due to compensatory mechanisms of other transferrin-like proteins in mammals (Tiklová et al., 2010). To date however, MTf has not been associated with TJs in mammals. It can cross the blood-brain barrier, which is formed by TJs, but it has been suggested that MTf is taken up by a cell-surface receptor (Demeule et al., 2003) rather than any interaction with TJs being observed. As TJs are more similar to *Drosophila* sSJs rather than pSJs, and as MTf expression levels in normal mammalian tissues is generally low, this suggests that MTf may not have a role in TJs in mammals.

4.3.6 Future directions

While Tsf2 knockdown and overexpression in ISCs/EBs appear to be showing reciprocal results, which could suggest that these are true phenotypes of changing Tsf2 expression in ISCs/EBs in the *Drosophila* midgut, validation of the lines is required. Short-term future work could include loss of function mutants, as these would further aid in clarifying the contradictory phenotypes seen when using the different RNAi lines. Repeating experiments that failed due to technical difficulties, such as the Su(H)GBE reporter experiments looking at GFP levels, is another initial follow-up step.

Carrying out repeats of lifespan experiments using a non-leaky system may yield more insight into the relationship between Tsf2-induced ISC/EB cell fate changes and their effect on lifespan. And finally, the creation of new genetic tools, such as Tsf2 reporters, would not only provide an alternative to look at Tsf2 expression patterns, but it would also greatly advance the exploration of downstream effects.

Chapter 5: The role of Laminin B2 in regulating homeostasis of the *Drosophila* midgut

5.1 Introduction

Another hit in the RNAi screen that acts as the preliminary work to this thesis is Laminin B2. It showed the largest increase in the proportion of stem and progenitor cells upon ISC/EB-specific knockdown in the adult midgut (**Figure 8**).

Laminins are glycoproteins that form one of the core components of the extracellular matrix. They have integral roles in both tissue structure and mediating signalling pathways. They are found in many species and tissues, showing their importance in both development and adult organisms.

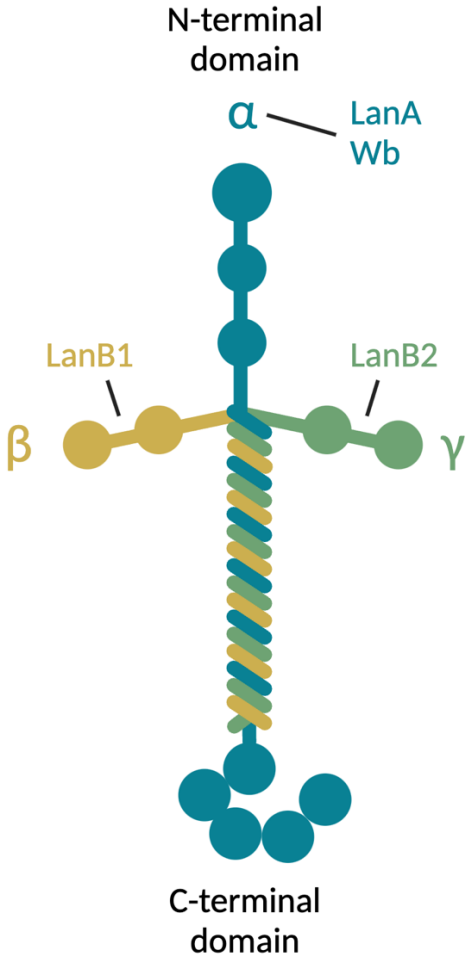

Figure 29: The laminin heterotrimer.

Drosophila has two α chains (LanA, Wb), one β chain (LanB1) and one γ chain (LanB2). This figure was made with Biorender.

5.1.1 Laminin structure

The *Drosophila* genome contains four Laminin subunits: two α chains encoded by Laminin A (LanA) and Wing blister (Wb), which most resemble human Laminin α3 and 5 and α1 and 2 respectively, one β chain Laminin B1 (LanB1), and the γ chain Laminin B2 (LanB2) (**Figure 29**). They can form two heterotrimers, LamininA with the LanA α chain, and LamininW with the Wb α chain (Fessler et al., 1987; Henchcliffe et al., 1993; D. Martin et al., 1999; Montell & Goodman, 1988; Urbano et al., 2009).

5.1.2 Laminin integration into the ECM

It has been shown that αβγ heterotrimers form in the endoplasmic reticulum (ER) before being secreted, shown with murine, human, and *Drosophila* Laminin. This can only occur if the β and γ chain form a disulphide bond preceding α chain interaction (Hunter et al., 1990; Kumagai et al., 1997; Yurchenco et al., 1985, 1997). Once deposited in the ECM, N-terminal Laminin ends form a polymeric meshwork with other ECM proteins, while C-terminal ends mediate cell receptor binding and signalling (Colognato et al., 1999; Deutzmann et al., 1990; Rousselle et al., 1995; Schittny & Yurchenco, 1990). While individual α chain secretion was not seen in the developing *Drosophila* larva (Urbano et al., 2009), both intact and truncated α chain can be secreted from human embryonic kidney 293 cells (Yurchenco et al., 1997), and murine embryoid bodies can also secrete a truncated α chain in the absence of γ chain expression (Smyth et al., 1999). It is not clear whether this occurs in adult *Drosophila* or in humans.

5.1.3 Laminins are required for morphogenesis

Studying LanB2 during *Drosophila* embryogenesis revealed several roles during the development of the midgut and its surrounding VM (Wolfstetter & Holz, 2012). Loss of either α subunit shows that the two Laminin trimers have slightly different functions in different tissues, both in mammalian systems (Colognato et al., 1999) and in *Drosophila*, seen by the varying phenotypes of *lanA* vs *wb* mutants (Pitsidianaki et al., 2021; Urbano et al., 2009; Wolfstetter & Holz, 2012). One heterotrimer can partially compensate for the loss of the other, as *wb;lanA* double mutants have a more severe phenotype than single mutants. Loss of either the LanB1 or LanB2 subunit prevents any Laminin trimer secretion, which comes with an increase in the severity of the phenotypes (Urbano et al., 2009; Wolfstetter et al., 2019; Wolfstetter & Holz, 2012).

Laminins interact both directly and indirectly with a host of other ECM proteins. Their presence is required for initial BM assembly during *Drosophila* development (Henchcliffe et al., 1993) and they are expressed before other ECM components (Matsubayashi et al., 2017). This Laminin requirement during development is highly conserved, seen also in mice and in *C. elegans* (Colognato et al., 1999; C. Huang et al., 2003; S. Li et al., 2002; Smyth et al., 1999) and is also important during adult BM remodelling (Colognato et al., 1999; Gialeli et al., 2011). Localisation of other BM components is reduced and disrupted in *lanB2* mutants (Wolfstetter & Holz, 2012), such as Nidogen/Entactin, which interacts directly with LanB2 (Mayer et al., 1993), SPARC/BM-40, and Collagen IV (Wolfstetter & Holz, 2012). Dystroglycan expression does not rely on Laminins (Schneider et al., 2006; Wolfstetter & Holz, 2012).

Loss of a fully formed ECM disrupts cell migration, which is required for fusion of the anterior and posterior *Drosophila* midgut primordia, causing gaps in the midgut (Pitsidianaki et al., 2021; Wolfstetter & Holz, 2012). The close association with the VM is lost. *LanB2* mutant phenotypes are enhanced by mutations in other proteins such as Thrombospondin and Kon-tiki, proteins thought to act during tendon and muscle target site recognition. This makes an interaction between Laminin trimers and these proteins likely during muscle development, possibly indirectly via integrins (Urbano et al., 2009; Wolfstetter & Holz, 2012). Eventually these disruptions lead to lethality at the end of embryogenesis (Henchcliffe et al., 1993; Smyth et al., 1999).

Unlike other epithelia which rely only on polarity factors, the *Drosophila* midgut is comparable to vertebrates as both also require Laminin-integrin interactions for cell polarity. Loss of the integrin adhesion complex prevents Cadherin localisation and apical junction formation, which is necessary for polarity and for MET during gut development (J. Chen et al., 2018; Klein et al., 1988; Wolfstetter & Holz, 2012; Yarnitzky & Volk, 1995; Yu et al., 2005). This process is initiated by the mesoderm-derived LamininW trimer and reinforced by the midgut-derived LamininA trimer (Pitsidianaki et al., 2021).

5.1.4 Laminin expression is required to maintain certain stem cell populations

Not only is Laminin-integrin signalling between epithelial cells and the BM required for migration and polarity, it has also been shown to be necessary for proliferation and maintenance of ISC fate in the adult *Drosophila* midgut. Mutations of integrin subunits αPS1, αPS3 and βPS, as well as the main integrin ligand LanA, cause a reduction in ISC number (Lin et al.,

2013), and while the reduction in ISCs/EBs in the RNAi screen upon LanA knockdown was not significant, there was a significant decrease in total cell number (**Figure 8**). The ISCs of *lanA* or integrin mutant guts are not lost by apoptosis, but rather through differentiation into ECs and EEs, with cell type proportions equivalent to wild-type midgut differentiation. This cannot be rescued by activation of individual proliferation pathways, showing a key role for integrin signalling in the intestine (Lin et al., 2013). The study, which was looking specifically at the requirement for integrin signalling to maintain ISCs, used *lanA* MARCM ISC clones in the posterior midgut to show that LanA levels are reduced but not fully depleted surrounding these ISCs, with the remaining expression likely coming from the surrounding VM (Lin et al., 2013).

Similar results were seen in the *Drosophila* ovary: Follicle stem cells require αPS1βPS and αPS2βPS integrins as well as the αPS1βPS ligand LanA to be maintained in the germarium, with mutant clones being lost over time by differentiation and lack of proliferation (Gotwals et al., 1994; O'Reilly et al., 2008).

In direct contrast to the loss of ISC maintenance and proliferation seen by Lin et al., Goulas et al. found that knockdown of integrins in midgut ISCs using several RNAi lines increased their proliferation (Goulas et al., 2012). Lin et al. hypothesised that the opposing results may be due to varying genetic background, off-target effects of the RNAi, or residual low-level expression during knockdown being sufficient for ISC maintenance (Lin et al., 2013).

The *lanA* phenotype seen in the preliminary work to this thesis is consistent with published literature (Lin et al., 2013), but is the opposite of that seen when LanB1 or LanB2 are knocked down (**Figure 8**). While LamininA knockdown does not prevent LamininW formation, LanB1 or LanB2 knockdown prevents the secretion of both trimers, which may be causing the difference in phenotype.

5.1.5 Chapter aims

Many previous studies looked at Laminin changes as a whole rather than from specific cell types. This chapter aims to investigate the involvement of ISC/EB-derived LanB2 in intestinal homeostasis and how changes in its expression are linked to age-related intestinal dysplasia.

5.2 Results

5.2.1 Knocking down LanB2 in stem and progenitor cells affects midgut homeostasis

As LanB2 knockdown in ISCs/EBs resulted in the largest increase in the proportion of ISCs/EBs in the initial knockdown screen (**Figure 8**), it was chosen for follow-up experiments. Because the screen only used one RNAi line, a repeat of the 7-day ISC/EB-specific knockdown driven by *esg^{ts}GFP* was carried out with three separate RNAi lines targeting different sequences to minimise the risk of phenotypes occurring from off-target effects. In addition to the original line used (BL55388, named *LanB2_RNAi_1*, **Figure 30B**), two other *lanB2-RNAi* lines were tested and compared to the control *luc-RNAi* BL31603 (**Figure 30A,D**): BL62002 (named *LanB2_RNAi_2*, **Figure 30C**) and v42559 (named *LanB2_RNAi_3*, **Figure 30E**). *LanB2_RNAi_3* was run in a separate set of experiments with its own control BL31603, which is indicated by the line separating them in the figures below. While *LanB2_RNAi_1* and *LanB2_RNAi_2* showed similar results, including trends in the same direction when the results were not statistically significant, *LanB2_RNAi_3* had opposing results (**Figure 31**).

LanB2_RNAi_1 and *LanB2_RNAi_2* showed no significant changes in cell number per field of view (FOV), whereas *LanB2_RNAi_3* showed a significant decrease from 306 ± 14 cells to 221 ± 12 cells (mean ± SEM) (**Figure 31A**). For both the proportion of stem and progenitor cells (*esg>GFP*) and of EE cells (*pros^{+}*), the Bloomington lines also followed the same trend, while the VDRC line showed the opposite. The proportion of stem/progenitor cells increased for *LanB2_RNAi_1* (27.2% ± 1.2 to 32.1% ± 1.4) and *LanB2_RNAi_2* (27.2% ± 1.2 to 32.7% ± 1.1), but decreased for *LanB2_RNAi_3* (30.6% ± 0.9 to 21.4% ± 2.1, **Figure 31B**). The proportion of EE cells increased with *LanB2_RNAi_1* (5.2% ± 0.6 to 7.7% ± 0.7) and did not change significantly for *LanB2_RNAi_2* or *LanB2_RNAi_3* (**Figure 31C**).

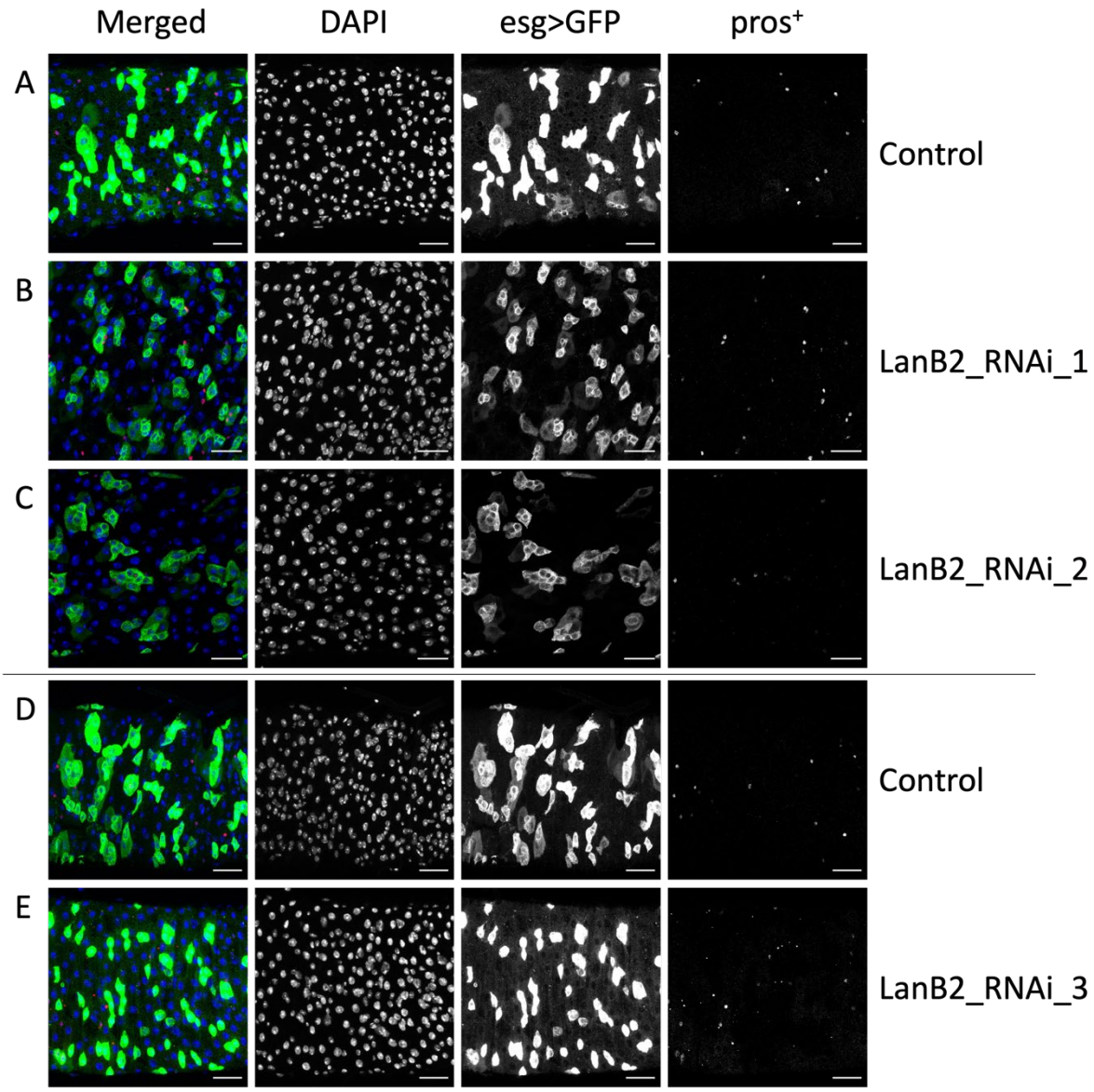

Figure 30: The effect of 7 days of LanB2 knockdown on cell number and the proportion of stem/progenitor cells and EE cells.

Representative projected confocal z stack images with brightness and contrast enhanced for clarity of control (A,D), and LanB2 knockdown (B,C,E) lines. D and E were run in a separate set of experiments from A-C. Grey-scale images show cells per field of view (DAPI), ISCs/EBs (esg>GFP), and EE cells (pros^{+}). Merged images show nuclei (blue), ISCs/EBs (green), and EE cells (red). Quantified in the figure below, representative of n≥15. Scale bars = 30 μm.

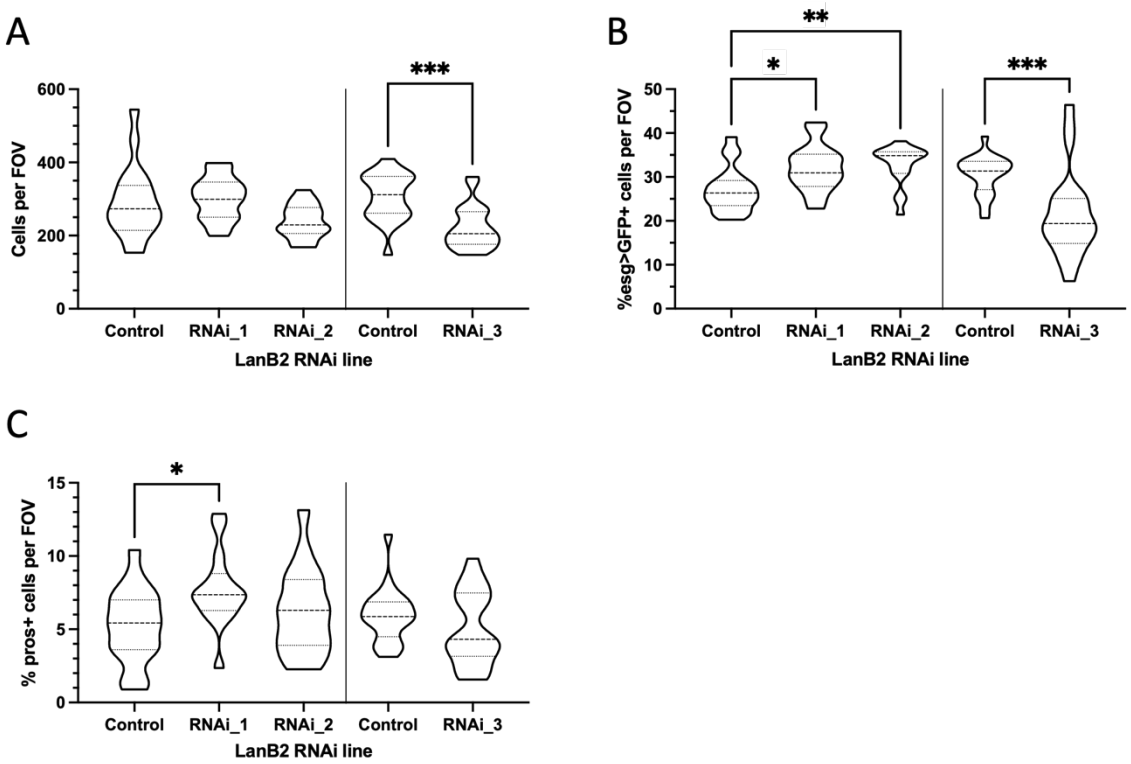

Figure 31: Quantification of the effect of 7 days of LanB2 knockdown on cell number and the proportion of stem/progenitor cells and EE cells.

*Changes in cell number per field of view (A), the proportion of stem/progenitor cells (B), and the proportion of EE cells (C) have been quantified. LanB2_RNAi_3 was run separately with its own control, denoted by the vertical line separating them. The plotted lines represent the median and quartiles. The ordinary one-way ANOVA with Holm-Šidák's multiple comparisons was used for normally distributed data, and the Kruskal-Wallis test with Dunn's multiple comparisons was used for non-normally distributed data. n≥15 guts over 3 replicates. No * = ns, *p<0.05, **p,0.01, ***p<0.001.*

5.2.2 LanB2 knockdown validation

As cells other than ISCs and EBs express Laminins, the ubiquitous driver *tubGAL4^{ts}* was used to knock down LanB2 in all cells in adult flies to test the efficacy of the RNAi lines compared to the control BL31603. This showed the *LanB2_RNAi_2* line to have the strongest whole gut knockdown (including crop, cardia, and Malpighian tubules), with an 83.8% reduction (mean ΔΔCt to 1dp). Interestingly, even though *LanB2_RNAi_3* had the opposite phenotypic results to the other two lines, it also showed a strong reduction in *lanB2* RNA levels (62.6%). *LanB2_RNAi_1* had the lowest knockdown with 19.0% (**Figure 32**).

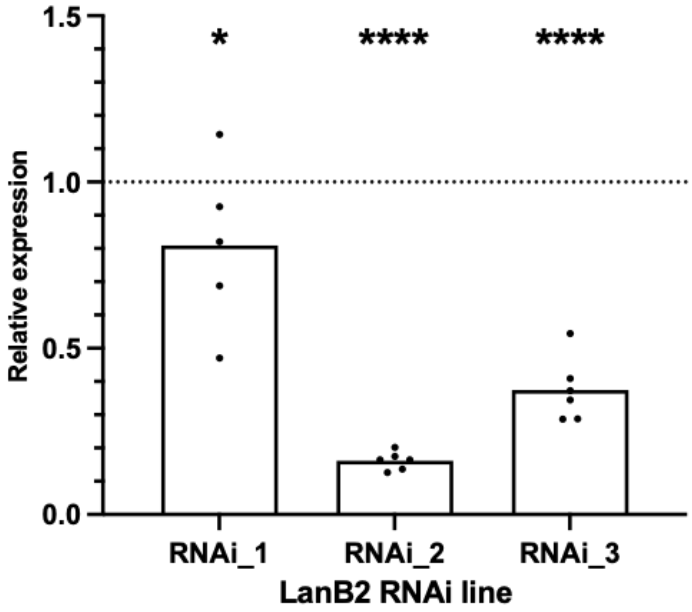

Figure 32: Validation of lanB2-RNAi lines.

*Changes in LanB2 expression levels in whole gut samples using the ubiquitous driver tubGAL4;GAL80^{ts} with specified RNAi lines compared to control BL31603 (denoted by line at 1), relative to GAPDH. The bars show mean ΔΔCt values. Calculated using an ordinary one-way ANOVA test with Holm-Šidák multiple comparisons. n=10 guts/sample, ≥5 replicates. *p<0.05, ****p<0.0001.*

5.2.3 Laminin expression in the midgut

5.2.3.1 Laminin B2

Looking at protein expression with an antibody or a reporter provides the ability to confirm its expression pattern as well as look at changes with age or upon genetic manipulation. As there is no longer an anti-LanB2 antibody commercially available, the CRIMIC GAL4 line BL91283 was used to drive *UAS-EGFP* (BL6874), *UAS-GFPnls* (BL4775), and *UAS-mCherrynls* (BL38425). Although the CRIMIC stock line was ordered on two separate occasions, neither version of the line showed any distinctive staining pattern with any reporter line (images not shown). As there was also no staining visible for the surrounding VM or the trachea, which are known to express Laminins (Klußmann-Fricke et al., 2022; D. Martin et al., 1999; Pitsidianaki et al., 2021; Sarov et al., 2016) and would have served as a positive control for this line, it was not possible to determine exact LanB2 expression or localisation.

There are however fosmid lines available for both of the other Laminin subunits, LanB1 and LanA (Sarov et al., 2016), which may be used to infer further information about LanB2 as they contain constructs for the expression of GFP-tagged *lanA* and *lanB1* transgenes.

5.2.3.2 Laminin A

The fosmid line v318155 (*LanAGFP*) was used to look at LanA localisation compared to ISCs/EBs (*esg-lacZ* reporter) and just EBs (*Su(H)GBE-lacZ* reporter). Anti-GFP immunofluorescent antibody staining on *esg-lacZ* flies not crossed to the fosmid line was used as a negative control (images not shown).

Due to strong laminin expression from the surrounding the VM and trachea (see example z stack projection, **Figure 33**), individual image slices rather than a z stack were used to look at subunit expression within the epithelium. Although the 3D shape of the gut provided some difficulties in getting clear images, representative figures are shown below. A more concentrated ring of GFP was seen surrounding ISCs and EBs, shown with the reporter line *esg-lacZ*, than the background level of LanAGFP in the epithelium (**Figure 34A**). This was the case across almost all images taken from several replicates. Furthermore, occasionally a few other $lacZ^-$ cells also had a brighter GFP ring surrounding them. These were exclusively small nuclei, which may be either EEs or cells from the tissues surrounding the gut.

Comparing LanAGFP to the *Su(H)GBE-lacZ* reporter also showed increased GFP levels around $lacZ^+$ cells, as well as other $lacZ^-$ cells (**Figure 34B**) which may be ISCs not labelled by the *Su(H)GBE-lacZ* reporter. This was again seen in several images across different replicates.

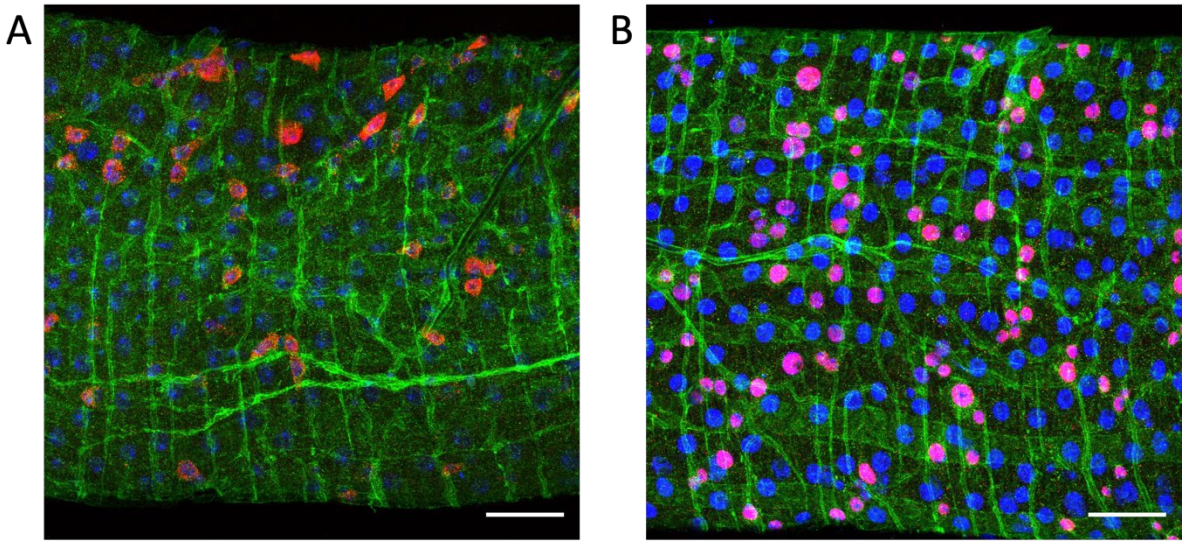

Figure 33: LanA and LanB1GFP expression in the gut and surrounding tissues.

Z stack projections of LanAGFP crossed to Su(H)GBE-lacZ (A), and LanB1GFP crossed to esg-lacZ (B), showing extensive expression from non-epithelial tissues. The brightness and contrast are enhanced for clarity. Representative of n≥15 guts per condition. Scale bar = 30 µm.

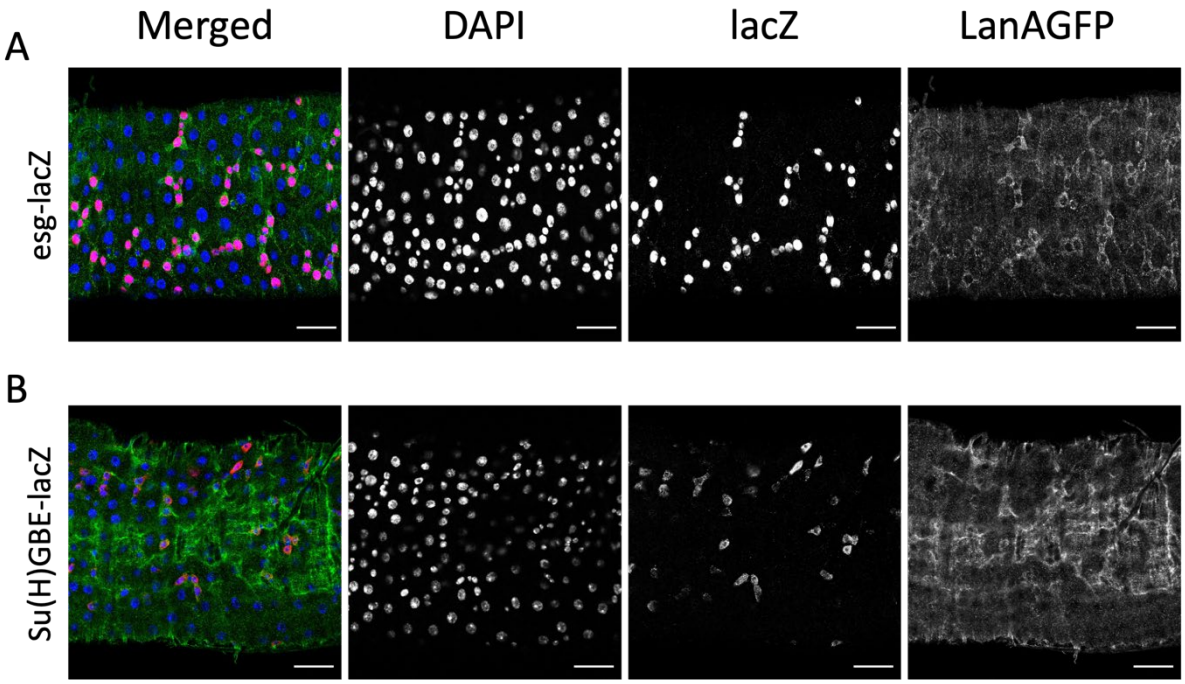

Figure 34: LanA expression pattern in the adult midgut.

Representative images showing LanAGFP expression pattern in the midgut, with brightness and contrast enhanced for clarity. Single slice confocal images of the midgut showing LanAGFP staining in relation to esg-lacZ (A) and Su(H)GBE-lacZ (B) antibody staining. Grey-scale images show nuclei (DAPI), ISCs/EBs (lacZ), and LanA (GFP). Merged images show nuclei (blue), ISCs/EBs (red), and LanAGFP (green). Representative of n=26 across 3 replicates (esg-lacZ), n=23 across 3 replicates (Su(H)GBE-lacZ). Scale bars = 30 µm.

5.2.3.3 Laminin B1

The fosmid line v318180 (*LanB1GFP*) was used to look at LanB1 localisation. When crossed to the *esg-lacZ* (ISC/EB) and *Su(H)GBE-lacZ* (EB) reporter lines, the epithelial localisation pattern followed that of LanA as described above, with increased localisation surrounding the stem and progenitor cells (**Figure 35**). This can be expected as Laminins are secreted as a heterotrimer.

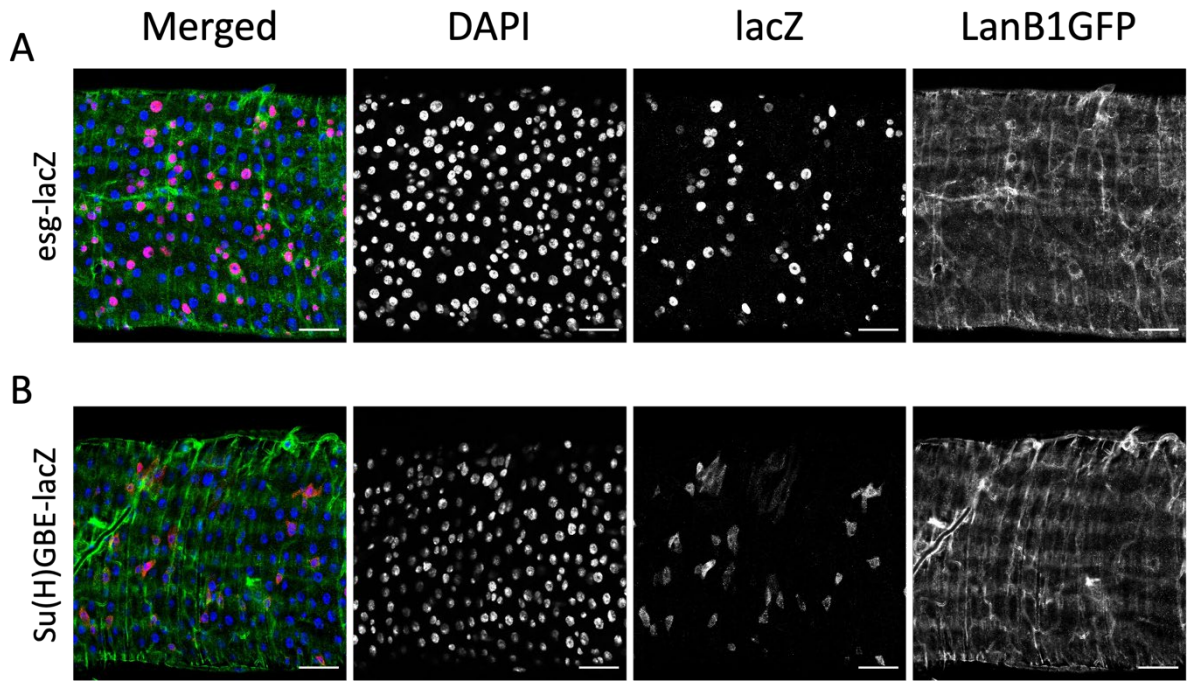

Figure 35: LanB1 expression pattern in the adult midgut.

Representative images showing LanB1GFP expression pattern in the midgut, with brightness and contrast enhanced for clarity. Single slice confocal images of the midgut showing LanB1GFP staining in relation to esg-lacZ (A) and Su(H)GBE-lacZ (B) antibody staining. Grey-scale images show nuclei (DAPI), ISCs/EBs (lacZ), and LanB1 (GFP). Merged images show nuclei (blue), ISCs/EBs (red), and LanB1GFP (green). Representative of n=18 across 3 replicates (esg-lacZ), n=15 across 2 replicates (Su(H)GBE-lacZ). Scale bars = 30 µm

5.2.4 The effect of changing LanB2 levels on other laminins

In order to assess potential effects of changes in LanB2 expression by stem/progenitor cells, the ISC/EB-specific GeneSwitch driver *5961^{GS}* was used to knock down LanB2 using the strongest RNAi line (*LanB2_RNAi_2*, **Figure 32**). After 7 days on RU50 treatment, no change in *lanB2* RNA levels was seen in midguts (**Figure 36**). This may be due to strong expression levels by the surrounding tissues masking changes in ISCs/EBs, which make up only a small percentage of the cells in the midgut.

5961^{GS}>LanB2_RNAi_2 did not change the levels of *lanA* or *lanB1* mRNA expression after 7 days of knockdown to a statistically significant level (**Figure 36**).

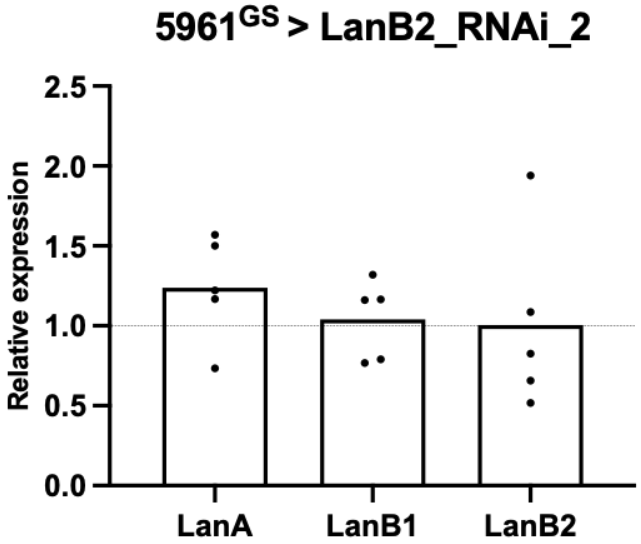

Figure 36: Expression of laminin subunits after ISC/EB-specific LanB2 knockdown.

Changes in expression levels of LanA, LanB1 and LanB2 with 7 days of LanB2 knockdown in stem/progenitor cells using 5961^{GS}>LanB2_RNAi_2, relative to GAPDH. The bars show mean ΔΔCt values. Calculated using unpaired t test to compare RU0 and RU50 as all data sets were normal. n=10 midguts/sample, 5 replicates. No = ns.*

5.2.5 The effect of LanB2 knockdown on lifespan and gut barrier function

As shown in Chapter 3, both *lanB1* and *lanA* showed increased RNA expression in 51-day old flies, with a 46.9% and a 70.0% increase of the mean from day 10 to day 51 respectively (**Figure 13B,C**), and *lanB2* shows a slight, non-significant trend towards an increase at day 51 (**Figure 13D**). This raised the question whether changing LanB2 throughout adult life would change the lifespan. Age-matched *5961^{GS}>lanB2-RNAi* flies were mated for 2 days on normal cornmeal food, after which the females were randomly split in half into control and knockdown vials (10 vials of 30 flies each per condition), aged to day 7 (± 1 day), and then put onto RU0 or RU50 cornmeal food. Deaths were recorded every 2 - 3 days when the flies were transferred onto fresh food.

The knockdown was initially carried out using the *LanB2_RNAi_3* line (**Figure 37C-E**). Three lifespans were carried out, each set up independently at different times. While the first showed a significant increase in lifespan with knockdown when comparing the lifespan curves with the log-rank (Mantel-Cox) test, with the graphs converging for the median survival at day 43 (**Figure 37C**), the lifespan curves of the second replicate were not significantly different (medians were day 34 (control) and day 38 (knockdown), (**Figure 37D**)), and the third replicate

had a significant decrease, with medians at day 53 for the control and at day 46 for the knockdown (**Figure 37E**).

The same experiments were carried out with *LanB2_RNAi_2* (**Figure 37A,B**). The first replicate was not statistically significant, with median survival at day 62 for the control and day 55 for the knockdown, while for the second replicate the knockdown lifespan survived significantly longer, with medians at day 66 for the control and 71 for the knockdown. Overall, this shows that there is no reproducible, significant effect on lifespan using this method.

Separate lifespans to measure gut barrier function using the Smurf assay were set up from the same crosses concurrently with the lifespans. The flies were tested every 10 days and the proportion of Smurf flies were counted and analysed using the chi-square test. The Smurf lifespans were set up with *LanB2_RNAi_3* lifespans replicate 1 and 3. The second Smurf set had a significant increase in Smurf proportions in the RU50 cohort on day 39 (5.91% vs 11.17%) and a significant decrease on day 60 (8.11% vs 1.90%), but given that these results were only seen in one of the replicates and only at two time points, this was not taken as a meaningful result (**Figure 37F**). This suggests that LanB2 does not have an effect on the *Drosophila* gut barrier function.

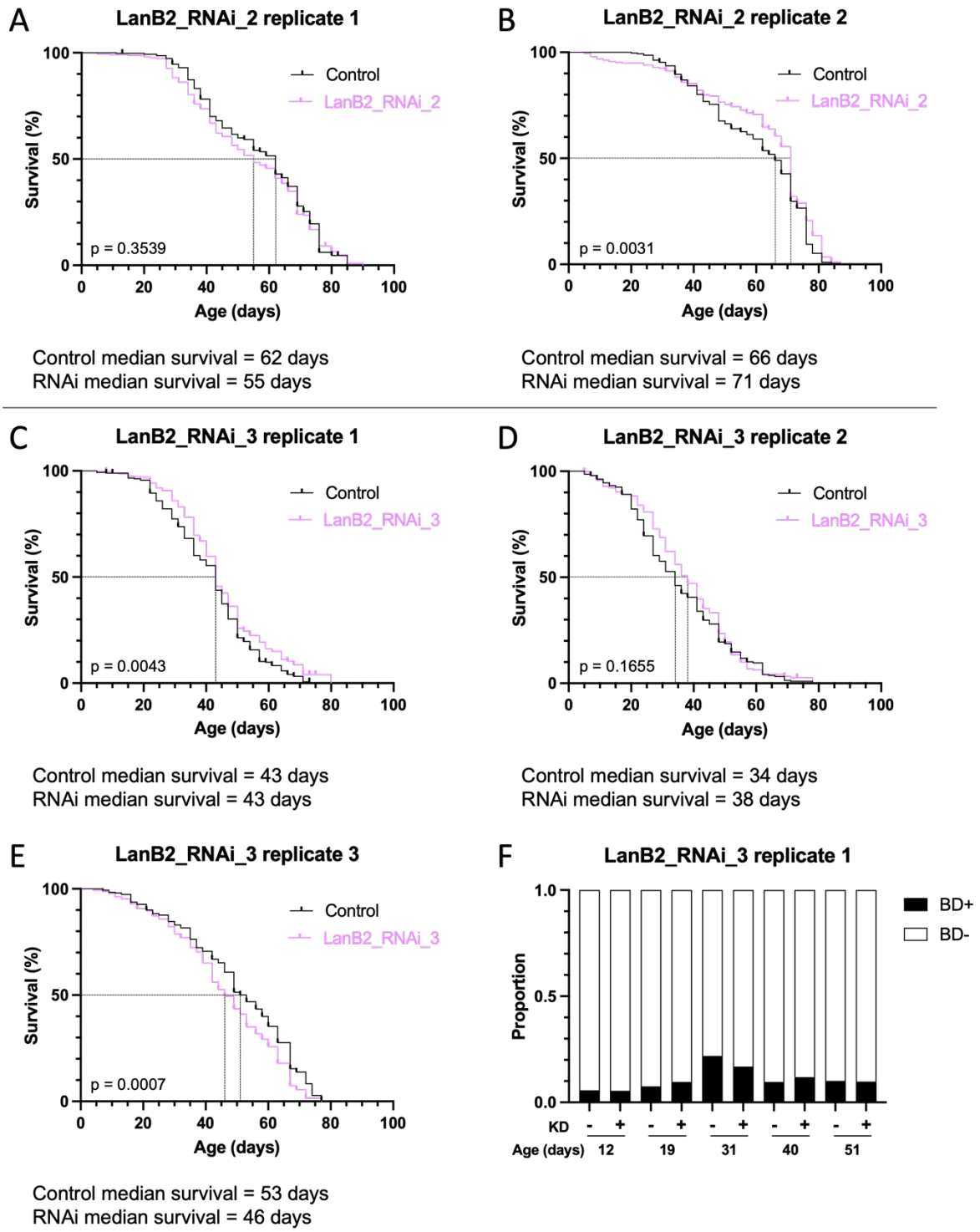

Figure 37: The effect of LanB2 knockdown on lifespan and gut barrier function.

Lifespan graphs of LanB2 knockdown with LanB2_RNAi_2 (A,B) and LanB2_RNAi_3 (C,D,E). Smurf proportions of a representative LanB2_RNAi_3 lifespan (F) taken at 10-day intervals, comparing control (KD-) and knockdown (KD+) flies. BD denotes barrier dysfunction. All Smurf proportions were not significant (chi-square test). Lifespans were tested with log-rank (Mantel-Cox) test, p values are indicated on each plot. n=300 flies/condition.

5.2.6 The effect of LanB2 knockdown on signalling pathway components

In order to test which signalling pathways may be mediating the changes seen upon LanB2 knockdown, RT-qPCRs were run using the previously mentioned *5961^{GS}>LanB2_RNAi_2* samples. None of the three genes tested showed any significant changes (**Figure 38**).

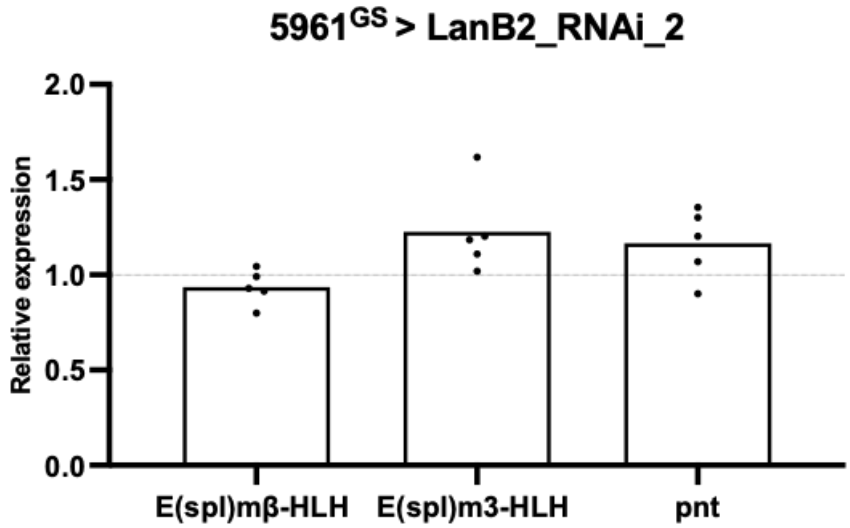

Figure 38: The effect of LanB2 knockdown on signalling pathway component expression.

Changes in expression levels of E(spl)mβ-HLH, E(spl)m3-HLH, and pnt with 7 days of LanB2 knockdown in stem/progenitor cells using 5961^{GS}>LanB2_RNAi_2, relative to GAPDH. The bars show mean ΔΔCt values. Calculated using unpaired t test to compare RU0 and RU50 as all data sets were normal. n=10 midguts/sample, 5 replicates. No = ns.*

As Laminin expression is required for Collagen arrangement during embryogenesis, an antibody against human Collagen IV was used to look for changes after 7 days of LanB2 knockdown using *esg^{ts}GFP* with all three RNAi lines. This did not show Collagen staining in any of the samples, including the control (data not shown), suggesting that this antibody is unsuitable for *Drosophila* intestinal staining.

5.3 Discussion

This chapter has looked at the involvement of Laminin B2 in midgut homeostasis and age. LanB2 knockdown in stem and progenitor cells was found to disrupt homeostasis by affecting the proportions of different cell types in the posterior midgut, but showed no significant effects on lifespan using the GeneSwitch system, and it has not yet been identified which signalling pathways mediate the phenotypes seen.

5.3.1 Variable phenotypic effect of LanB2 knockdown on midgut homeostasis

Of the three RNAi lines used to knock down LanB2 expression, two (*LanB2_RNAi_1* and *LanB2_RNAi_2*) showed similar effects on changes in the proportion of stem/progenitor cells and EE cells, while the third (*LanB2_RNAi_3*) showed very different results (**Figure 31**). This does not seem to be due to varying knockdown levels, as *LanB2_RNAi_3* knockdown levels (62.2%) were in between *LanB2_RNAi_1* (19.0%) and *LanB2_RNAi_2* (83.8%). It is important to note that cell counting experiments with *LanB2_RNAi_3* were run separately from *LanB2_RNAi_1* and *LanB2_RNAi_2*, although as the results are combining three replicates set up at different times that all showed the same trends, this suggests it was not due to an artefact. Furthermore, as *LanB2_RNAi_3* was ordered from a different stock centre than *LanB2_RNAi_1* and *LanB2_RNAi_2* and the control, it is likely to have a different genetic background that may not have the same homeostatic turnover rate as the other two RNAi lines. Such differences could be overcome by using a drug-inducible system with an ISC/EB reporter, e.g., *esgsfGFP*, as the control flies will have the exact same genetic background as treated flies. This could also be used to determine whether the GeneSwitch system is inducing knockdown to a sufficient level to give the same phenotype that is seen when using $esg^{ts}GFP$. Alternatively, differences between the three RNAi lines could be due to off-target effects unrelated to LanB2 knockdown.

A further way of addressing this problem would be to create *lanB2* mutants, as this might give more conclusive results. A new transgenic line (5961^{GS},*UAS-GFP,UAS-mCas9*) was created during the course of this thesis. While no guide RNA currently exists for *lanB2*, there are lines available for CRISPR-mediated *lanB1* overexpression (Ewen-Campen et al., 2017; Jia et al., 2018) and knockout (Zirin et al., 2020) and the generation of new sgRNAs is now relatively straightforward, so this could be a logical next step. Another method of inducing ISC mutants can be done by creating MARCM clones (T. Lee & Luo, 2001).

The initial RNAi screen that was run in 2018/19 before this PhD also tested *LanB2_RNAi_1* and showed very similar results, with a significant increase in cells per FOV and %ISCs/EBs (**Figure 8**). RNAi lines against LanB1 (BL42616) and LanA (BL28071) were also tested in the screen. While *lanB1-RNAi* showed a non-significant increase in %ISCs/EBs, *lanA-RNAi* showed the opposite result to *LanB2_RNAi_1* and *lanB1-RNAi*, with a significant decrease in the number of cells per FOV and a non-significant decrease in %ISCs/EBs. A similar *lanA* phenotype was also seen by Lin et al when looking at integrin signalling. They found that

LanA-integrin signalling is required for ISC maintenance and proliferation, with a mild decrease in ISC number after seven days that became more pronounced two weeks after *lanA* mutant clone induction (Lin et al., 2013). As Laminin turnover is slower than other ECM proteins, the phenotypes of *lanB2* driven by *esg^{ts}GFP* knockdown may become more pronounced if the knockdown were to be carried out for longer than 7 days.

5.3.2 Laminin expression pattern in the posterior midgut

As the results described above occurred when LanB2 was knocked down only in ISCs and EBs, this shows that along with other tissues such as the surrounding VM and trachea, there is also an epithelial Laminin source that has not been described previously. Although it was not possible to visualise LanB2 expression, looking at the other Laminin subunits can provide a good insight into where LanB2 is likely to be localised. LanAGFP and LanB1GFP staining patterns were in alignment with each other, with almost all guts showing the same brighter rings of GFP around stem and progenitor cells. These fosmid lines have previously been used to show Laminin surrounding the VM encircling the midgut but did not look specifically at the midgut epithelium itself (Sarov et al., 2016). An earlier study showed that *lanA* mutant ISC clones have reduced LanA protein levels surrounding those ISCs in adult midguts, which suggests that this reduced localisation around stem cells is likely due to loss of expression by these cells themselves (Lin et al., 2013). *Drosophila* follicle stem cells, unlike other ovarian stem cells, have also been shown to require their own LanA secretion in order to maintain stemness and proliferation via cell-autonomous LanA-integrin signalling (O'Reilly et al., 2008). In addition to the targeted DamID transcriptomics that formed the basis for the original screen (Doupé et al., 2018), a recent scRNA-seq study looking at expression patterns in different cell types in the gut found that *lanA*, *wb*, *lanB1*, and *lanB2* are all expressed by ISCs/EBs (Hung et al., 2020).

A few individual smaller cells that were not labelled ISCs and EBs also had brighter GFP staining surrounding them. These may be EE cells, which are the only other posterior midgut cell type to have small nuclei, or they could also be cells from the tissues encircling the gut, such as the VM and trachea, as it was not always possible to get images of the gut showing exclusively epithelial cells due to the 3D shape of the gut.

In order to determine the functions and sources of Laminins, it would be useful to create additional reporters, both to determine which cell types express LanB2 as well as where those

proteins localise in the tissue. This can be done using CRISPR-based approaches to make enhancer traps or tagged proteins (Bosch et al., 2020). It would provide the possibility to distinguish what part ISC/EB-derived Laminins play in homeostasis and how this changes in old flies, as well as measuring changes in protein levels with age, as this does not always correlate with changes in mRNA levels (Becker et al., 2018). Using an overexpression line would provide a good complement to the experiments carried out so far in order to elucidate further by which mechanisms ISC/EB-derived LanB2 acts. As increased LAMC1, the human ortholog of LanB2, has been associated with more aggressive metastatic cancer (Y. Fang et al., 2022), looking at LanB2 expression in *Drosophila* tumour models or knocking down/overexpressing LanB2 in this context could also be investigated.

While individual α chain secretion has not been detected in *Drosophila* embryos (Urbano et al., 2009), it has been seen in human embryonic kidney cell culture and in mouse embryoid bodies (Smyth et al., 1999; Yurchenco et al., 1997). It has not been shown whether this happens in the adult fly. This may however be a reason why knocking down an α chain gives different results to the β or γ chain. If individual α chains are secreted, they may have other functions than the Laminin trimers. Furthermore, as there are two α chains that can partially compensate for one another in various tissues (Wolfstetter & Holz, 2012), knocking down one of them may not prevent total laminin secretion. Only one β and one γ chain exist in the *Drosophila* genome and as a result, knocking down one of them has been shown to cause build-up of the other subunit in the cell, which has been seen in human embryonic kidney (Yurchenco et al., 1997) and bovine adrenocortical cell culture (Pellerin et al., 1997) as well as in *C. elegans* embryos (C. Huang et al., 2003; Kao et al., 2006) and in *Drosophila* larval glial cells (Petley-Ragan et al., 2016). This was studied in more detail in *Drosophila* larval glia, which showed that β or γ chain knockdown causes accumulation of the other subunit in the ER, leading to ER stress and the unfolded protein response (UPR); lowering the level of the accumulating subunit decreases the phenotype. When Laminin trimer secretion is reduced by knockdown of a transmembrane ER protein Tango1, which is thought to help secrete Laminins in glia, this phenotype is much milder, suggesting that the build-up of individual unbound Laminin subunits is the cause (Petley-Ragan et al., 2016). Future work could explore the possibility of ER stress in adult midgut progenitor cells upon LanB2 knockdown. This can be done by looking at changes in expression of PERK, ATF6, and IRE1, which activate the UPR, as well as downstream TF Xbp1 and phosphorylation of eIF2α. It has been shown that changing Xbp1 expression levels

in ISCs, EBs or ECs to simulate or repress the UPR affects ISC proliferation (L. Wang et al., 2014).

5.3.3 The effect of LanB2 knockdown on age

Figure 13 showed an increase in RNA levels in 51-day old CS flies for both *lanA* and *lanB1*, although it is not clear if this translates to increased protein levels, as no commercially available antibodies exist. This would be something that could possibly be measured using GFP levels of the fosmid lines, or by making new antibodies or additional protein traps, including for LanB2. The increase in RNA levels may be resulting in increased protein levels, or it may be trying to compensate for age-related decline in ECM function (reviewed by Statzer et al., 2023). Increased mRNA levels of some Laminin chains (Denisenko et al., 2018) and Laminin B1 protein levels (Abrass et al., 1995) have been seen in old compared to young rat kidneys. An increase in Laminin α2 has also been detected during heart failure in old humans (E. H. Kim et al., 2016). *LanA-RNAi* in *Drosophila* heart has been shown to preserve heart contractility and increase lifespan by reducing aberrant ECM build-up (Sessions et al., 2017). These studies show that there is still much to be learned about the role that Laminins play in ageing.

Lifespan analyses of LanB2 knockdown in intestinal stem and progenitor cells did not yield consistent effects on lifespan. *LanB2_RNAi_2* had one replicate with a significant increase and one with no significant difference, while *LanB2_RNAi_3* had one replicate with a significant increase, one with a significant decrease, and one with no change (**Figure 37**). It was not possible to test the level of LanB2 knockdown in these experiments, as the high level of Laminin expression from other tissues masks any changes in ISC/EB expression levels, as was shown by the 7-day knockdown samples (**Figure 36**). It cannot be known therefore if the knockdown using 5961^{GS} was strong enough to induce the equivalent phenotypic changes seen when using $esg^{ts}GFP$ (**Figure 30**). Additionally, it has been shown that the GeneSwitch system can be unreliable and "leaky" when driving RNAi expression and with age, and expression can be induced without RU486 present (Poirier et al., 2008; Scialo et al., 2016). Possible aberrant expression in control flies could be overcome using a different system, for example the AGES system, which induces expression by degradation of GAL80, as this has been shown not to be leaky in old flies (McClure et al., 2022).

Additionally, there may be compensatory mechanisms at play with age. While overall midgut mRNA levels of *lanA* and *lanB1* seem to be increasing at day 51 (**Figure 13**), a study looking

at age-related changes in ISCs specifically found that in geriatric flies (>70 days), the chromatin regions for *lanB1* and *lanB2* were less accessible, and *lanB2* RNA levels in ISCs were decreased at that age (Tauc et al., 2021). As the contribution of Laminins from ISCs/EBs is likely to be much smaller than from other sources, these other tissues may adapt their own Laminin secretion to compensate for a decreased expression from ISCs/EBs, which could lead to a different BM composition.

The ECM is a dynamic system, containing more stable Collagen IV and Laminin meshworks while other ECM proteins move about more freely within this scaffold, shown in *C. elegans* and mice (Keeley et al., 2020; Trier et al., 1990). Modifications to BM Laminins have been implicated in various effects on cell migration. While a Laminin meshwork is required for cell migration during tissue formation in development, cleaving Laminin to promote cell detachment is also a method used to enhance some types of metastases (Gialeli et al., 2011). Meanwhile, cleaving Laminin subunits can also increase cell attachment (H. Lee et al., 2023). This shows that there are many different functions for Laminins in different situations and tissues, and further study is needed to determine the role of Laminins within the adult midgut and how protein levels and localisation change with age.

5.3.4 Signalling pathways downstream of laminins

In adult *Drosophila* ISCs, several integrin subunits are required for ISC maintenance and proliferation, as are the proteins Talin/Rhea and Integrin-linked kinase, which convey integrin signals to the cytoskeleton. Downstream pathways have not been identified, as individually activating the Wg, JAK/STAT, or EGFR pathways in ISCs does not rescue the loss of integrin-mediated ISC maintenance and it was therefore hypothesised that integrin-mediated adhesion to the BM may facilitate short-range signalling from the VM to maintain the ISC niche (Lin et al., 2013). Targets of the Notch and EGFR signalling pathways were tested for changes in expression levels upon ISC/EB-specific LanB2 knockdown for 7 days using RT-qPCR, but this did not show any significant results.

An initial foray into looking at the effect of LanB2 knockdown on other BM components did not yield any results, with the antibody against Collagen IV not showing any staining on control or knockdown samples. The antibody was designed against human Collagen IV and may therefore not detect *Drosophila* Collagen well. Additionally, as this knockdown was only

induced for seven days, it may not have had any substantial effect on Collagen deposition, as both Collagen and Laminin turnover in the ECM are much slower than other components.

Short-term future work should include testing further signalling pathway components using RT-qPCR with the samples that already exist, as this was unfortunately not possible within the time given, as well as creating samples with longer LanB2 knockdown which might show stronger results.

5.3.5 Future directions

While the results described above give an initial insight into epithelium-derived Laminin, there are still many questions that need to be answered. As a way of addressing the problem that the three different RNAi lines did not all show the same results, *lanB2* knockout rather than knockdown could be used to clarify these contradicting results.

Due to a lack of LanB2-specific antibody commercially available, enhancer or protein traps would be useful tools for further study of LanB2 expression.

Changing LanB2 expression in different contexts, such as inducing knockdown/overexpression at different timepoints or after injury when the ECM has been disrupted, could provide more insight into the role that ISC/EB-derived LanB2 can play and which signalling pathways it may be involved in. Making a driver line with *lanA* or *lanB1* reporters could also be used to look at the effect of LanB2 knockdown/overexpression on the other Laminin subunits, e.g., to see if LanB1 accumulates in the ER and leads to a UPR, as was seen in other tissues (Petley-Ragan et al., 2016).

As described above, the AGES system could provide a better alternative when looking at changes in expression in later life to prevent knockdown in control samples.

Chapter 6: Conservation of Tsf2 and LanB2 expression in mammalian epithelia

6.1 Introduction

The results described in the chapters above were carried out using *Drosophila melanogaster* as a simple *in vivo* model system. In order to see if any phenotypes seen in *Drosophila* may be found in mammalian systems, both human prostate tissue samples and iPSC-derived endodermal spheroids were analysed as no human intestinal tissue was available. As both the prostate and the *Drosophila* midgut are made of an endoderm-derived epithelium that contains stem cells, these similarities allow for a comparison between the two systems.

6.1.1 The roles of Tsf2 and LanB2 in mammalian systems

DIOPT Version 9.0 (Y. Hu et al., 2011; http://www.flyrnai.org/diopt) was used to identify the closest human orthologs for *Drosophila* LanB2 and Tsf2. Laminin subunit gamma 1 (LAMC1, 58% protein similarity) and Melanotransferrin (MTf, 46% protein similarity) were identified as having the best score and reverse score for LanB2 and Tsf2, respectively. Due to time constraints, only one of the Laminin γ subunits was investigated.

6.1.1.1 Melanotransferrin

As described above in Chapter 4, MTf was discovered as a melanoma marker and has been found to be expressed in several types of cancer. It plays a role in tumour growth and metastasis, with a high expression correlating with poor patient outcome. While one study using immunohistochemistry (IHC) did not find MTf expression in the normal adult prostate and only one out of five prostate cancer samples showed positive staining (Natali et al., 1987), a later study using the dot blot method did see MTf expression in the adult prostate, albeit at low levels (Richardson, 2000).

The Human Protein Atlas reports low MTf expression in normal prostate tissue, with a mix of both low and moderate expression in prostate cancer (Uhlen et al., 2015, 2017; https://www.proteinatlas.org/).

6.1.1.2 Laminin C1

As in *Drosophila*, mammalian Laminins consist of a heterotrimer made up of α, β, and γ chains. The human genome contains five α chains, three β chains, and three γ chains, creating a much more complex interplay between the different subunit combinations compared to the two Laminin trimer combinations possible in *Drosophila*. Different tissues express different Laminin trimers, and developmental expression also differs from adult tissues (reviewed by Aumailley, 2013).

Like with *Drosophila* LanB2, complete loss of LAMC1 during development is lethal in mice due to the requirement of basement membrane formation during embryogenesis (Smyth et al., 1999). LAMC1 is the most commonly expressed γ chain (Siler et al., 2000). A study looking at adult mouse LAMC1 expression found that loss of the protein in adult mice is lethal, and that the small intestine may be the tissue with the highest Laminin turnover in mice as it experienced a large reduction in Laminin protein upon LAMC1 knockout, whereas other tissues (heart, lung, liver, kidney, and spleen) showed minimal protein level changes after three weeks. LAMC1 deletion causes intestinal proliferation and loss of gut barrier function, potentially by affecting Indian hedgehog signalling (Fields et al., 2019). The mesenchyme of the small intestine is thought to be the main source of LAMC1 (Fields et al., 2019).

Increased LAMC1 expression has been associated with several cancers, including gliomas (J. Liu et al., 2019), malignant meningiomas (H.-L. Ke et al., 2013), later stage endometrial cancer (Kunitomi et al., 2020), uterine carcinoma (Kashima et al., 2015), ovarian cancer (Diao & Yang, 2021; Kuhn et al., 2012), triple negative breast cancer (Piovan et al., 2012), hepatocellular carcinoma (Liétard et al., 1997; Zhang et al., 2017), oesophageal squamous cell carcinoma (L. Fang et al., 2021), colorectal cancer (Lou et al., 2016; Peters et al., 2013), and prostate cancer (Nishikawa et al., 2014), and higher expression levels generally correlate with a worse patient outcome and faster recurrence.

Several of these studies have shown that reducing LAMC1 expression in cancers reduces cell migration and invasion and in some cases proliferation as well. Migration and invasion are also reduced upon LAMC1 knockdown in prostate cancer (PCa) (Nishikawa et al., 2014). Post-translational cleaving of the α chain of α5β1γ1 laminin and of the β chain in α3β3γ2 Laminin have been associated with increased PCa cell migration by reducing adhesion of cancer cells to the extracellular matrix (Bair et al., 2005; Udayakumar et al., 2003). The Laminin receptor

integrin α6β1, which binds Laminin α5β1γ1 in PCa, is expressed by the tumour cells and is important for PCa metastasis (Pawar et al., 2007).

In hepatocellular cancer, several potential mechanisms of action have been identified to promote tumorigenesis. The transcription factor Sp1 has been shown to function upstream of LAMC1, and it modulates expression of other genes involved in proliferation and growth as well (Liétard et al., 1997). LAMC1 mRNA is bound by micro-RNA-124 (mi-RNA-124) in hepatocellular cancer. Increased LAMC1 mRNA expression reduces mi-RNA-124 levels and prevents mi-RNA-124 from binding to and downregulating CD151 mRNA, an oncogene involved in proliferation and invasion (Yang et al., 2017).

The Human Protein Atlas reports low glandular expression of LAMC1 in normal prostate tissue, with a mix of both low and moderate expression in PCa (Uhlen et al., 2015, 2017; https://www.proteinatlas.org/).

Other diseases in addition to cancer have been linked to misregulation of Laminin expression, such as the autoimmune disease anti-Laminin γ1 pemphigoid, a skin-blistering disease (Akasaka et al., 2015), ulcerative colitis (Schmehl et al., 2000), and Crohn's disease (Spenlé et al., 2012). This wide range of diseases shows that it is important to understand how LAMC1 functions and what affects its expression.

In order to study these genes in the context of a mammalian epithelium, the prostate was selected as a model system as expression of both genes has been observed in PCa and collaboration with researchers at Newcastle University was able to provide access to prostate tissue samples and generation of endodermal spheroids, with the hopes that this system can be used for further work in the future.

6.1.2 The structure of the prostate

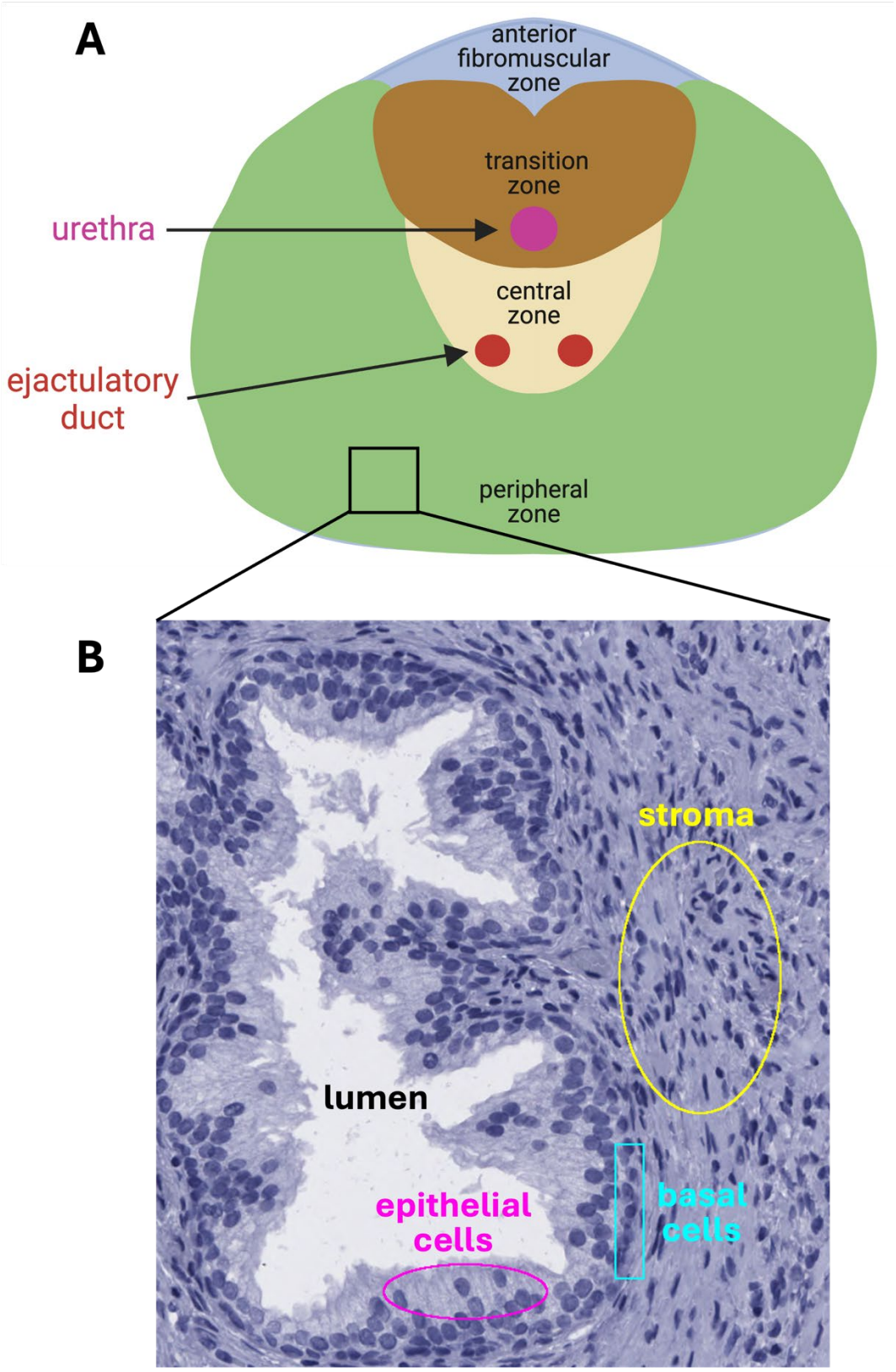

Figure 39: The structure of the human prostate.

(A*) A simplified schematic of a transverse section of the prostate, showing the four regions of the organ. This figure was made with Biorender. (B) Glandular prostate tissue of the peripheral zone stained with H&E, showing the lumen surrounded by columnar epithelial cells (pink) and basal cells (blue). Stromal tissue surrounds the glands (yellow).*

The prostate is an endoderm-derived, walnut-shaped gland located at the base of the bladder, consisting of four main anatomical regions: the anterior fibromuscular zone, the central zone, the transition zone, and the peripheral zone (**Figure 39A**). The peripheral zone is the area that gives rise to most prostatic cancers, while the transition zone is where benign prostate hyperplasia occurs (McNeal, 1969, 1981).

The prostate consists of ducts that branch out into secretory acini, similar to alveoli in the lungs. They are made up of a fluid-filled lumen surrounded by epithelial cells, which are encased by stroma. The epithelial cells are comprised of luminal/glandular, basal, and neuroendocrine cells. The apical side of luminal cells face the lumen as columnar cells (**Figure 39B**, pink), with a thin row of basal cells surrounding them (**Figure 39B**, blue), while occasional neuroendocrine cells are interspersed. The stromal tissue (**Figure 39B**, yellow) consists of smooth muscle cells, fibroblasts, nerve cells, and blood vessels (Foster & Ke, 1997; Fullwood et al., 2019; Henry et al., 2018; Isaacs, 1994; Shen & Abate-Shen, 2010).

Several stem cell populations have been identified in the murine prostate. There are two unipotent progenitor populations that are responsible for replacing luminal cells and basal cells, while an additional multipotent stem cell population exists in the basal layer that can differentiate into all epithelial cell types (Choi et al., 2012; Ousset et al., 2012). Prostate cancers derived from the different stem cells give rise to slightly different tumour phenotypes (Z. A. Wang et al., 2013).

In humans, prostate stem cells are less well defined. A lineage tracing-like experiment looking at inherited mutations in mitochondrial DNA suggests that there are also stem cells that can form all three epithelial cell types (Blackwood et al., 2011). Further research found bipotent basal progenitor cells that can differentiate into both basal and luminal cells, as well as a unipotent luminal progenitor. Both of these progenitor cells are thought to come from basal stem cells found in niches near the urethra, from which cells move outwards along the glands (Moad et al., 2017).

Delta expression has been identified in prostate basal stem cells (Moad et al., 2017) and Notch signalling is required to for differentiation and to limit hyperproliferation (X.-D. Wang et al., 2006).

6.1.3 Prostatic diseases

With age, there is an increased risk of prostate problems, mainly prostatitis (inflammation), benign prostatic hyperplasia (BPH), and PCa. BPH has been described as a "reawakening" of the proliferation-induction potential of the stroma, with new ducts forming in the transition zone (McNeal, 1978). By the age of 50 - 60 years old, half of people with prostates will have developed symptomatic BPH, although the process is likely to start at an age as early as 30 years old (Berry et al., 1984). While the disease does not develop into cancer, the tissue enlargement does cause a decrease in quality of life, e.g., lower urinary tract symptoms due to the prostate's proximity to the bladder. The cause for BPH development is not known, although it has been linked to several factors including obesity, metabolic anomalies, and hormonal changes (Aaron et al., 2016).

After lung cancer, PCa is the second leading cause of cancer-related deaths in men, with the five-year survival rate dropping to 30% for metastatic PCa (Buskin et al., 2023). Initial PCa treatment consists of surgical options and radiotherapy, followed by androgen depletion therapy, as androgens are required for the development and maintenance of the prostate tissue, and depletion has an inhibitory effect on tumour growth (Cunha et al., 1987; Huggins & Hodges, 1941). The cancer can return as metastatic castration-resistant prostate cancer, which is lethal (Saad & Hotte, 2010).

6.1.4 Methods to study prostate disease

As there are several big differences in prostrate structure and development between humans and mice (Ittmann, 2018) and access to tissue samples is not always readily available, there has been a big drive towards both 3D cell culture as well as other preclinical models to further investigate normal development and changes that occur in PCa (reviewed by Buskin et al., 2023).

Organoids are *in vitro* 3D models, established from stem cells (embryonic, adult, or induced pluripotent stem cells), that self-organise, are self-sustaining, and recapitulate the *in vivo* structure of the tissue they are forming. They provide an advantage over 2D models as it is possible to incorporate multiple cell types and a better representation of the environment including the surrounding extracellular matrix. They can be established using cells from patients, both from healthy and from diseased tissues. Spheroids are also 3D *in vitro* models,

although less complex than organoids as they do not have the same level of organisation (reviewed by Białkowska et al., 2020; Buskin et al., 2023; X. Jiang et al., 2023).

6.1.5 Chapter aims

This chapter aims to look for conserved expression of the orthologs of *Drosophila* LanB2 and Tsf2 in mammalian epithelia, which may suggest that the orthologs share a conserved role. Additionally, spheroid formation is explored to see whether it can be used in the future as a cell culture system to study the expression and functions of target genes identified in *Drosophila*.

6.2 Results

6.2.1 Definitive endoderm generation using 3D spheroid culture

3D cell culture was used to grow spheroids. 30 wells were set up with 1000 iPSCs each in a 96-well plate. While half were treated with standard stem cell growth medium as a control, the rest were treated additionally with 100ng/mL of Activin A in order to induce endoderm development. Three spheroids for each condition were selected and imaged on day 0, 1, 3, and 5 of differential treatment (**Figure 40**). While not statistically significant, there is a trend towards a difference in area between the control and treated spheroids on day 5, with control spheroid area measuring 3773 ± 480 μm (mean ± SEM) and treated spheroid area measuring 2265 ± 414 μm (**Figure 41**).

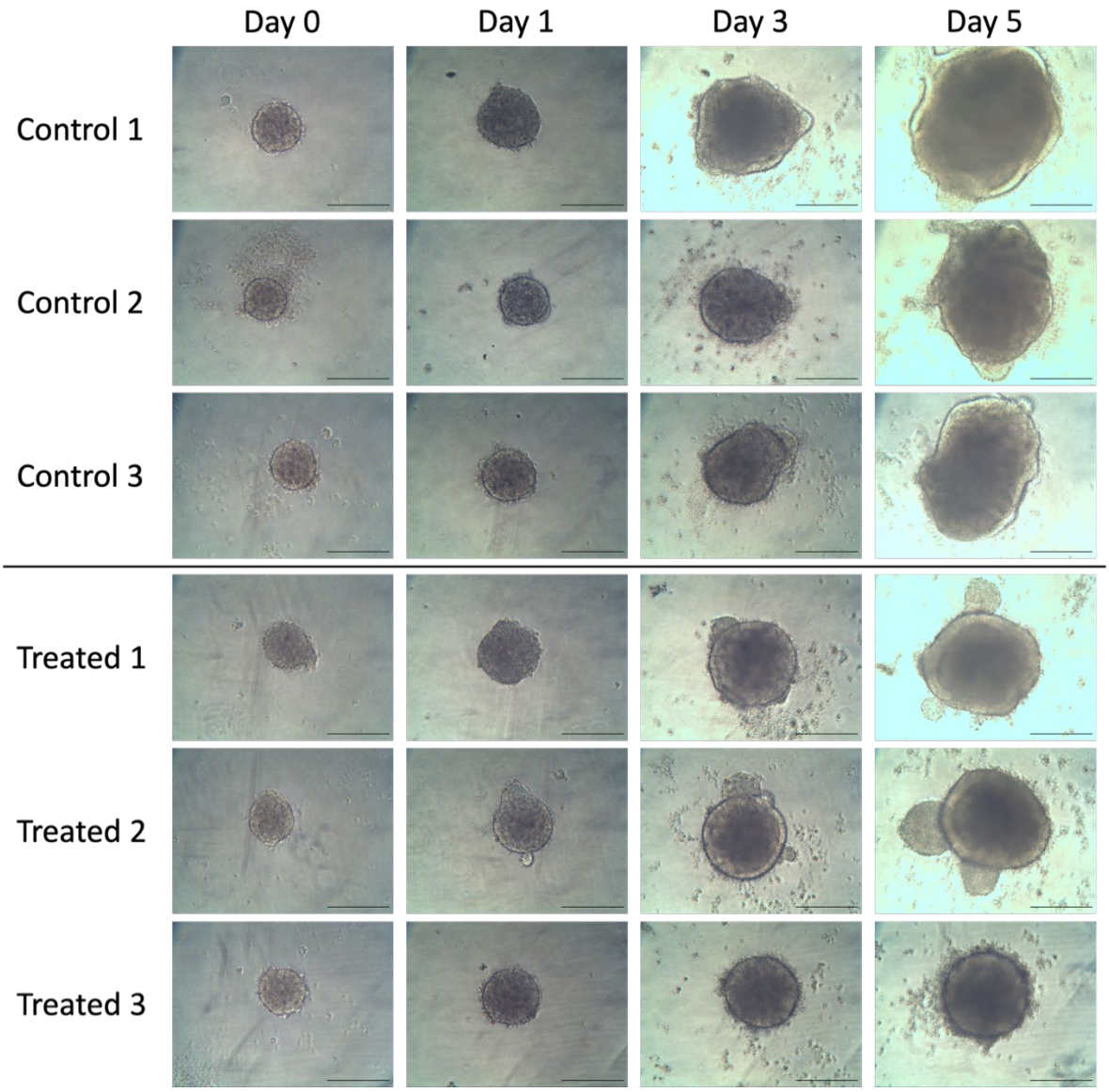

Figure 40: iPSC spheroid growth over the course of 5 days.

Images of spheroids taken at 10X zoom on day 0, 1, 3, and 5 after culture set-up. Control = growth medium only, Treated = growth medium + 100ng/mL Activin A for definitive endoderm differentiation. n = 3. Scale bar = 30 µm.

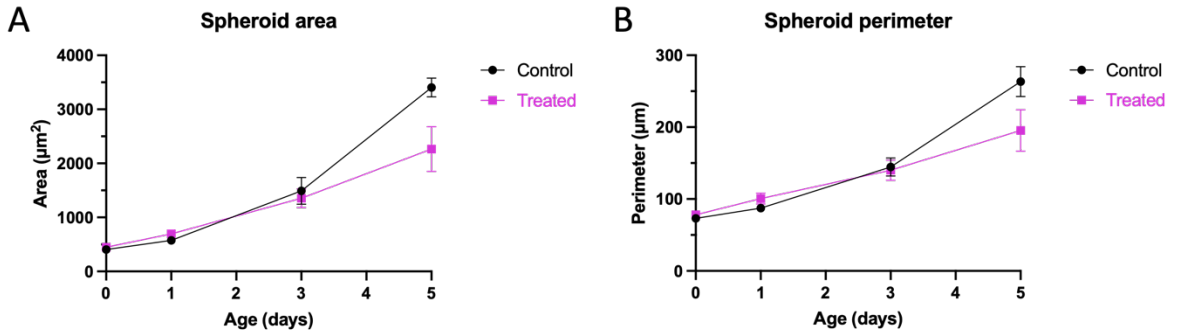

Figure 41: Quantification of iPSC spheroid growth over the course of 5 days.

(A) Change in spheroid area of control and treated spheroids over time. (B) Change in spheroid perimeter of control and treated spheroids over time. Control = growth medium only. Treated = growth medium + 100ng/mL Activin A for definitive endoderm differentiation. Data is shown as mean ± SEM, n = 3 per condition. Calculated using an unpaired t test.

6.2.2 Gene expression in definitive endoderm

Two sets of five spheroids per condition were taken and sectioned for IHC staining. This was not successful, as neither the antibody stain nor the Haematoxylin & Eosin (H&E) stain were visible on the slides (data not shown).

10 spheroids each were combined to create samples for control and treated spheroid RNA extraction and cDNA synthesis on day 5. Due to delayed arrival of primers the RT-qPCR analysis could not be carried out.

6.2.3 Immunohistochemistry staining of prostate tissue

BPH as well as primary PCa patient tissue samples were stained for MTf and LAMC1 expression using immunohistochemistry. Patient 1 (sample 11972) was taken from a prostate displaying BPH. Patients 2 (sample 12910) and 3 (sample 12782) had primary PCa, with less and more severe stages of the disease, respectively.

The negative controls without primary antibody show the structure of the prostate tissue. **Figure 42A** shows BPH, with frequent glands visible throughout the tissue. **Figure 42B** and **C** show PCa, with a loss of the clear gland structure due to tumour growth and uncontrolled proliferation. Some non-specific binding can be seen in the negative controls, mainly at the edge of the tissues and very occasionally in the stroma (**Figure 43**).

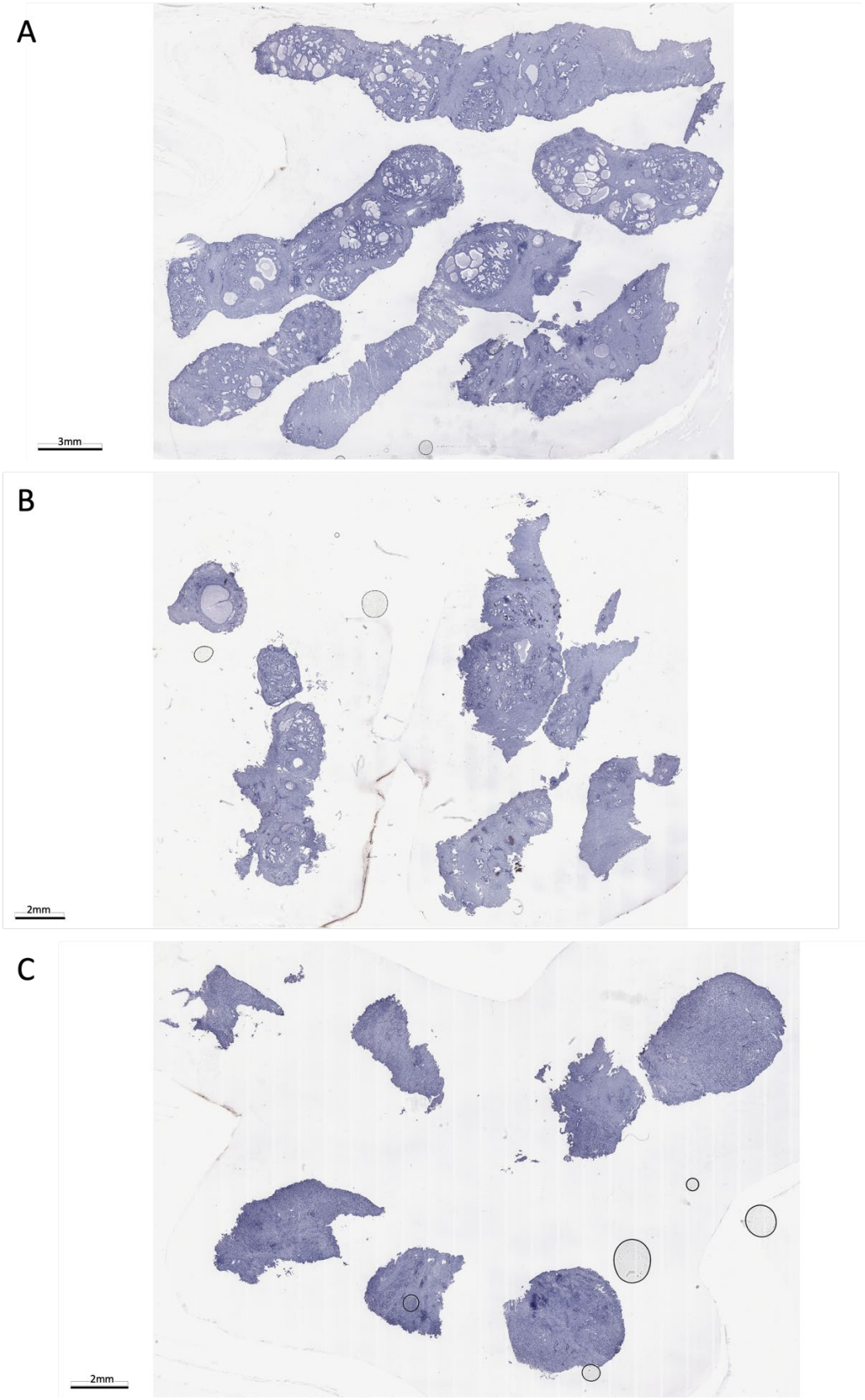

Figure 42: Negative control IHC staining of prostate tissue samples.

No-primary negative control staining shows tissue structure in benign prostate hyperplasia from patient 1 (A), and primary prostate cancer, with both less (B, patient 2) and more advanced (C, patient 3) stages. Scale bars shown in the bottom left corner on the images (A = 3mm, B+C = 2mm).

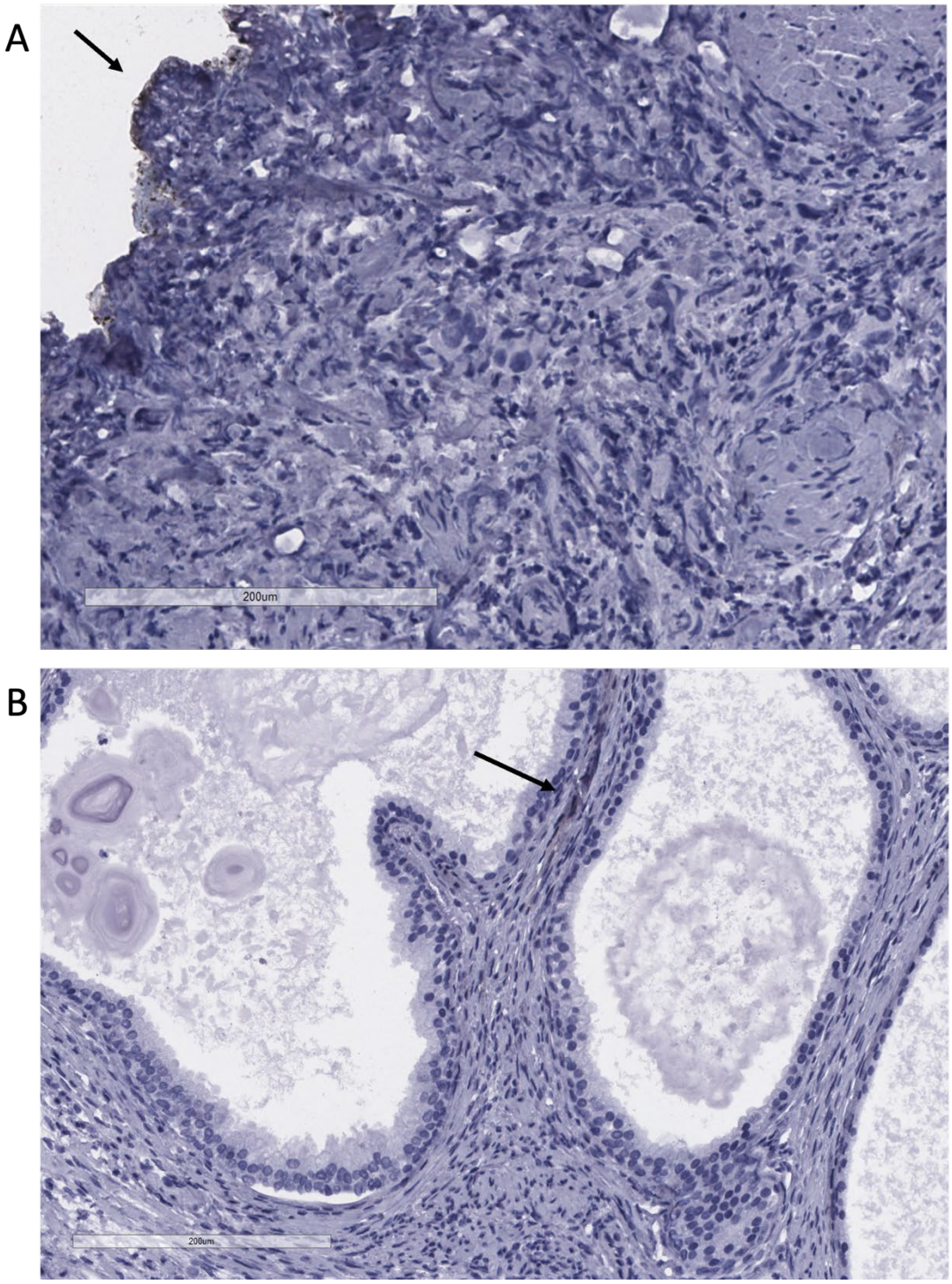

Figure 43: No-primary negative control IHC staining.

Some non-specific binding is visible in the negative controls at the edge of the samples (A) and in the stroma (B), shown with arrows. Scale bar = 200 µm.

6.2.3.1 Melanotransferrin

Figure 44 shows an overview of the staining of all three samples for MTf. The following three figures show higher magnification of MTf staining. In BPH tissue, there is occasional stromal staining visible, although this is very sparse (**Figure 45**). In PCa tissue, the staining is again of varying intensity, with some areas in the sample from patient 2 showing light stromal expression (**Figure 46A**), while others also show luminal cell cytoplasmic staining (**Figure 46C**). In the sample from patient 3, which is the more advanced PCa sample, less staining was visible, with the staining looking very similar to the non-specific binding that was seen in the negative control samples (**Figure 47**).

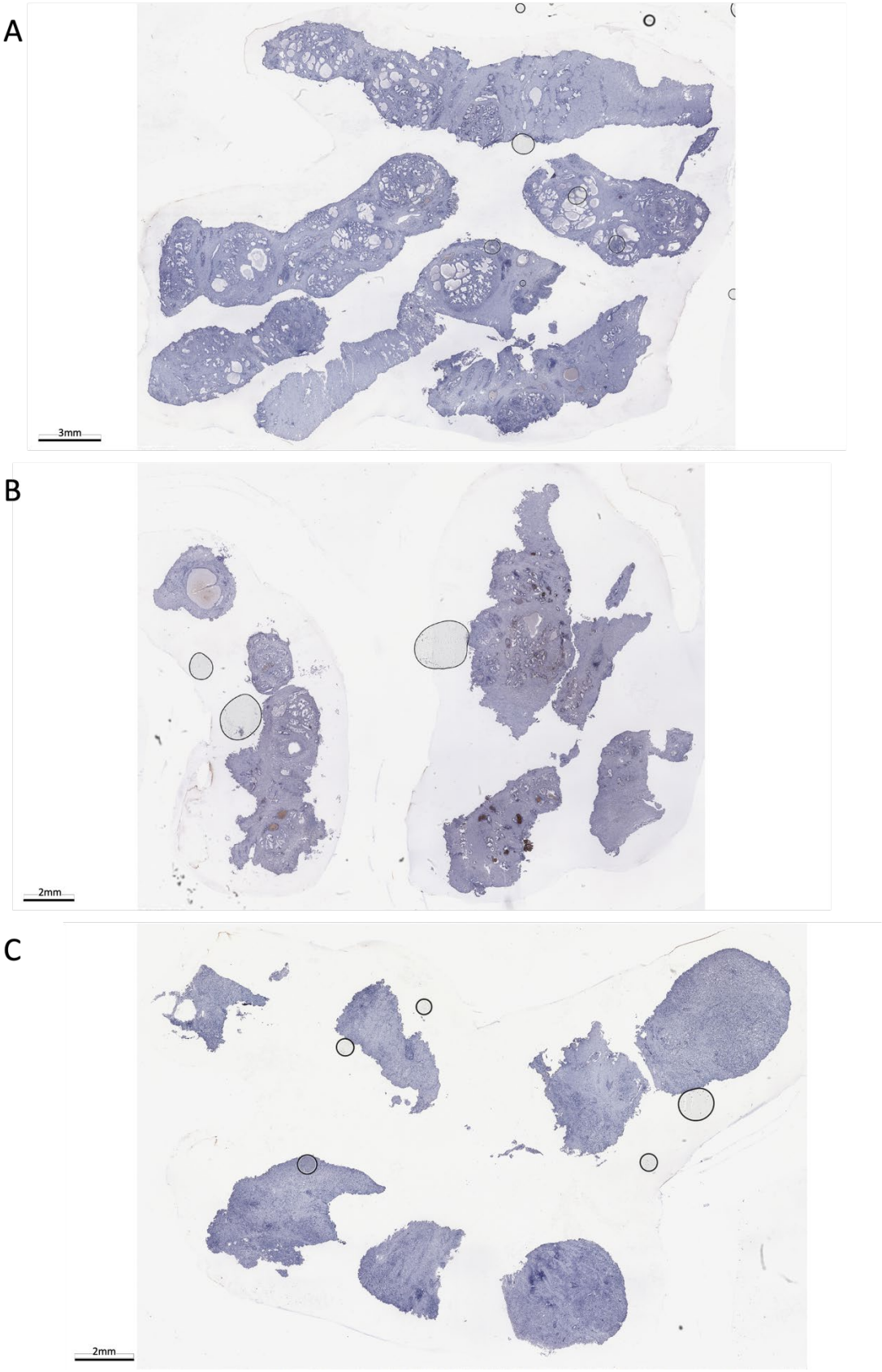

Figure 44: Melanotransferrin IHC staining of prostate tissue samples.

MTf expression in benign prostate hyperplasia of patient 1 (A), and primary prostate cancer, with both less (B) and more advanced (C) stages in patients 2 and 3, respectively. Scale bars shown in the bottom left corner on the images (A = 3mm, B+C = 2mm).

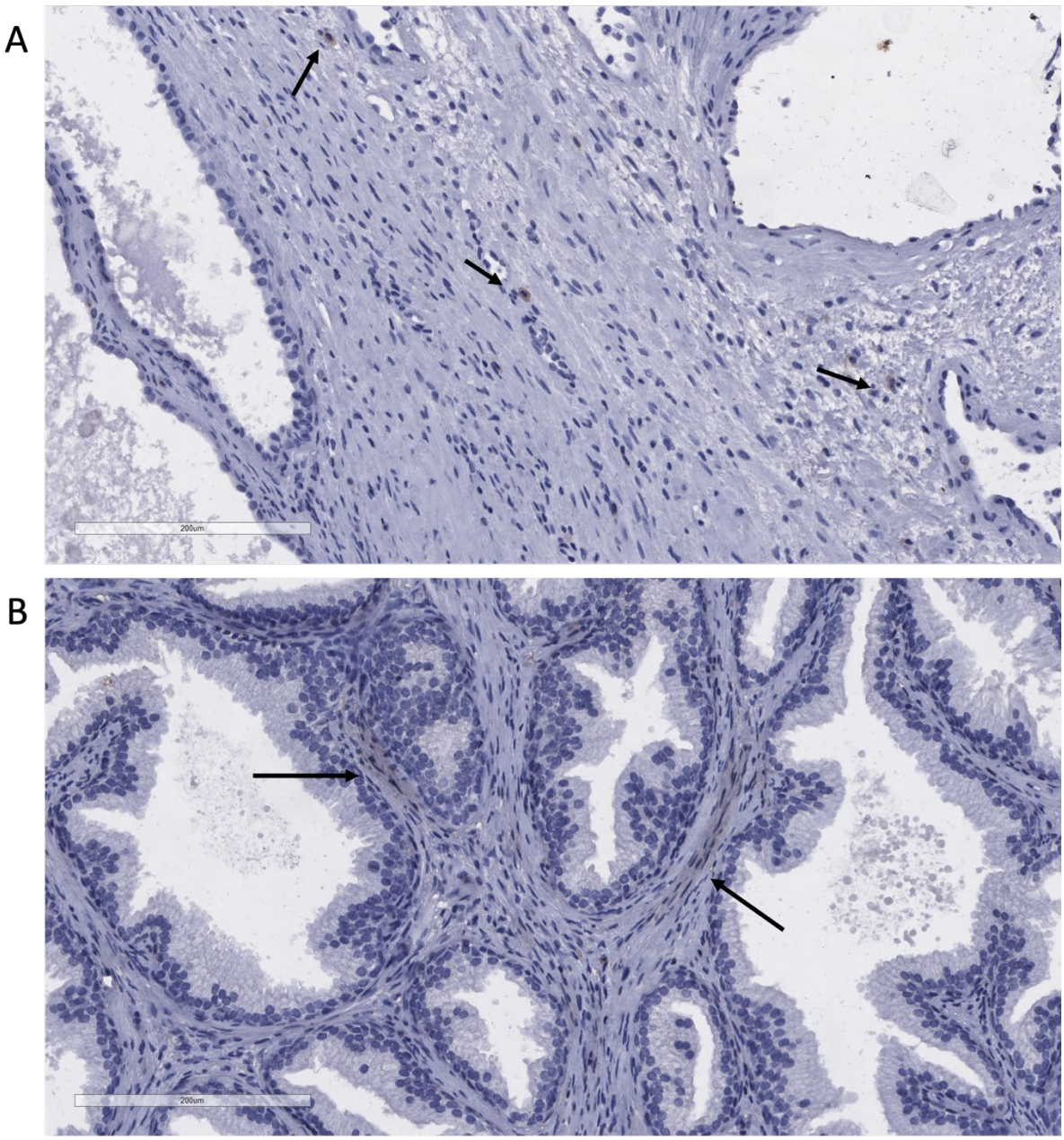

Figure 45: Melanotransferrin expression in BPH tissue, patient 1.

Variable staining levels of MTf are seen in prostate BPH, with examples of positive stains annotated with arrows. Scale bar = 200 μm.

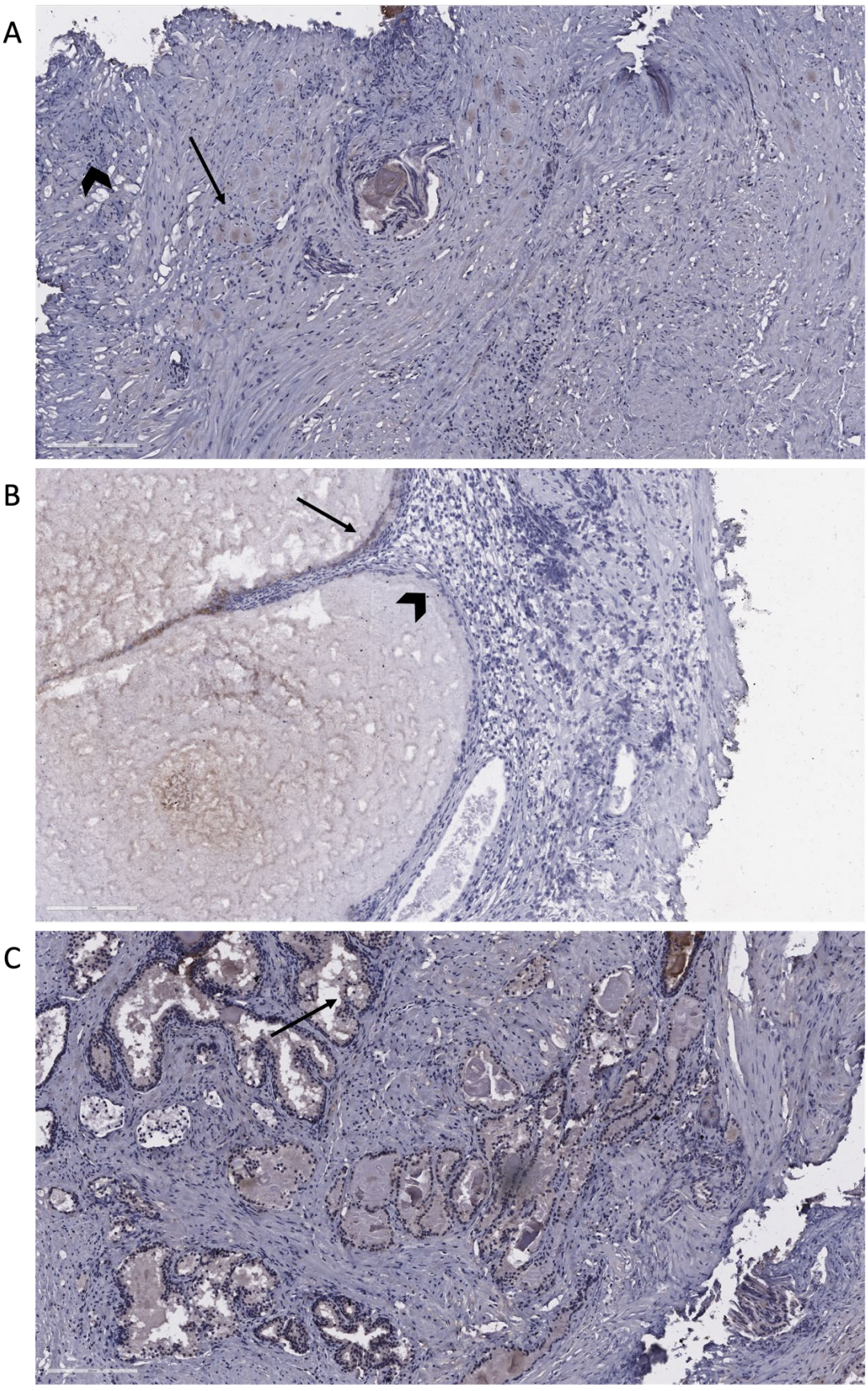

Figure 46: Melanotransferrin expression in primary PCa tissue, patient 2.

Variable MTf staining levels are seen in prostate cancer, with both positive stain (arrow) and absence of staining (arrowhead) in similar areas annotated. Scale bar = 200 µm.

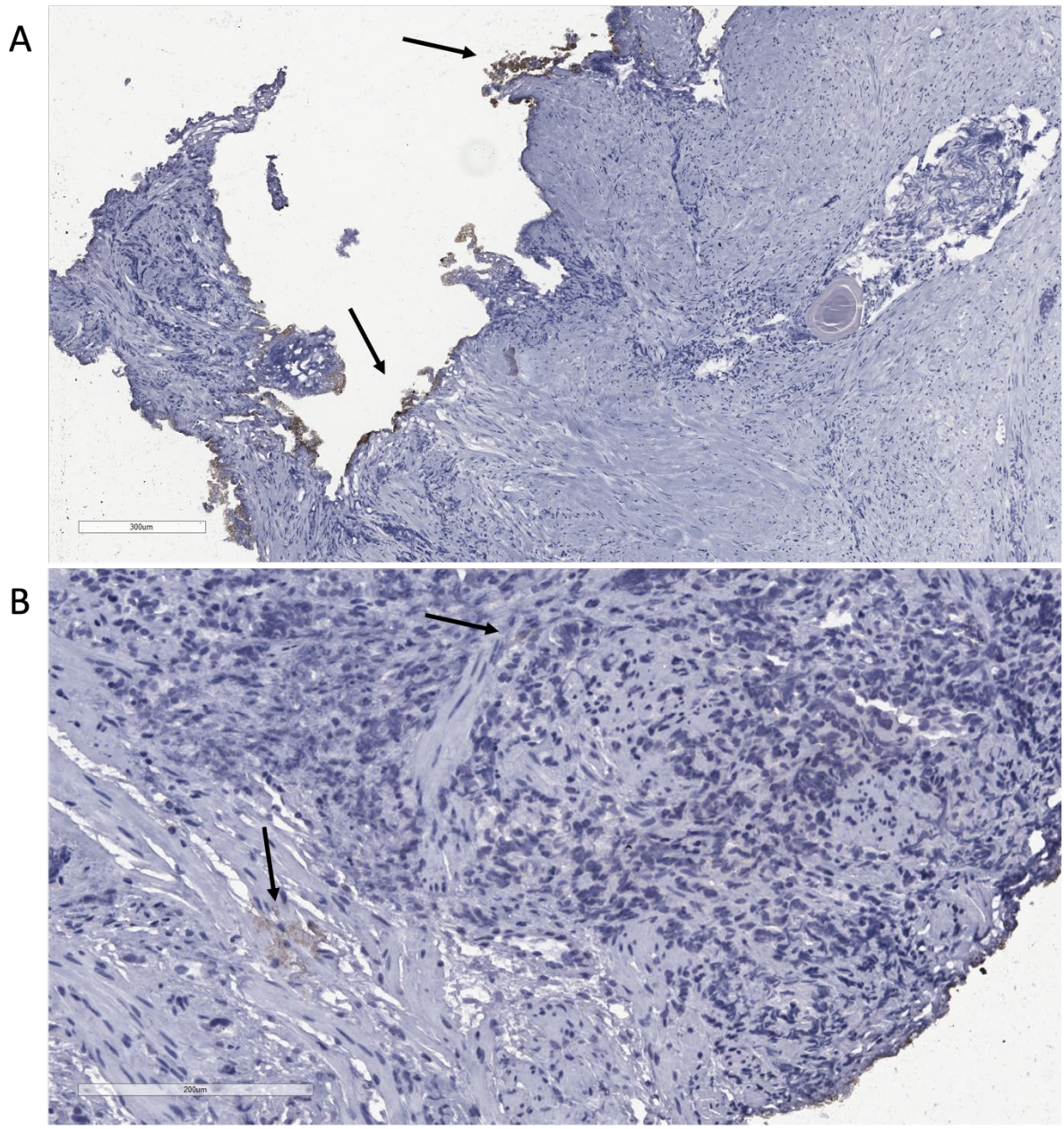

Figure 47: Melanotransferrin expression in more advanced PCa tissue, patient 3.

Variable MTf staining levels are seen in prostate cancer. Scale bars shown on image (A = 300 µm, B = 200 µm).

6.2.3.2 Laminin C1

LAMC1 staining was also variable, with different areas on the slides showing different levels of staining (**Figure 48**). In BPH tissue, most stromal tissue showed LAMC1 to be present. Several glands also showed LAMC1 located around the basal cells (**Figure 49B,C**), and occasionally positive stain was also visible in luminal cells (**Figure 49A**). In PCa tissue, some areas of the samples had very high expression, e.g., **Figure 50A** and **Figure 51A,B**, while other areas had less. The areas with increased staining had expression both in the stroma as well as basal and luminal cells.

Due to the image format it was not possible to split the image channels into H&E and antibody staining in order to quantify antibody staining intensity.

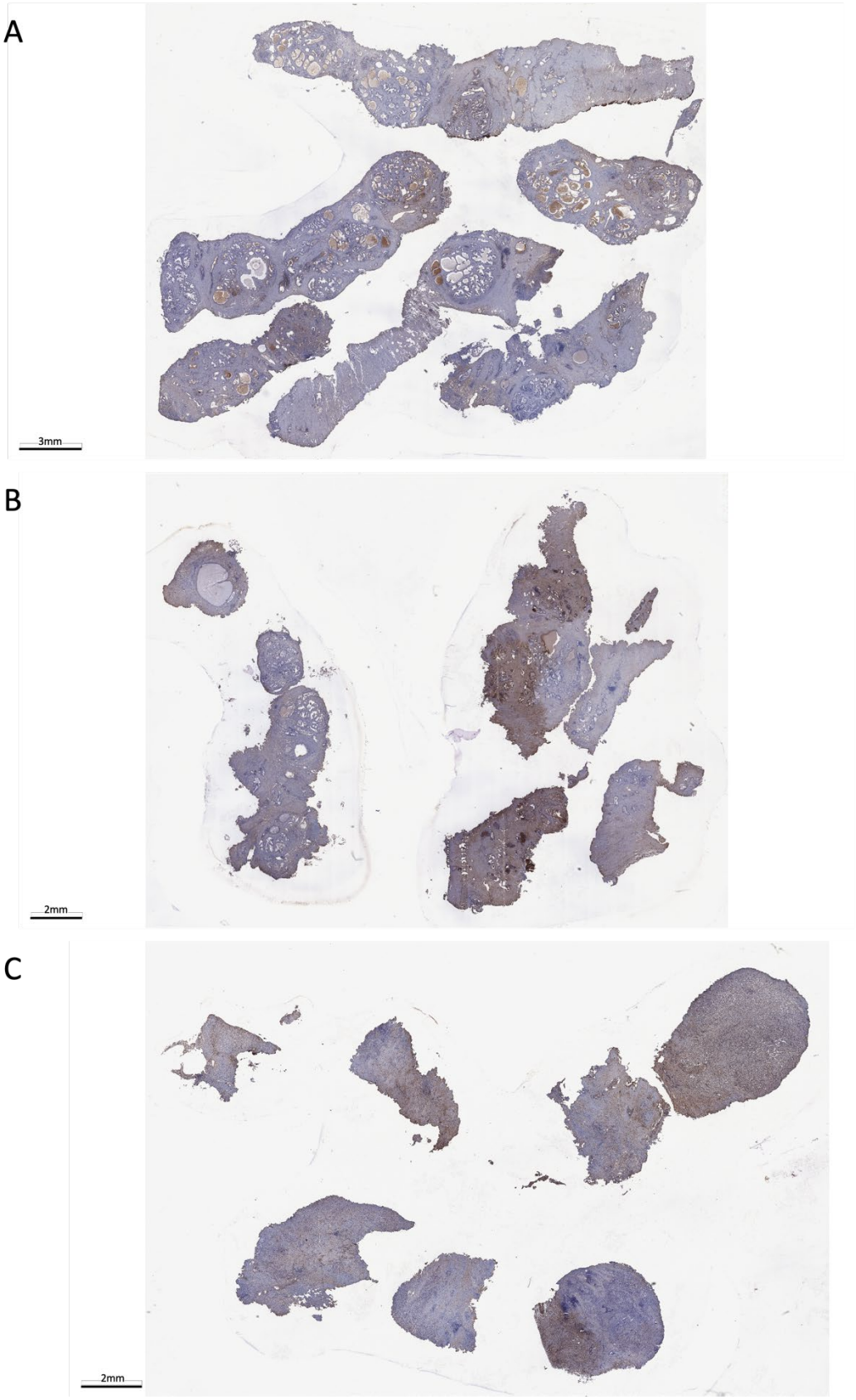

Figure 48: Laminin C1 IHC staining of prostate tissue samples.

LAMC1 expression in benign prostate hyperplasia of patient 1 (A), and primary prostate cancer, with both less (B) and more advanced (C) stages in patients 2 and 3, respectively. Scale bars shown in the bottom left corner on the images (A = 3mm, B+C = 2mm).

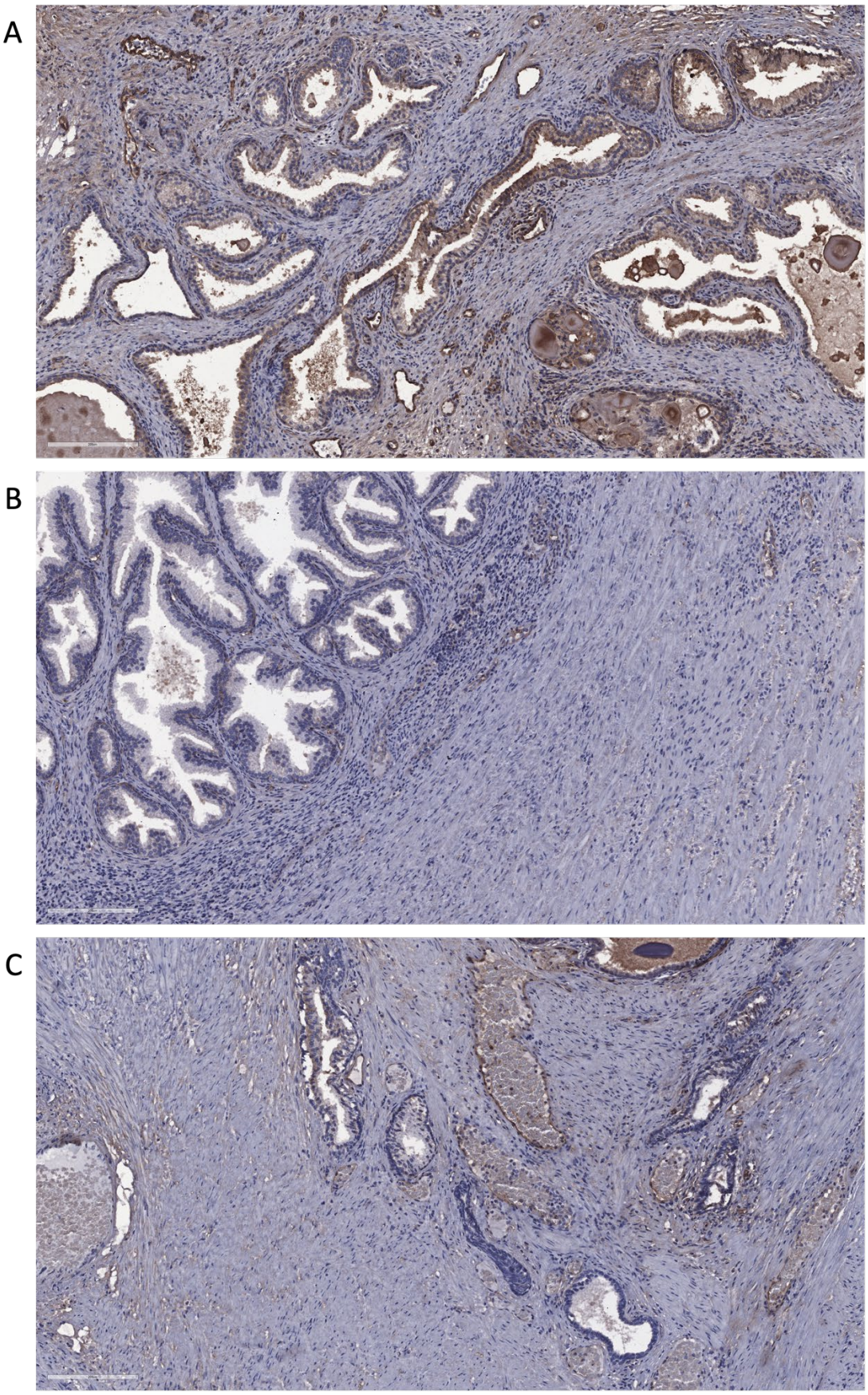

Figure 49: Laminin C1 expression in BPH tissue, patient 1.

Variable LAMC1 staining levels are seen in prostate BPH. Scale bar = 200 µm.

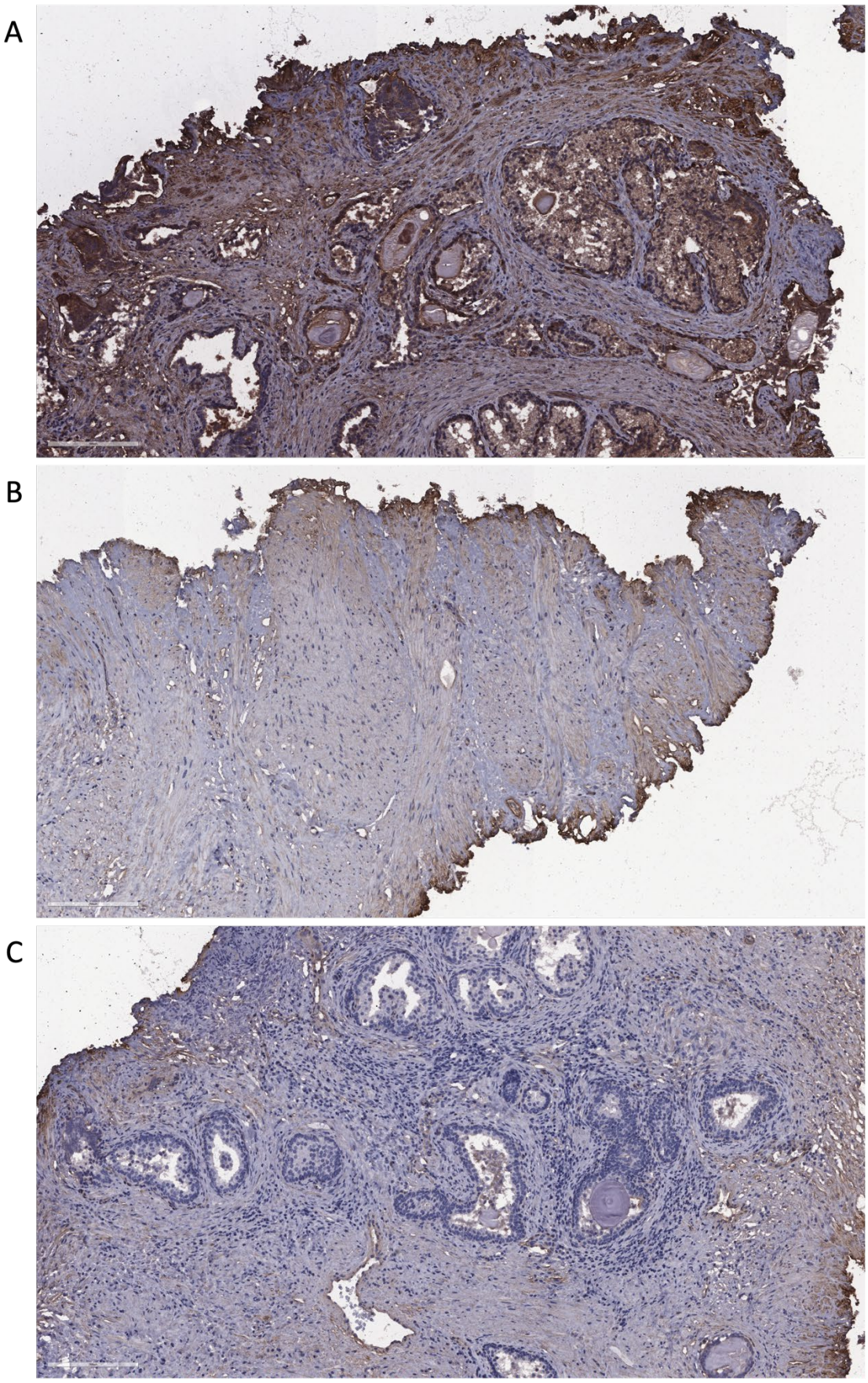

Figure 50: Laminin C1 expression in primary PCa tissue, patient 2.

Variable LAMC1 staining levels are seen in prostate cancer. Scale bar = 200 µm.

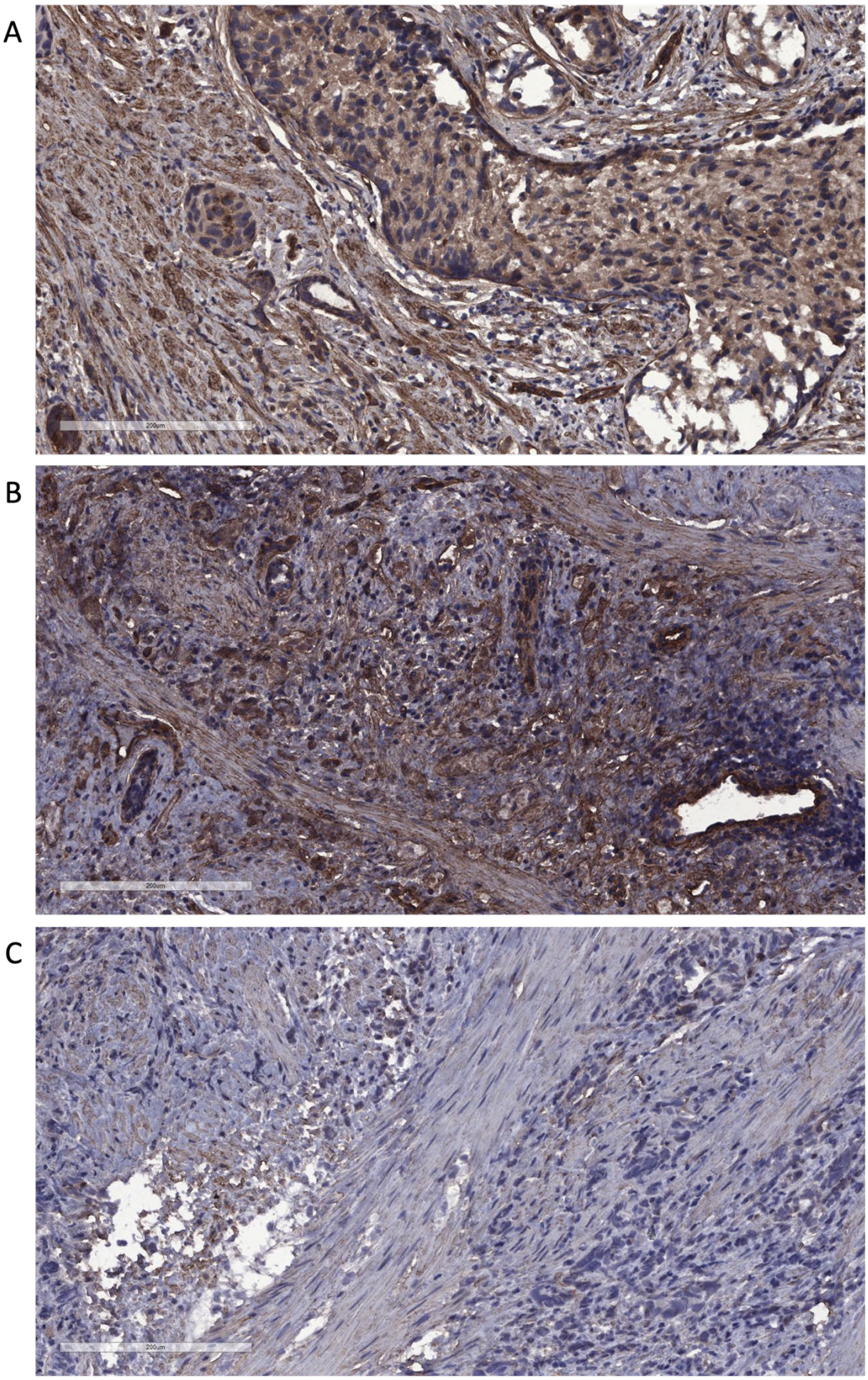

Figure 51: Laminin C1 expression in primary PCa tissue, patient 3.

Variable LAMC1 staining levels are seen in prostate cancer. Scale bar = 200 µm.

6.3 Discussion

In this chapter, expression of the human orthologs of LanB2 and Tsf2 were looked at in the context of prostate tissue. While staining results were variable, they do seem to indicate that both proteins are expressed in the prostate at a range of levels. Furthermore, iPSC-derived spheroids were grown for 5 days and showed signs of endoderm development.

6.3.1 Spheroid differentiation into definitive endoderm

The trend towards a difference in area between the control and treated spheroid areas, as well as the budding seen in the spheroid images, may indicate that the treated spheroids were indeed differentiating into definitive endoderm, as they were not purely proliferating and increasing in size as was seen in the control spheroids. This suggests they could be used as pre-clinical models for endoderm development.

6.3.2 MTf and LAMC1 expression in prostate tissue

On all slides that had visible staining, the stain intensity was very variable, with some tissue sections having regions with both strong and with almost no staining. This may be due to some difficulties that occurred during the staining process, meaning some areas of slides may not have been adequately exposed to the reagents. This makes it hard to draw conclusions from the IHC staining.

Another thing that may have contributed to varied staining is the grade of cellular heterogeneity that is found in cancer, with a potential six different types of cancer-associated fibroblasts (CAFs) suggested in human PCa (Sugimoto et al., 2006; Vickman et al., 2020). Different fibroblast types have also been discovered in BPH (Joseph et al., 2021). These can express different genes and at different levels and can have a tumour-promoting or -suppressing effect in a context-dependent manner (Kalluri, 2016). Not only do CAFs themselves express different genes, but they also respond differently to signalling pathways (Kiskowski et al., 2011). Signalling niches can be created on as small a scale as individual glands (Joseph et al., 2021). CAFs, unlike fibroblasts taken from healthy tissue, have the ability to induce tumorigenesis in BPH cells, even though BPH is not normally a precursor to cancer (Ao et al., 2007; Franco et al., 2011).

6.3.2.1 Melanotransferrin

Although some areas of the tissue samples seemed to show real staining, e.g., **Figure 46C**, the overall level was extremely low. While the antibody used for this experiment was labelled as unsuitable for IHC, which may have led to an insensitivity to any MTf present, this does line up with results found in other studies that showed only low MTf expression in the prostate (Natali et al., 1987; Richardson, 2000). Due to the scarcity of expression visible it is difficult to determine the localisation of MTf in the prostate, however **Figure 46C** showed luminal cell cytoplasmic staining, while some other images also show stromal localisation. The fact that there was only staining visible in the earlier PCa sample (patient 2) but not the more advanced stage sample (patient 3) suggests that these staining results may not be representative of real MTf expression, as MTf expression correlates positively with a worse outcome in cancers (Yen et al., 2023). Alternatively, this may be due to differences in tumours between patients showing heterogeneous expression.

Without further research it is difficult to determine whether prostatic stem or progenitor cells express MTf, but if this is the case, luminal progenitor cells may be a source as some MTf expression was seen in luminal cells.

6.3.2.2 Laminin C1

The staining of LAMC1 was also very variable. Strong staining in some samples suggests that LAMC1 is indeed expressed in the prostate, and the PCa samples had several regions with stronger staining than was seen in BPH tissue, which may indicate that LAMC1 expression was upregulated in those samples.

Prostate-derived fibroblasts have been shown to produce Laminins, including LAMC1, in 3D spheroid culture, although the study did not find an upregulation of expression of LAMC1 when the fibroblasts were co-cultured with PCa cells (Ojalill et al., 2020). Ojalill et al also showed that one of the two PCa cancer cell lines tested in the study was able to produce α3, β3, and γ2 Laminin subunits when cultured on its own (Ojalill et al., 2020). Laminin α3β3γ2 is upregulated in co-culture of fibroblasts and PCa cells and has also been found to be expressed by cancer cells in other cancer tissues, for example in cutaneous squamous cell carcinoma (Siljamäki et al., 2020).

The time given only allowed for one attempt at IHC staining, so a repeat may be able to clarify further the expression levels and pattern. As fibroblasts produce a lot of ECM components in

the prostate (Ojalill et al., 2018), it is not surprising that there is LAMC1 staining in the stromal tissue. Similarly in the small intestine, the mesenchyme has higher LAMC1 expression than epithelial cells (Fields et al., 2019). Staining was also visible in the region of the basal cells, which is where multipotent progenitor cells are thought to be located. Further experiments such as additional staining and cell type-specific gene expression analysis would need to be carried out to determine whether these progenitor cells express LAMC1. Other γ chain Laminins could also be investigated to give a wider picture of *Drosophila* LanB2 orthologs, but this was not possible within the scope of this project.

6.3.3 Conclusion and future directions

The results shown above were an initial, mainly qualitative foray into the mammalian significance of the research carried out in *Drosophila*. Following this up with immunofluorescent staining could be used to complement the IHC analysis in a more quantitative way. Furthermore, it may offer more sensitivity to detect low level expression, as it is difficult to determine if the MTf staining is real or non-specific as seen in some of the negative controls. It would also allow for easier co-staining with cell type-specific antibodies to better determine exact localisation of the genes of interest. It was not possible to do this within the timescale of this project.

Additional MTf IHC staining could be carried out using an alternative antibody to compare whether the lack of visualisation was due to a lack of expression or due to antibody unsuitability.

It would also be interesting to compare the staining patterns to healthy tissue. In this thesis BPH was used to compare to cancer expression, however BPH, while less dangerous, is also diseased, non-homeostatic tissue. Unfortunately, no healthy tissue was available for this thesis.

As the work in the previous chapters carried out in *Drosophila* focuses on the posterior midgut, comparing this to human small intestinal tissue samples or to intestinal models may provide a better comparison of any conclusions that may be drawn between the two. Intestinal organoids have been successfully generated (Sato et al., 2009, 2011) and may allow an easier and quicker alternative to tissue samples.

Chapter 7: Thesis discussion

It has long been known that it is of vital importance that stem cell populations adapt their proliferation rates and the cell fate of their progeny to local demand, and that this is continuously signalled to stem cells from progeny and specific niche cells. However, the stem cells' own contribution to this control has not yet been studied in great detail. It is becoming more evident with a growing list of examples that stem cells are indeed active participants in niche signalling, both to themselves as well as to their progeny.

The *Drosophila* midgut has been used extensively as a model system for looking at stem cells. It is a simplified version of the mammalian small intestine with high enough degree of cell type similarity and genetic conservation to allow conclusions drawn from research in *Drosophila* to give insight into how this organ functions in humans. This thesis has aimed to expand on previous research which has identified *Drosophila* intestinal stem and progenitor cell-specific gene expression (Doupé et al., 2018); in particular, a list of secreted proteins thought to be expressed in ISCs and EBs was studied. Preliminary work to this thesis looked at whether knocking down these genes specifically in adult ISCs and EBs affected midgut homeostasis by looking for potential changes to cell proportions in the midgut. The screen was able to identify several genes that may be involved in normal homeostasis of the adult midgut, as changing their expression led to a change in the proportion of ISCs/EBs, which could indicate a change in proliferation or differentiation. While this is not able to identify genes involved only in non-homeostatic control of stem cells, for example during regeneration, it is a good first indicator as to whether the genes may be important for stem cell regulation.

With age, stem cell populations undergo a range of changes that lead to a loss of homeostasis. This eventually leads to a decrease in health, which is of particular importance as the average lifespan of the human population is increasing due to advancements in science and technology. It is difficult to study ageing in humans as active manipulation of gene expression or tracking cells or proteins is not ethically possible, therefore the use of model organisms such as *Drosophila* is essential to understand how organisms age.

7.1 Age-related changes in midgut gene expression

RT-qPCR analysis of several of the genes thought to encode stem/progenitor cell-secreted proteins was able to give further insight into their expression by comparing midgut expression of three different timepoints in wild-type flies. Day 10 represented young, healthy guts, day 30 represented intestines that are likely to have lost homeostasis and could be in the hyperproliferative stage which occurs prior to the exhaustion of functional stem cells, which was represented by day 51 samples according to previous research carried out in the lab. Unfortunately, this method is a crude approach and not cell type-specific as guts were dissected and the whole midgut was included in the sample, meaning that any expression by tissue surrounding the gut that may have been included in the sample was included in the results. This may mask stem or progenitor cell-specific changes as they make up only a small number of the cells in the gut. Several of the genes tested did however have significant differences in expression between the timepoints and this provides a list of candidates for future work into age-related changes in the intestine.

7.2 Laminin expression in the midgut

The rest of the work in this thesis focused on two of the genes that were found to increase the proportion of stem and progenitor cells in the gut in the preliminary RNAi screen. Knockdown of LanB2, which codes for the only γ chain Laminin subunit in the *Drosophila* genome, resulted in the largest increase in the proportion of stem and progenitor cells. Previous research into Laminins in *Drosophila* has mostly focused on Laminins as a whole and has not looked at individual sources of Laminin in detail. The results in this thesis suggest however that there is an epithelial source of Laminins in addition to the surrounding tissues, which is backed up by single cell sequencing data (Hung et al., 2020) in addition to the targeted DamID results (Doupé et al., 2018). Interestingly, other single cell RNA sequencing research has shown that all *Drosophila* Laminin subunits decrease in expression in ISCs with age, although only the *lanB2* decrease is statistically significant (Tauc et al., 2021). RT-qPCR results described in this thesis however suggest that *lanA* and *lanB1* but not *lanB2* RNA expression increases in midguts with age. This is an interesting contradiction that would benefit from further study, not only on the RNA level but also how this relates to protein expression and variations in expression from different Laminin sources adjacent to the gut such as the muscle and trachea.

As the ECM is essential for supporting the gut, and Laminin meshworks make up one of the main components of the ECM, it was surprising that knocking down the only γ chain, and thereby essentially preventing Laminin secretion from ISCs/EBs, did not show any changes in lifespan, especially as ISC-specific LanA has been shown to be required to maintain normal ISC function via integrin signalling (Lin et al., 2013). It may be possible that ISC/EB-secreted Laminin has a specific role that can be compensated long-term by other sources. Testing the level of LanB2 knockdown in samples with long-term ISC/EB-specific knockdown, as well as carrying out knockout experiments, would be a helpful step to validate the lifespan data in order to integrate it into the existing literature. This is particularly important as the three RNAi lines used did not give consistent phenotypes for how they affect midgut homeostasis.

When looking at conservation of expression and function between *Drosophila* LanB2 and mammalian Laminin, the comparison is complicated somewhat by the fact that there are several γ chains in mammals that have differing expression patterns. LAMC1 is the most similar to LanB2 in terms of protein similarity. Its expression was investigated in relation to prostate cancer through work with collaborators, but no clear conclusions could be drawn from the data available.

7.3 Transferrin 2 expression in the midgut

Not much research has been published on Tsf2 in the fly gut. The main body of work consists of its involvement in hindgut and tracheal septate junction formation during development (Tiklová et al., 2010). The results of this thesis did not show the phenotypes that are typical of loss of SJ components upon Tsf2 knockdown, such as mislocalisation of other SJ components, significantly decreased lifespan, or a Smurf phenotype. Similarly, another SJ protein Neuroglian also acts as a SJ component in other epithelia but not in the midgut. There it is expressed by stem and progenitor cells and regulates proliferation via an independent mechanism (Resnik-Docampo et al., 2021).

As with LanB2, knocking down or overexpressing Tsf2 did not show any significant effect on lifespan. As nothing is known about its function in the midgut, it is hard to say whether any effect on lifespan can be expected as there may be compensatory mechanisms that kick in after an initial loss of homeostasis. It is noteworthy though that while RT-qPCR showed an increase

in *tsf2* mRNA expression in the whole midgut, protein levels decreased in ISCs/EBs, shown with antibody staining.

A very tentative connection was shown between changing Tsf2 expression levels and the JNK pathway. Increased Tsf2 expression showed a decrease in JNK phosphorylation, while Tsf2 knockdown led to significant, albeit very minor, reduced expression of the negative feedback regulator Puc. A decrease in JNK phosphorylation lines up with the phenotypes seen in the midgut, as JNK pathway activation leads to increased ISC proliferation. These results are preliminary and require follow-up experiments for consolidation.

As Tsf2 knockdown/overexpression phenotypes mirrored those of Notch, this was investigated as a possible mechanism by which Tsf2 may be affecting midgut homeostasis. Using a reporter such as *Su(H)GBE-GFPnls* would be likely to give the most representative result of changes in Notch signalling, but these experiments unfortunately did not work and there was not enough time to repeat them. Other avenues of investigating this pathway did not give a concise outcome, with only E(spl)m3-HLH showing a small reduction in expression upon Tsf2 knockdown, while Tsf2 knockdown did not affect E(spl)mβ-HLH and Tsf2 overexpression showed no significant changes in the expression of either gene. This seems to suggest that Notch signalling could be ruled out as a target for mediating the effects of Tsf2 expression changes on homeostasis, but further validation is necessary.

The three different *tsf2-RNAi* lines also showed varying phenotypes on homeostasis. Like for LanB2 these differences need to be examined further to give a reliable result, although the fact that Tsf2 overexpression showed the opposite results when looking at changes in progenitor cell number to the RNAi line used for the majority of this thesis suggests that this RNAi line displays the real phenotype of Tsf2 knockdown in contrast with the other two *tsf2-RNAi* lines.

So far there is no research to suggest that MTf, the mammalian ortholog of Tsf2, has any involvement in cell junctions. MTf expression has been found at low levels in various tissues, but its expression is much higher in cancers and higher MTf expression correlates with a worse outcome for the patients as it results in increased tumour growth and cell migration. This seems to be the opposite to what is seen in the *Drosophila* midgut, where increased expression leads to a decrease in proliferative cells. This is an interesting avenue for future research. Various signalling pathway components can have opposing effects in different tissues, acting in an

oncogenic manner in some and having a tumour-suppressive function in others. This should also be considered when comparing results from different tissues and organisms.

7.4 Limitations of this work

There are several limitations to take into consideration when interpreting the results shown in this thesis.

As mentioned previously, the results comparing gene expression at different ages were not cell type-specific and therefore it cannot be concluded that any statistically significant changes in expression levels occur specifically in ISCs and EBs. The expression of targets selected from this data can be compared to other published resources on age-related changes.

A major point to consider is the differences in phenotypes seen when using RNAi lines from BDSC compared to VDRC, and this could be cleared up by carrying out knockout experiments and/or looking at changes in protein levels after changing gene expression. This could also give stronger phenotypes, as it is not clear if a low level of remaining expression might be sufficient to mask some effects that could be seen with total protein loss.

It is also not clear how strong the knockdown of the genes of interest was with the GeneSwitch system, which was used for the majority of experiments. As a functioning Tsf2 primer was only identified towards the end of this project, there was not enough time to carry out experiments to measure knockdown or overexpression levels. The presence of GFP was initially used as evidence that the overexpression line *UAS-Tsf2-GFP* was being induced in RU50 treated samples, but it was later discovered that the 5961^{GS} line had its own inducible *UAS-GFP* that had not been annotated by the lab that supplied it. When looking at LanB2 knockdown, using a ubiquitous driver did show that the gene was being knocked down, but no significant changes were seen when using the ISC/EB-specific GeneSwitch driver. This could be due to either low knockdown induction using GeneSwitch or, more likely, expression from other cells masking changes in ISCs/EBs. While the GeneSwitch system has been shown to be leaky, with transgene expression in the absence of RU, this has not been seen with the newly developed, auxin-inducible AGES system and so this could be used as an alternative to confirm the results shown.

7.5 Future perspectives

The production of reporters and antibodies for both LanB2 and Tsf2, as well as for any other genes of interest from the RNAi screen that might be studied in the future, will provide a lot of additional information. This can be used to help answer several questions, including exact localisation in the midgut, how protein levels change with age, which different cell types express these proteins, and whether there is any compensation from other sources upon knockdown in stem and progenitor cells.

The loss of homeostasis seen after a 7-day knockdown of both LanB2 and Tsf2 compared to a seeming lack of effect on lifespan is an intriguing relationship that will be interesting to decipher in the future, in particular when comparing *Drosophila* and mammalian orthologs, as complete loss of LAMC1 in mice, both during development and inducible loss during adulthood, is sufficient for lethality.

Overall, these results provide an initial look at two stem- and progenitor-specific secreted proteins and how their expression relates to midgut homeostasis and loss of homeostasis with age. There is still much to learn about how stem cells regulate their environment and change with age, and how this knowledge can be applied to maintain health in old age.

Bibliography

Aaron, L., Franco, O. E., & Hayward, S. W. (2016). Review of Prostate Anatomy and Embryology and the Etiology of Benign Prostatic Hyperplasia. *Urologic Clinics of North America*, *43*(3), 279–288. https://doi.org/10.1016/j.ucl.2016.04.012

Abrass, C. K., Adcox, M. J., & Raugi, G. J. (1995). Aging-associated changes in renal extracellular matrix. *The American Journal of Pathology*, *146*(3), 742–752. http://www.ncbi.nlm.nih.gov/pubmed/7887455

Akasaka, E., Nakano, H., Korekawa, A., Fukui, T., Kaneko, T., Koga, H., Hashimoto, T., & Sawamura, D. (2015). Anti-laminin γ1 pemphigoid associated with ulcerative colitis and psoriasis vulgaris showing autoantibodies to laminin γ1, type XVII collagen and laminin-332. *European Journal of Dermatology*, *25*(2), 198–199. https://doi.org/10.1684/ejd.2014.2499

Alemany, R., Vila, M. R., Franci, C., Egea, G., Real, F. X., & Thomson, T. M. (1993). Glycosyl phosphatidylinositol membrane anchoring of melanotransferrin (p97): apical compartmentalization in intestinal epithelial cells. *Journal of Cell Science*, *104*, 1155–1162.

Amcheslavsky, A., Song, W., Li, Q., Nie, Y., Bragatto, I., Ferrandon, D., Perrimon, N., & Ip, Y. T. (2014). Enteroendocrine Cells Support Intestinal Stem-Cell-Mediated Homeostasis in Drosophila. *Cell Reports*, *9*(1), 32–39. https://doi.org/10.1016/j.celrep.2014.08.052

Antonello, Z. A., Reiff, T., Ballesta-Illan, E., & Dominguez, M. (2015). Robust intestinal homeostasis relies on cellular plasticity in enteroblasts mediated by miR-8–Escargot switch. *The EMBO Journal*, *34*(15), 2025–2041. https://doi.org/10.15252/embj.201591517

Ao, M., Franco, O. E., Park, D., Raman, D., Williams, K., & Hayward, S. W. (2007). Cross-talk between Paracrine-Acting Cytokine and Chemokine Pathways Promotes Malignancy in Benign Human Prostatic Epithelium. *Cancer Research*, *67*(9), 4244–4253. https://doi.org/10.1158/0008-5472.CAN-06-3946

Assémat, E., Bazellières, E., Pallesi-Pocachard, E., Le Bivic, A., & Massey-Harroche, D. (2008). Polarity complex proteins. *Biochimica et Biophysica Acta (BBA) - Biomembranes*, *1778*(3), 614–630. https://doi.org/10.1016/j.bbamem.2007.08.029

Auld, V. J., Fetter, R. D., Broadie, K., & Goodman, C. S. (1995). Gliotactin, a novel transmembrane protein on peripheral glia, is required to form the blood-nerve barrier in drosophila. *Cell*, *81*(5), 757–767. https://doi.org/10.1016/0092-8674(95)90537-5

Aumailley, M. (2013). The laminin family. *Cell Adhesion and Migration*, *7*(1), 48–55. https://doi.org/10.4161/cam.22826

Ayyaz, A., Li, H., & Jasper, H. (2015). Haemocytes control stem cell activity in the Drosophila intestine. *Nature Cell Biology*, *17*(6), 736–748. https://doi.org/10.1038/ncb3174

Bailey, A. M., & Posakony, J. W. (1995). Suppressor of Hairless directly activates transcription of Enhancer of split Complex genes in response to Notch receptor activity. *Genes & Development*, *9*(21), 2609–2622. https://doi.org/10.1101/gad.9.21.2609

Bair, E. L., Chen, M. L., McDaniel, K., Sekiguchi, K., Cress, A. E., Nagle, R. B., & Bowden, G. T. (2005). Membrane Type 1 Matrix Metalloprotease Cleaves Laminin-10 and Promotes Prostate Cancer Cell Migration. *Neoplasia*, *7*(4), 380–389. https://doi.org/10.1593/neo.04619

Bardin, A. J., Perdigoto, C. N., Southall, T. D., Brand, A. H., & Schweisguth, F. (2010). Transcriptional control of stem cell maintenance in the *Drosophila* intestine. *Journal of Cell Science*, *123*(5), e1–e1. https://doi.org/10.1242/jcs.069401

Barker, N., van Es, J. H., Kuipers, J., Kujala, P., van den Born, M., Cozijnsen, M., Haegebarth, A., Korving, J., Begthel, H., Peters, P. J., & Clevers, H. (2007). Identification of stem cells in small intestine and colon by marker gene Lgr5. *Nature*, *449*(7165), 1003–1007. https://doi.org/10.1038/nature06196

Bätz, T., Förster, D., & Luschnig, S. (2014). The transmembrane protein Macroglobulin complement-related is essential for septate junction formation and epithelial barrier function in *Drosophila*. *Development*, *141*(4), 899–908. https://doi.org/10.1242/dev.102160

Baumann, O. (2001). Posterior Midgut Epithelial Cells Differ in Their Organization of the Membrane Skeleton from Other Drosophila Epithelia. *Experimental Cell Research*, *270*(2), 176–187. https://doi.org/10.1006/excr.2001.5343

Baumgartner, S., Littleton, J. T., Broadie, K., Bhat, M. A., Harbecke, R., Lengyel, J. A., Chiquet-Ehrismann, R., Prokop, A., & Bellen, H. J. (1996). A Drosophila neurexin is required for septate junction and blood-nerve barrier formation and function. *Cell*, *87*(6), 1059–1068. https://doi.org/10.1016/S0092-8674(00)81800-0

Becker, K., Bluhm, A., Casas-Vila, N., Dinges, N., Dejung, M., Sayols, S., Kreutz, C., Roignant, J.-Y., Butter, F., & Legewie, S. (2018). Quantifying post-transcriptional regulation in the development of Drosophila melanogaster. *Nature Communications*, *9*(1), 4970. https://doi.org/10.1038/s41467-018-07455-9

Beebe, K., Lee, W. C., & Micchelli, C. A. (2010). JAK/STAT signaling coordinates stem cell proliferation and multilineage differentiation in the Drosophila intestinal stem cell lineage. *Developmental Biology*, *338*(1), 28–37. https://doi.org/10.1016/j.ydbio.2009.10.045

Behr, M., Riedel, D., & Schuh, R. (2003). The Claudin-like Megatrachea Is Essential in Septate Junctions for the Epithelial Barrier Function in Drosophila. *Developmental Cell*, *5*(4), 611–620. https://doi.org/10.1016/S1534-5807(03)00275-2

Berry, S. J., Coffey, D. S., Walsh, P. C., & Ewing, L. L. (1984). The Development of Human Benign Prostatic Hyperplasia with Age. *Journal of Urology*, *132*(3), 474–479. https://doi.org/10.1016/S0022-5347(17)49698-4

Bertrand, Y., Demeule, M., Michaud-Levesque, J., & Béliveau, R. (2007). Melanotransferrin induces human melanoma SK-Mel-28 cell invasion in vivo. *Biochemical and Biophysical Research Communications*, *353*(2), 418–423. https://doi.org/10.1016/j.bbrc.2006.12.034

Białkowska, K., Komorowski, P., Bryszewska, M., & Miłowska, K. (2020). Spheroids as a Type of Three-Dimensional Cell Cultures—Examples of Methods of Preparation and the Most Important Application. *International Journal of Molecular Sciences*, *21*(17), 6225. https://doi.org/10.3390/ijms21176225

Bilder, D., Li, M., & Perrimon, N. (2000). Cooperative Regulation of Cell Polarity and Growth by *Drosophila* Tumor Suppressors. *Science*, *289*(5476), 113–116. https://doi.org/10.1126/science.289.5476.113

Bilder, D., Schober, M., & Perrimon, N. (2003). Integrated activity of PDZ protein complexes regulates epithelial polarity. *Nature Cell Biology*, *5*(1), 53–58. https://doi.org/10.1038/ncb897

Biteau, B., Hochmuth, C. E., & Jasper, H. (2008). JNK Activity in Somatic Stem Cells Causes Loss of Tissue Homeostasis in the Aging Drosophila Gut. *Cell Stem Cell*, *3*(4), 442–455. https://doi.org/10.1016/j.stem.2008.07.024

Biteau, B., & Jasper, H. (2011). EGF signaling regulates the proliferation of intestinal stem cells in *Drosophila*. *Development*, *138*(6), 1045–1055. https://doi.org/10.1242/dev.056671

Biteau, B., & Jasper, H. (2014). Slit/Robo Signaling Regulates Cell Fate Decisions in the Intestinal Stem Cell Lineage of Drosophila. *Cell Reports*, *7*(6), 1867–1875. https://doi.org/10.1016/j.celrep.2014.05.024

Biteau, B., Karpac, J., Hwangbo, D., & Jasper, H. (2011). Regulation of Drosophila lifespan by JNK signaling. *Experimental Gerontology*, *46*(5), 349–354. https://doi.org/10.1016/j.exger.2010.11.003

Biteau, B., Karpac, J., Supoyo, S., DeGennaro, M., Lehmann, R., & Jasper, H. (2010). Lifespan Extension by Preserving Proliferative Homeostasis in Drosophila. *PLoS Genetics*, *6*(10), e1001159. https://doi.org/10.1371/journal.pgen.1001159

Blackwood, J. K., Williamson, S. C., Greaves, L. C., Wilson, L., Rigas, A. C., Sandher, R., Pickard, R. S., Robson, C. N., Turnbull, D. M., Taylor, R. W., & Heer, R. (2011). *In situ* lineage tracking of human prostatic epithelial stem cell fate reveals a common clonal origin for basal and luminal cells. *The Journal of Pathology*, *225*(2), 181–188. https://doi.org/10.1002/path.2965

Blice-Baum, A. C., Guida, M. C., Hartley, P. S., Adams, P. D., Bodmer, R., & Cammarato, A. (2019). As time flies by: Investigating cardiac aging in the short-lived Drosophila model. *Biochimica et Biophysica Acta (BBA) - Molecular Basis of Disease*, *1865*(7), 1831–1844. https://doi.org/10.1016/j.bbadis.2018.11.010

Bond, D., & Foley, E. (2012). Autocrine platelet-derived growth factor-vascular endothelial growth factor receptor-related (Pvr) pathway activity controls intestinal stem cell proliferation in the adult Drosophila midgut. *Journal of Biological Chemistry*, *287*(33), 27359–27370. https://doi.org/10.1074/jbc.M112.378018

Bonnay, F., Cohen-Berros, E., Hoffmann, M., Kim, S. Y., Boulianne, G. L., Hoffmann, J. A., Matt, N., & Reichhart, J.-M. (2013). *big bang* gene modulates gut immune tolerance in *Drosophila*. *Proceedings of the National Academy of Sciences*, *110*(8), 2957–2962. https://doi.org/10.1073/pnas.1221910110

Bosch, J. A., Colbeth, R., Zirin, J., & Perrimon, N. (2020). Gene Knock-Ins in *Drosophila* Using Homology-Independent Insertion of Universal Donor Plasmids. *Genetics*, *214*(1), 75–89. https://doi.org/10.1534/genetics.119.302819

Brand, A. H., & Perrimon, N. (1993). Targeted gene expression as a means of altering cell fates and generating dominant phenotypes. *Development (Cambridge, England)*, *118*(2), 401–415. https://doi.org/10.1242/dev.118.2.401

Broderick, N. A., Buchon, N., & Lemaitre, B. (2014). Microbiota-Induced Changes in Drosophila melanogaster Host Gene Expression and Gut Morphology. *MBio*, *5*(3), 1117–1131. https://doi.org/10.1128/mBio.01117-14

Brown, J. P., Hewick, R. M., Hellström, I., Hellström, K. E., Doolittle, R. F., & Dreyer, W. J. (1982). Human melanoma-associated antigen p97 is structurally and functionally related to transferrin. *Nature*, *296*(5853), 171–173. https://doi.org/10.1038/296171a0

Brown, J. P., Nishiyama, K., Hellström, I., & Hellström, K. E. (1981). Structural characterization of human melanoma-associated antigen p97 with monoclonal antibodies. *The Journal of Immunology*, *127*(2), 539–546. https://doi.org/10.4049/jimmunol.127.2.539

Brown, J. P., Woodbury, R. G., Hart, C. E., Hellström, I., & Hellström, K. E. (1981). Quantitative analysis of melanoma-associated antigen p97 in normal and neoplastic tissues. *Proceedings of the National Academy of Sciences*, *78*(1), 539–543. https://doi.org/10.1073/pnas.78.1.539

Brown, J. P., Wright, P. W., Hart, C. E., Woodbury, R. G., Hellström, K. E., & Hellström, I. (1980). Protein antigens of normal and malignant human cells identified by immunoprecipitation with monoclonal antibodies. *Journal of Biological Chemistry*, *255*(11), 4980–4983. https://doi.org/10.1016/S0021-9258(19)70731-5

Buchon, N., Broderick, N. A., Chakrabarti, S., & Lemaitre, B. (2009). Invasive and indigenous microbiota impact intestinal stem cell activity through multiple pathways in *Drosophila*. *Genes & Development*, *23*(19), 2333–2344. https://doi.org/10.1101/gad.1827009

Buchon, N., Broderick, N. A., Kuraishi, T., & Lemaitre, B. (2010). DrosophilaEGFR pathway coordinates stem cell proliferation and gut remodeling following infection. *BMC Biology*, *8*(1), 152. https://doi.org/10.1186/1741-7007-8-152

Buchon, N., Broderick, N. A., Poidevin, M., Pradervand, S., & Lemaitre, B. (2009). Drosophila Intestinal Response to Bacterial Infection: Activation of Host Defense and Stem Cell Proliferation. *Cell Host & Microbe*, *5*(2), 200–211. https://doi.org/10.1016/j.chom.2009.01.003

Buchon, N., & Osman, D. (2015). All for one and one for all: Regionalization of the Drosophila intestine. *Insect Biochemistry and Molecular Biology*, *67*, 2–8. https://doi.org/10.1016/j.ibmb.2015.05.015

Bunt, S., Denholm, B., & Skaer, H. (2011). Characterisation of the Drosophila procollagen lysyl hydroxylase, dPlod. *Gene Expression Patterns*, *11*(1–2), 72–78. https://doi.org/10.1016/j.gep.2010.09.006

Buskin, A., Scott, E., Nelson, R., Gaughan, L., Robson, C. N., Heer, R., & Hepburn, A. C. (2023). Engineering prostate cancer in vitro: what does it take? *Oncogene*, *42*(32), 2417–2427. https://doi.org/10.1038/s41388-023-02776-6

Byri, S., Misra, T., Syed, Z. A., Bätz, T., Shah, J., Boril, L., Glashauser, J., Aegerter-Wilmsen, T., Matzat, T., Moussian, B., Uv, A., & Luschnig, S. (2015). The Triple-Repeat Protein Anakonda Controls Epithelial Tricellular Junction Formation in Drosophila. *Developmental Cell*, *33*(5), 535–548. https://doi.org/10.1016/j.devcel.2015.03.023

Casali, A., & Batlle, E. (2009). Intestinal Stem Cells in Mammals and Drosophila. *Cell Stem Cell*, *4*(2), 124–127. https://doi.org/10.1016/j.stem.2009.01.009

Castilho, R. M., Squarize, C. H., Chodosh, L. A., Williams, B. O., & Gutkind, J. S. (2009). mTOR Mediates Wnt-Induced Epidermal Stem Cell Exhaustion and Aging. *Cell Stem Cell*, *5*(3), 279–289. https://doi.org/10.1016/j.stem.2009.06.017

Chen, H.-J., Li, Q., Nirala, N. K., & Ip, Y. T. (2020). The Snakeskin-Mesh Complex of Smooth Septate Junction Restricts Yorkie to Regulate Intestinal Homeostasis in Drosophila. *Stem Cell Reports*, *14*(5), 828–844. https://doi.org/10.1016/j.stemcr.2020.03.021

Chen, J., Sayadian, A. C., Lowe, N., Lovegrove, H. E., & St Johnston, D. (2018). An alternative mode of epithelial polarity in the Drosophila midgut. *PLoS Biology*, *16*(10). https://doi.org/10.1371/journal.pbio.3000041

Chen, J., & St Johnston, D. (2022). De novo apical domain formation inside the Drosophila adult midgut epithelium. *ELife*, *11*. https://doi.org/10.7554/eLife.76366

Choi, N., Kim, J., Yang, D., Kim, Y., & Yoo, M. (2008). Age-related changes in *Drosophila* midgut are associated with PVF2, a PDGF/VEGF-like growth factor. *Aging Cell*, *7*(3), 318–334. https://doi.org/10.1111/j.1474-9726.2008.00380.x

Choi, N., Zhang, B., Zhang, L., Ittmann, M., & Xin, L. (2012). Adult Murine Prostate Basal and Luminal Cells Are Self-Sustained Lineages that Can Both Serve as Targets for Prostate Cancer Initiation. *Cancer Cell*, *21*(2), 253–265. https://doi.org/10.1016/j.ccr.2012.01.005

Chung, H. Y., Cesari, M., Anton, S., Marzetti, E., Giovannini, S., Seo, A. Y., Carter, C., Yu, B. P., & Leeuwenburgh, C. (2009). Molecular inflammation: Underpinnings of aging and age-related diseases. *Ageing Research Reviews*, *8*(1), 18–30. https://doi.org/10.1016/j.arr.2008.07.002

Claesson, M. J., Jeffery, I. B., Conde, S., Power, S. E., O'Connor, E. M., Cusack, S., Harris, H. M. B., Coakley, M., Lakshminarayanan, B., O'Sullivan, O., Fitzgerald, G. F., Deane, J., O'Connor, M., Harnedy, N., O'Connor, K., O'Mahony, D., van Sinderen, D., Wallace, M.,

Brennan, L., … O'Toole, P. W. (2012). Gut microbiota composition correlates with diet and health in the elderly. *Nature*, *488*(7410), 178–184. https://doi.org/10.1038/nature11319

Clark, R. I., Salazar, A., Yamada, R., Fitz-Gibbon, S., Morselli, M., Alcaraz, J., Rana, A., Rera, M., Pellegrini, M., Ja, W. W., & Walker, D. W. (2015). Distinct Shifts in Microbiota Composition during Drosophila Aging Impair Intestinal Function and Drive Mortality. *Cell Reports*, *12*(10), 1656–1667. https://doi.org/10.1016/j.celrep.2015.08.004

Colognato, H., Winkelmann, D. A., & Yurchenco, P. D. (1999). Laminin Polymerization Induces a Receptor–Cytoskeleton Network. *The Journal of Cell Biology*, *145*(3), 619–631. https://doi.org/10.1083/jcb.145.3.619

Cordero, J. B., Stefanatos, R. K., Myant, K., Vidal, M., & Sansom, O. J. (2012). Non-autonomous crosstalk between the Jak/Stat and Egfr pathways mediates *Apc1* -driven intestinal stem cell hyperplasia in the *Drosophila* adult midgut. *Development*, *139*(24), 4524–4535. https://doi.org/10.1242/dev.078261

Cordero, J. B., Stefanatos, R. K., Scopelliti, A., Vidal, M., & Sansom, O. J. (2012). Inducible progenitor-derived Wingless regulates adult midgut regeneration in *Drosophila*. *The EMBO Journal*, *31*(19), 3901–3917. https://doi.org/10.1038/emboj.2012.248

Cordero, J. B., Vidal, M., & Sansom, O. (2009). APC as a master regulator of intestinal homeostasis and transformation: From flies to vertebrates. *Cell Cycle*, *8*(18), 2927–2932. https://doi.org/10.4161/cc.8.18.9472

Cunha, G. R., Donjacour, A. A., Cooke, P. S., Mee, S., Bigsby, R. M., Higgins, S. J., & Sugimura, Y. (1987). The Endocrinology and Developmental Biology of the Prostate. *Endocrine Reviews*, *8*(3), 338–362. https://doi.org/10.1210/edrv-8-3-338

Dambroise, E., Monnier, L., Ruisheng, L., Aguilaniu, H., Joly, J.-S., Tricoire, H., & Rera, M. (2016). Two phases of aging separated by the Smurf transition as a public path to death. *Scientific Reports*, *6*(1), 23523. https://doi.org/10.1038/srep23523

de Navascués, J., Perdigoto, C. N., Bian, Y., Schneider, M. H., Bardin, A. J., Martínez-Arias, A., & Simons, B. D. (2012). *Drosophila* midgut homeostasis involves neutral competition between symmetrically dividing intestinal stem cells. *The EMBO Journal*, *31*(11), 2473–2485. https://doi.org/10.1038/emboj.2012.106

Delidakis, C., Monastirioti, M., & Magadi, S. S. (2014). E(spl): Genetic, Developmental, and Evolutionary Aspects of a Group of Invertebrate Hes Proteins with Close Ties to Notch Signaling [Bookitem]. In *Current Topics in Developmental Biology* (Vol. 110, pp. 217–262). Academic Press. https://doi.org/10.1016/B978-0-12-405943-6.00006-3

Deligiannaki, M., Casper, A. L., Jung, C., & Gaul, U. (2015). Pasiflora proteins are novel core components of the septate junction. *Development*, *142*(17), 3046–3057. https://doi.org/10.1242/dev.119412

Demeule, M., Bertrand, Y., Michaud-Levesque, J., Jodoin, J., Rolland, Y., Gabathuler, R., & Béliveau, R. (2003). Regulation of plasminogen activation: a role for melanotransferrin (p97) in cell migration. *Blood*, *102*(5), 1723–1731. https://doi.org/10.1182/blood-2003-01-0166

Demeule, M., Poirier, J., Jodoin, J., Bertrand, Y., Desrosiers, R. R., Dagenais, C., Nguyen, T., Lanthier, J., Gabathuler, R., Kennard, M., Jefferies, W. A., Karkan, D., Tsai, S., Fenart, L., Cecchelli, R., & Béliveau, R. (2002). High transcytosis of melanotransferrin (P97) across the blood–brain barrier. *Journal of Neurochemistry*, *83*(4), 924–933. https://doi.org/10.1046/j.1471-4159.2002.01201.x

Denisenko, O., Mar, D., Trawczynski, M., & Bomsztyk, K. (2018). Chromatin changes trigger laminin genes dysregulation in aging kidneys. *Aging*, *10*(5), 1133–1145. https://doi.org/10.18632/aging.101453

Desrosiers, R. R., Bertrand, Y., Nguyen, Q.-T., Demeule, M., Gabathuler, R., Kennard, M. L., Gauthier, S., & Béliveau, R. (2003). Expression of melanotransferrin isoforms in human serum: relevance to Alzheimer's disease. *Biochemical Journal*, *374*(2), 463–471. https://doi.org/10.1042/bj20030240

Deutzmann, R., Aumailley, M., Wiedemann, H., Pysny, W., Timpl, R., & Edgar, D. (1990). Cell adhesion, spreading and neurite stimulation by laminin fragment E8 depends on maintenance of secondary and tertiary structure in its rod and globular domain. *European Journal of Biochemistry*, *191*(2), 513–522. https://doi.org/10.1111/j.1432-1033.1990.tb19151.x

Diao, B., & Yang, P. (2021). Comprehensive Analysis of the Expression and Prognosis for Laminin Genes in Ovarian Cancer. *Pathology and Oncology Research*, *27*. https://doi.org/10.3389/pore.2021.1609855

Dippold, W. G., Lloyd, K. O., Li, L. T., Ikeda, H., Oettgen, H. F., & Old, L. J. (1980). Cell surface antigens of human malignant melanoma: definition of six antigenic systems with mouse monoclonal antibodies. *Proceedings of the National Academy of Sciences*, *77*(10), 6114–6118. https://doi.org/10.1073/pnas.77.10.6114

Doupé, D. P., Marshall, O. J., Dayton, H., Brand, A. H., & Perrimon, N. (2018). *Drosophila* intestinal stem and progenitor cells are major sources and regulators of homeostatic niche

signals. *Proceedings of the National Academy of Sciences*, *115*(48), 12218–12223. https://doi.org/10.1073/pnas.1719169115

Dunn, L. L., Sekyere, E. O., Suryo Rahmanto, Y., & Richardson, D. R. (2006). The function of melanotransferrin: a role in melanoma cell proliferation and tumorigenesis. *Carcinogenesis*, *27*(11), 2157–2169. https://doi.org/10.1093/carcin/bgl045

Duś-Szachniewicz, K., Ostasiewicz, P., Woźniak, M., Kołodziej, P., Wiśniewski, J. R., & Ziółkowski, P. (2015). Pattern of Melanotransferrin Expression in Human Colorectal Tissues: An Immunohistochemical Study on Potential Clinical Application. *Anticancer Research*, *35*(12), 6551–6561. http://www.ncbi.nlm.nih.gov/pubmed/26637869

Esmangart de Bournonville, T., & Le Borgne, R. (2020). Interplay between Anakonda, Gliotactin, and M6 for Tricellular Junction Assembly and Anchoring of Septate Junctions in Drosophila Epithelium. *Current Biology*, *30*(21), 4245-4253.e4. https://doi.org/10.1016/J.CUB.2020.07.090

Estin, C. D., Stevenson, U., Kahn, M., Hellstrom, I., & Hellstrom, K. E. (1989). Transfected Mouse Melanoma Lines That Express Various Levels of Human Melanoma-Associated Antigen p97. *JNCI Journal of the National Cancer Institute*, *81*(6), 445–448. https://doi.org/10.1093/jnci/81.6.445

Estin, C. D., Stevenson, U. S., Plowman, G. D., Hu, S. L., Sridhar, P., Hellström, I., Brown, J. P., & Hellström, K. E. (1988). Recombinant vaccinia virus vaccine against the human melanoma antigen p97 for use in immunotherapy. *Proceedings of the National Academy of Sciences*, *85*(4), 1052–1056. https://doi.org/10.1073/pnas.85.4.1052

Ewen-Campen, B., Yang-Zhou, D., Fernandes, V. R., González, D. P., Liu, L.-P., Tao, R., Ren, X., Sun, J., Hu, Y., Zirin, J., Mohr, S. E., Ni, J.-Q., & Perrimon, N. (2017). Optimized strategy for in vivo Cas9-activation in *Drosophila*. *Proceedings of the National Academy of Sciences*, *114*(35), 9409–9414. https://doi.org/10.1073/pnas.1707635114

Eyford, B. A., Singh, C. S. B., Abraham, T., Munro, L., Choi, K. B., Hill, T., Hildebrandt, R., Welch, I., Vitalis, T. Z., Gabathuler, R., Gordon, J. A., Adomat, H., Guns, E. S. T., Lu, C.-J., Pfeifer, C. G., Tian, M. M., & Jefferies, W. A. (2021). A Nanomule Peptide Carrier Delivers siRNA Across the Intact Blood-Brain Barrier to Attenuate Ischemic Stroke. *Frontiers in Molecular Biosciences*, *8*. https://doi.org/10.3389/fmolb.2021.611367

Faivre-Sarrailh, C., Banerjee, S., Li, J., Hortsch, M., Laval, M., & Bhat, M. A. (2004). *Drosophila* contactin, a homolog of vertebrate contactin, is required for septate junction organization and paracellular barrier function. *Development*, *131*(20), 4931–4942. https://doi.org/10.1242/dev.01372

Fang, L., Che, Y., Zhang, C., Huang, J., Lei, Y., Lu, Z., Sun, N., & He, J. (2021). LAMC1 upregulation via TGFβ induces inflammatory cancer-associated fibroblasts in esophageal squamous cell carcinoma via NF-κB–CXCL1–STAT3. *Molecular Oncology*, *15*(11), 3125–3146. https://doi.org/10.1002/1878-0261.13053

Fang, Y., Dou, R., Huang, S., Han, L., Fu, H., Yang, C., Song, J., Zheng, J., Zhang, X., Liu, K., Xiang, Z., Zhang, X., Wang, S., & Xiong, B. (2022). LAMC1-mediated preadipocytes differentiation promoted peritoneum pre-metastatic niche formation and gastric cancer metastasis. *International Journal of Biological Sciences*, *2022*(7), 3082–3101. https://doi.org/10.7150/ijbs.70524

Fehon, R. G., Dawson, I. A., & Artavanis-Tsakonas, S. (1994). A *Drosophila* homologue of membrane-skeleton protein 4.1 is associated with septate junctions and is encoded by the *coracle* gene. *Development*, *120*(3), 545–557. https://doi.org/10.1242/dev.120.3.545

Ferraces-Riegas, P., Galbraith, A. C., & Doupé, D. P. (2022). Epithelial Stem Cells: Making, Shaping and Breaking the Niche. In *Adv Exp Med Biol-Cell Biology and Translational Medicine* (Vol. 16, pp. 1–12). https://doi.org/10.1007/5584_2021_686

Fessler, L. I., Campbell, A. G., Duncan, K. G., & Fessler, J. H. (1987). Drosophila laminin: characterization and localization. *The Journal of Cell Biology*, *105*(5), 2383. https://doi.org/10.1083/JCB.105.5.2383

Fields, B., DeLaForest, A., Zogg, M., May, J., Hagen, C., Komnick, K., Wieser, J., Lundberg, A., Weiler, H., Battle, M. A., & Carlson, K.-S. (2019). The Adult Murine Intestine is Dependent on Constitutive Laminin-γ1 Synthesis. *Scientific Reports*, *9*(1), 19303. https://doi.org/10.1038/s41598-019-55844-x

Fischer, J. A., Giniger, E., Maniatis, T., & Ptashne, M. (1988). GAL4 activates transcription in Drosophila. *Nature*, *332*(6167), 853–856. https://doi.org/10.1038/332853a0

Food, M. R., Rothenberger, S., Gabathuler, R., Haidl, I. D., Reid, G., & Jefferies, W. A. (1994). Transport and expression in human melanomas of a transferrin-like glycosylphosphatidylinositol-anchored protein. *Journal of Biological Chemistry*, *269*(4), 3034–3040. https://pubmed.ncbi.nlm.nih.gov/8300636/

Food, M. R., Sekyere, E. O., & Richardson, D. R. (2002). The soluble form of the membrane-bound transferrin homologue, melanotransferrin, inefficiently donates iron to cells via nonspecific internalization and degradation of the protein. *European Journal of Biochemistry*, *269*(18), 4435–4445. https://doi.org/10.1046/J.1432-1033.2002.03140.X

Fortini, M. E., Skupski, M. P., Boguski, M. S., & Hariharan, I. K. (2000). A Survey of Human Disease Gene Counterparts in the *Drosophila* Genome. *The Journal of Cell Biology*, *150*(2), F23–F30. https://doi.org/10.1083/jcb.150.2.F23

Foster, C. S., & Ke, Y. (1997). Stem cells in prostatic epithelia. *International Journal of Experimental Pathology*, *78*(5), 311–329. https://doi.org/10.1046/j.1365-2613.1997.380368.x

Franco, O. E., Jiang, M., Strand, D. W., Peacock, J., Fernandez, S., Jackson, R. S., Revelo, M. P., Bhowmick, N. A., & Hayward, S. W. (2011). Altered TGF-β Signaling in a Subpopulation of Human Stromal Cells Promotes Prostatic Carcinogenesis. *Cancer Research*, *71*(4), 1272–1281. https://doi.org/10.1158/0008-5472.CAN-10-3142

Fullwood, N. J., Lawlor, A. J., Martin-Hirsch, P. L., Matanhelia, S. S., & Martin, F. L. (2019). An analysis of benign human prostate offers insights into the mechanism of apocrine secretion and the origin of prostasomes. *Scientific Reports*, *9*(1), 4582. https://doi.org/10.1038/s41598-019-40820-2

Furriols, M., & Bray, S. (2001). A model Notch response element detects Suppressor of Hairless–dependent molecular switch. *Current Biology*, *11*(1), 60–64. https://doi.org/10.1016/S0960-9822(00)00044-0

Gabathuler, R., Vitalis, T. Z., Nounou, M. I., Iqbal, U., Moreno, M., Adkins, C. E., Torrell, T. O., Jefferies, W. A., & Lockman, P. R. (2013). Abstract A247: BT2111, a new anticancer agent composed of trastuzumab and transcend a vector for brain delivery for the treatment of metastatic Her2+ breast cancer. *Molecular Cancer Therapeutics*, *12*(11_Supplement), A247–A247. https://doi.org/10.1158/1535-7163.TARG-13-A247

Garmany, A., Yamada, S., & Terzic, A. (2021). Longevity leap: mind the healthspan gap. *Npj Regenerative Medicine*, *6*(1), 57. https://doi.org/10.1038/s41536-021-00169-5

Garratt, R. C., & Jhoti, H. (1992). A molecular model for the tumour-associated antigen, p97, suggests a Zn-binding function. *FEBS Letters*, *305*(1), 55–61. https://doi.org/10.1016/0014-5793(92)80654-Y

Genova, J. L., & Fehon, R. G. (2003). Neuroglian, Gliotactin, and the Na+/K+ ATPase are essential for septate junction function in *Drosophila*. *The Journal of Cell Biology*, *161*(5), 979–989. https://doi.org/10.1083/jcb.200212054

Gerber, H.-P., & Ferrara, N. (2003). The role of VEGF in normal and neoplastic hematopoiesis. *Journal of Molecular Medicine*, *81*(1), 20–31. https://doi.org/10.1007/s00109-002-0397-4

Gialeli, C., Theocharis, A. D., & Karamanos, N. K. (2011). Roles of matrix metalloproteinases in cancer progression and their pharmacological targeting. *The FEBS Journal*, *278*(1), 16–27. https://doi.org/10.1111/j.1742-4658.2010.07919.x

Golic, K. G., & Lindquist, S. (1989). The FLP recombinase of yeast catalyzes site-specific recombination in the drosophila genome. *Cell*, *59*(3), 499–509. https://doi.org/10.1016/0092-8674(89)90033-0

Gotwals, P. J., Fesslert, L. I., Wehrlii, M., & Hynes, R. 0. (1994). Drosophila PS1 integrin is a laminin receptor and differs in ligand specificity from PS2. *Cell Biology*, *91*, 11447–11451.

Goulas, S., Conder, R., & Knoblich, J. A. (2012). The Par Complex and Integrins Direct Asymmetric Cell Division in Adult Intestinal Stem Cells. *Cell Stem Cell*, *11*(4), 529–540. https://doi.org/10.1016/j.stem.2012.06.017

Gudipaty, S. A., Lindblom, J., Loftus, P. D., Redd, M. J., Edes, K., Davey, C. F., Krishnegowda, V., & Rosenblatt, J. (2017). Mechanical stretch triggers rapid epithelial cell division through Piezo1. *Nature*, *543*(7643), 118–121. https://doi.org/10.1038/nature21407

Guisoni, N., Martinez-Corral, R., Garcia Ojalvo, J., & de Navascués, J. (2017). Diversity of fate outcomes in cell pairs under lateral inhibition. *Development*. https://doi.org/10.1242/dev.137950

Guo, Y., Pan, W., Liu, S., Shen, Z., Xu, Y., & Hu, L. (2020). ERK/MAPK signalling pathway and tumorigenesis (Review). *Experimental and Therapeutic Medicine*. https://doi.org/10.3892/etm.2020.8454

Guo, Z., Driver, I., & Ohlstein, B. (2013). Injury-induced BMP signaling negatively regulates *Drosophila* midgut homeostasis. *Journal of Cell Biology*, *201*(6), 945–961. https://doi.org/10.1083/jcb.201302049

He, L., Si, G., Huang, J., Samuel, A. D. T., & Perrimon, N. (2018). Mechanical regulation of stem-cell differentiation by the stretch-activated Piezo channel. *Nature*, *555*(7694), 103–106. https://doi.org/10.1038/nature25744

Henchcliffe, C., Garcia-Alonso, L., Tang, J., & Goodman, C. S. (1993). Genetic analysis of laminin A reveals diverse functions during morphogenesis in Drosophila. *Development*, *118*(2), 325–337. https://doi.org/10.1242/DEV.118.2.325

Henry, G. H., Malewska, A., Joseph, D. B., Malladi, V. S., Lee, J., Torrealba, J., Mauck, R. J., Gahan, J. C., Raj, G. V., Roehrborn, C. G., Hon, G. C., MacConmara, M. P., Reese, J. C., Hutchinson, R. C., Vezina, C. M., & Strand, D. W. (2018). A Cellular Anatomy of the

Normal Adult Human Prostate and Prostatic Urethra. *Cell Reports*, *25*(12), 3530-3542.e5. https://doi.org/10.1016/j.celrep.2018.11.086

Hepburn, A. C., Curry, E. L., Moad, M., Steele, R. E., Franco, O. E., Wilson, L., Singh, P., Buskin, A., Crawford, S. E., Gaughan, L., Mills, I. G., Hayward, S. W., Robson, C. N., & Heer, R. (2020). Propagation of human prostate tissue from induced pluripotent stem cells. *Stem Cells Translational Medicine*, *9*(7), 734–745. https://doi.org/10.1002/sctm.19-0286

Hijazi, A., Masson, W., Augé, B., Waltzer, L., Haenlin, M., & Roch, F. (2009). *boudin* is required for septate junction organisation in *Drosophila* and codes for a diffusible protein of the Ly6 superfamily. *Development*, *136*(13), 2199–2209. https://doi.org/10.1242/dev.033845

Hildebrandt, A., Pflanz, R., Behr, M., Tarp, T., Riedel, D., & Schuh, R. (2015). Bark beetle controls epithelial morphogenesis by septate junction maturation in Drosophila. *Developmental Biology*, *400*(2), 237–247. https://doi.org/10.1016/j.ydbio.2015.02.008

Hochmuth, C. E., Biteau, B., Bohmann, D., & Jasper, H. (2011). Redox Regulation by Keap1 and Nrf2 Controls Intestinal Stem Cell Proliferation in Drosophila. *Cell Stem Cell*, *8*(2), 188–199. https://doi.org/10.1016/j.stem.2010.12.006

Hollander, D., & Tarnawski, H. (1985). Aging-Associated Increase in Intestinal Absorption of Macromolecules. *Gerontology*, *31*(3), 133–137. https://doi.org/10.1159/000212694

Hu, D. J.-K., & Jasper, H. (2019). Control of Intestinal Cell Fate by Dynamic Mitotic Spindle Repositioning Influences Epithelial Homeostasis and Longevity. *Cell Reports*, *28*(11), 2807-2823.e5. https://doi.org/10.1016/j.celrep.2019.08.014

Hu, S. L., Plowman, G. D., Sridhar, P., Stevenson, U. S., Brown, J. P., & Estin, C. D. (1988). Characterization of a recombinant vaccinia virus expressing human melanoma-associated antigen p97. *Journal of Virology*, *62*(1), 176–180. https://doi.org/10.1128/jvi.62.1.176-180.1988

Hu, Y., Comjean, A., Perkins, L. A., Perrimon, N., & Mohr, S. E. (2015). GLAD: an Online Database of Gene List Annotation for *Drosophila* . *Journal of Genomics*, *3*, 75–81. https://doi.org/10.7150/jgen.12863

Hu, Y., Flockhart, I., Vinayagam, A., Bergwitz, C., Berger, B., Perrimon, N., & Mohr, S. E. (2011). An integrative approach to ortholog prediction for disease-focused and other functional studies. *BMC Bioinformatics*, *12*, 357. https://doi.org/10.1186/1471-2105-12-357

Hu, Y., Sopko, R., Foos, M., Kelley, C., Flockhart, I., Ammeux, N., Wang, X., Perkins, L., Perrimon, N., & Mohr, S. E. (2013). FlyPrimerBank: an online database for Drosophila

melanogaster gene expression analysis and knockdown evaluation of RNAi reagents. *G3 (Bethesda, Md.)*, *3*(9), 1607–1616. https://doi.org/10.1534/g3.113.007021

Huang, C., Hall, D. H., Hedgecock, E. M., Kao, G., Karantza, V., Vogel, B. E., Hutter, H., Chisholm, A. D., Yurchenco, P. D., & Wadsworth, W. G. (2003). Laminin α subunits and their role in *C. elegans* development. *Development*, *130*(14), 3343–3358. https://doi.org/10.1242/dev.00481

Huang, X., Warren, J. T., Buchanan, J., Gilbert, L. I., & Scott, M. P. (2007). *Drosophila Niemann-Pick Type C-2* genes control sterol homeostasis and steroid biosynthesis: a model of human neurodegenerative disease. *Development*, *134*(20), 3733–3742. https://doi.org/10.1242/dev.004572

Huggins, C., & Hodges, C. V. (1941). Studies on Prostatic Cancer I. The Effect of Castration, of Estrogen and of Androgen Injection on Serum Phosphatases in Metastatic Carcinoma of the Prostate*. *Cancer Research*, *1*(4), 293–297. http://aacrjournals.org/cancerres/article-pdf/1/4/293/2368295/crs0010040293.pdf

Hung, R.-J., Hu, Y., Kirchner, R., Liu, Y., Xu, C., Comjean, A., Tattikota, S. G., Li, F., Song, W., Ho Sui, S., & Perrimon, N. (2020). A cell atlas of the adult *Drosophila* midgut. *Proceedings of the National Academy of Sciences*, *117*(3), 1514–1523. https://doi.org/10.1073/pnas.1916820117

Hunter, I., Schulthess, T., Bruch, M., Beck, K., & Engel, J. (1990). Evidence for a specific mechanism of laminin assembly. *European Journal of Biochemistry*, *188*(2), 205–211. https://doi.org/10.1111/J.1432-1033.1990.TB15391.X

Ile, K. E., Tripathy, R., Goldfinger, V., & Renault, A. D. (2012). Wunen, a *Drosophila* lipid phosphate phosphatase, is required for septate junction-mediated barrier function. *Development*, *139*(14), 2535–2546. https://doi.org/10.1242/dev.077289

Inoue, H., Imamura, T., Ishidou, Y., Takase, M., Udagawa, Y., Oka, Y., Tsuneizumi, K., Tabata, T., Miyazono, K., & Kawabata, M. (1998). Interplay of Signal Mediators of Decapentaplegic (Dpp): Molecular Characterization of Mothers against dpp, Medea, and Daughters against dpp. *Molecular Biology of the Cell*, *9*(8), 2145–2156. https://doi.org/10.1091/mbc.9.8.2145

Isaacs, J. T. (1994). Role of Androgens in Prostatic Cancer. In *Vitamins and Hormones* (Vol. 49, pp. 433–502). https://doi.org/10.1016/S0083-6729(08)61152-8

Ittmann, M. (2018). Anatomy and Histology of the Human and Murine Prostate. *Cold Spring Harbor Perspectives in Medicine*, *8*(5), a030346. https://doi.org/10.1101/cshperspect.a030346

Izumi, Y., Furuse, K., & Furuse, M. (2019). Septate junctions regulate gut homeostasis through regulation of stem cell proliferation and enterocyte behavior in Drosophila. *Journal of Cell Science*, *132*(18), 582148. https://doi.org/10.1101/582148

Izumi, Y., Furuse, K., & Furuse, M. (2020). A novel membrane protein Hoka regulates septate junction organization and stem cell homeostasis in the Drosophila gut. *BioRxiv*, 2020.11.10.376210. https://doi.org/10.1101/2020.11.10.376210

Izumi, Y., Furuse, K., & Furuse, M. (2021). The novel membrane protein Hoka regulates septate junction organization and stem cell homeostasis in the *Drosophila* gut. *Journal of Cell Science*, *134*(6). https://doi.org/10.1242/jcs.257022

Izumi, Y., & Furuse, M. (2014). Molecular organization and function of invertebrate occluding junctions. *Seminars in Cell & Developmental Biology*, *36*, 186–193. https://doi.org/10.1016/j.semcdb.2014.09.009

Izumi, Y., Motoishi, M., Furuse, K., & Furuse, M. (2016). A tetraspanin regulates septate junction formation in Drosophila midgut. *Journal of Cell Science*, *129*(6), 1155–1164. https://doi.org/10.1242/jcs.180448

Izumi, Y., Yanagihashi, Y., & Furuse, M. (2012). A novel protein complex, mesh-ssk, is required for septate junction formation in *drosophila* midgut. *Journal of Cell Science*, *125*(20), 4923–4933. https://doi.org/10.1242/jcs.112243

Jasper, H. (2020). Intestinal Stem Cell Aging: Origins and Interventions. *Annual Review of Physiology*, *82*(1), 203–226. https://doi.org/10.1146/annurev-physiol-021119-034359

Jefferies, W. A., Food, M. R., Gabathuler, R., Rothenberger, S., Yamada, T., Yasuhara, O., & McGeer, P. L. (1996). Reactive microglia specifically associated with amyloid plaques in Alzheimer's disease brain tissue express melanotransferrin. *Brain Research*, *712*(1), 122–126. https://doi.org/10.1016/0006-8993(95)01407-1

Jennings, B. H. (2011). Drosophila – a versatile model in biology & medicine. *Materials Today*, *14*(5), 190–195. https://doi.org/10.1016/S1369-7021(11)70113-4

Jia, Y., Xu, R.-G., Ren, X., Ewen-Campen, B., Rajakumar, R., Zirin, J., Yang-Zhou, D., Zhu, R., Wang, F., Mao, D., Peng, P., Qiao, H.-H., Wang, X., Liu, L.-P., Xu, B., Ji, J.-Y., Liu, Q., Sun, J., Perrimon, N., & Ni, J.-Q. (2018). Next-generation CRISPR/Cas9 transcriptional activation in *Drosophila* using flySAM. *Proceedings of the National Academy of Sciences*, *115*(18), 4719–4724. https://doi.org/10.1073/pnas.1800677115

Jiang, H., Grenley, M. O., Bravo, M.-J., Blumhagen, R. Z., & Edgar, B. A. (2011). EGFR/Ras/MAPK Signaling Mediates Adult Midgut Epithelial Homeostasis and

Regeneration in Drosophila. *Cell Stem Cell*, *8*(1), 84–95. https://doi.org/10.1016/j.stem.2010.11.026

Jiang, H., Patel, P. H., Kohlmaier, A., Grenley, M. O., McEwen, D. G., & Edgar, B. A. (2009). Cytokine/Jak/Stat Signaling Mediates Regeneration and Homeostasis in the Drosophila Midgut. *Cell*, *137*(7), 1343–1355. https://doi.org/10.1016/j.cell.2009.05.014

Jiang, X., Oyang, L., Peng, Q., Liu, Q., Xu, X., Wu, N., Tan, S., Yang, W., Han, Y., Lin, J., Xia, L., Peng, M., Tang, Y., Luo, X., Su, M., Shi, Y., Zhou, Y., & Liao, Q. (2023). Organoids: opportunities and challenges of cancer therapy. *Frontiers in Cell and Developmental Biology*, *11*. https://doi.org/10.3389/fcell.2023.1232528

Jones, P. H., Harper, S., & Watt, F. M. (1995). Stem cell patterning and fate in human epidermis. *Cell*, *80*(1), 83–93. https://doi.org/10.1016/0092-8674(95)90453-0

Jones, P. H., & Watt, F. M. (1993). Separation of human epidermal stem cells from transit amplifying cells on the basis of differences in integrin function and expression. *Cell*, *73*(4), 713–724. https://doi.org/10.1016/0092-8674(93)90251-K

Joseph, D. B., Henry, G. H., Malewska, A., Reese, J. C., Mauck, R. J., Gahan, J. C., Hutchinson, R. C., Malladi, V. S., Roehrborn, C. G., Vezina, C. M., & Strand, D. W. (2021). Single-cell analysis of mouse and human prostate reveals novel fibroblasts with specialized distribution and microenvironment interactions. *The Journal of Pathology*, *255*(2), 141–154. https://doi.org/10.1002/path.5751

Kalluri, R. (2016). The biology and function of fibroblasts in cancer. *Nature Reviews Cancer*, *16*(9), 582–598. https://doi.org/10.1038/nrc.2016.73

Kao, G., Huang, C., Hedgecock, E. M., Hall, D. H., & Wadsworth, W. G. (2006). The role of the laminin β subunit in laminin heterotrimer assembly and basement membrane function and development in C. elegans. *Developmental Biology*, *290*(1), 211–219. https://doi.org/10.1016/j.ydbio.2005.11.026

Karkan, D., Pfeifer, C., Vitalis, T. Z., Arthur, G., Ujiie, M., Chen, Q., Tsai, S., Koliatis, G., Gabathuler, R., & Jefferies, W. A. (2008). A Unique Carrier for Delivery of Therapeutic Compounds beyond the Blood-Brain Barrier. *PLoS ONE*, *3*(6), e2469. https://doi.org/10.1371/journal.pone.0002469

Karpowicz, P., Perez, J., & Perrimon, N. (2010). The Hippo tumor suppressor pathway regulates intestinal stem cell regeneration. *Development*, *137*(24), 4135–4145. https://doi.org/10.1242/dev.060483

Karpowicz, P., Zhang, Y., Hogenesch, J. B., Emery, P., & Perrimon, N. (2013). The Circadian Clock Gates the Intestinal Stem Cell Regenerative State. *Cell Reports*, *3*(4), 996–1004. https://doi.org/10.1016/j.celrep.2013.03.016

Kashima, H., Wu, R.-C., Wang, Y., Sinno, A. K., Miyamoto, T., Shiozawa, T., Wang, T.-L., Fader, A. N., & Shih, I.-M. (2015). Laminin C1 expression by uterine carcinoma cells is associated with tumor progression. *Gynecologic Oncology*, *139*(2), 338–344. https://doi.org/10.1016/j.ygyno.2015.08.025

Kaufman, T. C. (2017). A Short History and Description of *Drosophila melanogaster* Classical Genetics: Chromosome Aberrations, Forward Genetic Screens, and the Nature of Mutations. *Genetics*, *206*(2), 665–689. https://doi.org/10.1534/genetics.117.199950

Kawamoto, T., Pan, H., Yan, W., Ishida, H., Usui, E., Oda, R., Nakamasu, K., Noshiro, M., Kawashima-Ohya, Y., Fujii, M., Shintani, H., Okada, Y., & Kato, Y. (1998). Expression of membrane-bound transferrin-like protein p97 on the cell surface of chondrocytes. *European Journal of Biochemistry*, *256*(3), 503–509. https://doi.org/10.1046/j.1432-1327.1998.2560503.x

Ke, H., Feng, Z., Liu, M., Sun, T., Dai, J., Ma, M., Liu, L. P., Ni, J. Q., & Pastor-Pareja, J. C. (2018). Collagen secretion screening in Drosophila supports a common secretory machinery and multiple Rab requirements. *Journal of Genetics and Genomics*, *45*(6), 299–313. https://doi.org/10.1016/J.JGG.2018.05.002

Ke, H.-L., Ke, R.-H., Li, B., Wang, X.-H., Wang, Y.-N., & Wang, X.-Q. (2013). Association between laminin γ1 expression and meningioma grade, recurrence, and progression-free survival. *Acta Neurochirurgica*, *155*(1), 165–171. https://doi.org/10.1007/s00701-012-1512-0

Keeley, D. P., Hastie, E., Jayadev, R., Kelley, L. C., Chi, Q., Payne, S. G., Jeger, J. L., Hoffman, B. D., & Sherwood, D. R. (2020). Comprehensive Endogenous Tagging of Basement Membrane Components Reveals Dynamic Movement within the Matrix Scaffolding. *Developmental Cell*, *54*(1), 60-74.e7. https://doi.org/10.1016/j.devcel.2020.05.022

Kennard, M. L., Feldman, H., Yamada, T., & Jefferies, W. A. (1996). Serum levels of the iron binding protein p97 are elevated in Alzheimer′s disease. *Nature Medicine*, *2*(11), 1230–1235. https://doi.org/10.1038/nm1196-1230

Kennard, M. L., Richardson, D. R., Gabathuler, R., Ponka, P., & Jefferies, W. A. (1995). A novel iron uptake mechanism mediated by GPI-anchored human p97. *The EMBO Journal*, *14*(17), 4178–4186. https://doi.org/10.1002/j.1460-2075.1995.tb00091.x

Khadilkar, R. J., & Tanentzapf, G. (2019). Septate junction components control *Drosophila* hematopoiesis through the Hippo pathway. *Development*, *146*(7). https://doi.org/10.1242/dev.166819

Kim, D. K., Seo, M. Y., Lim, S. W., Kim, S., Kim, J. W., Carroll, B. J., Kwon, D. Y., Kwon, T., & Kang, S. S. (2001). Serum Melanotransferrin, p97 as a Biochemical Marker of Alzheimer's Disease. *Neuropsychopharmacology*, *25*(1), 84–90. https://doi.org/10.1016/S0893-133X(00)00230-X

Kim, E. H., Galchev, V. I., Kim, J. Y., Misek, S. A., Stevenson, T. K., Campbell, M. D., Pagani, F. D., Day, S. M., Johnson, T. C., Washburn, J. G., Vikstrom, K. L., Michele, D. E., Misek, D. E., & Westfall, M. V. (2016). Differential protein expression and basal lamina remodeling in human heart failure. *Proteomics. Clinical Applications*, *10*(5), 585–596. https://doi.org/10.1002/PRCA.201500099

Kim, S.-H., & Lee, W.-J. (2014). Role of DUOX in gut inflammation: lessons from Drosophila model of gut-microbiota interactions. *Frontiers in Cellular and Infection Microbiology*, *3*. https://doi.org/10.3389/fcimb.2013.00116

Kiskowski, M. A., Jackson, R. S., Banerjee, J., Li, X., Kang, M., Iturregui, J. M., Franco, O. E., Hayward, S. W., & Bhowmick, N. A. (2011). Role for Stromal Heterogeneity in Prostate Tumorigenesis. *Cancer Research*, *71*(10), 3459–3470. https://doi.org/10.1158/0008-5472.CAN-10-2999

Klämbt, C. (1993). The *Drosophila* gene *pointed* encodes two ETS-like proteins which are involved in the development of the midline glial cells. *Development*, *117*(1), 163–176. https://doi.org/10.1242/dev.117.1.163

Klein, G., Langegger, M., Timpl, R., & Ekblom, P. (1988). Role of laminin a chain in the development of epithelial cell polarity. *Cell*, *55*(2), 331–341. https://doi.org/10.1016/0092-8674(88)90056-6

Klußmann-Fricke, B.-J., Martín-Bermudo, M. D., & Llimargas, M. (2022). The basement membrane controls size and integrity of the Drosophila tracheal tubes. *Cell Reports*, *39*(4), 110734. https://doi.org/10.1016/j.celrep.2022.110734

Königsmann, T., Parfentev, I., Urlaub, H., Riedel, D., & Schuh, R. (2020). The bicistronic gene würmchen encodes two essential components for epithelial development in Drosophila. *Developmental Biology*, *463*(1), 53–62. https://doi.org/10.1016/j.ydbio.2020.04.005

Korinek, V., Barker, N., Morin, P. J., van Wichen, D., de Weger, R., Kinzler, K. W., Vogelstein, B., & Clevers, H. (1997). Constitutive Transcriptional Activation by a β-Catenin-Tcf

Complex in APC $^{-/-}$ Colon Carcinoma. *Science*, *275*(5307), 1784–1787. https://doi.org/10.1126/science.275.5307.1784

Korzelius, J., Naumann, S. K., Loza-Coll, M. A., Chan, J. S., Dutta, D., Oberheim, J., Gläßer, C., Southall, T. D., Brand, A. H., Jones, D. L., & Edgar, B. A. (2014). Escargot maintains stemness and suppresses differentiation in Drosophila intestinal stem cells. *The EMBO Journal*, *33*(24), 2967–2982. https://doi.org/10.15252/embj.201489072

Kuhn, E., Kurman, R. J., Soslow, R. A., Han, G., Sehdev, A. S., Morin, P. J., Wang, T.-L., & Shih, I.-M. (2012). The Diagnostic and Biological Implications of Laminin Expression in Serous Tubal Intraepithelial Carcinoma. *American Journal of Surgical Pathology*, *36*(12), 1826–1834. https://doi.org/10.1097/PAS.0b013e31825ec07a

Kumagai, C., Kadowaki, T., & Kitagawa, Y. (1997). Disulfide-bonding between Drosophila laminin β and γ chains is essential for α chain to form αβγ trimer. *FEBS Letters*, *412*(1), 211–216. https://doi.org/10.1016/S0014-5793(97)00780-1

Kunitomi, H., Kobayashi, Y., Wu, R.-C., Takeda, T., Tominaga, E., Banno, K., & Aoki, D. (2020). LAMC1 is a prognostic factor and a potential therapeutic target in endometrial cancer. *Journal of Gynecologic Oncology*, *31*(2). https://doi.org/10.3802/jgo.2020.31.e11

Landis, G. N., Hilsabeck, T. A. U., Bell, H. S., Ronnen-Oron, T., Wang, L., Doherty, D. V., Tejawinata, F. I., Erickson, K., Vu, W., Promislow, D. E. L., Kapahi, P., & Tower, J. (2021). Mifepristone Increases Life Span of Virgin Female Drosophila on Regular and High-fat Diet Without Reducing Food Intake. *Frontiers in Genetics*, *12*, 1870. https://doi.org/10.3389/fgene.2021.751647

Landis, G. N., Salomon, M. P., Keroles, D., Brookes, N., Sekimura, T., & Tower, J. (2015). The progesterone antagonist mifepristone/RU486 blocks the negative effect on life span caused by mating in female Drosophila. *Aging*, *7*(1), 53–69. https://doi.org/10.18632/aging.100721

Laprise, P., Beronja, S., Silva-Gagliardi, N. F., Pellikka, M., Jensen, A. M., McGlade, C. J., & Tepass, U. (2006). The FERM Protein Yurt Is a Negative Regulatory Component of the Crumbs Complex that Controls Epithelial Polarity and Apical Membrane Size. *Developmental Cell*, *11*(3), 363–374. https://doi.org/10.1016/j.devcel.2006.06.001

Lee, H., Ibrahimi, L., Azar, D. T., & Han, K.-Y. (2023). The Role of Membrane-Type 1 Matrix Metalloproteinase–Substrate Interactions in Pathogenesis. *International Journal of Molecular Sciences*, *24*(3), 2183. https://doi.org/10.3390/ijms24032183

Lee, T., & Luo, L. (1999). Mosaic Analysis with a Repressible Cell Marker for Studies of Gene Function in Neuronal Morphogenesis. *Neuron*, *22*(3), 451–461. https://doi.org/10.1016/S0896-6273(00)80701-1

Lee, T., & Luo, L. (2001). Mosaic analysis with a repressible cell marker (MARCM) for Drosophila neural development. *Trends in Neurosciences*, *24*(5), 251–254. https://doi.org/10.1016/S0166-2236(00)01791-4

Lee, W.-C., Beebe, K., Sudmeier, L., & Micchelli, C. A. (2009). *Adenomatous polyposis coli* regulates *Drosophila* intestinal stem cell proliferation. *Development*, *136*(13), 2255–2264. https://doi.org/10.1242/dev.035196

Lei, Y., Lu, Z., Huang, J., Zang, R., Che, Y., Mao, S., Fang, L., Liu, C., Wang, X., Zheng, S., Sun, N., & He, J. (2020). The membrane-bound and soluble form of melanotransferrin function independently in the diagnosis and targeted therapy of lung cancer. *Cell Death & Disease*, *11*(10), 933. https://doi.org/10.1038/s41419-020-03124-2

Li, H., Qi, Y., & Jasper, H. (2013). Dpp Signaling Determines Regional Stem Cell Identity in the Regenerating Adult Drosophila Gastrointestinal Tract. *Cell Reports*, *4*(1), 10–18. https://doi.org/10.1016/j.celrep.2013.05.040

Li, H., Qi, Y., & Jasper, H. (2016). Preventing Age-Related Decline of Gut Compartmentalization Limits Microbiota Dysbiosis and Extends Lifespan. *Cell Host & Microbe*, *19*(2), 240–253. https://doi.org/10.1016/j.chom.2016.01.008

Li, S., Harrison, D., Carbonetto, S., Fässler, R., Smyth, N., Edgar, D., & Yurchenco, P. D. (2002). Matrix assembly, regulation, and survival functions of laminin and its receptors in embryonic stem cell differentiation. *The Journal of Cell Biology*, *157*(7), 1279–1290. https://doi.org/10.1083/jcb.200203073

Li, Z., Guo, Y., Han, L., Zhang, Y., Shi, L., Huang, X., & Lin, X. (2014). Debra-Mediated Ci Degradation Controls Tissue Homeostasis in Drosophila Adult Midgut. *Stem Cell Reports*, *2*(2), 135–144. https://doi.org/10.1016/j.stemcr.2013.12.011

Li, Z., Zhang, Y., Han, L., Shi, L., & Lin, X. (2013). Trachea-Derived Dpp Controls Adult Midgut Homeostasis in Drosophila. *Developmental Cell*, *24*(2), 133–143. https://doi.org/10.1016/j.devcel.2012.12.010

Liang, J., Balachandra, S., Ngo, S., & O'Brien, L. E. (2017). Feedback regulation of steady-state epithelial turnover and organ size. *Nature*, *548*(7669), 588–591. https://doi.org/10.1038/nature23678

Liétard, J., Musso, O., Théret, N., L'Helgoualc'h, A., Campion, J. P., Yamada, Y., & Clément, B. (1997). Sp1-mediated transactivation of LamC1 promoter and coordinated expression

of laminin-gamma1 and Sp1 in human hepatocellular carcinomas. *The American Journal of Pathology*, *151*(6), 1663–1672. http://www.ncbi.nlm.nih.gov/pubmed/9403717

Lim, X., Tan, S. H., Koh, W. L. C., Chau, R. M. W., Yan, K. S., Kuo, C. J., van Amerongen, R., Klein, A. M., & Nusse, R. (2013). Interfollicular Epidermal Stem Cells Self-Renew via Autocrine Wnt Signaling. *Science*, *342*(6163), 1226–1230. https://doi.org/10.1126/science.1239730

Lin, G., Xu, N., & Xi, R. (2008). Paracrine Wingless signalling controls self-renewal of Drosophila intestinal stem cells. *Nature*, *455*(7216), 1119–1123. https://doi.org/10.1038/nature07329

Lin, G., Xu, N., & Xi, R. (2010). Paracrine Unpaired Signaling through the JAK/STAT Pathway Controls Self-renewal and Lineage Differentiation of Drosophila Intestinal Stem Cells. *Journal of Molecular Cell Biology*, *2*(1), 37–49. https://doi.org/10.1093/jmcb/mjp028

Lin, G., Zhang, X., Ren, J., Pang, Z., Wang, C., Xu, N., & Xi, R. (2013). Integrin signaling is required for maintenance and proliferation of intestinal stem cells in Drosophila. *Developmental Biology*, *377*(1), 177–187. https://doi.org/10.1016/j.ydbio.2013.01.032

Liu, J., Liu, D., Yang, Z., & Yang, Z. (2019). High LAMC1 expression in glioma is associated with poor prognosis . *OncoTargets and Therapy*, *Volume 12*, 4253–4260. https://doi.org/10.2147/OTT.S205333

Liu, W., Singh, S. R., & Hou, S. X. (2010). JAK–STAT is restrained by Notch to control cell proliferation of the *Drosophila* intestinal stem cells. *Journal of Cellular Biochemistry*, *109*(5), 992–999. https://doi.org/10.1002/jcb.22482

Llimargas, M., Strigini, M., Katidou, M., Karagogeos, D., & Casanova, J. (2004). Lachesin is a component of a septate junction-based mechanism that controls tube size and epithelial integrity in the *Drosophila* tracheal system. *Development*, *131*(1), 181–190. https://doi.org/10.1242/dev.00917

López de Andrés, J., Griñán-Lisón, C., Jiménez, G., & Marchal, J. A. (2020). Cancer stem cell secretome in the tumor microenvironment: a key point for an effective personalized cancer treatment. *Journal of Hematology & Oncology*, *13*(1), 136. https://doi.org/10.1186/s13045-020-00966-3

López-Otín, C., Blasco, M. A., Partridge, L., Serrano, M., & Kroemer, G. (2013). The Hallmarks of Aging. *Cell*, *153*(6), 1194–1217. https://doi.org/10.1016/j.cell.2013.05.039

Lorenzon, E., Colladel, R., Andreuzzi, E., Marastoni, S., Todaro, F., Schiappacassi, M., Ligresti, G., Colombatti, A., & Mongiat, M. (2012). MULTIMERIN2 impairs tumor

angiogenesis and growth by interfering with VEGF-A/VEGFR2 pathway. *Oncogene*, *31*(26), 3136–3147. https://doi.org/10.1038/onc.2011.487

Lou, J., Gong, J., Ke, J., Tian, J., Zhang, Y., Li, J., Yang, Y., Zhu, Y., Gong, Y., Li, L., Chang, J., Zhong, R., & Miao, X. (2016). A functional polymorphism located at transcription factor binding sites, rs6695837 near *LAMC1* gene, confers risk of colorectal cancer in Chinese populations. *Carcinogenesis*, *38*(2), bgw204. https://doi.org/10.1093/carcin/bgw204

Loza-Coll, M. A., Southall, T. D., Sandall, S. L., Brand, A. H., & Jones, D. L. (2014). Regulation of Drosophila intestinal stem cell maintenance and differentiation by the transcription factor Escargot. *The EMBO Journal*, *33*(24), 2983–2996. https://doi.org/10.15252/embj.201489050

Lucchetta, E. M., & Ohlstein, B. (2012). The *Drosophila* midgut: a model for stem cell driven tissue regeneration. *WIREs Developmental Biology*, *1*(5), 781–788. https://doi.org/10.1002/wdev.51

Mao, Y., Wang, M., Xiong, Y., Wen, X., Zhang, M., Ma, L., & Zhang, Y. (2023). MELTF Might Regulate Ferroptosis, Pyroptosis, and Autophagy in Platelet-Rich Plasma-Mediated Endometrial Epithelium Regeneration. *Reproductive Sciences*, *30*(5), 1506–1520. https://doi.org/10.1007/s43032-022-01101-y

Marianes, A., & Spradling, A. C. (2013). Physiological and stem cell compartmentalization within the Drosophila midgut. *ELife*, *2*(2). https://doi.org/10.7554/eLife.00886

Martin, D., Zusman, S., Li, X., Williams, E. L., Khare, N., Darocha, S., Chiquet-Ehrismann, R., & Baumgartner, S. (1999). wing blister , A New Drosophila Laminin Chain Required for Cell Adhesion and Migration during Embryonic and Imaginal Development. *The Journal of Cell Biology*, *145*(1). http://www.jcb.org

Martin, J. L., Sanders, E. N., Moreno-Roman, P., Jaramillo Koyama, L. A., Balachandra, S., Du, X., & O'Brien, L. E. (2018). Long-term live imaging of the Drosophila adult midgut reveals real-time dynamics of division, differentiation and loss. *ELife*, *7*. https://doi.org/10.7554/eLife.36248

Martin-Blanco, E., Gampel, A., Ring, J., Virdee, K., Kirov, N., Tolkovsky, A. M., & Martinez-Arias, A. (1998). puckered encodes a phosphatase that mediates a feedback loop regulating JNK activity during dorsal closure in Drosophila. *Genes & Development*, *12*(4), 557–570. https://doi.org/10.1101/gad.12.4.557

Matsubayashi, Y., Louani, A., Dragu, A., Sánchez-Sánchez, B. J., Serna-Morales, E., Yolland, L., Gyoergy, A., Vizcay, G., Fleck, R. A., Heddleston, J. M., Chew, T.-L., Siekhaus, D. E.,

& Stramer, B. M. (2017). A Moving Source of Matrix Components Is Essential for De Novo Basement Membrane Formation. *Current Biology*, *27*(22), 3526-3534.e4. https://doi.org/10.1016/j.cub.2017.10.001

Mayer, U., Nischt, R., Poschl, E., Mann, K., Fukuda, K., Geri, M., Yamada, Y., & Timpl, R. (1993). A single EGF-like motif of laminin is responsible for high affinity nidogen binding. *The EMBO Journal*, *1*(5), 1–879.

Mazahreh, R., Mason, M. L., Gosink, J. J., Olson, D. J., Thurman, R., Hale, C., Westendorf, L., Pires, T. A., Leiske, C. I., Carlson, M., Nguyen, L. T., Cochran, J. H., Okeley, N. M., Yumul, R., Jin, S., Stone, I. J., Sahetya, D., Nesterova, A., Allred, S., … Sandall, S. (2023). SGN-CD228A Is an Investigational CD228-Directed Antibody–Drug Conjugate with Potent Antitumor Activity across a Wide Spectrum of Preclinical Solid Tumor Models. *Molecular Cancer Therapeutics*, *22*(4), 421–434. https://doi.org/10.1158/1535-7163.MCT-22-0401

McClure, C. D., Hassan, A., Aughey, G. N., Butt, K., Estacio-Gómez, A., Duggal, A., Ying Sia, C., Barber, A. F., & Southall, T. D. (2022). An auxin-inducible, GAL4-compatible, gene expression system for Drosophila. *ELife*, *11*. https://doi.org/10.7554/eLife.67598

McGuire, S. E., Le, P. T., Osborn, A. J., Matsumoto, K., & Davis, R. L. (2003). Spatiotemporal Rescue of Memory Dysfunction in *Drosophila*. *Science*, *302*(5651), 1765–1768. https://doi.org/10.1126/science.1089035

McNagny, K., Rossi, F., Smith, G., & Graf, T. (1996). The eosinophil-specific cell surface antigen, EOS47, is a chicken homologue of the oncofetal antigen melanotransferrin. *Blood*, *87*(4), 1343–1352. https://doi.org/10.1182/blood.V87.4.1343.bloodjournal8741343

McNeal, J. E. (1969). Origin and development of carcinoma in the prostate. *Cancer*, *23*(1), 24–34. https://doi.org/10.1002/1097-0142(196901)23:1<24::AID-CNCR2820230103>3.0.CO;2-1

McNeal, J. E. (1978). Origin and evolution of benign prostatic enlargement. *Investigative Urology*, *15*(4), 340–345. http://www.ncbi.nlm.nih.gov/pubmed/75197

McNeal, J. E. (1981). The zonal anatomy of the prostate. *The Prostate*, *2*(1), 35–49. https://doi.org/10.1002/pros.2990020105

Micchelli, C. A., & Perrimon, N. (2006). Evidence that stem cells reside in the adult Drosophila midgut epithelium. *Nature*, *439*(7075), 475–479. https://doi.org/10.1038/nature04371

Michaud-Levesque, J., Demeule, M., & Beliveau, R. (2006). In vivo inhibition of angiogenesis by a soluble form of melanotransferrin. *Carcinogenesis*, *28*(2), 280–288. https://doi.org/10.1093/carcin/bgl123

Michaud-Levesque, J., Rolland, Y., Demeule, M., Bertrand, Y., & Béliveau, R. (2005). Inhibition of endothelial cell movement and tubulogenesis by human recombinant soluble melanotransferrin: involvement of the u-PAR/LRP plasminolytic system. *Biochimica et Biophysica Acta (BBA) - Molecular Cell Research*, *1743*(3), 243–253. https://doi.org/10.1016/j.bbamcr.2004.10.010

Mitra, S. K., Hanson, D. A., & Schlaepfer, D. D. (2005). Focal adhesion kinase: in command and control of cell motility. *Nature Reviews Molecular Cell Biology*, *6*(1), 56–68. https://doi.org/10.1038/nrm1549

Moad, M., Hannezo, E., Buczacki, S. J., Wilson, L., El-Sherif, A., Sims, D., Pickard, R., Wright, N. A., Williamson, S. C., Turnbull, D. M., Taylor, R. W., Greaves, L., Robson, C. N., Simons, B. D., & Heer, R. (2017). Multipotent Basal Stem Cells, Maintained in Localized Proximal Niches, Support Directed Long-Ranging Epithelial Flows in Human Prostates. *Cell Reports*, *20*(7), 1609–1622. https://doi.org/10.1016/j.celrep.2017.07.061

Montagne, C., & Gonzalez-Gaitan, M. (2014). Sara endosomes and the asymmetric division of intestinal stem cells. *Development*, *141*(10), 2014–2023. https://doi.org/10.1242/dev.104240

Montell, D. J., & Goodman, C. S. (1988). Drosophila substrate adhesion molecule: Sequence of laminin B1 chain reveals domains of homology with mouse. *Cell*, *53*(3), 463–473. https://doi.org/10.1016/0092-8674(88)90166-3

Moroo, I., Ujie, M., Walker, B. L., Tiong, J. W. C., Vitalis, T. Z., Karkan, D., Gabathuler, R., Moise, A. R., & Jefferies, W. A. (2003). Identification of a Novel Route of Iron Transcytosis across the Mammalian Blood-Brain Barrier. *Microcirculation*, *10*(6), 457–462. https://doi.org/10.1038/sj.mn.7800213

Morris, R. J., Liu, Y., Marles, L., Yang, Z., Trempus, C., Li, S., Lin, J. S., Sawicki, J. A., & Cotsarelis, G. (2004). Capturing and profiling adult hair follicle stem cells. *Nature Biotechnology*, *22*(4), 411–417. https://doi.org/10.1038/nbt950

Morrison, S. J., & Spradling, A. C. (2008). Stem Cells and Niches: Mechanisms That Promote Stem Cell Maintenance throughout Life. *Cell*, *132*(4), 598–611. https://doi.org/10.1016/j.cell.2008.01.038

Moskalev, A., Proshkina, E., Zhavoronkov, A., & Shaposhnikov, M. (2019). Effects of unpaired 1 gene overexpression on the lifespan of Drosophila melanogaster. *BMC Systems Biology*, *13*(S1), 16. https://doi.org/10.1186/s12918-019-0687-x

Mundorf, J., Donohoe, C. D., McClure, C. D., Southall, T. D., & Uhlirova, M. (2019). Ets21c Governs Tissue Renewal, Stress Tolerance, and Aging in the Drosophila Intestine. *Cell Reports*, *27*(10), 3019-3033.e5. https://doi.org/10.1016/j.celrep.2019.05.025

Natali, P. G., Roberts, J. T., Difilippo, F., Bigotti, A., Dent, P. B., Ferrone, S., & Liao, S.-K. (1987). Immunohistochemical detection of antigen in human primary and metastatic melanomas by the monoclonal antibody 140.240 and its possible prognostic significance. *Cancer*, *59*(1), 55–63. https://doi.org/10.1002/1097-0142(19870101)59:1<55::AID-CNCR2820590115>3.0.CO;2-R

Naureckiene, S., Sleat, David. E., Lackland, H., Fensom, A., Vanier, M. T., Wattiaux, R., Jadot, M., & Lobel, P. (2000). Identification of *HE1* as the Second Gene of Niemann-Pick C Disease. *Science*, *290*(5500), 2298–2301. https://doi.org/10.1126/science.290.5500.2298

Nelson, K. S., Furuse, M., & Beitel, G. J. (2010). The Drosophila Claudin Kune-kune Is Required for Septate Junction Organization and Tracheal Tube Size Control. *Genetics*, *185*(3), 831–839. https://doi.org/10.1534/genetics.110.114959

Neophytou, C., Soteriou, E., & Pitsouli, C. (2023). The Sterol Transporter Npc2c Controls Intestinal Stem Cell Mitosis and Host–Microbiome Interactions in Drosophila. *Metabolites*, *13*(10), 1084. https://doi.org/10.3390/metabo13101084

Nilton, A., Oshima, K., Zare, F., Byri, S., Nannmark, U., Nyberg, K. G., Fehon, R. G., & Uv, A. E. (2010). Crooked, Coiled and Crimpled are three Ly6-like proteins required for proper localization of septate junction components. *Development*, *137*(14), 2427–2437. https://doi.org/10.1242/dev.052605

Nishikawa, R., Goto, Y., Kojima, S., Enokida, H., Chiyomaru, T., Kinoshita, T., Sakamoto, S., Fuse, M., Nakagawa, M., Naya, Y., Ichikawa, T., & Seki, N. (2014). Tumor-suppressive microRNA-29s inhibit cancer cell migration and invasion via targeting LAMC1 in prostate cancer. *International Journal of Oncology*, *45*(1), 401–410. https://doi.org/10.3892/ijo.2014.2437

Noirot-Timothée, C., & Noirot, C. (1980). Septate and Scalariform Junctions in Arthropods. In *International Review of Cytology* (Vol. 63, pp. 97–140). Academic Press. https://doi.org/10.1016/S0074-7696(08)61758-1

Nounou, M. I., Adkins, C. E., Rubinchik, E., Terrell-Hall, T. B., Afroz, M., Vitalis, T., Gabathuler, R., Tian, M. M., & Lockman, P. R. (2016). Anti-cancer Antibody

Trastuzumab-Melanotransferrin Conjugate (BT2111) for the Treatment of Metastatic HER2+ Breast Cancer Tumors in the Brain: an In-Vivo Study. *Pharmaceutical Research*, *33*(12), 2930–2942. https://doi.org/10.1007/s11095-016-2015-0

Obniski, R., Sieber, M., & Spradling, A. C. (2018). Dietary Lipids Modulate Notch Signaling and Influence Adult Intestinal Development and Metabolism in Drosophila. *Developmental Cell*, *47*(1), 98-111.e5. https://doi.org/10.1016/j.devcel.2018.08.013

O'Brien, L. E., Soliman, S. S., Li, X., & Bilder, D. (2011). Altered Modes of Stem Cell Division Drive Adaptive Intestinal Growth. *Cell*, *147*(3), 603–614. https://doi.org/10.1016/j.cell.2011.08.048

Ohlstein, B., & Spradling, A. (2006). The adult Drosophila posterior midgut is maintained by pluripotent stem cells. *Nature*, *439*(7075), 470–474. https://doi.org/10.1038/nature04333

Ohlstein, B., & Spradling, A. (2007). Multipotent *Drosophila* Intestinal Stem Cells Specify Daughter Cell Fates by Differential Notch Signaling. *Science*, *315*(5814), 988–992. https://doi.org/10.1126/science.1136606

Ojalill, M., Rappu, P., Siljamäki, E., Taimen, P., Boström, P., & Heino, J. (2018). The composition of prostate core matrisome in vivo and in vitro unveiled by mass spectrometric analysis. *The Prostate*, *78*(8), 583–594. https://doi.org/10.1002/pros.23503

Ojalill, M., Virtanen, N., Rappu, P., Siljamäki, E., Taimen, P., & Heino, J. (2020). Interaction between prostate cancer cells and prostate fibroblasts promotes accumulation and proteolytic processing of basement membrane proteins. *The Prostate*, *80*(9), 715–726. https://doi.org/10.1002/pros.23985

O'Reilly, A. M., Lee, H.-H., & Simon, M. A. (2008). Integrins control the positioning and proliferation of follicle stem cells in the *Drosophila* ovary. *The Journal of Cell Biology*, *182*(4), 801–815. https://doi.org/10.1083/jcb.200710141

Osman, D., Buchon, N., Chakrabarti, S., Huang, Y.-T., Su, W.-C., Poidevin, M., Tsai, Y.-C., & Lemaitre, B. (2012). Autocrine and paracrine unpaired signaling regulate intestinal stem cell maintenance and division. *Journal of Cell Science*, *125*(24), 5944–5949. https://doi.org/10.1242/jcs.113100

Osterwalder, T., Yoon, K. S., White, B. H., & Keshishian, H. (2001). A conditional tissue-specific transgene expression system using inducible GAL4. *Proceedings of the National Academy of Sciences*, *98*(22), 12596–12601. https://doi.org/10.1073/pnas.221303298

Ousset, M., Van Keymeulen, A., Bouvencourt, G., Sharma, N., Achouri, Y., Simons, B. D., & Blanpain, C. (2012). Multipotent and unipotent progenitors contribute to prostate

postnatal development. *Nature Cell Biology*, *14*(11), 1131–1138. https://doi.org/10.1038/ncb2600

Paluncic, J., Azad, M. G., Lane, D. J. R., Skoda, J., Park, K. C., Chiang, S., Bae, D. H., Scolyer, R., Afroz, R., Babu, G., Wilmott, J., Loh, K., Jansson, P. J., Dharmasivam, M., Huang, M. L., Zhao, X., Kovacevic, Z., & Richardson, D. R. (2023). Melanotransferrin Functions as a Pro-Oncogenic WNT Agonist: A Yin-Yang Relationship in Melanoma with the WNT Antagonist and Metastasis Suppressor, NDRG1. *BioRxiv*, 2023.02.27.530353. https://doi.org/10.1101/2023.02.27.530353

Pardo-Saganta, A., Tata, P. R., Law, B. M., Saez, B., Chow, R. D.-W., Prabhu, M., Gridley, T., & Rajagopal, J. (2015). Parent stem cells can serve as niches for their daughter cells. *Nature*, *523*(7562), 597–601. https://doi.org/10.1038/nature14553

Paul, S. M., Ternet, M., Salvaterra, P. M., & Beitel, G. J. (2003). The Na+/K+ ATPase is required for septate junction function and epithelial tube-size control in the *Drosophila* tracheal system. *Development*, *130*(20), 4963–4974. https://doi.org/10.1242/dev.00691

Pawar, S. C., Demetriou, M. C., Nagle, R. B., Bowden, G. T., & Cress, A. E. (2007). Integrin α6 cleavage: A novel modification to modulate cell migration. *Experimental Cell Research*, *313*(6), 1080–1089. https://doi.org/10.1016/j.yexcr.2007.01.006

Pellerin, S., Keramidas, M., Chambaz, E. M., & Feige, J.-J. (1997). Expression of Laminin and Its Possible Role in Adrenal Cortex Homeostasis. *Endocrinology*, *138*(3), 1321–1327. https://doi.org/10.1210/endo.138.3.4962

Perochon, J., Yu, Y., Aughey, G. N., Medina, A. B., Southall, T. D., & Cordero, J. B. (2021). Dynamic adult tracheal plasticity drives stem cell adaptation to changes in intestinal homeostasis in Drosophila. *Nature Cell Biology*, *23*(5), 485–496. https://doi.org/10.1038/s41556-021-00676-z

Peters, U., Jiao, S., Schumacher, F. R., Hutter, C. M., Aragaki, A. K., Baron, J. A., Berndt, S. I., Bézieau, S., Brenner, H., Butterbach, K., Caan, B. J., Campbell, P. T., Carlson, C. S., Casey, G., Chan, A. T., Chang–Claude, J., Chanock, S. J., Chen, L. S., Coetzee, G. A., … Hsu, L. (2013). Identification of Genetic Susceptibility Loci for Colorectal Tumors in a Genome-Wide Meta-analysis. *Gastroenterology*, *144*(4), 799-807.e24. https://doi.org/10.1053/j.gastro.2012.12.020

Petley-Ragan, L. M., Ardiel, E. L., Rankin, C. H., & Auld, V. J. (2016). Accumulation of Laminin Monomers in *Drosophila* Glia Leads to Glial Endoplasmic Reticulum Stress and Disrupted Larval Locomotion. *The Journal of Neuroscience*, *36*(4), 1151–1164. https://doi.org/10.1523/JNEUROSCI.1797-15.2016

Petri, J., Syed, M. H., Rey, S., & Klämbt, C. (2019). Non-Cell-Autonomous Function of the GPI-Anchored Protein Undicht during Septate Junction Assembly. *Cell Reports*, *26*(6), 1641-1653.e4. https://doi.org/10.1016/j.celrep.2019.01.046

Piovan, C., Palmieri, D., Di Leva, G., Braccioli, L., Casalini, P., Nuovo, G., Tortoreto, M., Sasso, M., Plantamura, I., Triulzi, T., Taccioli, C., Tagliabue, E., Iorio, M. V., & Croce, C. M. (2012). Oncosuppressive role of p53-induced miR-205 in triple negative breast cancer. *Molecular Oncology*, *6*(4), 458–472. https://doi.org/10.1016/j.molonc.2012.03.003

Pitsidianaki, I., Morgan, J., Adams, J., & Campbell, K. (2021). Mesenchymal-to-epithelial transitions require tissue-specific interactions with distinct laminins. *Journal of Cell Biology*, *220*(8). https://doi.org/10.1083/jcb.202010154

Poirier, L., Shane, A., Zheng, J., & Seroude, L. (2008). Characterization of the *Drosophila* Gene-Switch system in aging studies: a cautionary tale. *Aging Cell*, *7*(5), 758–770. https://doi.org/10.1111/j.1474-9726.2008.00421.x

Port, F., Strein, C., Stricker, M., Rauscher, B., Heigwer, F., Zhou, J., Beyersdörffer, C., Frei, J., Hess, A., Kern, K., Lange, L., Langner, N., Malamud, R., Pavlović, B., Rädecke, K., Schmitt, L., Voos, L., Valentini, E., & Boutros, M. (2020). A large-scale resource for tissue-specific CRISPR mutagenesis in Drosophila. *ELife*, *9*. https://doi.org/10.7554/eLife.53865

Puzanov, G. A. (2022). Identification of key genes of the ccRCC subtype with poor prognosis. *Scientific Reports*, *12*(1), 14588. https://doi.org/10.1038/s41598-022-18620-y

Rahmanto, Y. S., & Richardson, D. R. (2009). Generation and characterization of transgenic mice hyper-expressing melanoma tumour antigen p97 (Melanotransferrin): No overt alteration in phenotype. *Biochimica et Biophysica Acta - Molecular Cell Research*, *1793*(7), 1210–1217. https://doi.org/10.1016/j.bbamcr.2009.02.003

Ramírez-Gómez, F., Ortíz-Pineda, P. A., Rojas-Cartagena, C., Suárez-Castillo, E. C., & García-Ararrás, J. E. (2008). Immune-related genes associated with intestinal tissue in the sea cucumber Holothuria glaberrima. *Immunogenetics*, *60*(1), 57–71. https://doi.org/10.1007/s00251-007-0258-y

Real, F. X., Furukawa, K. S., Mattes, M. J., Gusik, S. A., Cordon-Cardo, C., Oettgen, H. F., Old, L. J., & Lloyd, K. O. (1988). Class 1 (unique) tumor antigens of human melanoma: identification of unique and common epitopes on a 90-kDa glycoprotein. *Proceedings of the National Academy of Sciences*, *85*(11), 3965–3969. https://doi.org/10.1073/pnas.85.11.3965

Reiff, T., Jacobson, J., Cognigni, P., Antonello, Z., Ballesta, E., Tan, K. J., Yew, J. Y., Dominguez, M., & Miguel-Aliaga, I. (2015). Endocrine remodelling of the adult intestine sustains reproduction in Drosophila. *ELife*, *4*(e06930). https://doi.org/10.7554/eLife.06930

Reiter, L. T., Potocki, L., Chien, S., Gribskov, M., & Bier, E. (2001). A Systematic Analysis of Human Disease-Associated Gene Sequences In *Drosophila melanogaster*. *Genome Research*, *11*(6), 1114–1125. https://doi.org/10.1101/gr.169101

Ren, F., Wang, B., Yue, T., Yun, E.-Y., Ip, Y. T., & Jiang, J. (2010). Hippo signaling regulates Drosophila intestine stem cell proliferation through multiple pathways. *Proceedings of the National Academy of Sciences*, *107*(49), 21064–21069. https://doi.org/10.1073/pnas.1012759107

Rera, M., Bahadorani, S., Cho, J., Koehler, C. L., Ulgherait, M., Hur, J. H., Ansari, W. S., Lo, T., Jones, D. L., & Walker, D. W. (2011). Modulation of Longevity and Tissue Homeostasis by the Drosophila PGC-1 Homolog. *Cell Metabolism*, *14*(5), 623–634. https://doi.org/10.1016/j.cmet.2011.09.013

Rera, M., Clark, R. I., & Walker, D. W. (2012). Intestinal barrier dysfunction links metabolic and inflammatory markers of aging to death in Drosophila. *Proceedings of the National Academy of Sciences of the United States of America*, *109*(52), 21528–21533. https://doi.org/10.1073/pnas.1215849110

Resnik-Docampo, M., Cunningham, K. M., Ruvalcaba, S. M., Choi, C., Sauer, V., & Jones, D. L. (2021). Neuroglian regulates Drosophila intestinal stem cell proliferation through enhanced signaling via the epidermal growth factor receptor. *Stem Cell Reports*, *16*(6), 1584–1597. https://doi.org/10.1016/j.stemcr.2021.04.006

Resnik-Docampo, M., Koehler, C. L., Clark, R. I., Schinaman, J. M., Sauer, V., Wong, D. M., Lewis, S., D'Alterio, C., Walker, D. W., & Jones, D. L. (2017). Tricellular junctions regulate intestinal stem cell behaviour to maintain homeostasis. *Nature Cell Biology*, *19*(1), 52–59. https://doi.org/10.1038/ncb3454

Richardson, D. R. (2000). The role of the membrane-bound tumour antigen, melanotransferrin (p97), in iron uptake by the human malignant melanoma cell. *European Journal of Biochemistry*, *267*(5), 1290–1298. https://doi.org/10.1046/j.1432-1327.2000.01079.x

Richardson, D. R., & Morgan, E. H. (2004). The transferrin homologue, melanotransferrin (p97), is rapidly catabolized by the liver of the rat and does not effectively donate iron to the brain. *Biochimica et Biophysica Acta (BBA) - Molecular Basis of Disease*, *1690*(2), 124–133. https://doi.org/10.1016/j.bbadis.2004.06.002

Rincón-Ortega, L., Valencia-Expósito, A., Kabanova, A., González-Reyes, A., & Martin-Bermudo, M. D. (2023). Integrins control epithelial stem cell proliferation in the Drosophila ovary by modulating the Notch pathway. *Frontiers in Cell and Developmental Biology*, *11*. https://doi.org/10.3389/fcell.2023.1114458

Rodriguez-Fernandez, I. A., Qi, Y., & Jasper, H. (2019). Loss of a proteostatic checkpoint in intestinal stem cells contributes to age-related epithelial dysfunction. *Nature Communications*, *10*(1), 1050. https://doi.org/10.1038/s41467-019-08982-9

Rodriguez-Fernandez, I. A., Tauc, H. M., & Jasper, H. (2020). Hallmarks of aging Drosophila intestinal stem cells. *Mechanisms of Ageing and Development*, *190*, 111285. https://doi.org/10.1016/j.mad.2020.111285

Röhn, T. A., Reitz, A., Paschen, A., Nguyen, X. D., Schadendorf, D., Vogt, A. B., & Kropshofer, H. (2005). A Novel Strategy for the Discovery of MHC Class II–Restricted Tumor Antigens: Identification of a Melanotransferrin Helper T-Cell Epitope. *Cancer Research*, *65*(21), 10068–10078. https://doi.org/10.1158/0008-5472.CAN-05-1973

Rolland, Y., Demeule, M., Fenart, L., & Béliveau, R. (2009). Inhibition of melanoma brain metastasis by targeting melanotransferrin at the cell surface. *Pigment Cell & Melanoma Research*, *22*(1), 86–98. https://doi.org/10.1111/j.1755-148X.2008.00525.x

Rolland, Y., Demeule, M., Michaud-Levesque, J., & Béliveau, R. (2007). Inhibition of tumor growth by a truncated and soluble form of melanotransferrin. *Experimental Cell Research*, *313*(13), 2910–2919. https://doi.org/10.1016/j.yexcr.2007.04.013

Roman, G., Endo, K., Zong, L., & Davis, R. L. (2001). P{Switch}, a system for spatial and temporal control of gene expression in *Drosophila melanogaster*. *Proceedings of the National Academy of Sciences*, *98*(22), 12602–12607. https://doi.org/10.1073/pnas.221303998

Rose, T. M., Plowman, G. D., Teplow, D. B., Dreyer, W. J., Hellström, K. E., & Brown, J. P. (1986). Primary structure of the human melanoma-associated antigen p97 (melanotransferrin) deduced from the mRNA sequence. *Proceedings of the National Academy of Sciences*, *83*(5), 1261–1265. https://doi.org/10.1073/pnas.83.5.1261

Rothenberger, S., Food, M. R., Gabathuler, R., Kennard, M. L., Yamada, T., Yasuhara, O., L. McGeer, P., & Jefferies, W. A. (1996). Coincident expression and distribution of melanotransferrin and transferrin receptor in human brain capillary endothelium. *Brain Research*, *712*(1), 117–121. https://doi.org/10.1016/0006-8993(96)88505-2

Rousselle, P., Golbik, R., van der Rest, M., & Aumailley, M. (1995). Structural Requirement for Cell Adhesion to Kalinin (Laminin-5). *Journal of Biological Chemistry*, *270*(23), 13766–13770. https://doi.org/10.1074/jbc.270.23.13766

Saad, F., & Hotte, S. J. (2010). Guidelines for the management of castrate-resistant prostate cancer. *Canadian Urological Association Journal*, *4*(6), 380–384. https://doi.org/10.5489/cuaj.10167

Sala, R., Jefferies, W. A., Walker, B., Yang, J., Tiong, J., Law, S. K. A., Carlevaro, M. F., Di Marco, E., Vacca, A., Cancedda, R., Cancedda, F. D., & Ribatti, D. (2002). The human melanoma associated protein melanotransferrin promotes endothelial cell migration and angiogenesis in vivo. *European Journal of Cell Biology*, *81*(11), 599–607. https://doi.org/10.1078/0171-9335-00280

Salazar, A. M., Aparicio, R., Clark, R. I., Rera, M., & Walker, D. W. (2023). Intestinal barrier dysfunction: an evolutionarily conserved hallmark of aging. *Disease Models & Mechanisms*, *16*(4). https://doi.org/10.1242/dmm.049969

Salazar, A. M., Resnik-Docampo, M., Ulgherait, M., Clark, R. I., Shirasu-Hiza, M., Jones, D. L., & Walker, D. W. (2018). Intestinal Snakeskin Limits Microbial Dysbiosis during Aging and Promotes Longevity. *IScience*, *9*, 229–243. https://doi.org/10.1016/j.isci.2018.10.022

Sancho, R., Cremona, C. A., & Behrens, A. (2015). Stem cell and progenitor fate in the mammalian intestine: Notch and lateral inhibition in homeostasis and disease. *EMBO Reports*, *16*(5), 571–581. https://doi.org/10.15252/embr.201540188

Sarov, M., Barz, C., Jambor, H., Hein, M. Y., Schmied, C., Suchold, D., Stender, B., Janosch, S., KJ, V. V., Krishnan, R., Krishnamoorthy, A., Ferreira, I. R., Ejsmont, R. K., Finkl, K., Hasse, S., Kämpfer, P., Plewka, N., Vinis, E., Schloissnig, S., … Schnorrer, F. (2016). A genome-wide resource for the analysis of protein localisation in Drosophila. *ELife*, *5*(FEBRUARY2016). https://doi.org/10.7554/eLife.12068

Sasaki, A., Nishimura, T., Takano, T., Naito, S., & Kan Yoo, S. (2021). white regulates proliferative homeostasis of intestinal stem cells during ageing in Drosophila. *Nat Metab*, *3*, 546–557. https://doi.org/10.1038/s42255-021-00375-x

Sato, T., van Es, J. H., Snippert, H. J., Stange, D. E., Vries, R. G., van den Born, M., Barker, N., Shroyer, N. F., van de Wetering, M., & Clevers, H. (2011). Paneth cells constitute the niche for Lgr5 stem cells in intestinal crypts. *Nature*, *469*(7330), 415–418. https://doi.org/10.1038/nature09637

Sato, T., Vries, R. G., Snippert, H. J., van de Wetering, M., Barker, N., Stange, D. E., van Es, J. H., Abo, A., Kujala, P., Peters, P. J., & Clevers, H. (2009). Single Lgr5 stem cells build

crypt-villus structures in vitro without a mesenchymal niche. *Nature*, *459*(7244), 262–265. https://doi.org/10.1038/nature07935

Sawaki, K., Kanda, M., Umeda, S., Miwa, T., Tanaka, C., Kobayashi, D., Hayashi, M., Yamada, S., Nakayama, G., Omae, K., KOIKE, M., & KODERA, Y. (2019). Level of Melanotransferrin in Tissue and Sera Serves as a Prognostic Marker of Gastric Cancer. *Anticancer Research*, *39*(11), 6125–6133. https://doi.org/10.21873/anticanres.13820

Schindelin, J., Arganda-Carreras, I., Frise, E., Kaynig, V., Longair, M., Pietzsch, T., Preibisch, S., Rueden, C., Saalfeld, S., Schmid, B., Tinevez, J.-Y., White, D. J., Hartenstein, V., Eliceiri, K., Tomancak, P., & Cardona, A. (2012). Fiji: an open-source platform for biological-image analysis. *Nature Methods*, *9*(7), 676–682. https://doi.org/10.1038/nmeth.2019

Schittny, J. C., & Yurchenco, P. D. (1990). Terminal short arm domains of basement membrane laminin are critical for its self-assembly. *The Journal of Cell Biology*, *110*(3), 825–832. https://doi.org/10.1083/jcb.110.3.825

Schmehl, K., Florian, S., Jacobasch, G., Salomon, A., & Körber, J. (2000). Deficiency of epithelial basement membrane laminin in ulcerative colitis affected human colonic mucosa. *International Journal of Colorectal Disease*, *15*(1), 39–48. https://doi.org/10.1007/s003840050006

Schneider, M., Khalil, A. A., Poulton, J., Castillejo-Lopez, C., Egger-Adam, D., Wodarz, A., Deng, W.-M., & Baumgartner, S. (2006). Perlecan and Dystroglycan act at the basal side of the Drosophila follicular epithelium to maintain epithelial organization. *Development*, *133*, 3805–3815. https://doi.org/10.1242/dev.02549

Schulte, J., Tepass, U., & Auld, V. J. (2003). Gliotactin, a novel marker of tricellular junctions, is necessary for septate junction development in Drosophila. *Journal of Cell Biology*, *161*(5), 991–1000. https://doi.org/10.1083/jcb.200303192

Scialo, F., Sriram, A., Stefanatos, R., & Sanz, A. (2016). Practical Recommendations for the Use of the GeneSwitch Gal4 System to Knock-Down Genes in Drosophila melanogaster. *PLOS ONE*, *11*(8), e0161817. https://doi.org/10.1371/journal.pone.0161817

Sciot, R., De Vos, R., van Eyken, P., van der Steen, K., Moerman, P., & Desmet, V. J. (1989). In situ localization of melanotransferrin (melanoma-associated antigen P97) in human liver. A light- and electronmicroscopic immunohistochemical study. *Liver*, *9*(2), 110–119. https://doi.org/10.1111/J.1600-0676.1989.TB00387.X

Scopelliti, A., Cordero, J. B., Diao, F., Strathdee, K., White, B. H., Sansom, O. J., & Vidal, M. (2014). Local Control of Intestinal Stem Cell Homeostasis by Enteroendocrine Cells in

the Adult Drosophila Midgut. *Current Biology*, *24*(11), 1199–1211. https://doi.org/10.1016/j.cub.2014.04.007

Sekyere, E. O., Dunn, L. L., Rahmanto, Y. S., & Richardson, D. R. (2006). Role of melanotransferrin in iron metabolism: studies using targeted gene disruption in vivo. *Blood*, *107*(7), 2599–2601. https://doi.org/10.1182/blood-2005-10-4174

Sessions, A. O., Kaushik, G., Parker, S., Raedschelders, K., Bodmer, R., Van Eyk, J. E., & Engler, A. J. (2017). Extracellular matrix downregulation in the Drosophila heart preserves contractile function and improves lifespan. *Matrix Biology*, *62*, 15–27. https://doi.org/10.1016/j.matbio.2016.10.008

Shaw, R. L., Kohlmaier, A., Polesello, C., Veelken, C., Edgar, B. A., & Tapon, N. (2010). The Hippo pathway regulates intestinal stem cell proliferation during *Drosophila* adult midgut regeneration. *Development*, *137*(24), 4147–4158. https://doi.org/10.1242/dev.052506

Shen, M. M., & Abate-Shen, C. (2010). Molecular genetics of prostate cancer: new prospects for old challenges. *Genes & Development*, *24*(18), 1967–2000. https://doi.org/10.1101/gad.1965810

Shi, X.-Z., Zhong, X., & Yu, X.-Q. (2012). Drosophila melanogaster NPC2 proteins bind bacterial cell wall components and may function in immune signal pathways. *Insect Biochemistry and Molecular Biology*, *42*(8), 545–556. https://doi.org/10.1016/j.ibmb.2012.04.002

Siler, U., Seiffert, M., Puch, S., Richards, A., Torok-Storb, B., Müller, C. A., Sorokin, L., & Klein, G. (2000). Characterization and functional analysis of laminin isoforms in human bone marrow. *Blood*, *96*(13), 4194–4203. https://doi.org/10.1182/blood.V96.13.4194

Siljamäki, E., Rappu, P., Riihilä, P., Nissinen, L., Kähäri, V.-M., & Heino, J. (2020). H-Ras activation and fibroblast-induced TGF-β signaling promote laminin-332 accumulation and invasion in cutaneous squamous cell carcinoma. *Matrix Biology*, *87*, 26–47. https://doi.org/10.1016/j.matbio.2019.09.001

Singh, C. S. B., Eyford, B. A., Abraham, T., Munro, L., Choi, K. B., Okon, M., Vitalis, T. Z., Gabathuler, R., Lu, C.-J., Pfeifer, C. G., Tian, M. M., & Jefferies, W. A. (2021). Discovery of a Highly Conserved Peptide in the Iron Transporter Melanotransferrin that Traverses an Intact Blood Brain Barrier and Localizes in Neural Cells. *Frontiers in Neuroscience*, *15*, 596976. https://doi.org/10.3389/fnins.2021.596976

Siudeja, K., Nassari, S., Gervais, L., Skorski, P., Lameiras, S., Stolfa, D., Zande, M., Bernard, V., Frio, T. R., & Bardin, A. J. (2015). Frequent Somatic Mutation in Adult Intestinal Stem

Cells Drives Neoplasia and Genetic Mosaicism during Aging. *Cell Stem Cell*, *17*(6), 663–674. https://doi.org/10.1016/j.stem.2015.09.016

Smyth, N., Seda Vatansever, H., Murray, P., Meyer, M., Frie, C., Paulsson, M., & Edgar, D. (1999). Absence of Basement Membranes after Targeting the LAMC1 Gene Results in Embryonic Lethality Due to Failure of Endoderm Differentiation. *The Journal of Cell Biology*, *144*(1), 151–160. http://www.jcb.org

Snow, P. M., Bieber, A. J., & Goodman, C. S. (1989). Fasciclin III: A novel homophilic adhesion molecule in Drosophila. *Cell*, *59*(2), 313–323. https://doi.org/10.1016/0092-8674(89)90293-6

Southall, T. D., Gold, K. S., Egger, B., Davidson, C. M., Caygill, E. E., Marshall, O. J., & Brand, A. H. (2013). Cell-Type-Specific Profiling of Gene Expression and Chromatin Binding without Cell Isolation: Assaying RNA Pol II Occupancy in Neural Stem Cells. *Developmental Cell*, *26*(1), 101–112. https://doi.org/10.1016/j.devcel.2013.05.020

Spenlé, C., Hussenet, T., Lacroute, J., Lefebvre, O., Kedinger, M., Orend, G., & Simon-Assmann, P. (2012). Dysregulation of laminins in intestinal inflammation. *Pathologie Biologie*, *60*(1), 41–47. https://doi.org/10.1016/j.patbio.2011.10.005

Staley, B. K., & Irvine, K. D. (2010). Warts and Yorkie Mediate Intestinal Regeneration by Influencing Stem Cell Proliferation. *Current Biology*, *20*(17), 1580–1587. https://doi.org/10.1016/j.cub.2010.07.041

Statzer, C., Park, J. Y. C., & Ewald, C. Y. (2023). Extracellular Matrix Dynamics as an Emerging yet Understudied Hallmark of Aging and Longevity. *Aging and Disease*, *14*(3), 670. https://doi.org/10.14336/AD.2022.1116

Stec, W., Vidal, O., & Zeidler, M. P. (2013). *Drosophila* SOCS36E negatively regulates JAK/STAT pathway signaling via two separable mechanisms. *Molecular Biology of the Cell*, *24*(18), 3000–3009. https://doi.org/10.1091/mbc.e13-05-0275

Strand, D., Raska, I., & Mechler, B. M. (1994). The Drosophila lethal(2)giant larvae tumor suppressor protein is a component of the cytoskeleton. *The Journal of Cell Biology*, *127*(5), 1345–1360. https://doi.org/10.1083/jcb.127.5.1345

Suardita, K., Fujimoto, K., Oda, R., Shimazu, A., Miyazaki, K., Kawamoto, T., & Kato, Y. (2002). Effects of Overexpression of Membrane-bound Transferrin-like Protein (MTf) on Chondrogenic Differentiation in Vitro. *Journal of Biological Chemistry*, *277*(50), 48579–48586. https://doi.org/10.1074/jbc.M209243200

Sugimoto, H., Mundel, T. M., Kieran, M. W., & Kalluri, R. (2006). Identification of fibroblast heterogeneity in the tumor microenvironment. *Cancer Biology & Therapy*, *5*(12), 1640–1646. https://doi.org/10.4161/cbt.5.12.3354

Suryo Rahmanto, Y., Dunn, L. L., & Richardson, D. R. (2007a). Identification of distinct changes in gene expression after modulation of melanoma tumor antigen p97 (melanotransferrin) in multiple models in vitro and in vivo. *Carcinogenesis*, *28*(10), 2172–2183. https://doi.org/10.1093/carcin/bgm096

Suryo Rahmanto, Y., Dunn, L. L., & Richardson, D. R. (2007b). The melanoma tumor antigen, melanotransferrin (p97): a 25-year hallmark – from iron metabolism to tumorigenesis. *Oncogene*, *26*(42), 6113–6124. https://doi.org/10.1038/sj.onc.1210442

Tadokoro, T., Gao, X., Hong, C. C., Hotten, D., & Hogan, B. L. M. (2016). BMP signaling and cellular dynamics during regeneration of airway epithelium from basal progenitors. *Development*, *143*(5), 764–773. https://doi.org/10.1242/dev.126656

Tamamouna, V., Panagi, M., Theophanous, A., Demosthenous, M., Michail, M., Papadopoulou, M., Teloni, S., Pitsouli, C., & Apidianakis, Y. (2020). Evidence of two types of balance between stem cell mitosis and enterocyte nucleus growth in the *Drosophila* midgut. *Development*, *147*(11). https://doi.org/10.1242/dev.189472

Tauc, H. M., Rodriguez-Fernandez, I. A., Hackney, J. A., Pawlak, M., Ronnen Oron, T., Korzelius, J., Moussa, H. F., Chaudhuri, S., Modrusan, Z., Edgar, B. A., & Jasper, H. (2021). Age-related changes in polycomb gene regulation disrupt lineage fidelity in intestinal stem cells. *ELife*, *10:e62250*. https://doi.org/10.7554/eLife.62250

Tempesta, C., Hijazi, A., Moussian, B., & Roch, F. (2017). Boudin trafficking reveals the dynamic internalisation of specific septate junction components in Drosophila. *PLoS ONE*, *12*(10). https://doi.org/10.1371/journal.pone.0185897

Thom, G., Tian, M.-M., Hatcher, J. P., Rodrigo, N., Burrell, M., Gurrell, I., Vitalis, T. Z., Abraham, T., Jefferies, W. A., Webster, C. I., & Gabathuler, R. (2018). A peptide derived from melanotransferrin delivers a protein-based interleukin 1 receptor antagonist across the BBB and ameliorates neuropathic pain in a preclinical model. *Journal of Cerebral Blood Flow & Metabolism*, *39*(10), 2074–2088. https://doi.org/10.1177/0271678X18772998

Tian, A., Benchabane, H., Wang, Z., & Ahmed, Y. (2016). Regulation of Stem Cell Proliferation and Cell Fate Specification by Wingless/Wnt Signaling Gradients Enriched at Adult Intestinal Compartment Boundaries. *PLOS Genetics*, *12*(2), e1005822. https://doi.org/10.1371/journal.pgen.1005822

Tian, A., & Jiang, J. (2014). Intestinal epithelium-derived BMP controls stem cell self-renewal in Drosophila adult midgut. *ELife*, *3*(3), e01857. https://doi.org/10.7554/eLife.01857

Tian, A., & Jiang, J. (2017). Dual role of BMP signaling in the regulation of *Drosophila* intestinal stem cell self-renewal. *Fly*, *11*(4), 297–302. https://doi.org/10.1080/19336934.2017.1384104

Tian, A., Shi, Q., Jiang, A., Li, S., Wang, B., & Jiang, J. (2015). Injury-stimulated Hedgehog signaling promotes regenerative proliferation of *Drosophila* intestinal stem cells. *Journal of Cell Biology*, *208*(6), 807–819. https://doi.org/10.1083/jcb.201409025

Tian, A., Wang, B., & Jiang, J. (2017). Injury-stimulated and self-restrained BMP signaling dynamically regulates stem cell pool size during *Drosophila* midgut regeneration. *Proceedings of the National Academy of Sciences*, *114*(13), E2699–E2708. https://doi.org/10.1073/pnas.1617790114

Tiklová, K., Senti, K. A., Wang, S., Gräslund, A., & Samakovlis, C. (2010). Epithelial septate junction assembly relies on melanotransferrin iron binding and endocytosis in Drosophila. *Nature Cell Biology*, *12*(11), 1071–1077. https://doi.org/10.1038/ncb2111

Tiwari, N., Meyer-Schaller, N., Arnold, P., Antoniadis, H., Pachkov, M., van Nimwegen, E., & Christofori, G. (2013). Klf4 Is a Transcriptional Regulator of Genes Critical for EMT, Including Jnk1 (Mapk8). *PLoS ONE*, *8*(2), e57329. https://doi.org/10.1371/journal.pone.0057329

Töpfer, U. (2023). Basement membrane dynamics and mechanics in tissue morphogenesis. *Biology Open*, *12*(8). https://doi.org/10.1242/bio.059980

Tower, J., Landis, G. N., Shen, J., Choi, R., Fan, Y., Lee, D., & Song, J. (2017). Mifepristone/RU486 acts in Drosophila melanogaster females to counteract the life span-shortening and pro-inflammatory effects of male Sex Peptide. *Biogerontology*, *18*(3), 413–427. https://doi.org/10.1007/s10522-017-9703-y

Tran, L., & Greenwood-Van Meerveld, B. (2013). Age-Associated Remodeling of the Intestinal Epithelial Barrier. *The Journals of Gerontology Series A: Biological Sciences and Medical Sciences*, *68*(9), 1045–1056. https://doi.org/10.1093/gerona/glt106

Trier, J. S., Allan, C. H., Abrahamson, D. R., & Hagen, S. J. (1990). Epithelial basement membrane of mouse jejunum. Evidence for laminin turnover along the entire crypt-villus axis. *Journal of Clinical Investigation*, *86*(1), 87–95. https://doi.org/10.1172/JCI114720

Udayakumar, T. S., Chen, M. L., Bair, E. L., Von Bredow, D. C., Cress, A. E., Nagle, R. B., & Bowden, G. T. (2003). Membrane Type-1-Matrix Metalloproteinase Expressed by Prostate Carcinoma Cells Cleaves Human Laminin-5 3 Chain and Induces Cell Migration

1. *Cancer Research*, *63*(9), 2292–2299. http://aacrjournals.org/cancerres/article-pdf/63/9/2292/2513662/ch0903002292.pdf

Uhlen, M., Fagerberg, L., Hallström, B. M., Lindskog, C., Oksvold, P., Mardinoglu, A., Sivertsson, Å., Kampf, C., Sjöstedt, E., Asplund, A., Olsson, I., Edlund, K., Lundberg, E., Navani, S., Szigyarto, C. A.-K., Odeberg, J., Djureinovic, D., Takanen, J. O., Hober, S., … Pontén, F. (2015). Tissue-based map of the human proteome. *Science*, *347*(6220). https://doi.org/10.1126/science.1260419

Uhlen, M., Zhang, C., Lee, S., Sjöstedt, E., Fagerberg, L., Bidkhori, G., Benfeitas, R., Arif, M., Liu, Z., Edfors, F., Sanli, K., von Feilitzen, K., Oksvold, P., Lundberg, E., Hober, S., Nilsson, P., Mattsson, J., Schwenk, J. M., Brunnström, H., … Ponten, F. (2017). A pathology atlas of the human cancer transcriptome. *Science*, *357*(6352). https://doi.org/10.1126/science.aan2507

Ullman, T., Odze, R., & Farraye, F. A. (2009). Diagnosis and management of dysplasia in patients with ulcerative colitis and Crohn's disease of the colon. *Inflammatory Bowel Diseases*, *15*(4), 630–638. https://doi.org/10.1002/ibd.20766

Urbano, J. M., Torgler, C. N., Molnar, C., Tepass, U., Lopez-Varea, A., Brown, N. H., de Celis, J. F., Martin-Bermudo, M. D., López-Varea, A., Brown, N. H., de Celis, J. F., & Martín-Bermudo, M. D. (2009). Drosophila laminins act as key regulators of basement membrane assembly and morphogenesis. *Development*, *136*(24), 4165–4176. https://doi.org/10.1242/dev.044263

Vickman, R. E., Broman, M. M., Lanman, N. A., Franco, O. E., Sudyanti, P. A. G., Ni, Y., Ji, Y., Helfand, B. T., Petkewicz, J., Paterakos, M. C., Crawford, S. E., Ratliff, T. L., & Hayward, S. W. (2020). Heterogeneity of human prostate carcinoma-associated fibroblasts implicates a role for subpopulations in myeloid cell recruitment. *The Prostate*, *80*(2), 173–185. https://doi.org/10.1002/pros.23929

Wang, L., Ryoo, H. D., Qi, Y., & Jasper, H. (2015). PERK Limits Drosophila Lifespan by Promoting Intestinal Stem Cell Proliferation in Response to ER Stress. *PLOS Genetics*, *11*(5), e1005220. https://doi.org/10.1371/journal.pgen.1005220

Wang, L., Zeng, X., Ryoo, H. D., & Jasper, H. (2014). Integration of UPRER and Oxidative Stress Signaling in the Control of Intestinal Stem Cell Proliferation. *PLoS Genetics*, *10*(8), e1004568. https://doi.org/10.1371/journal.pgen.1004568

Wang, X.-D., Leow, C. C., Zha, J., Tang, Z., Modrusan, Z., Radtke, F., Aguet, M., de Sauvage, F. J., & Gao, W.-Q. (2006). Notch signaling is required for normal prostatic epithelial cell

proliferation and differentiation. *Developmental Biology*, *290*(1), 66–80. https://doi.org/10.1016/j.ydbio.2005.11.009

Wang, Z. A., Mitrofanova, A., Bergren, S. K., Abate-Shen, C., Cardiff, R. D., Califano, A., & Shen, M. M. (2013). Lineage analysis of basal epithelial cells reveals their unexpected plasticity and supports a cell-of-origin model for prostate cancer heterogeneity. *Nature Cell Biology*, *15*(3), 274–283. https://doi.org/10.1038/ncb2697

Watt, F. M., & Fujiwara, H. (2011). Cell-Extracellular Matrix Interactions in Normal and Diseased Skin. *Cold Spring Harbor Perspectives in Biology*, *3*(4), a005124–a005124. https://doi.org/10.1101/cshperspect.a005124

Wolfstetter, G., Dahlitz, I., Pfeifer, K., Töpfer, U., Alt, J. A., Pfeifer, D. C., Lakes-Harlan, R., Baumgartner, S., Palmer, R. H., & Holz, A. (2019). Characterization of Drosophila Nidogen/entactin reveals roles in basement membrane stability, barrier function and nervous system patterning. *Development (Cambridge)*, *146*(2), dev168948. https://doi.org/10.1242/dev.168948

Wolfstetter, G., & Holz, A. (2012). The role of LamininB2 (LanB2) during mesoderm differentiation in Drosophila. *Cellular and Molecular Life Sciences*, *69*(2), 267–282. https://doi.org/10.1007/s00018-011-0652-3

Woodbury, R. G., Brown, J. P., Loop, S. M., Hellström, K. E., & Hellström, I. (1981). Analysis of normal neoplastic human tissues for the tumor-associated protein p97. *International Journal of Cancer*, *27*(2), 145–149. https://doi.org/10.1002/ijc.2910270204

Woodbury, R. G., Brown, J. P., Yeh, M. Y., Hellström, I., & Hellström, K. E. (1980). Identification of a cell surface protein, p97, in human melanomas and certain other neoplasms. *Proceedings of the National Academy of Sciences of the United States of America*, *77*(4), 2183–2187. https://doi.org/10.1073/pnas.77.4.2183

Woods, D. F., & Bryant, P. J. (1991). The discs-large tumor suppressor gene of Drosophila encodes a guanylate kinase homolog localized at septate junctions. *Cell*, *66*(3), 451–464. https://doi.org/10.1016/0092-8674(81)90009-X

Wu, V. M., Schulte, J., Hirschi, A., Tepass, U., & Beitel, G. J. (2004). Sinuous is a *Drosophila* claudin required for septate junction organization and epithelial tube size control. *The Journal of Cell Biology*, *164*(2), 313–323. https://doi.org/10.1083/jcb.200309134

Wu, V. M., Yu, M. H., Paik, R., Banerjee, S., Liang, Z., Paul, S. M., Bhat, M. A., & Beitel, G. J. (2007). *Drosophila* Varicose, a member of a new subgroup of basolateral MAGUKs, is required for septate junctions and tracheal morphogenesis. *Development*, *134*(5), 999–1009. https://doi.org/10.1242/dev.02785

Xu, C., Tang, H.-W., Hung, R.-J., Hu, Y., Ni, X., Housden, B. E., & Perrimon, N. (2019). The Septate Junction Protein Tsp2A Restricts Intestinal Stem Cell Activity via Endocytic Regulation of aPKC and Hippo Signaling. *Cell Reports*, *26*(3), 670-688.e6. https://doi.org/10.1016/j.celrep.2018.12.079

Xu, M., Tchkonia, T., & Kirkland, J. L. (2016). Perspective: Targeting the JAK/STAT pathway to fight age-related dysfunction. *Pharmacological Research*, *111*, 152–154. https://doi.org/10.1016/j.phrs.2016.05.015

Xu, N., Wang, S. Q., Tan, D., Gao, Y., Lin, G., & Xi, R. (2011). EGFR, Wingless and JAK/STAT signaling cooperatively maintain Drosophila intestinal stem cells. *Developmental Biology*, *354*(1), 31–43. https://doi.org/10.1016/j.ydbio.2011.03.018

Yamada, T., Tsujioka, Y., Taguchi, J., Takahashi, M., Tsuboi, Y., Moroo, I., Yang, J., & Jefferies, W. A. (1999). Melanotransferrin is produced by senile plaque-associated reactive microglia in Alzheimer's disease. *Brain Research*, *845*(1), 1–5. https://doi.org/10.1016/S0006-8993(99)01767-9

Yanagihashi, Y., Usui, T., Izumi, Y., Yonemura, S., Sumida, M., Tsukita, S., Uemura, T., & Furuse, M. (2012). Snakeskin, a membrane protein associated with smooth septate junctions, is required for intestinal barrier function in Drosophila. *Journal of Cell Science*, *125*(8), 1980–1990. https://doi.org/10.1242/jcs.096800

Yang, Z., Ma, H., Wang, S., Wang, L., & Liu, T. (2017). LAMC1 mRNA promotes malignancy of hepatocellular carcinoma cells by competing for MicroRNA-124 binding with CD151. *IUBMB Life*, *69*(8), 595–605. https://doi.org/10.1002/iub.1642

Yarnitzky, T., & Volk, T. (1995). Laminin is required for heart, somatic muscles, and gut development in the Drosophila embryo. *Developmental Biology*, *169*(2), 609–618. https://doi.org/10.1006/dbio.1995.1173

Yen, W.-C., Chang, K.-P., Chen, C.-Y., Huang, Y., Chen, T.-W., Cheng, H.-W., Yi, J.-S., Cheng, C.-C., Wu, C.-C., & Wang, C.-I. (2023). MFI2 upregulation promotes malignant progression through EGF/FAK signaling in oral cavity squamous cell carcinoma. *Cancer Cell International*, *23*(1), 112. https://doi.org/10.1186/s12935-023-02956-0

Yu, W., Datta, A., Leroy, P., O'Brien, L. E., Mak, G., Jou, T. S., Matlin, K. S., Mostov, K. E., & Zegers, M. M. P. (2005). β1-integrin orients epithelial polarity via Rac1 and laminin. *Molecular Biology of the Cell*, *16*(2), 433–445. https://doi.org/10.1091/mbc.E04-05-0435

Yurchenco, P. D., Quan, Y., Colognato, H., Mathus, T., Harrison, D., Yamada, Y., & O'Rear, J. J. (1997). The α chain of laminin-1 is independently secreted and drives secretion of its β-

and γ-chain partners. *Proceedings of the National Academy of Sciences*, *94*(19), 10189–10194. https://doi.org/10.1073/pnas.94.19.10189

Yurchenco, P. D., Tsilibary, E. C., Charonis, A. S., & Furthmayr, H. (1985). Laminin polymerization in vitro. Evidence for a two-step assembly with domain specificity. *Journal of Biological Chemistry*, *260*(12), 7636–7644. https://doi.org/10.1016/S0021-9258(17)39656-4

Zappia, M. P., Brocco, M. A., Billi, S. C., Frasch, A. C., & Ceriani, M. F. (2011). M6 Membrane Protein Plays an Essential Role in Drosophila Oogenesis. *PLoS ONE*, *6*(5), e19715. https://doi.org/10.1371/journal.pone.0019715

Zeng, X., & Hou, S. X. (2015). Enteroendocrine cells are generated from stem cells through a distinct progenitor in the adult *Drosophila* posterior midgut. *Development*, *142*(4), 644–653. https://doi.org/10.1242/dev.113357

Zerofsky, M., Harel, E., Silverman, N., & Tatar, M. (2005). Aging of the innate immune response in *Drosophila melanogaster*. *Aging Cell*, *4*(2), 103–108. https://doi.org/10.1111/j.1474-9728.2005.00147.x

Zhang, Y., Xi, S., Chen, J., Zhou, D., Gao, H., Zhou, Z., Xu, L., & Chen, M. (2017). Overexpression of LAMC1 predicts poor prognosis and enhances tumor cell invasion and migration in hepatocellular carcinoma. *Journal of Cancer*, *8*(15), 2992–3000. https://doi.org/10.7150/jca.21038

Zhou, F., Rasmussen, A., Lee, S., & Agaisse, H. (2013). The UPD3 cytokine couples environmental challenge and intestinal stem cell division through modulation of JAK/STAT signaling in the stem cell microenvironment. *Developmental Biology*, *373*(2), 383–393. https://doi.org/10.1016/j.ydbio.2012.10.023

Zhou, J., Florescu, S., Boettcher, A.-L., Luo, L., Dutta, D., Kerr, G., Cai, Y., Edgar, B. A., & Boutros, M. (2015). Dpp/Gbb signaling is required for normal intestinal regeneration during infection. *Developmental Biology*, *399*(2), 189–203. https://doi.org/10.1016/j.ydbio.2014.12.017

Zirin, J., Hu, Y., Liu, L., Yang-Zhou, D., Colbeth, R., Yan, D., Ewen-Campen, B., Tao, R., Vogt, E., VanNest, S., Cavers, C., Villalta, C., Comjean, A., Sun, J., Wang, X., Jia, Y., Zhu, R., Peng, P., Yu, J., … Perrimon, N. (2020). Large-Scale Transgenic *Drosophila* Resource Collections for Loss- and Gain-of-Function Studies. *Genetics*, *214*(4), 755–767. https://doi.org/10.1534/genetics.119.302964